

A1757

Encl In Pac. 2

A-1757

POR
LPOR - WM-10(3)
WM-11(2)
WM-16(2)

WM Record File
A-1757

WM Project 10, 11, 16
Docket No. _____
PDR K
HPDR B, N, S

FEB -3 A11 08

Distribution:
X Coleman

(Return to WM, 623-SS)

NUMERICAL MODELING OF GROUND-WATER FLOW SYSTEMS IN THE
VICINITY OF THE REFERENCE REPOSITORY LOCATION,
HANFORD SITE, WASHINGTON

DRAFT

- Paul Davis
- Walt Beyeler
- Mark Logston
- Neil Coleman
- Ken Brinster

8702200227 870203
PDR WMRES EXISANL
A-1757 PDR

DRAFT

3652

ENC. to cover letter DATED 2/3/87
RCD 2E-E1

A1757
DRAFT

1. INTRODUCTION.....2

2. GEOLOGY.....4

2.1. GEOLOGIC SETTING.....5

2.2. STRATIGRAPHY.....7

2.2.1. GRANDE RONDE BASALT.....8

2.2.1.1. UMTANUM FLOW.....9

2.2.1.2. MCCOY CANYON FLOW.....9

2.2.1.3. COHASSETT FLOW.....10

2.2.1.4. ROCKY COULEE FLOW.....10

2.2.2. WANAPUM BASALT.....11

2.2.2.1. FRENCHMAN SPRINGS MEMBER.....11

2.2.2.2. ROZA MEMBER.....11

2.2.2.3. PRIEST RAPIDS MEMBER.....12

2.2.3. SADDLE MOUNTAINS BASALT.....12

2.2.3.1. UMATILLA MEMBER.....12

2.2.3.2. ESQUATZEL MEMBER.....13

2.2.3.3. POMONA MEMBER.....13

2.2.3.4. ELEPHANT MOUNTAIN MEMBER.....13

2.2.4. ELLENSBURG FORMATION.....14

2.2.5. RINGOLD FORMATION.....14

2.2.6. PLIO-PLEISTOCENE UNIT.....15

2.2.7. HANFORD FORMATION.....16

2.3. REGIONAL GEOLOGIC STRUCTURES.....16

2.3.1. WAHLUKE SYNCLINE.....17

2.3.2. UMTANUM RIDGE-GABLE MOUNTAIN STRUCTURE.....17

2.3.3. COLD CREEK SYNCLINE.....18

2.3.4. YAKIMA RIDGE STRUCTURE.....18

DRAFT

2.3.5. BENSON RANCH SYNCLINE.....19

2.3.6. PASCO SYNCLINE.....19

2.3.7. CLE ELUM - WALLULA ALIGNMENT.....20

2.4. INTERNAL BASALT STRUCTURES.....20

3. HYDROLOGY.....21

3.1. SURFACE WATER.....21

3.2. GROUND WATER.....23

3.2.1. DEFINITION AND EXAMPLES OF CONCEPTUAL MODELS.....23

3.2.2. FACTORS CONTROLLING GROUND-WATER FLOW IN BASALTS.....28

3.2.3. DEFINITION AND PROPERTIES OF BWIP HYDROSTRATIGRAPHIC
UNITS.....34

3.2.3.1. ALLUVIUM.....34

3.2.3.2. BASALTS.....37

3.2.3.2.1. SADDLE MOUNTAINS BASALTS.....38

3.2.3.3. WANAPUM BASALTS.....39

3.2.3.4. GRANDE RONDE BASALTS.....41

3.2.4. RECHARGE AND DISCHARGE TO THE HYDROSTRATIGRAPHIC
UNITS.....43

3.2.5. GROUND-WATER MOVEMENT WITHIN THE HYDROSTRATIGRAPHIC
UNITS.....46

4. HYDROCHEMISTRY.....58

4.1. HYDROCHEMICAL DATA BASE.....58

4.2. MAJOR APPLICATIONS OF HYDROCHEMISTRY TO CONCEPTUAL
MODEL EVALUATION.....61

4.2.1. BWIP SITE CHARACTERIZATION REPORT (DOE, 1982).....61

4.2.2. U S. GEOLOGICAL SURVEY CRITIQUE OF SCR
(USGS, 1983).....63

4.2.3. LEHMAN REVIEW OF 1983 BWIP HYDROCHEMICAL DATA
 (LEHMAN, 1983).....65

4.2.4. ROCKWELL 1984 (DOE-NRC GEOCHEMISTRY WORKSHOP,
 JANUARY, 1984).....68

4.3. SUMMARY AND CONCLUSIONS.....70

5. SUMMARY AND EVALUATION OF CONCEPTUAL MODELS.....73

5.1. HYDROSTRATIGRAPHIC UNITS.....73

5.2. BOUNDARY CONDITIONS.....80

6. PREVIOUS NUMERICAL MODELING EFFORTS.....89

6.1. GENERAL DESCRIPTION OF THE MAJOR STUDIES.....89

6.1.1. LA SALA AND OTHERS, 1973.....89

6.1.2. ARNETT, 1980.....91

6.1.3. ARNETT AND OTHERS, 1981.....92

6.1.4. RIGDON AND OTHERS (LATA), 1981.....94

6.1.5. DOVE AND OTHERS, 1982.....94

6.1.6. LEHMAN AND QUINN, 1982 and QUINN, 1982.....96

6.1.7. BONANO AND OTHERS, 1986.....98

6.2. OVERALL REVIEW AND EVALUATION OF NUMERICAL MODELS.....100

6.2.1. EVALUATION OF NUMERICAL MODELS.....100

6.2.2. COMPARISON OF NUMERICAL MODELS.....102

6.2.3. COMPARISON OF MODEL RESULTS.....104

6.2.4. SUMMARY OF NUMERICAL MODELS.....107

7. CURRENT NUMERICAL MODELING OF BWIP.....108

7.1. REGIONAL MODEL OF THE EXTENDED PASCO BASIN.....109

7.1.1. INITIAL REGIONAL MODEL.....109

7.1.1.1. MODEL DESCRIPTION.....110

7.1.1.2. MODEL RESULTS.....115

7.1.2. ANALYSIS OF THE INITIAL MODEL.....	124
7.1.3. REVISED REGIONAL MODEL.....	125
7.1.3.1. DESCRIPTION OF THE REVISED MODEL.....	130
7.1.3.2. MODEL RESULTS.....	133
7.2. LOCAL MODEL.....	136
8. SUMMARY AND RECOMMENDATIONS.....	140

List of Tables

DRAFT

Table 3.1 Representative Hydraulic Properties of the Unconfined Aquifer (Gephart and others, 1979)

Table 3.2 Grande Ronde Conductivities at RRL-2 from RHO Interval Reports (Strait and Spane, 1982a,b,c,d, and e and 1983)

Table 3.3 Pasco Basin Water Budget (Leonhart , 1979)

Table 3.4 Hydraulic Heads within Selected Stratigraphic Intervals in the Saddle Mountains Basalt (Modified from DOE, 1982, Gephart and others 1979)

Table 7.1 Hydrostratigraphic Units Represented in the Local Model

Table A.1.1 Baseline Material Hydraulic Conductivities used in Calculating Basalt Composite Conductivities

Table A.1.2 Ratios of K_v to K_h used to Produce Model-Calculated Heads in RHO-BWI-80-100

Table A.2.1 MAGNUM3D Values for Hydraulic Parameters

Table A.2.2 Material Properties

**Table A.2.3 Annual Pumpage Rates Used in the Initial
MAGNUM-3D Pasco Basin Simulation**

Table A.2.4 Hydraulic Head Data

Table A.2.5 Results of Different Boundary Conditions

Table A.3.1 Model Parameters for Rigdon and others, 1981

Table A.4.1 Initial and Calibrated Hydraulic Parameters

**Table A.4.2 Porosities Used in Ground-Water Travel Time
Calculation (Reproduced from Dove and others,
Table B.27)**

**Table A.4.3 Average, rms, Maximum and Minimum Error
Comparisons Between Well Data and Model
Predictions and Well Data and the
Interpreted Potentials for Layer 1
(Reproduced from Dove and others, Table B.26)**

DRAFT

Table A.4.4 Summary of Comparison Statistics Between Model-Predicted Potential Distributions Interpreted from Water Level Data for Four Illustrative Model Calibration Runs and the Base Case. (Comparisons are shown for both the current condition scenario and the preman scenario. All values are in feet.) (Reproduced from Dove and others, Table B.31)

Table A.4.5 Calculated Fluxes in the Regional Model

List of Figures

DRAFT

- Figure 2.1 Location of the Hanford Site, Southeastern Washington State. (DOE, 1984)
- Figure 2.2 Reference Repository and Alternate Repository Locations. (DOE, 1984)
- Figure 2.3 Map of Major Landform Systems of the Pasco Basin. (DOE, 1984)
- Figure 2.4 Geomorphic Map of the Reference Repository Location. (DOE, 1984)
- Figure 2.5 Stratigraphic Nomenclature for the Columbia River Basalt Group of the Columbia Plateau (after Swanson and others, 1979b in DOE, 1984)
- Figure 2.6 Distribution of Columbia River Basalt Group (after Wright and others, 1973 in DOE, 1984)
- Figure 2.7 Geologic Cross Section Through the Reference Repository Location. (DOE, 1984)
- Figure 2.8 Umtanum Flow Isopach Map. (DOE, 1984)
- Figure 2.9 Isopach Map of the Dense Interior of the Umtanum Flow. (DOE, 1984)

DRAFT

Figure 2.11 Isopach Map of the Dense Interior of the
McCoy Canyon Flow. (DOE, 1984)

Figure 2.12 Sentinel Bluffs Sequence Isopach Map. (DOE, 1984)

Figure 2.13 Cohasset Flow Isopach Map.

Figure 2.14 Isopach Map of the Dense Interior of the Cohasset
Flow above the Vesicular Zone. (DOE, 1984)

Figure 2.15 Isopach Map of the Dense Interior of the Cohasset
Flow below the Vesicular Zone. (DOE, 1984)

Figure 2.16 Rocky Coulee Flow Isopach Map. (DOE, 1984)

Figure 2.17 Isopach Map of the Dense Interior of the Rocky
Coulee Flow. (DOE, 1984)

Figure 2.18 Suprabasalt Stratigraphy
in the Reference Repository
Location. (DOE, 1984)

Figure 2.19 Distribution of Ringold Formation Section Types.

Figure 2.20 Top of the Ringold Formation. Contour Pattern
Indicates Maximum Post-Ringold Incision Occurred
near the Trend of the Present Cold Creek Valley.
(DOE, 1984)

Figure 2.21 Generalized Geologic Structure Map of the Central

Figure 2.22 Cross Section of a Typical Flow in the Columbia
River Basalt Group Illustrating, in Idealized
Form, Jointing Patterns and other Structures
(from Swanson and Wright, 1976 in DOE, 1984)

DRAFT

Figure 3.1 Water-Table Map within the Pasco Basin.
(Gephart and others, 1979)

Figure 3.2 Water-Table Rise beneath the Hanford Site,
1944-1978. (Gephart and others, 1979)

Figure 3.3 Comparison of Hydraulic Heads in the Rattlesnake
Ridge Interbed to Water-Table Elevation (DOE, 1982)

Figure 3.4 Potentiometric Map and Inferred Flow Directions for the Mabton Interbed beneath the Hanford Site.
(Gephart and others, 1979)

Figure 3.5 Potentiometric Map of Saddle Mountains Basalts, Spring 1984.

Figure 3.6 Potentiometric Map of Wanapum Basalts, Spring 1984.

Figure 3.7 Potentiometric Map of Grande Ronde Basalts, Spring 1984.

Figure 3.8 Measured Water Levels in DC-19, DC-20, and DC-22 for the Wanapum and Grande Ronde Basalts, Spring 1986.

Figure 3.9 Location of Wells DC-19, DC-20, DC-22, DC-23W, and RRL-14 (Rockwell Hanford Operations, December 1985)

Figure 3.10 Response at DC-19, DC-20, and DC-22 to Bridge Plug Removal at RRL-14

Figure 3.11 Response at DC-19, DC-20, and DC-22 to Drilling, Piezometer Installation, and Cleanup of DC-23W

Figure 3.12 Location of Section A-A'

Figure 3.13 Section Through A-A' Showing Inferred Stratigraphy After Myers (1979) and Heads Measured in Spring

Figure 4.1 Piper Trilinear Plot of all Data Received from DOE
Richland Office 2/15/83

Figure 4.2 Distribution of Water Types within the Pasco Basin
(Lehman, 1983)

Figure 4.3 Chloride Concentrations (Mg/L) - Mabton Interbed
(RHO, 1984)

Figure 4.4 Chloride Contours (Mg/L) - U. Wanapum Groundwaters
(RHO, 1984)

Figure 4.5 Chloride Contours (Mg/L) - L. Wanapum Groundwaters
(RHO, 1984)

Figure 4.6 Sodium Contours (Mg/L) - U. Grande Ronde (RHO, 1984)

Figure 4.7 Dissolved Gases in the Grande Ronde Formation
(RHO, 1984)

- Figure 4.8 Tentative Flow Model Based on Hydrochemistry
(RHO, 1984)
- Figure 4.9 Schematic Cross Section AA' Showing Location of
Hypothesized Mixing Plume (RHO, 1984)
- Figure 6.1 Ground-Water Flow Directions Postulated by
LaSala and Doty, 1973
- Figure 6.2 Plan View of Streamlines from Hypothetical
Repository to Boundary
- Figure 6.3 Cross Section of Model-Calculated Streamlines
- Figure 7.1 Regional Model Grid
- Figure 7.2 Boundary Conditions for the Regional Model
- Figure 7.3 No-Flow and Constant Head Boundaries for Layer 4
- Figure 7.4 No-Flow and Constant Head Boundaries for Layer 3
- Figure 7.5 No-Flow and Constant Head Boundaries for Layer 2
- Figure 7.6 No-Flow and Constant Head Boundaries for Layer 1
- Figure 7.7 Generalized Stratigraphy of the Pasco Basin

Figure 7.9 Kriged Heads for the Grande Ronde Basalts

Figure 7.10 Kriged Heads for the Wanapum Basalts

Figure 7.11 Kriged Heads for the Saddle Mountains Basalts

**Figure 7.12 Composite Vertical Profile of Kriged Hydraulic
Heads near the RRL, McGee Well, and 200 Ponds Areas**

Figure 7.13 Simulated Heads for the Grande Ronde Basalts

Figure 7.14 Simulated Heads for the Wanapum Basalts

Figure 7.15 Simulated Heads for the Saddle Mountains Basalts

Figure 7.16 Simulated Heads for the Alluvium

**Figure 7.17 Simulated Heads
East-West Section through the RRL**

**Figure 7.18 Composite Vertical Profile of Simulated Hydraulic
Heads at the RRL, McGee Well, and 200 Ponds Areas**

Figure 7.19 Simulated Heads for the Saddle Mountains Basalts with and without the Cold Creek Barrier

Figure 7.20 Simulated Heads for the Wanapum Basalts with and without the Cold Creek Barrier

Figure 7.21 Simulated Heads for the Grande Ronde Basalts with and without the Cold Creek Barrier

Figure 7.22 Vertical Profile of Simulated Heads with the Cold Creek Barrier Included

Figure 7.23 Simulated Heads in an East-West Section through the RRL with and without the Cold Creek Barrier

Figure 7.24 Simulated Heads for the Grande Ronde Basalts with and without Gable Mountain/Gable Butte

Figure 7.25 Simulated Heads for the Wanapum Basalts with and without Gable Mountain/Gable Butte

Figure 7.26 Simulated Heads for the Saddle Mountains Basalts with and without Gable Mountain/Gable Butte

Figure 7.27 Simulated Heads for the Alluvium with and without Gable Mountain/Gable Butte

Figure 7.28 Simulated Heads in an East-West Section through the RRL with and without Gable Mountain/Gable Butte

Figure 7.29 Vertical Profile of Simulated Heads with Gable Mountain/Gable Butte Included

Figure 7.30 Simulated Heads for the Grande Ronde Basalts with and without Ponds

Figure 7.31 Simulated Heads for the Wanapum Basalts with and without Ponds

Figure 7.32 Simulated Heads for the Saddle Mountains Basalts with and without Ponds

Figure 7.33 Simulated Heads for the Alluvium with and without ponds

Figure 7.34 Simulated Heads in an East-West Section through the RRL with and without Ponds

Figure 7.35 Simulated Heads for the Grande Ronde Basalts with and without Gable Mountain/Gable Butte and the Cold Creek Barrier

- Figure 7.36 Simulated Heads for the Wanapum Basalts with and without Gable Mountain/Gable Butte and the Cold Creek Barrier**
- Figure 7.37 Simulated Heads for the Saddle Mountains Basalts with and without Gable Mountain/Gable Butte and the Cold Creek Barrier**
- Figure 7.38 Simulated Heads in an East-West Section through the RRL with and without Gable Mountain/Gable Butte and the Cold Creek Barrier**
- Figure 7.39 Simulated Heads in the Wanapum for Various Values of Leakance**
- Figure 7.40 Boundary Conditions for the Revised BWIP Regional Flow Model - Layer 1: Grande Ronde Basalts**
- Figure 7.41 Boundary Conditions for the Revised BWIP Regional Flow Model - Layer 2: Wanapum Basalts**
- Figure 7.42 Boundary Conditions for the Revised BWIP Regional Flow Model - Layer 3: Saddle Mountains Basalts**
- Figure 7.43 Boundary Conditions for the Revised BWIP Regional Flow Model - Layer 4: Saturated Ringold, Hanford, and Alluvium**

- Figure 7.44** Percentage of Rainfall Assumed to Recharge Groundwater
- Figure 7.45** Inferred Interbed Boundaries from Myers (1979) and the Model Blocks Modified to Reflect Interbed Influence
- Figure 7.46** Potentiometric Maps for the Grande Ronde Basalts showing Kriged Heads and Model-Predicted Heads for the Initial Simulation of the Revised Model and for the Revised Regional Simulations with and without Interbeds
- Figure 7.47** Potentiometric Maps for the Wanapum Basalts showing Kriged Heads and Model-Predicted Heads for the Initial Simulation of the Revised Model and for the Revised Regional Simulations with and without Interbeds
- Figure 7.48** Potentiometric Maps for the Saddle Mountains Basalts showing Kriged Heads and Model-Predicted Heads for the Initial Simulation of the Revised Model and for the Revised Regional Simulations with and without Interbeds
- Figure 7.49** Location of the Local Scale Model Grid Within the Regional Scale Model Grid

- Figure A.1.1 Vertical Layering for Pasco Basin
Three-Dimensional Model at Well DC-15
- Figure A.1.2 Preliminary Hydrogeologic and Hydrochemical Data
within the Saddle Mountains and Wanapum Basalts
at Borehole DB-15
- Figure A.1.3 Pasco Basin and Hanford Site
- Figure A.1.4 Plan View of Three-Dimensional Finite Element
Network for Pasco Basin
- Figure A.1.5 Potentiometric Map for and Inferred Flow
Directions of Groundwater within the Mabton
Interbed beneath the Hanford Site
- Figure A.1.6 Model-Calculated Heads, Top of Wanapum Basalt
 K_z/K_x from 10^{-2} to 10^{-3}
- Figure A.1.7 Model-Calculated Heads, Top of Wanapum Basalt
 K_z/K_x from 10^{-4} to 10^{-5}
- Figure A.2.1 Typical Vertical Cross Section of the Pasco Basin
(adapted from cross section B-B' in Plate III-11
of Gephart and others, 1979) (from Arnett and
others, 1981)

- Figure A.2.2 Schematic Cross Section showing Generalized Stratigraphy (from Arnett and others, 1981)
- Figure A.2.3 Material Type Distribution for the 2-D Model (from Arnett and others, 1981)
- Figure A.2.4 Plan View of the Pasco Basin Three-Dimensional Finite-Element Network Showing Head Boundary Conditions and Major Rivers (from Arnett and others, 1981)
- Figure A.2.5 Plan View of the Pasco Basin Three-Dimensional Finite-Element Network Showing Recharge and Pumping Areas and Major Rivers (from Arnett and others, 1981)
- Figure A.2.6 Plan View of Two-Dimensional Cross-Section Model (from Arnett and others, 1981)
- Figure A.2.7 Finite-Element Network for the Cross-Section Model (from Arnett and others, 1981)
- Figure A.2.8 Typical Vertical Cross Section of the Pasco Basin Three-Dimensional Finite-Element Network (from Arnett and others, 1981)

- Figure A.2.9 Hydraulic Head Contours at Bottom of Grande Ronde Basalts (from Arnett and others, 1981)
- Figure A.2.10 Hydraulic Head Contours at Top of Grande Ronde Basalts (from Arnett and others, 1981)
- Figure A.2.11 Hydraulic Head Contours at Top of Wanapum Basalts (from Arnett and others, 1981)
- Figure A.2.12 Hydraulic Head Contours at Top of Basalt Sequence (from Arnett and others, 1981)
- Figure A.2.13 X-Z Projection of Model-Calculated Streamline (from Arnett and others, 1981)
- Figure A.2.14 X-Y Projection of Streamlines from Hypothetical Repository to Boundary (from Arnett and others, 1981)
- Figure A.2.15 Head Contours for the Two Dimensional Model (from Arnett and others, 1981)
- Figure A.2.16 Streamline for the Two Dimensional Model (from Arnett and others, 1981)
- Figure A.3.1 Layering Scheme for LATA-RHO-04-02-A Model
- Figure A.4.1 Assumed Regions of Equal Deformation Associated with Structures within the Local Model Area

1982)

Figure A.4.2 Regional Model Boundary (from Dove and others, 1982)

Figure A.4.3 Model Boundaries and Constant Hydraulic Heads for the Saddle Mountains/Wanapum Basalts (Layer 1) (from Dove and others, 1982)

Figure A.4.4 Model Boundaries and Constant Hydraulic Heads for the Grande Ronde Basalts (Layer 2) (from Dove and others, 1982)

Figure A.4.5 Regional and Local (Pasco Basin) Model Boundaries (from Dove and others, 1982)

Figure A.4.6 Finite-Element Grid used in the Pasco Basin Model (from Dove and others, 1982)

Figure A.4.7 Model-Predicted Hydraulic Heads for the Saddle Mountains/ Wanapum Basalts Layer (values are in feet above MSL) (from Dove and others, 1982)

Figure A.4.8 Model-Predicted Hydraulic Heads for the Grande
Ronde Basalts Layer (values are in feet above MSL)
(from Dove and others, 1982)

Figure A.4.9 Flow Directions in the Pasco Basin (from Dove and
others, 1982)

Figure A.4.10 Simulated Hydraulic Heads for the Top of the
Grande Ronde for "Preman Conditions" (values are
in feet above MSL) (from Dove and others, 1982)

Figure A.4.11 Simulated Hydraulic Heads for the Top of the
Grande Ronde for "Current Conditions" (values are
in feet above MSL) (from Dove and others, 1982)

Figure A.4.12 Simulated Hydraulic Heads for the Top of the
Saddle Mountains for "Preman Conditions" (values
are in feet above MSL) (from Dove and others,
1982)

Figure A.4.13 Simulated Hydraulic Heads for the Top of the
Saddle Mountains for "Current Conditions" (values
are in feet above MSL) (from Dove and others,
1982)

Figure A.5.1 Local Scale Model Grid

a) Local Scale Model Layering

b) Relationship Between the Regional and Local
Grids

**Figure A.5.2 Potentiometric Surface for Layers 1,2,3, and 4
for the Run Having the Lowest Error Index
(from Bonano and others, 1986)**

**Figure A.5.3 Potentiometric Surface from the Local Scale
Model in the Flow Tops adjacent to the
Hypothetical Repository, and in a Section
Through the Hypothetical Repository
(from Bonano and others, 1986)**

1. INTRODUCTION

The U.S. Department of Energy (DOE) has identified the Reference Repository Location (RRL) at the Hanford Site, Washington as one of the three potentially acceptable sites for a mined geologic repository for spent nuclear fuel and high-level radioactive waste (HLW). To demonstrate suitability of the site, the DOE will be required to predict travel-times of ground-water and amounts of radionuclides released from the repository to the accessible environment. These predictions will inevitably rely on numerical simulations of the area's ground-water flow system.

In addition, the DOE is using ground-water flow simulations to design and analyze in-situ tests. Thus, in order to implement the appropriate regulations, the U.S. Nuclear Regulatory Commission (NRC) must understand the validity of and uncertainty associated with these simulations. In this report these topics are addressed from two directions. First, a review of published RRL numerical and conceptual models has been performed. Second, and perhaps more important, independent numerical models are being built and maintained for use in evaluating DOE plans and results. The current status of these models is included in this report. In addition, brief discussions of the regional geology, hydrology, and geochemistry are included to provide a framework for the following discussions. These sections are not meant to provide a complete description of these topics but only to cover the most important aspects of the ground-water flow system. For

a more detailed presentation of the geology and hydrology of the BWIP area the reader is referred to the following references. Unfortunately, the geochemistry of the natural ground waters has received much less attention. The few references that deal specifically with geochemistry are discussed in Section 4.

Previous Investigations

A general review of the Pasco Basin hydrology and geology prior to 1972 was done by Newcomb and others (1972). The report contains descriptions of the geologic and hydrologic units in the Pasco Basin and a review of the tectonic history of the area. There is also an extensive discussion of artificial recharge from industrial plants and radioactive waste disposal ponds and cribs. Gephart and others (1979) have summarized existing hydrogeologic reports pertaining to the Pasco Basin with emphasis on the deeper basalt flows. Meyers and others (1979) provided a compilation of borehole studies, geophysical surveys, and tectonic studies. The Site Characterization Report (1982) for BWIP contains a summary of Rockwell Hanford Operations (RHO) head measurements, injection tests, and water samples from wells in the RRL. Guzowski and others (1982) have compiled tables and figures illustrating hydrologic properties and other physical parameters from works prior to 1982. Also included is a discussion of the regional setting, geology, hydrogeology, and geochemistry of the Pasco Basin. Strait and Spane (1982a, 1982b, 1982c, 1982d, 1983) have completed numerous

hydrologic tests of the basalts and interbeds that will be referenced in this analysis. Reports that deal specifically with ground-water flow models are summarized in Section 5 of this report with detailed reviews of these reports provided in Appendix A.

2. GEOLOGY

DRAFT

The geology of the study area must be understood in order to formulate a conceptual model of the ground-water flow system. First of all, the geologic information must be combined with hydrologic data in order to define hydrostratigraphic units which are subsequently combined into model layers or used individually as a model layer. Second, a knowledge of the geology is required to define the areal extent of these units. And finally, inferences about the flow systems hydraulic behavior and transport characteristics are drawn from information on geologic structures and lithologic characteristics of the units. This last point is especially true for the Hanford study area where hydrologic information near geologic structures is lacking.

Following is a brief description of the sites geomorphology, the stratigraphic units, and geologic structures. While these descriptions are brief, they are meant to provide the reader with a framework for understanding the modeling efforts described in the remainder of the report.

2.1. GEOLOGIC SETTING

The RRL is located in the DOE's Hanford Reservation near Richland, Washington and is in the central portion of the Cold Creek Syncline within the Pasco Basin, a structural and topographic basin located in the Columbia Intermontaine Province (Figure 2.1). The area of interest is located in what will be informally referred to herein as the Columbia Plateau. The Columbia Plateau coincides with the distribution of Miocene flood basalts of the Columbia River Basalt Group in the Columbia Intermontaine Province. The Columbia Intermontaine Province is bounded to the west by the Cascade Mountains and to the east and north by the Rocky Mountains. The Columbia Basin subprovince is located in the northern part of the intermontaine province and is a large structural and topographic depression, with the low point (the Pasco Basin) near the location of the RRL. The Pasco Basin has undergone a long cycle of basalt deposition coupled with periods of fluvial erosion and deposition, tectonic activity and glacial activity.

Major surface features in the area include:

- 1) The Columbia River, Umtanum Ridge, Gable Butte, and Gable Mountain to the north;
- 2) Yakima Ridge to the west;
- 3) Rattlesnake Hills to the south;

4) The Columbia River to the east and Yakima River to the south east (Figure 2.2).

The RRL is located in the west-central portion of the Pasco Basin, near the boundary between the Yakima Folds and the Central Plains morphologic sections of the Columbia Intermontaine Province. Shown in Figure 2.3 are the major landform systems of the Pasco Basin. The basin and valley terrain in which the RRL is located consists of low-relief, sediment-filled portions of the Central Plains and synclinal valleys of the Yakima folds.

Four geomorphic units are defined within the RRL (Figure 2.4). The Umtanum Ridge Bar and the 200 Areas Bar are gravel bars formed during catastrophic Pleistocene flooding. The Central Hanford Sand Plain was formed by the deposition of finer grained sediments on the lee side of the Umtanum Ridge Bar. The predominant materials are granules of fine grained sand and silt. Holocene alluvium along Cold Creek is superimposed on the western portion of the Central Hanford Sand Plain and forms the western part of the reference repository location covering about 13 square kilometers.

2.2. STRATIGRAPHY

The major stratigraphic unit present in the Pasco Basin is the Columbia River Basalt Group which is composed of 5 formations with 19 members (Swanson and others, 1979) (Figure 2.5). The Grande Ronde, Wanapum, and Saddle Mountains Basalts crop out in the Pasco Basin area (Figure 2.6). The Imnaha and Picture Gorge Basalts will not be discussed because they do not crop out in the area of interest and because they are located well below the repository level. Interbedded with the basalts are Miocene sediments of the Ellensburg Formation. The basalt sequence is overlain by semi-consolidated to unconsolidated sediments of the Ringold and Hanford Formations and by unconsolidated surficial deposits.

The maximum thickness of the Columbia River Basalt Group, including its interbedded sediments, is approximately 5,000 meters (Mitchell and Bergstrom, 1983). The flood basalts, underlain by metamorphosed sedimentary and volcanic units, were erupted from a series of north-northwest-trending linear vents (e.g., Waters, 1961). Individual flows range in thickness from a few centimeters to approximately 100 meters with most flows ranging from 20 and 40 meters in thickness. The basic disposal concept for the Hanford Site is that the HLW would be placed in a repository that would be excavated from the dense interior of one of the Columbia River Basalt flows. Following is a brief description of each of the major geologic units in the region.

2.2.1. GRANDE RONDE BASALT

The oldest basalt of interest, the Grande Ronde Basalt, was extruded 17 to 15.6 mybp, and is the most areally extensive and voluminous member of the Columbia River Basalt Group. The known thickness ranges from tens of meters along the Plateau margins to over 1,000 meters in the Pasco Basin. The only regional subdivisions [at the scale of the Plateau] are four magnetostratigraphic units (Figure 2.5). However, at a subregional scale, there are a number of flows that blanket areas of at least 250 square kilometers (Long and Landon, 1981). Four of these extensive flows within the Pasco Basin are currently being considered as candidate horizons for the geologic repository.

In the Pasco Basin the Grande Ronde basalt is comprised of at least 56 flows. The basalt is typically fine grained aphyric or sparsely microphyric with few consistent textural differences. Flows are correlated on the basis of magnetostratigraphy and chemical composition. Two informal "through-runner" units identified in the basin are termed the Schwana and Sentinel Bluffs sequences. Four flows in the Grande Ronde have been identified as potential candidate horizons: the Umtanum Flow of the Schwana Sequence and the McCoy Canyon, Cohasset and Rocky Coulee Flows of the Sentinel Bluffs Sequence (Figure 2.7).

2.2.1.1. UMTANUM FLOW

The Umtanum flow is the lowermost candidate horizon; the top of the flow ranges from 1059 to 1135 meters below ground surface in the RRL. The Umtanum appears to be thicker to the northwest and southeast of the RRL than at the center of the Cold Creek Syncline. In the RRL, the Umtanum varies in thickness, ranging from about 60 to 70 meters (Figure 2.8). The dense interior of the flow also varies in thickness (Figure 2.9), but appears everywhere to be greater than 24 meters, based on current borehole information. Within the RRL the brecciated flow top appears to be quite thick and highly variable, similar to the exposed section at Emerson Nipple where the anomalously thick flow top is 40 meters thick which is 50 percent of the flow (DOE, 1982). This thick flow top is particularly evident in borehole RRL-2.

2.2.1.2. McCoy CANYON FLOW

The McCoy Canyon flow is the lowermost of the Sentinel Bluffs flows; the top of the flow ranges from 1025 to 1090 meters below ground surface. The flow generally thins from northwest to southeast, ranging from about 34 meters to 45 meters thick across the RRL (Figure 2.10). Intraflow entablature and colonnade structures have a total thickness of about 30 meters for the dense interior across the RRL (Figure 2.11). The dense

interior, however, has sporadic vesicular zones that reduce the potential volume available for a repository.

2.2.1.3. COHASSETT FLOW

The Cohasset flow is stratigraphically near the middle of the Sentinel Bluffs sequence (Figure 2.12) and the top of the flow is 896 to 943 meters below the ground surface. The flow is thickest in central Pasco Basin thinning southeasterly and is consistently about 80 meters thick (Figure 2.13). Although the Cohasset flow is the thickest candidate flow within the RRL, the multi-layered entablature/colonnade structures cannot be correlated from borehole to borehole. A laterally continuous vesicular zone ranging from 3 to 8.5 meters in thickness, located about 30 meters from the top of the flow, divides the dense interior into an upper and a lower zone (Figure 2.14 and 2.15). The dense interior below the vesicular zone ranges from 36 to 46 meters in thickness.

2.2.1.4. ROCKY COULEE FLOW

The Rocky Coulee flow, the uppermost candidate horizon, occurs in the upper third of the Sentinel Bluffs Sequence. This flow thins from about 55 meters to about 43 meters in thickness from west to east across the RRL (Figure 2.16). The dense interior of the flow ranges in thickness from 27 to 47 meters and thins significantly to the northwest across the RRL as a result of vesiculation beneath the flow top (Figure 2.17).

2.2.2. WANAPUM BASALT

The Grande Ronde Basalt is unconformably overlain by the Wanapum Basalt and within the Pasco Basin, the Wanapum Basalt consists of three members: Frenchmen Springs, Roza, and Priest Rapids. The Vantage interbed separates the formation from the underlying Grande Ronde. The Mabton interbed separates the formation from the overlying Saddle Mountains Basalt. The total thickness of the Wanapum Basalt in the RRL is about 335 meters. Because these basalts are not being considered as for the location of a repository, isopach maps are not included.

2.2.2.1. FRENCHMAN SPRINGS MEMBER

The Frenchman Springs is the oldest Wanapum member and consists of 7 to 9 flows (lobes) within the Cold Creek syncline. These flows cannot be consistently correlated from hole to hole. In the RRL, the Frenchman Springs is about 215 meters thick but thins abruptly onto the Rattlesnake Mountain structure south of the Cold Creek Syncline.

2.2.2.2. ROZA MEMBER

The Roza Member is comprised of one to two flows in the RRL where it is about 53 meters thick. The Roza thins across

Rattlesnake Mountain and the Umtanum Ridge-Gable Mountain structure.

2.2.2.3. PRIEST RAPIDS MEMBER

The Priest Rapids Member consists of the Rosalia and Lolo flows, which appear to be present throughout the Cold Creek syncline. The Priest Rapids is about 46 meters thick in the RRL, but thins across the Rattlesnake Mountain and Umtanum Ridge-Gable Mountain structures.

2.2.3. SADDLE MOUNTAINS BASALT

The youngest formation of the Columbia River Basalt Group is the Saddle Mountains Basalt which has been divided into at least 10 members (Figure 2.5). In the RRL, the Saddle Mountains Basalt is represented by four members: Umatilla, Esquatzel, Pomona, and Elephant Mountain Members. The extrusion period 13.5 to 6 mybp, was characterized by declining volcanism, the deposition of interbedded sediments (Ellensburg Formation), folding, and canyon cutting.

2.2.3.1. UMATILLA MEMBER

The Umatilla Member consists of the Sillusi and Umatilla flows, which together total about 70 meters thickness in the RRL. The member is wedge-shaped, thins to the north, and pinches out

north of the Umtanum Ridge-Gable Mountain structure and east of the Cold Creek syncline.

2.2.3.2. ESQUATZEL MEMBER

The Esquatzel Member consists of one to two flows or flow lobes, locally separated by a vitric tuff. The total thickness of this member in the RRL is about 70 meters. The member is confined to the southern and eastern parts of the Pasco Basin, pinching out on the Rattlesnake Mountain and Umtanum Ridge-Gable Mountain structures.

2.2.3.3. POMONA MEMBER

The Pomona Member is represented by only one flow in the Pasco Basin at the RRL and is approximately 80 meters thick. As with the other members of the Saddle Mountains Basalt, the Pomona thins over the anticlinal structures that bound the Cold Creek syncline.

2.2.3.4. ELEPHANT MOUNTAIN MEMBER

Within the Pasco Basin the Elephant Mountain Member consists of two flows but in the RRL only the lower Elephant Mountain flow is present and is about 25 meters thick. The member is thickest in the eastern part of the Cold Creek syncline, thinning both toward the Rattlesnake Mountain anticline and to the northwest

of the syncline. The Elephant Mountain Member defines the top-of-basalt over most of the Cold Creek syncline on the Hanford reservation.

2.2.4. ELLENSBURG FORMATION

The Ellensburg Formation is a Miocene fluvial sequence with volcanoclastic sediments. It is interbedded primarily with the Wanapum and Saddle Mountains Basalts. There are two distinct lithologies, representing two distinct provenances: volcanoclastic sediments derived from the Cascade Range and clastic plutonic and metamorphic sediments from the Rocky Mountains. The volcanoclastic sediments were deposited as ashfalls and fluvial sediments and the clastics from the Rocky Mountains were deposited by westward flowing fluvial systems. Nomenclature of the Ellensburg Formation is given in Figure 2.18.

2.2.5. RINGOLD FORMATION

The Columbia River Basalt Group (and interbedded Ellensburg Formation) is overlain over most of the Pasco Basin by the Ringold Formation (figure 2.18). The Ringold formation is predominantly fluvial sediments with some lacustrine and fanglomerate facies (Figure 2.19). Within the RRL, the Ringold Formation ranges from 105 to 215 meters in thickness.

Within the RRL the Ringold unconformably overlies the Elephant Mountain Member of the Saddle Mountains Basalt. The basal Ringold represents a fluvial environment, being finer grained toward the top of the unit, and is capped by a paleosol formed on the fine grained uppermost materials of the cycle. Laminated silt and clay of the lower Ringold disconformably overlie the basal Ringold paleosol. Up to several meters of local erosional relief separate the sandy gravels (with some intercalated sand and mud) of the middle Ringold from the lower Ringold. The upper Ringold, bedded and laminated sand and mud, conformably overlies the middle Ringold. An incised paleochannel occurs in the Ringold across the RRL (Figure 2.20). The variation in thickness of the formation probably is due to erosion.

2.2.6. PLIO-PLEISTOCENE UNIT

The Ringold Formation is unconformably overlain across the RRL by a Plio-Pleistocene unit that consists of a fanglomerate and a paleosol. The fanglomerate represents mass wastage of material from the surrounding ridges. The fanglomerate is thickest (up to 24 meters) beneath the Cold Creek Valley which thins and becomes fine to the northeast, where it grades into a paleosol formed after the incision of the Ringold.

2.2.7. HANFORD FORMATION

Catastrophic late Pleistocene floods deposited coarse-grained (Pasco Gravels) and fine-grained (Touchet Beds) facies across much of the Pasco Basin. The gravels are present at the Umtanum Ridge Bar and its extension, the 200 Areas Bar (see figure 2.4). Slackwater facies were deposited away from the gravel bars and are most common in the southern and western parts of the RRL and beneath the gravels of the 200 Areas Bar.

2.3. REGIONAL GEOLOGIC STRUCTURES

The Pasco Basin is located along the eastern margin of the Yakima Fold Belt. Structures in the area are characterized by long, narrow anticlines and broad synclines trending generally eastward from the western part of the Columbia Plateau to the Pasco Basin, where they die out (Figure 2.21). Most of the major faulting is associated with the anticlinal folds. Most of the faults are reverse faults (including thrust faults) that are parallel or subparallel to the axial planes of the anticlines. These faults are likely to have formed during the deformation that resulted in the folding. Structural relief on the anticlinal basalt ridges is up to approximately 1200 meters while the wavelengths of the folds are typically 5 to 10 kilometers. Anticlines are typically concentric, gentle to tight and upright to inclined. The tighter, inclined folds are usually asymmetric, with the steep limb approaching vertical or, in some cases, overturned. The asymmetric folds usually converge to the north.

Significant characteristics of major structures in the Pasco Basin are summarized below.

2.3.1. WAHLUKE SYNCLINE

The Wahluke Syncline is a broad (up to 13 kilometers wide), asymmetric trough lying between the Saddle Mountains and the Umtanum Ridge-Gable Mountain. The southern limb is steeper than the northern limb. In the lowest part of the syncline, the top-of-basalt is approximately 61 meters below mean sea level.

2.3.2. UMTANUM RIDGE-GABLE MOUNTAIN STRUCTURE

This eastward-trending structure extends 110 kilometers from Ellensburg, Washington, to Gable Mountain. Within the Pasco Basin, the anticline is flanked by the Wahluke syncline to the north and the Cold Creek syncline to the south. Maximum structural relief is approximately 880 meters. The eastern Umtanum Ridge segment is a complex structure characterized by an asymmetric, overturned, eastward-plunging anticline with crestral surface splinters forming several en echelon folds along trend. Structural relief and complexity decrease toward the center of the Pasco Basin, where the structure appears to be an asymmetric, eastward-plunging anticline with a steeply dipping north limb. Thrust faulting within this anticline is observed

in the Priest Rapids Dam area to the west is believed to die out as structural relief decreases to the east.

Gable Mountain and Gable Butte are surface expressions of several eastward-trending, second-order anticlines and synclines that represent a structural segment of the large, first-order northward-trending anticline. Three significant eastward-trending reverse faults and one north-trending normal fault have been described at Gable Mountain. These tear faults are associated with second-order folds, and therefore are likely to have lengths of about 1.6 kilometers or less. Fractures in fluvioglacial sediments are continuous with the reverse faults in the underlying basalts.

2.3.3. COLD CREEK SYNCLINE

The Cold Creek syncline is a broad, open, asymmetric, eastward-plunging, almost flat-bottomed syncline between the Umtanum Ridge-Gable Mountain structure and the Yakima Ridge structure. The proposed repository location is within this syncline.

2.3.4. YAKIMA RIDGE STRUCTURE

A group of topographic ridges are the surface expression of the plunging anticlines, monoclines and faults that comprise the Yakima Ridge Structure. Within the Pasco Basin, the dominant

structure is a northward-trending asymmetric, southeastward-plunging anticline (Cairn Hope Peak anticline), whose southern flank includes two monoclines, one of which may extend into a major fault zone of uncertain geometry (Silver Dollar fault). The major structure plunges into the basin as a series of second-order folds probably associated with reverse faults. There is a buried structural high along the trend of the Yakima Ridge structure to the southeast of the surface expressions. A saddle or shallow syncline with possible faulting is believed to separate the two segments.

2.3.5. BENSON RANCH SYNCLINE

The shallow Benson Ranch syncline lies between the Yakima Ridge and the Rattlesnake Hills structures on the western side of the Pasco Basin. The syncline plunges to the east and apparently dies out toward the Wye Barricade depression.

2.3.6. PASCO SYNCLINE

The Pasco syncline is a broad, low amplitude depression with a sinuous trend to the southeast part of the Pasco Basin. Overall the syncline plunges to the north, dying out against the Wye Barricade depression.

2.3.7. CLE ELUM - WALLULA ALIGNMENT

The Cle Elum - Wallula lineament is a 200 kilometer - long, 40 kilometer - wide deformed belt that parallels the western and southern boundaries of the Pasco Basin. Along the southwestern boundary of the basin, the Rattlesnake Hills - Rattlesnake Mountain segment is a major anticlinal structure. Geomorphic continuity along strike to Wallula Gap is considered to reflect continuity of deformation, probably as a right lateral strike slip or oblique slip fault.

2.4. INTERNAL BASALT STRUCTURES

Internal structures associated with lava movement and cooling are termed "intraflow structures" (DOE, 1984). Particularly important are the cooling joints that produce polygonal columns and hackly blocks. In general, three major intraflow structures are recognized: vesicular or brecciated flow tops; irregular and discontinuously jointed entablature near the middle of a flow; and more regularly jointed colonnade near the bottom of the flow (Figure 2.22). The bottoms of flows are typically thin (approximately 0.5 meter) zones of fractured, glassy basalt. The three major intraflow structures may vary in thickness, be absent from a given flow, or occur repeatedly within a single flow. The orientation of joints and fractures is typically nearly vertical, but occasionally approach horizontal. Radiating columnar joints have been observed in surface exposures of basalt flows. Limited core data indicate that secondary mineralization occurs in most fractures.

3. HYDROLOGY

The Pasco Basin hydrologic system consists of four parts:

- Surface waters
- Unsaturated (vadose) zone
- Unconfined system
- Confined system

The proposed repository location is in the confined ground-water flow system which is made up of the deeper basalts and associated interbeds. These units are the focus of this report. The surface waters and vadose zone will be discussed only in the context of discharge and recharge to the ground-water system. The unconfined system which occurs primarily in fluvial and lacustrine sediments and locally in basalts serves both as a place of discharge of water from the basalts and, in some locations, provides recharge to the basalts.

3.1. SURFACE WATER

Surface water is both a source of water to the ground-water system in some areas and location of ground-water discharge in

others. Therefore, any discussion of the ground-water flow system must include information on the surface water system.

Because the Pasco Basin is one of the lowest basins in the intermontaine region, and because it is contiguous to several higher basins, all surface drainage from upper basins passes through it. Several large rivers flow through the basin. The largest, the Columbia River, enters the basin in the northwest region at an elevation of 480 feet at Priest Rapids Dam, flows easterly along the north-central part of the basin, turns abruptly south and flows in a southerly direction along the eastern boundary of the basin. Near the southern boundary the river changes direction again and flows west-southwest and exits the basin at an elevation of 260 feet. In the Pasco Basin the Columbia River has three perennial tributaries (see Figure 2.1): The Yakima River, the Snake River, and the Walla Walla River. The Yakima River flows easterly across the central basin and into the Columbia below the city of Richland, Washington. Below the Yakima-Columbia confluence, the Snake and Walla Walla Rivers enter from the east. Note that even though a large amount of surface water flows through the Pasco Basin, no perennial streams originate in the basin.

Only one small natural lake (about 10 acres) occurs in the basin in a topographic low near an anticlinal axis (Gephart and others, 1979). There are, however, several waste-water ponds associated with reactors and industrial and municipal activities.

Mean annual precipitation in the Pasco Basin ranges from less than 7 inches (18 centimeters) in the low areas to about 15 inches (38 centimeters) on Rattlesnake Mountain south of the RRL. Average total precipitation for the whole basin is about 800,000 acre feet with only about 25,000 acre feet of runoff.

3.2. GROUND WATER

All studies of ground-water flow systems are preceded by and integrated with the development of conceptual ground-water flow models. Therefore, this section begins with a general definition of conceptual models. Following that is a discussion of recharge and discharge in the Pasco Basin region, a description of the region's hydrostratigraphic units, and some general comments on the movement of water in the region.

3.2.1. DEFINITION AND EXAMPLES OF CONCEPTUAL MODELS

Ground-water flow is controlled by the complex geometry of the pores of the geologic media and the amount and location of water entering and leaving the rocks. However, direct measurement of the pore geometries is impossible. In addition, finding and measuring all of the recharge and discharge is nearly impossible. Thus, conceptual models are merely the simplifications and assumptions we use to understand ground-water flow.

In building a conceptual model, we generally begin by assuming that a certain rock layer or group of layers has distinct hydrologic characteristics which are the result of the pore geometries within that layer. We then attempt to measure the properties of this layer(s) as a function of space and in some cases, time. In addition, we attempt to define the limits of this layer and any discontinuities within this layer. This layer or group of layers is generally referred to as a hydrostratigraphic unit. The definition of a hydrostratigraphic unit is ultimately dependent on the purpose of the model. For example, lumping of many geologic layers into one hydrostratigraphic unit may be acceptable if the purpose is to predict hydraulic responses over large regions. However, the same lumping may be inappropriate for attempting to define the path that a given tracer follows through the rock layers. Note that the term aquifer is a special case of a hydrostratigraphic unit which yields significant quantities of water to wells. After defining the hydrostratigraphic layers, the amount and location of flux into or out of them (that is, the recharge and discharge) must be estimated. Generally, recharge and discharge are treated by dividing the flow system into regions within which the recharge or discharge is assumed to be constant.

Examples of two conceptual models are provided in the following sections. Note that, as with the definition of a hydrostratigraphic layer, the formulation of an overall conceptual model depends both on the type and the scale of the problem being addressed.

For the first example, take the problem of trying to predict the future response of an aquifer to pumping. We can not measure the geometry of all the pores that water moves through to get to the pumping well along with the geometry of all the aquifer boundaries and the sources and discharges of water to the aquifer . Instead, we assume ideal geometries and boundary conditions for the aquifer (in other words, we form a conceptual model of the system). Hopefully, these idealizations are derived from knowledge of the site geology. Then, to cause a hydraulic response within the system the well is pumped for a short time and the change in water level in the wells and/or in nearby wells is measured as a function of distance and/or time. The pumping rate is then related to the response through a empirical coefficient called the aquifer diffusivity (hydraulic conductivity times the aquifer thickness divided by the storativity). This parameter is subsequently used along with a specified pumping rate to predict the future behavior of the aquifer. This "coefficient" is only relevant for the conceptual model for which it was measured. In fact, only predictions of aquifer response to the same magnitude of stress applied at that well for the same length of time will be accurate. For larger pumping rates or longer pumping times, the degree to which the response can be predicted will be dependent on the accuracy of the conceptual model.

Now take the example of predicting ground-water travel times from a proposed repository to the accessible environment. Here, at least two conceptual models are required, one to provide a framework for a model of the flow system used to predict ground-water travel time and one for designing and analyzing tests needed to obtain the parameters for the travel-time model. The need for the separate models arises from the fact that neither the time nor the resources are available for directly testing the flow system at the required space and time scales. Therefore, small regions within the system are tested to obtain parameters. These regions generally do not display all of the complexities of the flow system, thus conceptual models of them are much simpler. For example, the flow system is always heterogeneous but parameter tests may only sample only small homogeneous regions of the system. In practice, more than two conceptual models are applied. First, a conceptual framework for the travel-time model is defined from in-situ geologic and hydrologic evidence. This model consists of the definition of the hydrostratigraphic units, including their boundaries, the expected interaction between them, and their regions of recharge and discharge. Another conceptual model, similar to the one described in the above section, is then formulated to design and analyze tests that measure the

hydraulic parameters of transmissivity and storativity. In almost all of the tests performed to date at BWIP, a laterally unbounded, homogeneous, isotropic porous media has been assumed for the conceptual model of each hydrostratigraphic unit. An extension of the previous conceptual model is then used to design and analyze a test for the effective thickness (the percentage of the rock through which water flows multiplied by the thickness of the tested interval). In many cases, the conceptual model for these tests is basically the same as it is for the hydraulic tests. In the case of BWIP, the same laterally unbounded, homogeneous, isotropic porous media has been assumed. However, additional assumptions concerning the interaction between the water, rock, and the injected tracer must be made. These tests produce values which are valid only for the flow path between the two wells used in the test. They are also strictly valid only for the same hydraulic conditions imposed during the test and for the particular tracers used in the test but these transport parameters are extended to the travel time model just as the hydraulic parameters are.

Next, in addition to the hydraulic parameters and the effective thickness, some measurement of the driving forces is needed to arrive at ground water velocities and therefore, travel times. If all of the boundaries of the travel-time model were identified and they all were within a distance that could reasonably be modeled, then only the amount and distribution of recharge and the location and hydraulic character of discharge

areas would be needed. Unfortunately, the limits of the numerical model used to calculate the travel time can not always be extended to coincide with the limits of the hydrostratigraphic units. Sometimes, this results from a lack of knowledge as to the extent of the units and other times extension of the model would incorporate phenomena which would greatly complicate the modeling effort. Consequently, some model boundaries will not coincide with the physical boundaries of the units and additional assumptions must be made concerning the boundaries. In many cases information about the hydraulic potentials is used to imply either constant potential or no-flux boundaries. Note, however, that measurement of the potentials still requires a conceptual model that is consistent with the model of the flow system. At a minimum, the measured zone must correspond to the hydrostratigraphic unit. While this may sound trivial, researchers modeling the BWIP site have had to rely on measurements taken from test intervals that are larger and/or smaller than the defined hydrostratigraphic units.

3.2.2. FACTORS CONTROLLING GROUND-WATER FLOW IN BASALTS

Ground-Water Flow in an Undisturbed Basalt Flow

As noted in early USGS investigations of the site (LaSala and Doty, 1971 and LaSala and others, 1973), undisturbed basalt has

a very limited ability to transmit water. In comparing field measurements of hydraulic conductivities with laboratory measurements from intact cores of basalt they observed that the core samples always had lower values of conductivity. From this, they concluded that fracturing of the basalts was responsible for the larger field values. They also noted that the flow contact zones were able to transmit larger quantities of water than the dense interiors. Thus, it appears that two basic types of fracturing control water flow through a single intact basalt layer. The first being the fracturing that occurs along the upper and lower surfaces of a lava flow during deposition, while the second type results from the cooling of the lava flow (see figure 2.22). The two types of fracturing are very different in character.

Fracturing near the flow contacts (i.e., the flow tops and bottoms) is very extensive with no apparent preferred orientation. However, many of these fractures have been found to be filled with weathering products of the basalt. This results in most of the ground-water being transmitted through zones within a given flow top which may be much thinner than the total thickness of the flow top.

On the other hand, fractures formed during cooling of the flow are generally vertical and form relatively large evenly spaced hexagonal blocks. The relatively large spacing between fractures may be the reason that these zones transmit much less

water than the flow tops and bottoms. Also, the preferred orientation of these fractures may result in a more direct vertical path for the water. In theory, a particle of water would have to travel about two to three times longer along a horizontal path to travel the same overall distance as it would along the vertical path (DOE, 1982 and 1984). Just as in the flow contact fractures, most of these fractures have been observed to be filled with clays from the weathering of the basalts. While this may impede water flow, the relative permeability of these fractures is probably still much larger than that of the dense basalt.

To date, the zones defined by the two types of fracturing (the flow tops/flow bottoms and the dense interiors) are the smallest hydrostratigraphic units that have been defined by BWIP investigators. In nearly all investigations, these zones have been assumed to behave as equivalent porous media. That is, flow is assumed to obey Darcy's law. Justification for this assumption has been based on arguments about the frequency of fractures relative to the size of the domain of interest, where the domain of interest is on the order of meters for stress tests and 100's to 1000's of meters for elements of flow models. In addition, responses of these zones to hydraulic stresses have been interpreted as being consistent with responses that are characteristic of porous media. However, these arguments have been based almost solely on the hydraulic behavior of the units not on their ability to transport

contaminates. It is easy to conceptualize a system that behaves hydrologically like a porous medium but whose transport characteristics are dominated by fractures. Therefore, it is impossible to conclude that the assumption of the porous media behavior for the flow tops and interiors is correct.

Effects of Geologic Structures on Ground-Water Flow

Major faulting in the Pasco Basin region is associated with anticlinal structures. Less extensive faulting is also known to occur along synclines and perhaps monoclines. Currently no direct hydraulic tests along or across known major faults have been performed. Hopefully, future BWIP studies will include direct testing of the hydraulic characteristics of these faults. Unfortunately, the smaller scale faults will be difficult to identify, let alone directly test. This is because the faults are generally oriented vertically and the separation distance between them may be on the order of 10's to 100's of meters. Thus, the probability of encountering a fault in BWIP's drill and test program is very small. While a few of these faults have been encountered and tested (DOE, 1984), implications regarding their effect on local and regional ground-water flow must be made by indirect evidence such as ground water chemistry or the results of large scale hydraulic stress tests.

Available evidence indicates that faults can act as either barriers or conduits for ground-water flow. One hydraulic test was performed on a suspected fault or fracture zone by Strait and Spane (1983). This test indicated that the fault has a relatively large hydraulic conductivity. On the other hand, Newcomb (1959) described the presence of structural "barriers" to ground-water flow in the Columbia basalts. Because of their generally vertical orientation, the major effect of low conductivity faults is probably to impede lateral flow while faults of high conductivity probably increase vertical flow more than they increase horizontal flow. Also, a fault that serves as both a lateral impediment and a vertical conduit is imaginable. This fault would consist of clayey fault gouge along the fracture plane and a rubble zone on either or both sides of the plane.

One remaining issue is whether or not the faults cause the hydrostratigraphic units to act hydraulically as a fractured media, or whether they are spaced closely enough to allow the units to be treated as a porous media. Another possible complication would be if the faults vertically connect different hydrostratigraphic units, say two flow tops. If this happens frequently enough, then one may want to define a new hydrostratigraphic unit which includes both flow tops. Hopefully, these issues will be resolved by the proposed large-scale hydrologic testing.

Ground-water Flow in Interbeds

In the study area, the basalt flows are interbedded with sediments that consist of silts and clays with intermittent sand and gravel lenses. The interbeds are thickest in the center of the Pasco Basin and thin toward the basin margin. Also, the percentage of sedimentary interbeds (Gephart and others, 1979) decreases with depth. These interbeds can form highly permeable or nearly impermeable layers. Therefore, they are similar to tectonically undisturbed flow tops and flow interiors. Several important differences should be mentioned, however. First, of course, is that there is little question that the interbeds behave as a porous media. Second, and perhaps most important, the interbeds appear to be continuous over much larger regions than individual basalt flows. Third, ground-water flow is probably more evenly distributed vertically across an interbed than it is across a flow top or flow interior. Thus, a small offset along a fault may not affect horizontal ground-water flow in an interbed but might significantly retard flow in a flow top where the contributing interval may be less than a meter thick. Finally, vertical flow through interbeds is probably not affected by minor faults. In general then, the interbeds probably act as horizontal conduits for and impediments to ground-water flow within the upper basalts in the Pasco Basin. Ground-water movement in the Pasco Basin occurs in the alluvium and in the dense interiors, flow contacts, and interbeds of the basalt flows. An unconfined system exists in the Pasco Basin

and is made up of the alluvium and the upper Saddle Mountains basalts where there is no overlying confining material. A confined system exists throughout most of the Columbia Plateau and consists of the Saddle Mountains, Wanapum, and Grande Ronde Basalts. The confined system is made up of many interbeds and flow tops separated by dense interior units that may act as confining beds.

3.2.3. DEFINITION AND PROPERTIES OF BWIP HYDROSTRATIGRAPHIC UNITS

Following is a description of the hydrostratigraphic units that have been defined in the Pasco Basin region. These descriptions include the units' hydraulic properties as well as their areal extent and variability. These units could also be combined in various ways to form other hydrostratigraphic units.

3.2.3.1. ALLUVIUM

Definition and Geometry

The alluvial aquifer is made up of the Ringold Formation, the Hanford Formation, and associated supra-basalt sediments (see

sections 2.2.5, 2.2.6, and 2.2.7). The lateral boundaries of this unconfined aquifer include the Saddle Mountains to the north, Umtanum and Yakima Ridges on the west, Rattlesnake and Horseheaven Hills on the south and a broad monocline on the east. The bottom boundary is a thick relatively impervious extensive layer of silts and clays at the base of the Hanford Formation above the Saddle Mountains Basalts. The alluvial aquifer is unconfined and ranges in thickness from 0, along the edges of the basin, to 250 feet thick along the eastern edge of the repository site.

Hydrologic Parameters

In the Pasco Basin the storativity, transmissivity, and horizontal hydraulic conductivity of the alluvial aquifer have been tested for. Within the Hanford Reservation these parameters have been derived from aquifer tests. Outside the reservation, parameters have been estimated from production tests on irrigation wells. Gephart and others (1979) and Guzowski and others (1982) have compiled lists of calculated hydraulic conductivities, transmissivities, and storativities for the unconfined unit. The reader is referred to Table III-14 in Gephart and others (1979) for a more complete table with comments on the duration of the tests, well construction and imposed stresses on the system. In addition, Guzowski and others (1982), in their Appendices A and B, provide two

extensive tables listing hydraulic conductivities, transmissivities, and their sources of information.

Listed in Table 3.1 are representative hydraulic parameters of the alluvium in the Hanford region. Most hydrologic parameters listed in Table 3.1 indicate a difference between the Hanford and Middle Ringold Formations. The Hanford Formation has a hydraulic conductivity ranging from 500 feet/day to 20,000 feet/day, the undifferentiated Hanford and Middle Ringold unit has a range from 100 ft/day to 7,000 feet/day, the Middle Ringold unit ranges from 20 feet/day to 600 feet/day, and the Lower Ringold unit has a significantly lower range of .1 to 10 feet/day (Gephart and others, 1979). A plot from Gephart and others (1979) indicating a correlation between hydraulic conductivity and geologic units is shown in Figure 3.4. Throughout the area the specific yield has been estimated to range from .01 to .1.

Outside of the Hanford site, hydraulic data have been obtained from production tests on irrigation wells. Gephart and others (1979, see Tables III-15 and III-16) list specific capacity test results. The specific capacity of a well is defined as the pumping rate divided by the drawdown which yields estimates of aquifer transmissivity. Generally, high specific capacities indicate high transmissivities. The data indicate that north of Gable Mountain and Gable Butte, the transmissivities range from 4,000 to 25,000 ft²/day and on the flanks of Gable Mountain

and Gable Butte the transmissivities range from 40,000 to 600,000 ft²/day. In other areas, transmissivities range from 2,000 to 40,000 ft²/day. However, these values are questionable because of the questionable assumptions used in this type of test analysis (especially the assumption of constant pumping rates) and because the lack of information about the completion of the wells.

3.2.3.2. BASALTS

Ground-water flow below the alluvial aquifer occurs in the dense interiors, flow contacts, and interbeds of the basalt flows of the Columbia River Basalts. The basalts have been grouped into five formations including the Saddle Mountains, the Wanapum, the Grande Ronde, the Imnaha, and Picture Gorge Basalts. Unfortunately, no hydrologic information has been obtained on the deepest units, the Imnaha and the Picture Gorge Basalts, in the Pasco Basin area. Therefore, their effect on the ground-water flow system in this region is currently unknown. The following discussions will focus on the remaining units.

3.2.3.2.1. SADDLE MOUNTAINS BASALTS

Definition and Geometry

The Saddle Mountains Basalt is the shallowest of the Columbia Basalts and is therefore, hydrologically, the best understood. It consists of numerous basalt flows and four sedimentary interbeds. Of these four, the hydrology of the Mabton interbed, which is at the bottom of the Saddle Mountains, has been the subject of the most study. The Saddle Mountains Basalts extend throughout the Pasco Basin but thin toward the west and disappear in areas west and northwest of the basin. This unit is also discontinuous across several of the major structures in the region and is dissected by the Columbia River in many locations.

Hydraulic Properties

Measurements of hydraulic parameters of the Saddle Mountains basalts have concentrated on the interbeds and interflows. Horizontal hydraulic conductivity for the interbeds ranges from 10^{-6} ft/s to 10^{-3} ft/s and 10^{-5} ft/s to 10^{-2} ft/s for interflows (Guzowski and others, 1982). DOE's Draft Environmental Assessment (DOE, 1984) reports that the range of measured conductivities for interflows and interbeds of both the Saddle Mountains and the Wanapum Basalts is from 10^{-7} to 10^{-4} m/s (10^{-7} to 10^{-4} ft/s). Because of the lack of observation well data in the Saddle Mountains Basalt very few

measurements of the storage coefficient have been made. Gephart and others (1979) have estimated that the storage coefficient for this unit in the Hanford area ranges from about 1.0×10^{-5} to 1.0×10^{-3} .

Guzowski and others (1982) estimated a range of porosity for basalts based on histograms compiled from laboratory data on Hanford and other basalts. This range was 0-40 per cent for total porosity (the volume percentage of void space) and 0 - 2.5 percent for the effective porosity (the void space through which flow can occur). DOE (1982 p. 5.2-3) estimated the range of effective porosity for flow tops to be less than 5 percent and for entablature/colonnade to be less than 1 percent. However, these values are based mainly on laboratory measurements which do not provide accurate estimates of the in-situ effective porosity.

3.2.3.3. WANAPUM BASALTS

Definition and Geometry

The Wanapum Basalts extend over the entire Pasco Basin and well beyond in all areas except the extreme northwest. They are dissected by a few of the major faults and by the Columbia River just below Priest Rapids dam. The top part of the unit is

dissected by the Columbia River in several locations. Ground-water flow in this layer occurs primarily in the flow tops. The only significant interbed in this layer is the Vantage. The Vantage is only present locally at the base of the Wanapum and is relatively thin. The Priest Rapids Member and the Frenchman Springs Member have flow tops that produce large quantities of water from the upper and lower parts of the Wanapum, respectively. DOE (1982) reported that the Priest Rapids has produced from 63,000 gal/min to 128,000 gal/min in irrigation wells outside the Pasco Basin and the same potential yields exist within the basin.

Hydraulic Properties

Guzowski and others (1982) report a range of horizontal hydraulic conductivities for the Priest Rapids flow top from 2.8×10^{-3} ft/d to 1.3×10^4 ft/d (10^{-8} ft/s to 10^{-1} ft/s) and a range of 10^{-6} ft/d to 10^{-2} ft/d for the Frenchman Springs interflow. They also state that interbeds of the Wanapum Basalts have a range of hydraulic conductivities from 10^{-6} ft/s to 10^{-4} ft/s. Transmissivities of the Wanapum Basalts have been estimated from specific capacity tests of irrigation wells. Using these tests, Gephart and others (1979) have estimated the range of transmissivity to be from 3 ft²/day to 2400 ft²/day.

In the Pasco Basin, a storage coefficient for the Wanapum basalts has been estimated from testing at DC-1 to be from 6.3×10^{-4} to 1.8×10^{-3} (Gephart and others, 1979). Lower storage coefficients are probably characteristic of columnar basalts which are denser and hydraulically tighter.

3.2.3.4. GRANDE RONDE BASALTS

Definition and Geometry

Less is known about this unit than those previously described because of its depth and the resulting paucity of well data. The major differences between this unit and the overlying basalt units is its areal extent and the relative lack of sedimentary interbeds. This unit extends over and well beyond the Pasco Basin. Unlike the other basalts, the unit is not dissected by any of the geologic structures in the basin. There is a point, however, below Priest Rapids dam where the Columbia River cuts into the top of this unit.

Hydraulic Parameters

Before 1960, most hydrologic testing was done in water supply wells in the Ringold and Hanford Formations. Thus, little was

known about any of the Basalts, especially the Grande Ronde. In the mid 1960's, a drill-stem test was conducted in the Grande Ronde and pre-Grande Ronde rocks in well RSH-1. Seven 76-foot long intervals were tested. Hydraulic conductivities and hydraulic heads were estimated from flow data and shut-in pressure data (DOE, 1982). Borehole RSH-1 was re-tested by Gephart and others (1979) with 11 additional production and injection tests that were conducted opposite specific zones. In December, 1979 and January, 1982, two recirculating ground-water tracer experiments were conducted on a deep basalt flow top, the McCoy Canyon (Leonhart and others, 1984). Since 1979 many aquifer tests have been performed at the Hanford site. Hydrologic tests of the Umtanum basalt entablature, fracture zone, and flow top and the Middle Sentinel Bluffs vesicular zone, flow bottom, and colonnade/entablature were performed in borehole RRL-2 in late 1982 and early 1983 (Strait and Spane, 1982a, 1982b, 1982c, 1982d, and 1982e and 1983). Table 3.2 is a summary of the preliminary interpretations of the results of these tests.

Reported horizontal hydraulic conductivity for the basalt flow interiors in the Grande Ronde range from 10^{-10} ft/day to 10^{-3} ft/day (Guzowski and others 1982). Deju and Fecht (1979) report a conductivity for an interbed in the Grande Ronde of 10^{-8} ft/s. Reported ranges of interflow conductivities are 10^{-4} to 1 ft/day (DOE 1984) and 10^{-7} to 10^{-1} ft/day (Guzowski and others 1982). A vertical hydraulic conductivity

test on the Rocky Coulee flow interior at DC-4/5 indicated a conductivity of less than 10^{-5} feet/day (Spane and others, 1983).

To date, only two tracer tests have been performed in any of the units below the top of the Saddle Mountains. These tests represent two measurements of the same parameter at the same location. That is, these tracer tests were both done on the McCoy Canyon flow top in the Grande Ronde using the same drill holes. The purpose of the tests was to determine ground-water flow and solute transport parameters, including effective porosity. From these tests, the effective thickness (the product of the aquifer thickness and the effective porosity) of the unit was estimated to be from .006 to .01 feet (DOE 1984). These values indicate an effective porosity of the unit between .01 and 1 percent.

3.2.4. RECHARGE AND DISCHARGE TO THE HYDROSTRATIGRAPHIC UNITS

Recharge and Discharge to the Alluvium

These sediments are recharged by precipitation, irrigation, and disposal ponds. Some recharge occurs where the hydraulic gradient from the underlying basalts is sufficient for upward movement of water. Other sources of recharge include losses

from ephemeral streams and losses of water from the Columbia and Yakima Rivers during high stages. Discharge from the alluvium is mainly to the major rivers with some flow going to the Saddle Mountains Basalts.

As mentioned above precipitation in the Pasco Basin has a range from less than 7 inches in the vicinity of the RRL to 15 inches in the higher regions at Rattlesnake Mountain. The estimated total precipitation over the entire basin totals about 756,000 acre feet annually or less than an 8 inch average over the basin (Table 3.3). By assuming zero runoff and most of the precipitation being lost through evapotranspiration, Leonhart (1979) estimated the recharge from precipitation to the ground-water system to be around 6,000 acre feet per year.

Gephart and others (1979) have estimated about 20 to 40 percent of water put on fields during irrigation becomes recharge while Leonhart (1979) estimated that 30 percent of the surface water, or about 270,000 acre-feet per year, that is used for irrigation could be accounted for as recharge to the ground-water.

Another significant component of recharge to the alluvium is from the disposal ponds on the Hanford site. Industrial activities at Hanford since the mid-1940's have produced large volumes of radioactive waste water. This water was subsequently placed in disposal glibs, trenches, and ponds near the 200-west

and 200-east areas (Figure 3.2). The total volume disposed between 1945 and 1959 is given by Belter (1963) as 1.3×10^5 acre feet. The Committee on Radioactive Waste Management (CRWM, 1978) report that, as of January, 1975 about 4×10^5 acre feet of effluent had been discharged. Leonhart (1979) estimated that about 10 percent of this water recharges the ground-water system. This recharge raised the water table approximately 25 meters at the 200-west area, and 9 meters at the 200-east area (CRWM, 1978).

Recharge to and Discharge from the Basalts

Recharge to shallow basalts most likely occurs at the margins of the basin in the uplands where precipitation is greatest. On the other hand, recharge to the deeper basalts occurs on a regional scale through interbasin flow, leakage along structural and stratigraphic discontinuities and leakage along non-deformed basalt flow interiors (DOE, 1984). Faults and folds in the western part of the basin may effect vertical and lateral flow by acting as conduits but in the eastern part of the basin no structures occur that would impede flow from neighboring basins. In areas where these conduits exist, ground water in the upper basalts may discharge to the overlying sediments and through paleochannels to the Columbia River. Guzowski and others (1982) discussed flow in the Saddle Mountains Basalts and concluded that flow may be upward to the sediments in some areas and ultimately to the river, whereas in other areas flow may be

downward to the older basalts (Wanapum and Grande Ronde). However, due to the sparseness of the data the location of discharge for deep basalts remains uncertain.

3.2.5. GROUND-WATER MOVEMENT WITHIN THE HYDROSTRATIGRAPHIC UNITS

Ground-Water Movement in the Alluvium

In order to determine general directions of ground-water flow, a potentiometric map of the alluvium in the Pasco Basin (Figure 3.1) was constructed from a plate in Gephart and others (1979). This map indicates that recharge occurs in the western uplands of the basin and that ground water generally flows toward the Columbia River. Liquid waste disposal ponds from ordinary industrial plant and radioactive waste disposal has caused "mounding" of the water table at two sites and produced minor changes in the water table elsewhere in the area (Newcomb and others, 1972). The widespread effects of the mounds show a rise of 80 feet below U pond in the 200 West area, a rise of 20 feet below B Pond in the 200 East area, and a rise of 10 feet below Gable Mountain Pond (Figure 3.2). The high conical shaped mound below U Pond and the lower ellipsoidal shaped mound below B Pond indicate that the alluvium is more transmissive below B Pond.

Ground-water flow into and out of the basalts is another component of flow in the alluvium that must be accounted for. Along the Columbia River the potentiometric heads of the Rattlesnake Ridge interbed are sufficient to cause upward leakage of water to the alluvium (Figure 3.3). On the other hand, piezometers placed near the Rattlesnake Mountains and the disposal ponds display decreasing heads with depth indicating recharge to the basalts from the alluvium. Unfortunately, quantification of the amount of water moving between the basalts and the alluvium is difficult without more information on the vertical hydraulic properties of both units.

Ground-Water Flow within the Saddle Mountains Basalt

No information on the hydraulic heads exists for the entire Saddle Mountains Basalt sequence. Of the individual units that make up the Saddle Mountains Basalts, the Mabton interbed has been studied the most. Therefore, indications of horizontal flow with the Saddle Mountains Basalts is derived from this unit.

A potentiometric map for the Mabton interbed in the vicinity of the RRL (Figure 3.4) has been constructed from 1979 data (Gephart and others, 1979). Contours of hydraulic heads on this map indicate that recharge occurs in the west-central region and

causes a mound in the potentiometric surface extending eastward toward the river. Another map was constructed from 1984 data (Figure 3.5) but for an area larger than the Pasco Basin. This map indicates a larger mound to the southwest of the basin near the Yakima River and that a similar mound exists in the Horse Heaven Hills region. Both maps indicate that ground water flows east and southeast toward the Columbia River and locally toward the Yakima River.

Borehole data needed for determining vertical hydraulic gradients within the Saddle Mountains is sparse. Water levels from more than one interbed have been collected from five wells, DB-12, DB-13, DB-14, DC-1, and DC-16A (Table 3.4). The hydraulic head in well DB-13 increases with depth indicating upward movement of water to the alluvial aquifer whereas head in the other wells decrease with depth, indicating the loss of water to the lower basalts. Hydraulic-head differences between the Rattlesnake Ridge interbed of the Saddle Mountains Basalts and the alluvial aquifer also confirm this pattern (Figure 3.3).

Ground-Water Flow in the Wanapum Basalts

Potentiometric data are scarce for distinct aquifers in the Wanapum. Therefore, a map of composite hydraulic heads from the Wanapum Basalts was constructed (Figure 3.6) from 1984 data (Olson, 1984). This map indicates that recharge to the Wanapum

Basalts occurs in the west and north in the upland areas and discharge is generally in the east and south in the vicinity of the Columbia River. Vertical hydraulic-head gradients are generally upward with absolute values that range from 400 feet to 425 feet (see Figures III-23 and III-24 in Gephart and others, 1979).

Ground-Water Flow in the Grande Ronde Basalts

Hydraulic-head data from Olson (1984) were used to produce a contour map of the potentiometric surface of the Grande Ronde Basalts (Figure 3.7). This map indicates that ground-water in the Grande Ronde flows toward the Columbia River, and that the hydraulic gradient in the vicinity of the RRL is relatively small. However, this potentiometric surface is based on very few data points and any conclusions about flow directions are highly speculative. Shown in Figure 3.8 is the vertical head profile in three wells near the RRL constructed from data collected in the spring of 1986. These profiles indicate that flow in the Grande Ronde converges on the Cohasset flow top, while flow is upward in the Wanapum sequence toward the Rosalia flow top. The cause for this horizontal ground-water divide between the Rocky Coulee and the Ginko flow tops has yet to be explained.

Continuous hydraulic-head data are also available for several units of the Grande Ronde Basalts. These data document responses to stresses applied at neighboring wells. The responses in turn provide information about the degree of connection between units. In addition, if the magnitude of the stress is known estimates hydrologic parameters can be made.

At BWIP, the hydrographs recorded at wells DC-19, DC-20, and DC-22 show responses corresponding to the removal of a bridge plug packer at RRL-14, and the drilling of DC-23. Figure 3.9 shows the location of wells DC-23, RRL-14, DC-19, DC-20, and DC-22 and the RRL. Shown in Figure 3.10. are the recorded responses to the packer removal at RRL-14. The spacing between wells in the figure represents their radial distance from RRL-14. The hydrographs all begin when the packer was removed from the hole. The packer was intended to isolate the Grande Ronde and Wanapum Formations, and so was presumably placed above the Rocky Coulee. Deflation of the packer apparently overpressured the zones below it, producing the transient increase in head evident in some of the hydrographs. Two aspects of the relationship between the observed hydrographs are inconsistent with the notion of the monitored units being pervasive and fairly uniform: the lack of response in the Rocky Coulee at DC-22; and the response in the Rocky Coulee at DC-20 in light of the lack of response at DC-22. Possible reasons for the absence of response at DC-22 are:

- 1) The packer was placed below the Rocky Coulee in RRL-14, and there is poor vertical connection between the Cohasset and the Rocky Coulee between RRL-14 and DC-22.
- 2) The Rocky Coulee is discontinuous between RRL-14 and DC-22.

The response at DC-20 might be the result of:

- 1) Good connection through the Rocky Coulee from RRL-14 to DC-20
- 2) Packer placement below the Rocky Coulee and good vertical connection between the Cohasset and Rocky Coulee between RRL-14 and DC-20
- 3) Leaky packer in DC-20

Shown in Figure 3.11 is the response at DC-19, DC-20, and DC-22 to drilling DC-23W. The well was drilled through the Vantage interbed. Mud lost during drilling affected units above the Vantage. The spacing between hydrographs represents the radial distance of the well from DC-23W. All hydrographs start at the beginning of construction at DC-23W. Some unusual aspects of the responses include:

- 1) The larger response in the Ginko flow top at DC-19 than at DC-22, the second well being much closer to the source of stress.

- 2) The large response in the Cohasset at DC-19 compared with the response in this unit at the closer wells, and the response in the overlying Rocky Coulee.

The response in the Ginko can be most easily explained by assuming a lower effective transmissivity between DC-23 and DC-22, possibly due to anisotropy or to thinning of the unit to the west. If response in the Cohasset is due to pervasive vertical connection to the overlying units, the Rocky Coulee would be expected to have responded with a greater water-level fluctuation. The response would be consistent with a localized vertical connection near DC-19. The relative lack of response in the Cohasset in the closer wells could indicate discontinuity of the formation. The response to the removal of the pack in RRL-14 neither supports or refutes the possibility of discontinuity of the Cohasset. The lack of response at DC-19 may be because of interruption of the formation, or because of natural attenuation with distance. The virtual identity of responses in the Rocky Coulee and the Cohasset at DC-20 suggest connection of these units through the well bore

Regional Ground-Water Movement Through the Major Units

Previous sections described lateral flow through each of the major units and vertical flow within each unit. In order to understand regional flow between the units the cross section shown in Figure 3.13 was constructed (see Figure 3.12 for the location of the cross section). This figure shows a geologic section through the RRL along with hydraulic heads for various hydrostratigraphic units. Unfortunately, there are not enough data to be able to draw a similar section in a north-south direction.

Generally flat horizontal and vertical hydraulic gradients are apparent in the central and eastern portions of the section. A slightly downward gradient is observed in the central part of the section and an upward gradient is evident below the Columbia River. West of the RRL, a horizontal hydraulic gradient of about 500 feet (150 meters) occurs in the Priest Rapids member of the Wanapum Basalts. In well DB-1, the hydraulic head for the Priest Rapids is 920 feet above mean sea level and 410 feet above mean sea level in well DC-22. A smaller hydraulic head drop, about 200 feet, is also observed across the same area in the Grande Ronde. In the upper units, however, much less change in the horizontal gradient (about a 40 foot head drop in the Pomona Member of the Saddle Mountains basalt) is apparent. The

vertical hydraulic head gradients are also much different in the west. The largest hydraulic heads are located in the Priest Rapids (about 900 feet) with a 240 foot head drop between that unit and the overlying Mabton interbed. An addition drop of about 200 feet between the Mabton and the Pomona Member of the Saddle Mountains Basalts. Only one data point exists below the Priest Rapids. This head in the top of the Grande Ronde Basalts is 602 feet or a drop of a 318 feet between it and the Priest Rapids.

Thus, the hydraulic-head data discussed above indicate the following flow patterns:

- 1) Within the Saddle Mountains Basalt, recharge occurring in the western highlands, flowing eastward and then upward through the alluvium to the Columbia River. In the area of wells DC-20 and DC-1/2, water could also flow from the Saddle Mountains into the Wanapum Basalts.
- 2) Recharge to the Wanapum Basalts correspondingly occurs in the west. This water then flows eastward, eventually discharging through the Saddle Mountains to the Columbia River. In the western region, however, there is a significant potential for water to flow from the Wanapum Basalts to both the Saddle Mountains and Grande Ronde Basalts.

- 3) Water recharging the Grande Ronde Basalts appears to come either from the west within this unit or from leakage from the Wanapum Basalts. This water then flows eastward and discharges through the Wanapum Basalts to the Columbia River.

As mentioned previously, insufficient data were available to allow for the construction of a similar map in the north-south direction. However, from Figures 3.5 - 3.7 (the potentiometric maps of each of the major basalt units), several overall similarities can be observed. First of all, steeper hydraulic gradients and much higher hydraulic heads not only occur to the west of the site but also in the north and northeast in all of the units. While the changes do not seem to be as abrupt as the those seen in Figure 3.13, very steep local gradients do occur. Perhaps even more interesting are the differences in hydraulic heads between the major units in areas outside the Pasco Basin. For example, 500 foot head differences between the Saddle Mountains and Wanapum basalts are apparent in the north- and southwestern part of the region. In summary then, any conceptual model must be able to explain not only the different horizontal gradient seen in the Pasco Basin but also its very different vertical hydraulic gradient.

DOE (1984) has suggested that these hydraulic-head data indicate some type of vertical flow "barrier" just west of the RRL. In fact, some BWIP modeling has assumed that there is a no-flow boundary located west of the RRL that extends through the basalts. This, of course, is not possible as rocks are never impermeable and there is a very large driving force (i.e., horizontal gradient) for flow across the "barrier". Also the concept of a zero or low permeability zone cutting across all of the basalt units is difficult to justify given the different horizontal gradients in the units above and below the Priest Rapids flow top. And finally, the barrier concept fails to explain such changes in the horizontal and vertical gradients also occur in other parts of the regions.

The hydraulic heads profile shown in Figure 3.13 could be explained by preferential recharge to and flow along the Priest Rapids flow top combined with some restriction to flow west of the RRL. This flow top is exposed in a horseshoe shaped pattern caused by the plunging Cold Creek syncline, Umtanum Ridge and Yakima Ridge. Given the very large relative transmissivity of this unit, preferential recharge to and flow along it is imaginable. Several possibilities could cause a later restriction to flow in the Priest Rapids. As this area is close to the edge of the Pasco Basin (the edge of many of the upper basalts) it is possible that the Priest Rapids may display a fingering effect with gaps at certain places. Such a gap could be between DB-11 and DC-22. Another possibility is a fault in the same area which has an offset just larger than the thickness

of the Priest Rapids flow top. Such a fault would not affect horizontal flow in the thicker flow tops, interbeds, and interiors. Unfortunately, this concept alone does not explain the other steep horizontal and vertical gradients seen around the Pasco Basin.

4. HYDROCHEMISTRY

Integration of hydrochemical data with existing knowledge of the boundary conditions and aquifer hydraulics is necessary in order to formulate a conceptual model(s) that is consistent with the total physico-chemical evolution of the ground-water system. This is particularly true for systems such as the Pasco Basin where the boundary conditions are poorly defined and/or the hydraulic characteristics permit the formulation of several alternative conceptual ground-water flow models. Unfortunately, hydrochemical data alone can rarely be used to define the flow system. Instead its main use is in screening flow models which are inconsistent with the evidence on the chemical evolution of the ground water.

The following sections provide a brief description of the available hydrochemical data from the Pasco Basin area. In addition, a summary and evaluation of each of the major applications of the data to conceptual model formulation is provided.

4.1. HYDROCHEMICAL DATA BASE

The major ion hydrochemistry of the ground water in the Pasco Basin has been summarized in Smith and others (1980) and

Guzowski and others (1982), and a great deal of hydrochemical data (in a variety of presentation forms) is given in DOE (1982) and DOE (1984). Selected hydrochemical data, originally presented at a 1982 DOE-NRC hydrology workshop, were compiled by the NRC staff and contractors (NRC, 1983, Appendix F). The most recent and most complete published compilation of chemical data from BWIP ground waters is given in BWIP Data Package SD-BWI-DP-61 which is partially reproduced in Appendix B of Williams and Associates (1985). Additionally, data has been presented in various DOE-NRC workshops controlled by the NRC Division of Waste Management Document Control Center. The major ion data are summarized on the Piper (trilinear) diagram (Figure 4.1). Trace element concentrations from ground waters of the Hanford Reservation are tabulated in Table 4.1 . At this time, there is no available compilation of the isotopic and dissolved gas data, though both DOE and NRC contractors are in the process of developing such a data base. What isotopic and dissolved gas data are available must be gleaned from individual borehole reports or interpreted from summary diagrams and tables in major DOE program documents.

Standard methods for screening hydrochemical data for analytical errors, that is, charge balance calculations, have shown that the laboratory analyses can generally be relied on as accurately representing the sample. (NRC, 1983, Appendix F; Williams, 1983). However, in all cases, including DOE (1982), subsequent RHO work, work of the NRC and other reviewers, the application

of hydrochemical data to flow system evaluation has been hampered by the difficulties of collecting and preserving high quality water samples that are representative of the chemistry of the water at depth. Three potential problems that introduce uncertainties about the quality of data are:

1. Contamination of the ground water with drilling fluids.
2. Mixing of ground waters across formations in open boreholes.
3. Changes in the chemistry of the fluids between the formation and the sampling point. This is primarily due to up-hole sample collections which may allow loss of dissolved gases, changes in pH, and changes in temperature, with subsequent changes in speciation of the dissolved constituents.

In some instances, waters that have been contaminated with drilling fluids can be identified, for example with the use of tracers. In most other instances it is possible to use borehole histories along with the sampling methods to aid in identifying samples where the chemistry may have been adversely affected. Williams and Associates (1985) have shown that screening of contaminated samples can be done with inferences based on

detailed statistical analyses. In these instances, the entire hydrochemical data set can be screened for spurious data. However, screening of the chemical data base for unreliable samples before applying it to flow system analysis and evaluations of conceptual models has rarely been done. The best example to date of data screening is probably NRC (1983, Appendix F). However, in most cases, authors and reviewers have side stepped the problem by assuming (explicitly or implicitly) that the data are reliable.

4.2. MAJOR APPLICATIONS OF HYDROCHEMISTRY TO CONCEPTUAL MODEL EVALUATION

4.2.1. BWIP SITE CHARACTERIZATION REPORT (DOE, 1982)

Since the publication of the BWIP Site Characterization Report (DOE, 1982), hydrochemical data have been invoked as evidence in support (or against) conceptual models of the Pasco Basin by DOE and by assorted reviewers of DOE's work . In DOE (1982), RHO asserted that the major geologic units (Saddle Mountains, Wanapum and Grande Ronde Basalts) are distinguishable on the basis of the chemistry of the ground waters in contact with those formations. RHO went on to state that the differences in hydrochemical data among the basalts formations indicate that there has been no mixing of waters at the BWIP site, and that, consequently, the hydrochemical data supports a conceptual model

in which the permeable flow tops and interbeds are hydraulically isolated by the dense interiors. (DOE, 1982; p. 5.1 - 139, -184, -202). That is, the hydrochemical data were used to support a conceptual model framework very similar to Concept A of Gephart and others (1983). In addition, RHO presented major dissolved ion (Na, Cl, SO₄) data and selected minor and trace element (particularly F) distributions in ground water from four Grande Ronde boreholes and applied selected reaction mechanisms (sulfate reduction/calcite precipitation and cation exchange) within the Cold Creek Syncline to support the concept of water flowing to the southeast toward Wallula Gap from the area of the RRL.

Support for RHO's contention that the chemistry of waters from each of the major basalt units is distinct is found in Williams and Associates (1983; 1985). They applied univariate and multivariate statistical analyses to the chemical (but not the isotopic or dissolved gas) data to confirm that water chemistry can be used to distinguish the three major basalt formations. However, Williams and Associates emphasized that their statistical analyses demonstrated distinctness but not hydraulic isolation, which would require an integrated analysis of hydraulic characteristics, geochemical evolution of the water rock interactions, and structural analysis of the basalt sequence. In fact, the NRC staff concluded in the Draft Site Characterization Analysis (NRC, 1983) that, based on the available hydrologic information, up to twenty percent mixing of

the Saddle Mountains and Wanapum waters with Grande Ronde water could occur before the mixed water would be distinguishable within the precision of the analytical procedures.

In addition to NRC (1983), major critiques of DOE's 1982 use of hydrochemical data in support of conceptual model evaluations and alternative applications of hydrochemical data to formulation of conceptual models have been made by the U.S. Geological Survey (USGS, 1983) and Lehman (1983). Because both of these authors also provide conceptual models of their own, they are treated separately in the following sections.

4.2.2. U S. GEOLOGICAL SURVEY CRITIQUE OF SCR (USGS, 1983)

The USGS (1983) provided the most complete critique of the BWIP hydrochemical model. The review is contained in a 1983 letter from the USGS to the DOE presenting the Survey's comments on DOE (1982), and as a set of collegial comments on a Federal document. The USGS's intent was to identify issues and raise questions rather than to provide a comprehensive analysis of their own. The USGS preliminary analysis of Hanford data is based on major ions, dissolved gases, stable isotopes and qualitative reaction mechanisms. This breadth in their approach is the major strength of the analysis. In particular, this was the first analysis to make significant use of the dissolved gas data and is still the only published report to extensively use

reaction mechanisms in flow system interpretation at BWIP. Based on the total data available at the time, the USGS (1983) concluded:

1. There are separate flow systems inside and outside the Cold Creek Syncline;
2. Inside the syncline, methane-bearing waters in the Grande Ronde (in which the methane was probably derived from the sedimentary sequence below the Columbia River Basalts) move upward into the Wanapum and Saddle Mountains Basalts, with progressive dilution by local recharge;
3. Continuous flow in the Grande Ronde southeastward from the area of the RRL to DC-15 near the Columbia River is impossible based on the chemistry as reported;
4. The Grande Ronde and Lower Wanapum contain excess helium and anomalous ratios of nitrogen/argon which indicate that they are not receiving local recharge. Either a deep source of recharge or a distant regional source could explain the data

The USGS (1983) hydrochemical analysis did not attempt to combine the chemical trends it identified with a comprehensive assessment of hydraulics or boundary conditions. However, the points itemized above can be considered as part of a "conceptual model", one which is very different from that of DOE (1982). The most important differences are: 1) the concept of high vertical leakage determined from dissolved gas data in the area of the RRL and; 2) the contention that the hydrochemical data is incompatible with confined flow in the Grande Ronde toward Wallula Gap.

4.2.3. LEHMAN REVIEW OF 1983 BWIP HYDROCHEMICAL DATA (LEHMAN, 1983)

In an unpublished review prepared for the Yakima Indian Nation, Lehman (1983) compiled a February, 1983 set of hydrochemical data prepared by BWIP and presented a discussion of the hydrochemical data based primarily on major ion chemistry of the ground waters. Figure 4.1 is a Piper Trilinear Diagram of the 1983 data, showing the major-ion relationships for waters from the Saddle Mountains, Wanapum and Grande Ronde Basalts. Based on the major-ion chemistry, Lehman distinguished "Type A" (essentially Na-HCO₃ waters) and "Type B" (essentially Ca-Mg-Cl-SO₄ waters). The Type A waters are found in the Grande Ronde and portions of the Wanapum Basalts; the Type B waters are found exclusively in the Saddle Mountains Basalts

near the margins of the Pasco Basin (i.e., near the presumed recharge areas for the Saddle Mountains Basalts). In addition, the trilinear diagram identifies mixing trends in both the cations and anions, and Lehman distinguishes a "Type C" water which is consistent with a mixing of Types A and B. The Type C water is identified in the Saddle Mountains and Wanapum Basalts in the central portion of the Pasco Basin, which is consistent with a zone of upwelling and mixing. Figure 4.2 is a southwest to northeast cross section of the Pasco Basin illustrating the distribution of major-ion water types based on the 1983 data. As illustrated in the cross section, the trace of the Gable Mountain - Gable Butte anticline crosses the zone of Type C (mixed) water. If the anticline represents a structural discontinuity that permits significant vertical leakage, then this zone could provide a conduit for fluid flow, which would ultimately lead to discharge to the Columbia River northeast of the RRL. Finally, Lehman (1983) also presents data to support a hypothesis that the distribution of the mixed water is controlled by the distribution of the sedimentary interbeds of the Ellensburg Formation, not by the dense flow interiors of the basalts.

The major strengths of the Lehman (1983) approach are: (1) it incorporates recharge and discharge information and potentiometric data to help interpret the major-ion chemical trends, and, (2) it attempts to develop a two-dimensional picture of the ground-water flow system. The principal

limitation of the brief paper is that the analysis is limited largely to major dissolved ions. Because these ions are not generally conservative in a ground-water system, it is difficult to develop fully defensible mixing scenarios, based on an assumption of conservation.

Note that the conclusions of Williams and Associates are in conflict with the conclusions of Lehman (1983). That is, Williams and Associates (1985) did not find a statistically discernible areal pattern to the hydrochemical data. The problems that each of these investigators considered were formulated in such different fashions that the conflict may reflect matters related to statistical methodology. However, the dissolved gas data, which was not considered by Williams and Associates, indicates significant differences in the areal distribution of nitrogen and argon. These gases should be highly conservative in the ground-water system and therefore, they should be reliable indicators of flow patterns. Additionally, the cluster analysis reported by Williams and Associates indicated "anomalous" placements for samples from Boreholes DC-2, DC-6 and DC-4, which they ascribe to potential contamination or other sampling and analytical difficulties. However, Williams and Associates did not consider that these samples may represent a mixed water, as illustrated in Lehman's cross section.

4.2.4. ROCKWELL 1984 (DOE-NRC GEOCHEMISTRY WORKSHOP, JANUARY,
1984

In the January 9-12, 1984 DOE-NRC Workshop on geochemistry, RHO staff presented results of ground-water chemistry evaluations that had been performed up to that date. The presentation was based largely on major-ion chemistry, with some information drawn from the dissolved gases. This work was based on the results of sampling in the then-recently completed RRL-area boreholes. However, very little of the actual data was presented. In addition to these results, the RHO staff discussed improvements to sampling procedures that were aimed at addressing concerns about representativeness of samples (see Section 4.1 above). Their principal conclusions concerning the flow system were:

1. There is upward movement of deep ground-waters in the vicinity of the RRL;
2. There is evidence for mixing of ground-waters in the RRL boreholes;
3. The so-called "Cold Creek Barrier" west of the RRL may be related to the mixing process;
4. Other structures may also permit vertical ground-water flow;

5. Ground-water flow in the Wanapum Basalts appears to be to the southeast.

6. There does not appear to be hydrochemical evidence for flow in the Mabton Interbed or the overlying Saddle Mountains Basalts.

Illustrated in figures 4.3-4.7 are the data that were presented as the basis for the above interpretations. Cross-sectional and plan views of the resulting conceptual model are shown in figures 4.8 and 4.9. The principal strength of the information presented appears to be the use of the dissolved gas data and a willingness to re-interpret old hypotheses in light of new data. The main limitations of the information appear to be that they still rely to a substantial extent on subsets of the hydrochemical data applied without specific introduction of hydraulic data.

The contention of RHO (1984) that the Cold Creek Barrier is reflected in the hydrochemical data is borne out by the much more detailed statistical analysis of Williams and Associates (1985). Unfortunately, all inferences are limited by the small number of sample points northwest of the Barrier. Also, the hydrochemical data do not throw significant light on the issue of how much, if any, flow crosses the barrier. For example, the concentrations of all parameters of interest are much lower on

the northwest side of the Barrier. This would permit substantial leakage to be masked by the much higher concentrations observed in the RRL boreholes. For example, the Cl concentration in the lower Wanapum in RRL-2 is 350 - 450 mg/l while the concentration in the McGee well is 5 mg/l (see Figure 4.5). Clearly, a 10% leakage (a totally arbitrary number) of McGee Well water across the Barrier would not be detectable given the analytical precision and the sample variability. However, the hydrochemical data does indicate that there can be very little leakage from the RRL to the northwest (even if this were energetically feasible), since this would have a significant effect on the observed chemistry. Finally, the RHO hypothesis of flow in the Wanapum to the southeast should be tested against reaction models that address as much of the relevant chemistry as possible.

4.3. SUMMARY AND CONCLUSIONS

Hydrochemical data needs to be integrated with the geologic and hydrologic data in order to formulate and test conceptual ground-water flow models. While hydrochemical data alone (and particularly subsets, such as major-ion concentrations alone) can not be used reliably to formulate conceptual models, any conceptual model which is valid must be able to explain the observed hydrochemistry of the system.

Thus far, hydrochemistry has been applied at BWIP to:

1. Determine that the DOE (1982) conceptual model of hydraulically isolated transmissive zones with flow in the Grande Ronde to the southeast is not an acceptable flow model (NRC, 1983, USGS, 1983; Lehman, 1983, RHO, 1984).
2. Show, with the best current data, that the Cold Creek Barrier separates chemically distinct (though not necessarily isolated) ground waters (RHO, 1984; Williams and Associates, 1985).
3. Identify what appears to be a zone of high vertical communication in the area of the RRL (USGS, 1983; RHO, 1984).

In addition, assorted hydrochemical data have been used to develop tentative interpretations of flow directions within the Wanapum (RHO, 1984) and/or Saddle Mountains (Lehman, 1983). Finally, differing approaches to handling the data on dissolved ions have led to conflicting interpretations of the degree of mixing that can be determined in the Pasco Basin.

To date, RHO is the only group that has made extensive use of hydrochemistry in evaluating conceptual models of groundwater flow in the Pasco Basin. Further application of hydrochemistry

by RHO, the NRC staff or any other parties will require additional evaluation of the hydrochemistry (particularly hydrochemical data and reaction models that have not been used extensively to date) as well as incorporation of hydraulic and boundary-condition information to fully evaluate the extent to which hydrochemical data is consistent with alternative conceptual models.

5. SUMMARY AND EVALUATION OF CONCEPTUAL MODELS

The previous sections began with a discussion of the site geology upon which all conceptual models are founded. Then the next section discussed aspects of the conceptual model which have been derived from hydrologic investigations. Finally, hydrochemical evidence for and against certain conceptual models was presented. In this section, an attempt is made to integrate what is known about BWIP conceptual models prior to discussing both previous modeling efforts and our own current effort. Many uncertainties of course remain and therefore, many conceptual models are equally plausible. Thus this section will point out what is currently known along with a list of the principal remaining uncertainties.

5.1. HYDROSTRATIGRAPHIC UNITS

In a sense the choice of hydrostratigraphic units has been made for us. That is, the personnel responsible for site investigations defined and then proceeded to measure properties of various hydrostratigraphic units. Thus, without performing additional field work we are limited to using the previously defined units. About our only option is to combine the defined units into larger ones.

Site investigators have defined the units to be the alluvium overlying the basalts and the flow tops, flow interiors, and sedimentary interbeds with the basalts as hydrostratigraphic units. For regional modeling efforts, the most appropriate combination of units results in layers which correspond to the alluvium, the Saddle Mountains Basalts, the Wanapum Basalts, and the Grande Ronde Basalts.

Several remaining questions concerning assumptions about the hydraulic behavior and transport characteristics of these units remain to be answered. These are listed below:

Continuity of Hydrostratigraphic Units

With respect to the major basalt units mentioned above, the concern about continuity is limited to the faults that are associated with anticlinal folds and the erosion along the major rivers. Several of these faults dissect the Saddle Mountains Basalt and a few dissect the Wanapum Basalts. In combination with local recharge, these faults cause ground-water divides in the Saddle Mountains and Wanapum Basalts along Horse Heaven Hills and Rattle Snake Ridge (Figures 3.5 and 3.6). However, none of them dissect the Grande Ronde Basalts and no hydrologic data exist in these areas for the Grande Ronde. Thus, the hydrologic effect of these faults on the Grande Ronde Basalts is unknown.

Another possible discontinuity that exists west of the RRL has been referred to as the "Cold Creek Barrier". Evidence for this feature includes the large hydraulic head difference across the feature in the Priest Rapids flow top, a difference in the quality of water on each side of the feature, and geochemical evidence of vertical mixing of ground waters on the east side of the feature. The only geologic evidence for the "barrier" is indicated in drill holes DH-27 and DH-28 where there is an offset in the top of the basalt across the "barrier". However, the cause of the offset is uncertain. It may be the result of faulting, or of a monoclinial fold, or even just a misinterpretation of the units that make up the top of basalt in the two drill holes. In any event, none of the evidence indicates that the feature is a no-flow barrier. On the contrary, the head gradient alone provides a significant driving force for flow across the "barrier". Thus at most, there may be some restriction to flow west of the RRL but, as discussed in the hydrology section, the restriction may be only in the Priest Rapids flow top. Perhaps more important, however, are the remaining questions about the "barrier", including: 1) why are both the horizontal and vertical gradients so different on either side of the "barrier"?; 2) how far does this feature extend to the north and south?; 3) what is the cause for the apparent vertical leakage east of the "barrier"?; 4) does the feature extend into the Grande Ronde Basalts?; and; 5) are the steep horizontal and vertical gradients in other areas around the Pasco Basin related to this feature? Obviously, the answer

to these questions will come only after the DOE has performed large scale hydraulic and tracer tests across the "barrier". and performed more detailed investigations of the regions outside the RRL.

At different locations in and near the Pasco Basin the Columbia River cuts through the Saddle Mountains Basalt and into the Wanapum Basalt. Just below Priest Rapids dam, the river cuts all the way into the top of the Grande Ronde Basalts. As hydrologic data near these structures and near the river are sparse, the effect of these discontinuities is difficult to determine. It may, for example, be possible to arrive at an adequate simulation of the regional hydrology without explicitly including these features.

Continuity of the smaller units (the flow top, interbeds, and interiors) is much more of a problem. For example, the Frenchman Springs member of the Wanapum basalts alone is composed of 7 to 9 flows which cannot be consistently correlated from drill hole to drill hole. In addition, the nature of the basalt flows themselves raises questions as to the continuity of permeable zones within them. As noted in the discussions of hydrographs in Section 3, channeling of ground-water in the flow tops is evident in several of the units monitored in by the well DC-19, DC-20, and DC-22. Unfortunately, these hydrographs provide the only information on large-scale behavior as, only small scale hydraulic testing and two tracer tests (at the same

location) have been performed at BWIP. Therefore, testing thus far has not provided information on the hydrologic continuity of the units. Hopefully, this problem of continuity of the smaller units will be resolved when the DOE performs more tracer tests and large-scale hydraulic tests.

Fracture versus Porous Media Behavior

Fractures undoubtedly control the flow of water within the basalts of the Columbia Plateau. The question is whether or not the fracture spacings, orientations, apertures, and frequencies are such that the basalts can be treated as a porous media. In answering this question it is useful to delineate the three basic types of behavior that can occur. First, of course, the basalt can be highly fractured resulting in porous media type of flow and transport characteristics. Second, the basalt can be sufficiently fractured such that the hydraulic behavior can be approximated by an equivalent porous media but the transport characteristics are dominated by the fracture and matrix interaction (the "dual porosity" concept). And finally, the fractures may be spaced sufficiently far apart and be continuous enough to result in a short-circuiting of large blocks of basalt. Also note that a hydrostratigraphic unit may display all of these types of behavior at different locations within a given study area. Another possibility is that combined units could have two types of characteristics at the same location. For example, one could choose a hydrostratigraphic unit as one

flow top and its adjacent interiors. Horizontal flow within this unit may then be controlled by the rubblized flow top (an equivalent porous media) and transport could be affected by a combination of adsorption on particles within the flow top and diffusion of contaminate into the dense basalt interior.

Hydraulic testing at BWIP has been based on the assumption of porous or equivalent porous media behavior. Whether or not the response of the tests has been that of porous media would require a review of the measured response curves. In reviewing these curves one should be able to separate porous or equivalent porous type of responses from discrete fracture type of responses. The question then becomes a matter of the transport characteristics of the media. To answer this question would require the results of both sorptive and non-sorptive tracer tests. Unfortunately, this type of testing has not been done. Therefore, the question regarding transport of contaminants through the basalts can not be answered without additional tracer tests.

Homogeneous versus Heterogeneous Behavior

Obviously, from the physical characteristics of the hydrostratigraphic units and their measured properties, the units are heterogeneous. However, if our study was only interested in the hydraulic behavior of relatively large regions

then a homogeneous representation of the system may be adequate. On the other hand, if the interest is in contaminant transport or the hydraulic behavior of small regions then the units may have to be treated as heterogeneous. In short, the representation of the units as either heterogeneous or homogeneous is dependent on the purpose of the study.

Isotropic versus Anisotropic Behavior

To date, hydraulic testing at BWIP has concentrated on single hole, single zone type of testing. Therefore, very little is known about the anisotropy of individual hydrostratigraphic units. If the assumption is made that the hydraulic conductivity values obtained thus far are representative of the units as a whole, then the anisotropy of combined hydrostratigraphic units can be determined. In all possible combinations, the resulting hydrostratigraphic unit would display a large horizontal to vertical anisotropy. This is because of the larger conductivities of the flow tops and interbeds relative to the flow interiors. Hopefully, large scale testing will provide information on lateral anisotropy.

Representativeness of Hydraulic Parameters

The representativeness of the measured hydraulic parameters is

in question due to the limited volume of rock that has been tested by the DOE. These problems include questions about the spacial variability of parameters and of the representativeness of the existing values. Current data may be useful for predicting the hydraulic behavior of the system in the vicinity of the RRL. However, needed to set boundary conditions are very sparse. In addition, it is the variation in conductivities that control the transport of contaminants. Therefore, many more locations within the RRL need to be tested to accurately characterize the site with respect to transport. The second question is mainly focused on the representativeness of the measured hydraulic conductivities of the basalt interiors. Because flow through the interiors is thought to be controlled by vertical fractures and drill holes are not likely to intersect vertical fractures, the measurements taken to date may reflect the conductivity of the relatively intact basalt and may not be useful in predicting or understanding flow and transport.

5.2. BOUNDARY CONDITIONS

Geologic Evidence

The physical limits of the basalt flows must obviously act as boundaries for the hydrostratigraphic units used to represent

them. The way a boundary of a hydrostratigraphic unit is treated depends on conditions at the edge of the flow. Three types of boundary conditions are possible. In areas where the basalt flow is discharging, the boundary can be established as a specified flux out of the system, or a held potential. If the basalt flow crops out in an area of significant recharge, a specified flux or a held potential can be imposed, depending on the availability of supporting data. If the formation is not discharging or receiving recharge, then the treatment of the boundary depends on whether the steady-state or transient behavior of the system is being simulated. If the formation exchanges no water through its' bottom boundary, a no-flow condition is appropriate for steady-state. However, the distance from the edge of the flow to the point of saturation is not generally known, resulting in uncertainty in the location of the no-flow boundary. The contribution of this uncertainty to the uncertainty in ground-water travel time is not known, but might possibly be addressed with an otherwise-calibrated model. In the absence of such an estimation, the boundaries of the hydrostratigraphic units can be assumed to coincide with the boundaries of the associated basalt flows, with an unknown effect on the uncertainty in GWTT calculation. Because the location of the saturated zone can change with time, it is properly represented as a moving boundary in transient simulations.

There is also uncertainty in the vertical boundaries. No

physical evidence exists for a flow barrier underlying the basalts, so the interface between the basalts and underlying sediments must be assumed permeable to some degree. The Hanford, Ringold, alluvial deposits, and parts of the Saddle Mountains Basalts are generally unsaturated. The perimeter of this hydrostratigraphic unit is therefore most accurately represented as a moving boundary in a transient simulation, or as a steady-state no-flow boundary.

Rainfall and irrigation may recharge exposed units throughout the study area. Such recharge would be primarily to the Hanford and Ringold formations within the Pasco Basin, to the Saddle Mountains Basalts in the Horse Heaven Hills Basin, and to the Wanapum Basalts along Umtanum, Yakima, and Rattlesnake Ridges.

Points of incision of the hydrostratigraphic units by rivers may be either recharge or discharge points, or neither, depending on the nature of the contact.

Hydrologic Evidence

As discussed in Section 3, hydrologic measurements presuppose conceptual models defining the hydrologic units. Interpretation of test results necessitates assumptions about the units, such as homogeneity and unboundedness. For this reason, most hydrologic evidence cannot be used to develop a conceptual model, but to evaluate the consistency between the assumed conceptual model and the observations, and to calculate parameters specific to the model.

The following remarks discuss the inferences that can be made concerning the boundary conditions of the defined hydrostratigraphic units from the available hydrologic data, given the assumption of continuity. They are a summary of the description of recharge and discharge in Section 3.2.4.

Water-level data can be used to infer areas of recharge and discharge. Downward vertical gradients in exposed units imply recharge from the surface. Local maxima in a hydrostratigraphic unit imply recharge from an adjacent unit or the surface.

Downward vertical gradients in the Ringold imply recharge to the alluvium in the western part of the Pasco Basin (Figure 3.3) and recharge to the Saddle Mountains along Horse Heaven Hills (Figures 3.5 and 3.6). The observed mounds in the potentiometric surface in the alluvium surrounding the disposal ponds indicate recharge from these areas. The large mounds in the Saddle Mountains Basalts to the east of the Columbia and in the Yakima Basin are presumably the result of extensive irrigation in these areas. High heads in the Wanapum Basalts (Figure 3.6) along Yakima, Umtanum, and Rattlesnake Ridges imply recharge from rainfall.

The 1984 head surfaces for the Saddle Mountains and Wanapum sequences (figures 3.5 and 3.6) show minima along the Columbia

River, suggesting discharge to the Columbia. The Saddle Mountains Basalts in the Yakima Basin apparently discharge to the Yakima River. The Columbia River below the confluence with the Walla Walla River receives discharge from the Horse Heaven Hills Basin. The influence of the river can be represented as a specified head at the river elevation, coupled through the river bed, which may have different hydraulic properties than the underlying material.

Several hydrographs (e.g., Figure 3.8) show heads in the Grande Ronde increasing with depth, indicating recharge from deeper basalts. The extent and magnitude of this flux are unknown.

Hydrochemical Evidence

Like hydrologic data, collection of hydrochemical data requires prior assumptions about hydrostratigraphic units. Analysis of major ion data for estimating flow directions requires assumptions about reaction mechanisms. There is consequently considerable latitude in the interpretations of hydrochemical data.

DOE (1982) used the existence of chemically distinct waters in the three major basalt sequences to infer hydraulic isolation of these sequences. Williams and Associates found distinct water types, but point out that chemical typing alone is not evidence

of hydrologic isolation without consideration of possible reaction mechanisms.

The USGS (1983) incorporated dissolved gas data and reaction mechanisms in their analysis and found evidence of upward movement from pre-basalt sediments within the cold creek syncline. Their work also suggests that the Grande Ronde and Lower Wanapum are not receiving local recharge.

Lehman (1983) identified three distinct water types: one in the Grande Ronde and parts of the Wanapum, another in the presumed recharge areas of the Saddle Mountains Basalts, and a third found in the central part of the basin, having a composition consistent with a mixture of the first two types.

The consensus of these interpretations of the geochemical data is that there is upward leakage of groundwater from the lower basalts. With a pervasive influx of water from below, the Columbia River would be the only possible means of discharge.

Summary

The geologic, hydrologic, and hydrochemical evidence taken together suggest the following boundaries for this conceptual model of the Pasco Basin:

A specified-flux boundary representing recharge to

exposed units from rainfall and irrigation.

A specified flux or specified potential boundary at discharging basalt flow edges.

An impermeable or moving boundary at the basalt perimeters which are neither discharging nor receiving recharge.

An impermeable or moving boundary at the edge of the saturated alluvium.

A permeable boundary at the base of the Grande Ronde basalts. In practice, this boundary would be implemented as a specified flux or specified potential boundary.

Specified head boundaries along river contacts, connected through an area of uncertain permeability representing the river bed.

Uncertainty

Values used to specify the boundary conditions in numerical models based on this conceptual model will have an associated uncertainty. The effect of this uncertainty on the uncertainty

in estimated ground water travel time is unknown. The following remarks discuss the information available for estimating boundary condition values, and possible ways of reducing the associated uncertainty:

There is considerable uncertainty in the amount of recharge due to rainfall and irrigation. The amount of rainfall varies over the basins, as does the amount of evapotranspiration and recharge. Estimates of the total influx vary widely. An estimate of the average amount of recharge could be made from accurate ground water data and estimates of effective porosity. Another approach would be to impose constant head values from measured data at recharge locations. The total amount of influx required to maintain these heads, compared with the range of estimates calculated from rainfall data, would bound the conductivity of the recharged unit.

There are little data available on discharge rates. Where the units discharge to the Columbia the efflux rate is completely masked by the flow in the river. These boundaries, like recharge boundaries, can be treated as constant heads, provided enough water level measurements are available near the discharge area.

The amount of water entering the system from the lower

basalts and pre-basalt sediments is unknown. This flux could be estimated from the composition of Lehman's "mixed" water, if the composition of type A water, the composition of type B water, and the amount of surficial recharge were known. Vertical gradients in the lower Wanapum could also be used to estimate influx rate, if the vertical conductivity were known with precision. This boundary, like other sources of recharge or discharge, may be treated as a fixed potential boundary. As the number of wells completed below the Grande Ronde is very small, values for these constant heads can't be estimated with any confidence.

The degree of connection of the principal rivers to underlying formations could be estimated by comparing heads in wells near the river to river elevations. Using heads from nearby wells, rather than river heads, as the head potentials at the discharging boundaries would incorporate the effect of flow through the river bed without requiring the conductivity of the river channel to be calculated.

6. PREVIOUS NUMERICAL MODELING EFFORTS

This section contains a summary and review of the published numerical modeling studies of the BWIP site. In this portion of the report, only a general description of these studies is provided. A more detailed critique of each of the studies is provided in Appendix A. Following these reviews is a discussion of the main problems and limitations shared by most or all of the modeling studies.

6.1. GENERAL DESCRIPTION OF THE MAJOR STUDIES

6.1.1. LA SALA AND OTHERS, 1973

This study was not a numerical modeling study but was included here because it represents one of the first attempts at formulating a conceptual flow model of the Hanford region. As many of this study's conclusions have remained unaltered, it provides a good basis for understanding the accuracy (or validity) of the numerical modeling studies. The purpose of this study was to obtain an initial appraisal of the direction of ground water flow in the Columbia basalts in south-central Washington. In addition, they were attempting to understand the mechanisms controlling flow and attempting to delineate areas of

recharge and discharge. This study followed the drilling of well ARH-DC-1 in order to capitalize on the data obtained from that drill hole.

With respect to the factors controlling the flow, the authors concluded that flow tops and interbeds are responsible for most of the water being transmitted through the basalts. From studying cores taken at the site, they noted that because hydraulic conductivities of the cores were much less than the in-situ values, fractures were probably affecting the basalts' water-transmitting properties. Also from the cores, they noticed that due to non-interconnected vesicles, the total porosity of the basalts is probably much larger than the effective porosity.

The authors arrived at a description of the regional ground-water flow system by utilizing hydraulic-head and geochemical data, and by inferring effects of geologic structures on ground-water flow. Generally, their picture of the flow system shows water being recharged in the northwest, northeast and along Rattlesnake Ridge and Horse Heaven Hills (Figure 6.1). The only exception to this is the recharge from the Columbia River and just north of the Snake River. All of the recharged water eventually discharges into the Columbia River with the direction of flow across the Hanford site being toward the southeast. Also, in the Hanford area, the authors note a downward hydraulic gradient revealed by the ARH-DC-1

well. They believe this gradient could be the result of: 1) the surface disposal of waste water at the Hanford site, 2) the anisotropy of the rocks (the mechanism by which this could cause a downward gradient is not discussed by the authors), or 3) a deep, separate, regional flow system.

6.1.2. ARNETT, 1980

This author used a three-dimensional finite-element model to simulate ground-water flow in the Pasco Basin. This modeling represents the Basalt Waste Isolation Project's first documented attempt at ground-water flow modeling. The purpose of the study was to understand the flow system in the Pasco Basin, to calculate preliminary ground-water travel times to the accessible environment, and to identify limitations of data and conceptual models.

The system modeled in this study included the three major basalt layers; the Saddle Mountains, the Wanapum, and the Grande Ronde. Boundaries of the model were set at the surface-water divides of the Pasco Basin. It appears that these boundaries were treated as constant hydraulic heads.

Several parameter variations were tested in an attempt to match the measured hydraulic heads. Using the combination of parameters that the author felt best represented the system produced flow to the north and then upward to the Columbia

River. This parameter set contained vertical-to-horizontal ratios of the hydraulic conductivity from $1e-2$ to $1e-3$. However, both of these simulations produced hydraulic heads which are well above the measured values.

6.1.3. ARNETT AND OTHERS, 1981

The authors attempted to integrate the hydrologic data, a conceptual model and a numerical model in this initial BWIP far-field analysis. Their goal in this effort was to calculate ground-water travel times from the repository to the accessible environment, estimate ground-water velocities, and provide input into transport and health-effects models.

Both two- and three-dimensional finite-element models were used to simulate the flow system in the Pasco Basin. The three-dimensional model contained the three major basalt layers and a top layer representing the Hanford and Ringold sediments. However, the top layer was only used to define the upper boundary conditions and was not active in the model. Lateral boundaries of this model corresponded to the surface-water divides of the Pasco Basin. The authors believe that the hydraulic heads produced by this model are "physically reasonable and generally consistent with available borehole measurements" even though the model-produced heads are from 5 to 20 meters above the measured heads. Ground-water travel times

from the proposed repository location to the accessible environment were predicted to be greater than 100,000 years. the predicted particle paths for this model traveled down the axis of the Cold Creek syncline, under the Columbia River, and then slightly upward.

The two-dimensional model documented in this report was based on the results of the previously described three-dimensional model. That is, the two-dimensional model is a more detailed vertical section of the three-dimensional model which is aligned with the flow direction predicted by the three-dimensional model. With respect to detail, the main difference between the two models is that in the two-dimensional model the three major basalt units have been subdivided into 9 layers, including individual flows and interbeds. these layers have then been further divided into a total of 16 material types, each material type having different hydraulic properties. The simulated hydraulic head surface produces a slightly better match with the observed heads than does the three-dimensional model. Heads from this model were 5.5 to 11.3 meters above the measured heads. Results from this model indicate flow from the proposed repository location downward and then out the southeast model boundary. The associated ground-water travel time was predicted to be greater than 1,000,000 years.

6.1.4. RIGDON AND OTHERS (LATA), 1981

Los Alamos Technical Associates (LATA) simulated the ground-water flow in the Pasco Basin in an attempt to predict ground-water flow direction and the resulting radionuclide transport away from a hypothetical repository. Their three-dimensional model consisted of five of the most permeable units, including the upper sediments, interbeds, and flow tops. The less permeable units between these were implicitly represented by altering the parameters that represent the vertical connection between the permeable layers. The limits of their model coincide with the surface-water divides of the Pasco Basin. A trial and error type of calibration of the model to a transient response produced by a test at well DC-2 and to the steady-state hydraulic head surface.

6.1.5. DOVE AND OTHERS, 1982

The modeling described in this report was part of a demonstration of a methodology developed for the Department of Energy to assess the performance of a mined geologic repository in Columbia Basin basalts. In order to encompass the major sources of recharge to the Pasco Basin along with other factors that affect flow in the Pasco Basin, a regional (most of the Columbia Plateau) model was built first. This model was then used to set boundary conditions for a more detailed local (Pasco Basin) model. The local model, in turn, was used to calculate

ground-water travel times to the accessible environment and to define the flow patterns to be used in subsequent radionuclide transport calculations.

Ground-water flow in two layers was simulated in the regional-scale model. These layers were meant to represent the Grande Ronde Basalts and a combination of the Wanapum and Saddle Mountains Basalts. In addition, the overlying alluvial aquifer was used as a top boundary condition by fixing hydraulic heads equal to the elevation of the water table in that layer. The local model used the same layering scheme with the exception that the Saddle Mountains/Wanapum Basalts were split into two layers. One key assumption used in constructing these models was that the Grande Ronde Basalts act hydraulically like the Wanapum Basalts. The authors state that this assumption was made mainly because of the lack of data on the Grande Ronde Basalts.

A considerable amount of effort was expended to define the locations and quantities of recharge to the regional and local models. Once defined, the recharge was fixed and only the transmissivities of the layers and the vertical hydraulic connections between the layers were adjusted during calibration. Both hydraulic head measurements and ground-water ages interpreted from isotopic data were used to compare with model results during the calibration effort. However, the authors acknowledged that the interpreted ground-water ages were

very uncertain and therefore not of great value in model calibration.

Local model results (which inherently include regional model results through the boundary conditions) indicated that a particle leaving the proposed repository location would travel upward to the alluvium and then laterally to the Columbia River. The travel time associated with this path was calculated to be 15,176 years.

6.1.6. LEHMAN AND QUINN, 1982 and QUINN, 1982

These reports represents the Nuclear Regulatory Commissions' first effort at modeling the ground-water flow system associated with a proposed high-level waste disposal site. The purpose of these studies was to try and understand why two of the models described above, Arnett and others, 1981 and Dove and others, 1982, predicted completely different ground-water travel paths. In order to accomplish this purpose, the authors constructed their own model of the site. Then they attempted to reproduce the results of the other studies by using the corresponding boundary conditions and parameters. Using their model, they were able to accurately reproduce the results of both studies. This indicated that the previous modelers results were consistent with their associated model input. The authors concluded that the difference in predicted flow paths was a

result mainly of the boundary conditions employed in the two models and secondarily, the ratio of vertical to horizontal hydraulic conductivity input to the two models. As pointed out in the preceding sections and Appendix A, the model by Arnett and others (1981) utilized interpolated hydraulic head data to arrive at boundary conditions while the model by Dove and others (1982) relied on the results of a larger scale model for bounding hydraulic heads. As an additional result of their study, Lehman and Quinn (1982) believe that boundary conditions implemented in the numerical model by Arnett and others (1981) were not consistent with those implied by the associated conceptual model. Namely, discharge was occurring in areas that where the conceptual model indicated recharge and visa versa. As a follow on effort, Quinn (1982) varied the parameters within the NRC model in an attempt to understand how sensitive the model was to the parameters and boundary conditions that control the ground-water flow direction. The results of this study, as well as those of Lehman and Quinn (1982) indicate that the model is extremely sensitive to the imposed boundary conditions, the ratio of vertical to horizontal hydraulic conductivity, and the effective porosity. In addition, these studies had the following recommendations: 1) model simulations and associated sensitivity analyses should be used to direct field activities; 2) more data are required to define model boundary conditions; 3) more data are needed on vertical permeabilities and porosities; and 4) the hydrologic character of important geologic structures, such as the Gable Mountain-Gable Butte

anticline needs to be investigated by field and numerical studies.

6.1.7. Bonano and others, 1986

The ground-water flow modeling in this report is similar to that of Dove and others (1982) in that it was part of a demonstration of a performance assessment methodology. This methodology was developed to aid the NRC in evaluating the performance of a mined geologic repository in basalt. Although the authors term their efforts as a demonstration for a hypothetical basalt site, the conceptual model and all of the data used in the demonstration were from the Hanford area.

This demonstration was designed to address radionuclide discharge across an imaginary line five kilometers away from the edge of the proposed repository location, that is , the accessible environment as defined by the Environmental Protection Agency. However, in an effort to reduce the uncertainty involved with the assignment of boundary conditions, two different scales of models were constructed to analyze normal ground-water flow and selected scenarios. The regional model contained four layers which represented the alluvium, the Saddle Mountains Basalt, the Wanapum Basalt, and the Grande Ronde Basalt. The limits of the regional model contained an area slightly larger than the Pasco Basin (see figure A.). The

model was extended beyond the accessible environment to: 1) correspond with the areal extent of the basalts along several of the boundaries; 2) incorporate regions where the basalts are incised by the major rivers and; 3) include the main areas of recharge to the basalts. The results of this regional model were then used to set boundaries for the local model. The local model also extends beyond the edge of the accessible environment. This was done so that the effects of scenarios that were simulated using only the local model would not reach the boundaries which, of course, had been defined by the regional model.

As the system being simulated in this exercise was meant to be hypothetical, there was no attempt to calibrate the models. Instead, ranges of parameters were used in conjunction with their assumed distributions in a Monte Carlo based sensitivity and uncertainty analyses. In order to assure consistency between the regional and local models, sampling of parameter values was performed at the local model level. For example, hydraulic conductivities were sampled from data on the twenty layers represented in the local model. These values were then combined to yield values for each of the four regional model layers. The results of this regional model simulation were then used in turn to define boundary conditions for a local model simulation. A local-model simulation was then performed that utilized these boundary conditions along with the original sampled values of conductivity.

Overall results of this modeling effort yielded ground-water travel times from the proposed location of the repository to the accessible environment ranging from about 7,000 to 500,000 years.

6.2. OVERALL REVIEW AND EVALUATION OF NUMERICAL MODELS

This section contains a comparison and general evaluation of the models discussed in the previous sections. As mentioned previously, detailed reviews of several of the models discussed above are included in Appendix A.

6.2.1. EVALUATION OF NUMERICAL MODELS

Before comparing the various models and their results, several important factors about the models should be pointed out. Namely, almost all of the models suffer from the following problems: 1) lack of adequate documentation; 2) lack of or inaccurate calibration and; 3) lack of uncertainty and sensitivity analyses. With the exception of the report by Dove and others (1982), none of the model reports contain enough information to allow for a complete review of the modeling effort. For example, the differences in interpolated hydraulic heads used for boundary conditions can not be evaluated because

none of the models provide a map or listing of the head values. Similar problems exist with respect to input parameters, measured hydraulic heads used for model comparison, and model discretization. An equally important aspect that has been omitted from most of the reports is the process by which a "calibrated" model has been achieved. As these models have all been made in the phase of the overall study that is concerned with understanding the flow system, the combinations of parameters and boundary conditions that were unsuccessfully applied would provide as much information as those that were successful. At a minimum this lack of documentation could result in future modelers making the same mistakes. Perhaps worst is that the reader is not provided with possible additional information about the flow system. The real exception to the above generalizations are the models described by Dove and others (1982). Although not complete, this report does describe many of the modeling details not given by the others.

The second problem shared by all of the models is either the lack of any calibration or a calibration which leaves the modeled heads being tens to hundreds of feet different from the measured heads. Obviously if the model is not adequately reproducing the measured heads, then the model results are questionable whether they are used to understand the flow system or whether they are used to predict ground-water flow and transport.

Also limiting the usefulness of the model results is the lack of sensitivity and uncertainty analyses. With the exception of the models described by Bonano and others (1986), the only sensitivity analyses involved a few selected parameters in a few of the models and none of the other studies attempted any uncertainty analyses. In addition, the models of Bonano and others (1986) were for a "hypothetical" study area and therefore were not calibrated. Thus, their uncertainty and sensitivity analyses are of limited use. Several of the studies did attempt a parametric type of sensitivity analysis whereby selected parameters were varied while all other parameters were held constant. This procedure does provide some insight into the particular model sensitivity but because most of the parameters are assumed to be "correct" (i.e., they are held at one value), the analysis tells us very little about the "true" system behavior. Finally, the lack of complete sensitivity and uncertainty analyses means that the key model parameters have not been identified and no degree of confidence can be associated with the models.

6.2.2. COMPARISON OF NUMERICAL MODELS

The results of the models described above are a function of boundary conditions (including the location and amount of recharge), assumed layering, and hydraulic parameters. With the

exception of the regional model by Dove and others (1982), both models of Bonano and others (1986), and the conceptual model of LaSala and Doty (1973), the lateral boundaries of all of the remaining models correspond to the extent of the Pasco Basin. The regional models of the Dove and others (1982) and of Bonano and others (1986) encompass areas larger than the Pasco Basin but smaller than the Columbia Plateau whereas the conceptual model described by LaSala and Doty (1973) is for the entire Columbia Plateau. Finally, the local model of Bonano and others (1986) represents an area smaller than the Pasco Basin. The top boundaries of most of the models coincides with the water table of the alluvial aquifer. The only exceptions to this are the models by Arnett (1980) and the two-dimensional model of Arnett and others (1981) where the upper surface corresponds to basalt flows in the Saddle Mountains Basalts. In every case, an impermeable boundary corresponding to the location of the bottom of the Grande Ronde Basalts has been assumed. This apparent agreement between the models is interesting in light of the fact that there are no data to support the assumption that this no-flow condition exists.

A second important point to compare between the models is the choice of hydrostratigraphic units or layers that are modeled. Shown in Table 5.1 are the layering schemes employed in each of the models. Note that the majority of models only simulate flow in layers that are roughly equivalent to the major basalt units. The only significant exception to this is the

local-scale model of Bonano and others (1986) which simulates flow in twenty-eight layers. While this is much more detailed than the layering found in the other models, all of the basalt flows were not simulated. The importance of the choice of layering is dependent on the purpose of the modeling effort. If the only purpose of the model is to predict general directions of flow with the intent of using the model to understand the flow system, then a coarse layering may be appropriate. On the other hand, if the model is designed to predict particle paths and be the first step in a transport analysis, then the finer layering should produce more accurate results.

Normally, a comparison between models would be of the hydraulic parameters. However, because the models did not simulate the exact same layers a comparison would not be meaningful.

6.2.3. COMPARISON OF MODEL RESULTS

In the regulatory framework for which these codes were constructed, the results of primary importance are predicted ground-water travel time (NRC rule 10CFR60) and model-defined flow field required for radionuclide transport analysis. A comparison of predicted ground-water travel times is, unfortunately, not possible. This is because at the time most of the models were constructed there was no clear definition of the accessible environment. Therefore, most of the travel times

produced by the models were for travel from a hypothetical repository to any natural discharge point. Because the models have predicted a variety of flow paths, there is no purpose in comparing their associated travel times. On the other hand, the predicted flow paths can be used to indicate the general directions that would be followed by radionuclides released from a repository. Therefore, shown in figures 6.2 and 6.3 are the model-predicted flow paths. Note the large variation displayed by the paths. As noted by Lehman and Quinn (1982), this variation is due to a combination of differences in the boundary conditions and the ratios of vertical to horizontal hydraulic conductivity. In reality, differences in the boundary conditions are responsible almost all of the differences between the models. This is because the hydraulic parameters used in any given model have been adjusted to make the model agree with the measured hydraulic heads. That is, the adjustable hydraulic parameters have been combined with the fixed boundary conditions to yield model-predicted hydraulic heads that resemble the field measurements. Thus, the boundary conditions are the root of the differences in model-predicted flow paths. The question then arises as to how models which are based on the same data set can interpret the data to indicate such differences in boundary conditions. The obvious answer lies in the inadequacy of the data base. To be specific, most of the models rely on interpolated hydraulic heads to fix their boundary conditions. This is especially true of the majority of Pasco Basin models. Because a large degree of uncertainty in the heads exists, the

interpolated values can be quite different, resulting in different boundary conditions and, therefore, different results. In addition, assumptions concerning the effect of geologic structures on ground-water flow result in different boundary conditions. However, these assumptions are not supportable given the limited amount of hydrologic data in the vicinity of the structures. Two of the modeling efforts (Dove and others (1982) and Bonano and others (1986)) have attempted to minimize the uncertainty in boundary conditions by using regional models to set boundary conditions for smaller scale local models. This approach is advantageous if there is less uncertainty in the regional boundary conditions than in the local boundary conditions. Although the regional boundary conditions of these studies were not identical, both sets of authors felt that their regional models reduced the boundary condition uncertainty by: 1) including the major areas of recharge; 2) extending the model to the physical limits of the basalt layers in several areas and; 3) by including areas where the major rivers are assumed to be in hydraulic communication with the basalts. In both models, however, boundaries remain that rely on interpolated hydraulic heads. It is interesting to note that although these two models do not encompass the same areas nor do they employ exactly the same boundary conditions at coincident locations, the predicted travel paths are very similar. On the other hand, the Pasco Basin models display a large variance in the predicted flow paths. This could be coincidental or it could be the result of reduced uncertainty associated with the regional models.

6.2.4. SUMMARY OF NUMERICAL MODELS

None of the models described above has produced results which can be believed to represent the "real" system. This is because of the large uncertainty in boundary conditions, the scarcity of hydraulic data (especially outside the Reference Repository Location, the RRL), and the inability of the models to adequately reproduce the measured hydraulic heads. In fact, given the current data set, the most appropriate use of numerical models at this time is to aid in understanding the system behavior or in other terms, evaluating conceptual models. The models will be of little use in predicting ground-water flow and transport until: 1) a sufficient number of hydraulic tests have been performed over much larger scales than those performed to date; 2) the hydraulic effects of geologic structures have been directly tested and; 3) a clearer definition of boundary conditions, including recharge, has been obtained.

7. CURRENT NUMERICAL MODELING OF BWIP

Ground-water flow models of the Pasco Basin region are being constructed in order to provide the NRC with the ability to independently evaluate DOE modeling efforts and to test conceptual models of the ground-water flow system. In addition, these models will have the capability of analyzing for ground-water travel times and be able to test the effects of various hypothetical scenarios on the flow system.

Our approach was to construct a regional model of an area slightly larger than the Pasco Basin. This model will then provide boundary conditions to a smaller scale but more detailed model of an area around the RRL. The purpose for the regional model is to reduce the uncertainty in boundary conditions which has plagued previous model studies (see Section 5). This reduction in uncertainty comes from extending the model to physical boundaries wherever possible. At this time the regional model has been constructed and to a degree, calibrated. The model has also been used to test several conceptual models. The smaller scale model has been constructed, including the assignment of boundary hydraulic heads taken from the calibrated regional model. However, we are currently having difficulty obtaining a convergent solution. The following sections describe both the regional and smaller scale models in detail.

7.1. REGIONAL MODEL OF THE EXTENDED PASCO BASIN

The approach to building a regional model of the area around the RRL was to start with a relatively simple conceptual (and numerical) model. Then calibration of the model was attempted by trying to reproduce the measured hydraulic heads while using hydraulic parameters that were within the range of their measured values. If calibration could not be obtained in this manner, then additional complexities were added to the conceptual model. This resulted in the testing of several conceptual models. For discussion purposes, the following sections have been divided into a description of the two major conceptual models.

7.1.1. INITIAL REGIONAL MODEL

The initial conceptual model for ground-water flow in the Pasco, Yakima, and Horse Heaven Hills basins consists of four homogeneous, isotropic layers. These layers correspond to the Grande Ronde Basalts, Wanapum Basalts, Saddle Mountains Basalts, and the alluvium which consists of the semi-consolidated Ringold and Hanford Formation. The sedimentary interbeds have been lumped into the three basalt layers. Water-table conditions have been assumed for the top layer. The lower layers are then considered to be confined.

7.1.1.1. MODEL DESCRIPTION

NUMERICAL IMPLEMENTATION

The computer code used to simulate regional ground-water flow was the New Mexico Finite-Difference 3-D model (NMFD3D) (Posson and others, 1980). This computer program simulates three-dimensional ground-water flow in a porous media. It solves the steady-state and transient isothermal ground-water flow equations using a block-centered finite-difference method which utilizes the strongly implicit procedure (SIP) for matrix solution.

The extended Pasco Basin model grid has 47 rows and 44 columns. All active nodes are 2 miles square (Figure 7.1). The NMFD3D code requires the outer rows and columns to be explicitly included as no-flow boundaries. The thicknesses of the represented layers were calculated from average reported thicknesses. These are 1784', 1096', 751', and 400' for the Grande Ronde, Wanapum, Saddle Mountains, and alluvium respectively.

BOUNDARY CONDITIONS

The boundary conditions for the regional model were taken from

the Interagency Hydrology Task Force Model constructed by Tony Zimmerman at PNL (Figure 7.2). No-flow boundaries were placed along outcrop areas and assumed ground-water divides. Where a layer is incised by a river, constant heads were used to represent assumed hydraulic communication between the layer and the river. Where it was not feasible to extend to the model to the limit of a layer or an incising river, constant-head boundaries were used. The values of the heads along these boundaries were interpolated from heads measured at nearby wells. The use of the kriging interpolation procedure to estimate these boundary conditions from measured head data is discussed in Appendix C.

Illustrated in Figures 7.3 to 7.6 are the boundaries for each layer. The boundaries of the alluvium (layer 4) are illustrated in figure 7.3. Constant heads represent contact with the Columbia River, Yakima River, Snake River, and Walla Walla River. No-flow boundaries represent the limits of the saturated portions of the alluvium.

The boundaries of the Saddle Mountain Basalts in Figure 7.4 consist of constant-head nodes where the rivers incise the basalt and where the Saddle Mountains extend beyond the modeled region. No-flow boundaries are enforced where this basalt sequence crops out in the west.

The Columbia and Yakima Rivers incise the Wanapum at points in

the north, southwest, southeast and in the west (Figure 7.5). However, the Grande Ronde is in contact with only small regions of the Columbia, Walla Walla, and Yakima Rivers (Figure 7.6).

Recharge to the system is represented as wells pumping water into the top active layer. The recharge distribution was estimated from contour maps of areal precipitation (see Bonano and others, 1986). The recharge rate was calculated from the amount of precipitation and the percentage of the precipitation that is assumed to recharge the system. This percentage ranged from 5% in the western highlands to 0 in the Pasco Basin area.

HYDRAULIC PARAMETERS

Hydraulic parameters used in this steady-state model included: 1) hydraulic conductivity for the unconfined layer; 2) transmissivities for the confined layers; and 3) leakances between the layers (that is, the effective vertical hydraulic conductivity between the layers divided by the distance between the centers of the layers). Very few reliable estimates of transmissivity have been obtained for the modeled layers. Therefore, initial transmissivities were estimated from hydraulic conductivity measurements of each of the units (flow tops, interiors, and interbeds) that make up each model layer. These initial values of hydraulic conductivity were taken from the median values of the ranges reported in Bonano and others

(1986). Model transmissivities were then calculated from the conductivity and thickness of the constituent units as shown in Figure 7.8. The model calculates a transmissivity for the unconfined layer from the user-input hydraulic conductivity times the difference between the predicted hydraulic head and the bottom elevation. These bottom elevations for the top layer were taken from U.S. Geological Survey maps and from geological maps from Meyers and others (1979). Vertical leakances were calculated from the vertical hydraulic conductivities and assumed thicknesses. The initial parameter values used by the model are listed below.

Initial Values of
Transmissivities and Vertical Leakance

Leakance for layer 1 .47E-14
Leakance for layer 2 .93E-13
leakance for layer 3 .24E-12
Transmissivity for layer 1 .36E-03
Transmissivity for layer 2 .13E-01
Transmissivity for layer 3 .22E-02

HYDRAULIC HEADS USED FOR BOUNDARY CONDITIONS
AND MODEL COMPARISON

As stated previously, measured hydraulic heads were used to interpolate values for constant-head boundary conditions. In addition, model calibration was performed by comparing measured and model-predicted hydraulic heads. Thus, a kriging procedure was used to produce the interpolated heads for boundary conditions and to provide an estimate of the hydraulic head at each model node for comparison during calibration (See Appendix C for a discussion of the application of kriging). Flow directions implied by the kriged head surface for the three basalt layers are illustrated in Figures 7.9, 7.10 and 7.11. Hydraulic heads in the alluvium were not kriged because no constant head boundaries are used in this layer and the calibration focused on comparisons between measured and model-predicted heads in the basalt layers. In the basalt layers, flow is generally toward the Columbia River and then to the southeast. In the vicinity of the RRL, in the Saddle Mountains Basalt, the horizontal gradient is nearly zero. The horizontal gradient for the Wanapum in the same area is .005 and for the Grande Ronde the gradient is .004. A comparison of hydraulic heads with depth shows an increase in heads from the Saddle Mountains Basalts to the Wanapum Basalts, and then a decrease in heads from the Wanapum Basalts to the Grande Ronde Basalts (Figure 7.12).

7.1.1.2. MODEL RESULTS

Results of the initial model are shown in Figures 7.13 through 7.18. As stated before, the measured hydraulic heads were kriged to provide a general picture of the flow system to be used in comparison with model results. While these surfaces allow for qualitative comparisons, they should not be given too much credence as they are based on relatively few data points, especially in the Grande Ronde Basalts. Therefore the following comparisons are based mainly on the features of the kriged map that would probably not change with additional data. In general, the simulated hydraulic heads are much higher than those implied by the kriged values. Additionally, simulated flow directions differ from those inferred from the kriged heads. Another obvious problem with the simulation is its inability to reproduce the large areas of very low gradient in the central to southeastern parts of the basalt layers. Among the possibilities for the model problems are: 1) either the amount of recharge to the system is too large or; 2) the input conductivities and therefore transmissivities and vertical leakances are too low.

Given that the initial model was unable to reproduce the kriged head, two types of modifications were made in an attempt to calibrate the model. First the influence of various geologic structures and hydrologic phenomena were tested. These included a hypothesized barrier transverse to the Cold Creek Syncline, the waste water disposal ponds, and the Gable Mountain-Gable

Butte structure . Following this, uniform changes to the transmissivities of the basalt layers, the conductivity of the alluvium layer, and the leakances connecting layers were made. Following is a summary of the various permutations of the initial model that were made:

1. Inclusion of an impermeable region simulating the Cold Creek Barrier;
2. Inclusion of high vertical connection at Gable Mountain and Gable Butte.
3. Inclusion of the waste-water ponds in 200 west and 200 east areas.
4. A combination of Gable Mountain/Gable Butte with the Cold creek Barrier.
5. Three simulations with the vertical conductivities increased from their initial values by increments of 2 orders of magnitude.
6. Three simulations with both the vertical and horizontal permeabilities varied.

Following is a discussion of the results of each of the above model variations.

COLD CREEK BARRIER

The "Cold Creek barrier" is known only from hydrologic evidence. That is, hydraulic heads in the Wanapum Basalts on the west side of the barrier are much higher (about 500 feet) than on the east side. Relatively large head differences also exist in the Grande Ronde (about 200 feet difference) and the Saddle Mountains Basalts (about 40 feet). Possible effects of this feature were tested by treating the it as a vertical zone of very low permeability. Specifically, the "barrier" was simulated by including a block of very low transmissivity nodes. These three nodes (a total of 6 miles) were located in column 25 and extended from row 13 to row 15. Vertically the model "barrier" extended down through the Wanapum Basalts from the Saddle Mountain Basalts. At the time the model was constructed, the available evidence was not clear as to whether or not the barrier penetrates the Grande Ronde. Therefore, it was not included in layer 1 in these simulations. All other hydraulic parameters were the same as those used initially

Results of this simulation are shown in Figures 7.19 through 7.21. Also shown on these figures are the results of the initial simulation so that the effects of the model changes can be more easily evaluated. As can be seen in Figure 7.19, ground-water flow in the Saddle Mountain Basalts was deflected

around the barrier, as was expected. This dropped the heads at the RRL from about 1200 feet to about 1120 feet, still much higher than the measured values. The horizontal gradient in the Saddle Mountains Basalts decreased from about .008 to .004 in the vicinity of the RRL. Ground-water flow in the Wanapum Basalts was also deflected around the barrier (Figure 7.20). These heads, at the RRL, dropped about 10 feet. More importantly, the ground-water flow changed direction. Flow was deflected away from the point where the Wanapum Basalts are incised by the Columbia River to the southwest. The horizontal gradients remained nearly the same, .001. Ground-water flow in the Grande Ronde was not affected (Figure 7.21).

Vertical hydraulic gradients were examined from model nodes that are near the McGee well west of the barrier, the RRL east of the barrier, and the 200 Ponds area east of the RRL (Figure 7.22). When compared to the vertical profile plot for the initial run (Figure 7.18), little change, other than a slight shift in the Saddle Mountains head elevation, can be noted. The vertical gradient is still upward from the Saddle Mountains Basalt where the alluvium exists above the Basalts and downward where the alluvium is absent. In the 200 ponds area, the vertical gradient is slightly downward in the Wanapum and Grande Ronde but upward from the Saddle Mountains Basalts.

Figure 7.23 is an east-west section of the model calculated heads through the repository showing the simulation with the

cold creek barrier as well as the initial simulation. The heads are virtually unchanged.

GABLE BUTTE/GABLE MOUNTAIN STRUCTURE

For variation from the initial model, fracturing along the anticline associated with Gable Mountain and Gable Butte was assumed to provide a high degree of vertical connection through the basalt units. The anticline's effect on the vertical flow was simulated by applying a vertical conductivity of about 1 ft/d at model nodes representing this structure. This value is approximately 10^5 larger than any other vertical conductivity in the model. All other hydraulic parameters remained unchanged from the initial simulation.

The addition of the Gable Butte and Gable Mountain features to the model caused an overall lowering of the simulated potentiometric surface in the vicinity of the RRL (Figures 7.24 -7.29). In the Grande Ronde (Figure 7.24), the horizontal gradient remained at .001 but the direction of flow away from the proposed repository location has changed from southeast to slightly northeast. Model-predicted flow directions in the vicinity of the RRL change in a similar manner for the Wanapum and Saddle Mountains Basalts. The direction of flow in the Wanapum from the RRL is toward Gable Mountain with a slight increase in the horizontal gradient (Figure 7.25). The

horizontal gradient in the Saddle Mountains Basalts near the RRL is toward the Gable Mountain area (Figure 7.26). This gradient is only slightly less than the gradient in the original model even though the piezometric surface is lower in the vicinity of the RRL when compared to the original simulation. The increased leakance used to simulate Gable Mountain and Gable Butte raised the potentiometric surface in the alluvium with flow at a steeper gradient away from the hills toward the Columbia River (Figure 7.27).

A vertical east-west cross-section through the RRL is shown in Figure 7.39. This figure demonstrates the decline in the potentiometric surface caused by the high conductivity zone at Gable Mountain and Gable Butte. This decline is about 100 feet near the RRL. However, the effect of this feature extends only over a small part of the modeled region.

The model-predicted vertical hydraulic gradient (Figure 7.29) between the Grande Ronde Basalt and Wanapum Basalts is small (.002) but the vertical gradient from the Wanapum Basalt to Saddle Mountains Basalts is larger and downward at the 200 pond area. Near the RRL the vertical gradient is downward from the Saddle Mountains to the Wanapum Basalts (.03) but not as large as in the 200 ponds area. At McGee Well the gradient from the Saddle Mountains Basalts to the Wanapum is also downward but much less than at the other 2 locations. The hydraulic gradient in the Saddle Mountains Basalts is strongly downward in areas where the alluvium is present.

SIMULATION WITH U-POND AND B-POND

The effect of disposal ponds in the 200 east and 200 west areas was also included in an attempt to calibrate the regional model. These ponds are used to collect waste water and cooling water from Hanford industrial activities. The largest ponds in the vicinity of the RRL are U-Pond and B-Pond. The amount of water that leaks to the alluvium was estimated by Newcomb (1978) and Gephart and others (1979) in order to determine the rate of recharge to the alluvial aquifer. The rates were calculated: one based on a 30 year average infiltration rate and one based on 1978 data. The model was used to simulate both rates, however, the predicted results were very similar. Therefore, the following discussion is limited to the results of the simulation which utilized the 30 year average. The recharge was simulated in the model by wells placed at the nodes corresponding to the locations of U-Pond (Row 13,column 26) and B Pond (row 13,column 30).

The recharge rates for wells at model nodes Row 13/column 26 and Row 13/column 30 were increased to simulate leakage from the waste water ponds. All other parameters remained identical to those used in the initial run. All other parameters were kept at the original values.

Including these ponds in the model had no effect on the hydraulic heads in the Grande Ronde Basalt and the Wanapum Basalt (Figures 7.30 and 7.31). Saddle Mountains heads were increased only in the immediate vicinity of the ponds (Figure 7.32). Its potentiometric surface rose 32 feet below B-Pond and 30 feet below U-Pond. As expected, the greatest effect was in the alluvium (Figure 7.33 and Figure 7.34).

GABLE MOUNTAIN/GABLE BUTTE WITH THE COLD CREEK BARRIER

This configuration combined the modifications used to represent both the Gable Mountain - Gable Butte feature and the hypothesized hydrologic barrier. The hydraulic parameters were identical to those used in the initial run with the exception of the changes needed to represent the simulated features.

The effects of the structures on the piezometric surface are illustrated in Figures 7.35 through 7.38. Model-predicted flow in the Grande Ronde Basalts near the RRL (Figure 7.35) is generally to the east-northeast. Ground-water flow in the same vicinity in the Wanapum Basalts is toward the Gable Mountains/Gable Butte area (Figure 7.36). Flow in the vicinity of the RRL in the Saddle Mountains is deflected around the barrier and toward the Gable Butte/Gable Mountain area (Figure 7.37).

The vertical gradient in the Gable Mountain and Gable Butte area is small from the Grande Ronde Basalt to the Saddle Mountain Basalts but increases noticeably from the Saddle Mountains to the alluvium (Figure 7.38). In the vicinity of the barrier, the gradient is very steep from the Saddle Mountain to the Wanapum Basalts.

UNIFORM PARAMETER MODIFICATIONS

Each of the simulations discussed above included a representation of some physical aspect of the system not considered in the initial run. Although each of these had some influence on nearby heads, none produced a large change in heads over a significant area. Therefore, the heads calculated in each of the above simulations were still considerably larger than the kriged heads. Thus, in order to achieve a general reduction in the piezometric surface, the model parameters were varied uniformly over the entire modeled region.

Both the vertical and horizontal conductivities were increased in order to reduce the simulated heads. Leakage values were increased uniformly by 2, 4, and 6 orders of magnitude. Horizontal conductivities were increased uniformly by factors of 2 and 4. The relative magnitude of these changes reflects our very subjective feeling about the relative uncertainty in these parameters.

Typical results of the parameter variation simulations are displayed in Figure 7.39 . Increasing leakance reduces heads by providing greater connection to the ultimate point of discharge, the Columbia River in layer 4. If the leakance is increased to 4 orders of magnitude or more, heads in the lower layers are dominated by heads in the alluvium. The vertical gradient effectively vanishes. If the increase in leakance is less than 4 orders of magnitude, the heads remain uniformly above the interpolated heads.

7.1.2. ANALYSIS OF THE INITIAL MODEL

A shortcoming of the initial extended Pasco Basin model was its failure to reproduce a prominent feature of the observed heads: the large area of low gradient, roughly underlying the Hanford Formation. Because of the assumed homogeneity of the units, the only possible mechanism for producing variations in gradient corresponding to the extent of the Hanford Formation with this model was through connection to the layer representing the Hanford Formation itself. Although the simulations with globally increased leakance coupled with increased alluvium conductivity did show an area of low gradient underlying the Pasco, the extreme increase in leakance required to produce this effect consequently reduced the vertical head difference between

the lower three layers outside the limits of the Hanford Formation. Contrarily, the head surface interpreted from measured values shows significant differences in heads between layers outside the Pasco Basin.

The implication is that the flow system, even in the deeper units, is significantly different in the area roughly corresponding to the Pasco Basin than the flow system outside this basin. The most dramatic demonstration of this contrast are the data used to infer the existence of the 'Cold Creek Barrier'. This does not mean, however, that the flow system inside of the Pasco Basin is in any way isolated from the remaining area. On the contrary, all of the kriged head maps indicate that the majority of flow in the system discharges in the Pasco Basin.

7.1.3. REVISED REGIONAL MODEL

A revised regional model of the extended Pasco Basin was constructed after the failure of the initial model to reproduce the measured hydraulic heads. Recall that the original model was based on a simple conceptual model of the site, that is, homogenous, continuous layers. Therefore, the approach to revising the model was not based on additional assumptions as much as just including the more complex geometry of the system that is known from drill holes and outcrops. In addition, the

boundary conditions that had been defined by the Interagency Task Force were reviewed and subsequently revised.

First of all, cross section maps and structural maps prepared by RHO (Myers and others, 1979) were examined for an indication of geologic correlates to the observed 'flat spot' underlying the Hanford Formation or the inferred boundaries of this region of low hydraulic gradient. Because of the paucity of data, particularly outside the RRL, the cross sectional maps are sketchy, and so amenable to many interpretations, as well as being occasionally inconsistent. One section, for example, shows undifferentiated Ringold extending through RRL-2, while another section through the same well shows the same formation pinching out thousands of feet from the well. Although the cross sections don't suggest structural boundaries for the 'flat spot', the area of low gradient seems to correspond to regions of significant sedimentary deposition, suggesting that interbeds may significantly affect flow in regions where they are present. Additional evidence for areas of interbed-dominated flow is supplied by Lehman (1983), who found a correlation between the presence of interbeds and the occurrence of a water type whose chemical composition is consistent with a mixture of water from deep basalts and shallow units. Additionally, any sharp slope defining the limits of depositional features also limits the extent of some of the basalt flows. In this case, flow tops may pinch out in the vicinity of interbed disappearance. The abrupt disappearance of both flow tops and

interbeds would result in a corresponding change in transmissivity.

Another problem with the initial model was the inability to produce the low vertical gradient in the Pasco Basin. This similarity of heads in all units in the Pasco Basin can be assumed to indicate vertical connection between units or that each unit is separately connected to a common discharge point. One such possibility is the fault postulated to coincide with the Columbia River north of Richland. Hydraulic connection along this fault coupled with relatively large horizontal conductivities of each layer could produce the region of low gradient evident from the head data. Note that the vertical connection assumed at Gable Mountains/Gable Butte did not extend over this large of a region nor did it provide as direct a connection to the Columbia River.

Another possible mechanism for vertical connection is through the sedimentary interbeds. If the assumption is made that vertical flow through the dense interiors is controlled by discrete fractures that are spaced a relatively large distance apart, then horizontal continuity along the top and bottom of the dense interior must be present to connect the fractures of one dense interior to those of the adjacent dense interior. In areas where the interbeds are absent, horizontal flow is mainly through flow tops and bottoms. These units are of varying thickness and extent, with complete pinch outs of flows being

quite common. The interbeds, on the other hand, extent continuously over a large part of the Pasco Basin. Thus, by providing a pervasive lateral connection, the interbeds may also connect vertical fractures through the interiors, thereby effectively increasing the vertical conductivity of the flow system in the basalts.

Finally, while reviewing the structural maps of the Pasco Basin for possible associates with the 'flat spot' in the potentiometric maps, the use of several structures to infer boundary conditions in the initial model was found to be questionable. That is, existing boundary conditions did not appear to correctly represent the actual boundaries of the basalts. For example, the southern and eastern edges of the Grande Ronde were represented as no-flow boundaries, while the formation extends well beyond the limits of the model. The same was true of the layer used to represent the Wanapum. A portion of the eastern edge of the Saddle Mountains Basalt was similarly truncated, while discontinuities in the northern and eastern edges were not included. Additionally, the water level data did not indicate any type of ground-water divides associated with these boundaries. Finally, the initial amounts of recharge taken from Bonano and others (1986) were recalculated. Thus, after considering structural data and extant water level data the following inferences were made regarding the influence of structures on the model boundary conditions

The Horse Heaven feature separates the flow system in the Horse Heaven basin from systems to the north in both the Saddle Mountains and Wanapum basalts. Because the Grande Ronde is continuous across this structure and because the available (sparse) water-level data do not indicate any ground-water divide in the Grande Ronde, it was assumed to be hydraulically continuous across this structure.

The Rattlesnake Hills, Yakima, and Umtanum anticlines bound three troughs of the exposed Wanapum basalt in the northwest. These independent systems are joined to the east approximately where the bounding features turn to the south.

The Saddle Mountains basalt is discontinuous across the Rattlesnake anticline. This discontinuity effectively isolates the Saddle Mountains in the Yakima Basin from the formation in the Pasco Basin. The two systems are joined in the vicinity of Badger Mountain.

In addition to the changes discussed above, the initial amounts of recharge taken from Bonano and others (1986) were recalculated. In order to do this, basin budgets given in RHO-BWI-ST-5 were used to suggest the following recharge percentages:

Pasco Basin - 1% of rainfall
Yakima Basin - 3% of rainfall
Horse Heaven Hills Basin - 6% of rainfall

7.1.3.1. DESCRIPTION OF THE REVISED MODEL

Boundary conditions and recharge distribution used in the revised model are shown in figures 7.40 through 7.44. No-flow conditions were imposed along the physical boundaries of the layers. Discontinuities due to faulting were represented in one of two ways: if the fault was oriented parallel to one of the grid axes only the directional transmissivity perpendicular to the fault was zeroed. If the orientation of the fault was not parallel to the grid, all components of transmissivity were zeroed. This later approach results in the discontinuities being represented as 2 miles wide. Therefore, the first approach is preferable because the node representing the discontinuity can also represent flow parallel to the discontinuity.

As with the initial model, wells were included to represent recharge to exposed layers. A recharge rate for a given node was calculated from precipitation data and the percentage of rainfall that was assumed to become recharge (see Figure 7.44). Constant head nodes were used to represent connection between

the layers and the rivers, as well as the influence of units extending beyond the modeled region. Calculation of head values for the revised model is described in Appendix C. Note that the measured heads had to be re-kriged not only because of the different boundary conditions but also to account for the discontinuities that were shown to exist in the Wanapum and Saddle Mountains Basalts.

Hydrologic Parameters

Initial parameter values were the same as those used in the original model (median values of the ranges given in Bonano and others, 1986). Calibration was approached by making order-of-magnitude changes in these values, and comparing the resulting error index in each layer (see Appendix C for a discussion of the error index). Conductivity and leakance were initially changed for each layer as a whole. The influence of more highly conductive interbeds was then simulated by making separate changes to conductivity in nodes thought to contain significant thicknesses of interbeds.

The extent and thickness of the interbeds through the basin is not well known. For this reason the data for all interbeds was used to define the limits of a generic interbed. Conductivities of the nodes within this region were varied separately in each layer, but the region of augmented conductivity was the same for

each layer. Estimated boundaries of various interbeds from Myers (1979) are shown in figure 7.45, along with the nodes considered to be influenced by the presence of interbeds. Because of the high conductivity of some of the interbeds, the effective horizontal conductivities of large intervals where these interbeds exist could easily be orders of magnitude higher than the conductivity of intervals where the interbeds are absent. On the other hand, the influence of the interbeds on the effective vertical leakance could be negligible or extreme (see Section 6). To check the possible effects of the interbeds, the following changes were made to the model.

First of all, horizontal hydraulic conductivities for the regions influenced by interbeds were adjusted independently of the conductivities in the rest of the model. By increasing the horizontal conductivities in the interbed regions hydraulic gradients in these regions can be substantially reduced, as expected. Then, selective increasing of the leakance to simulate greater effective vertical connection in the interbed regions reduced the heads and vertical gradients, while preserving the large head differences between layers seen outside these regions. Finally, by varying the conductivity and leakance regionally the error index was improved considerably over runs where the conductivity and leakance were changed uniformly over each region.

7.1.3.2. MODEL RESULTS

Contour plots of model results having the lowest error index are shown in Figures 7.46 through 7.48, along with the kriged head surface and the results of the revised model which used the initial values of the hydraulic parameters. As mentioned above, the kriging of the measured heads was redone to account for the discontinuities that occur in some of the basalt units along the major geologic structures. Therefore, prior to discussing the model results a brief description of the new interpolated head surface is provided in the following paragraphs.

For the Grande Ronde Basalts, flow from the northwest and the southwest into the Pasco Basin is indicated, as well as discharge to the Columbia to the east and south. However, note that this interpretation is based on very sparse data. Kriged heads for the Wanapum Basalts indicate the Pasco Basin area receives recharge through the tongues in northwest bounded by the Umtanum, Yakima, and Rattlesnake anticlinal ridges. East of the Columbia River, the Wanapum Basalts of the Pasco Basin are also recharged from the north. Discharge is probably through the Saddle Mountains formation to the Columbia. Gradients in the Yakima Basin are primarily to the east, suggesting discharge to the Columbia River. Heads in the Yakima also exhibit a region of low gradient north of the contact with the Yakima River, although data in this area is scanty. The few

water-level measurements in the Horse Heaven Hills basin suggest flow from the northwest to the Columbia River in the south. Flow directions in the Saddle Mountains are similar to those in the Wanapum with both recharge and discharge locations being almost identical. The only difference, of course, is the the Saddle Mountains Basalts discharge water through the alluvium to the Columbia River where they are not in direct contact with the river and in some areas the Saddle Mountains Basalts may recharge the Wanapum Basalts. Finally, note that the new kriged heads show the same marked 'flat spot' in the hydraulic gradient in the Pasco Basin that was indicated by the original kriged head surface. This 'flat spot' is apparent in all of the basalt layers.

Heads calculated using the initial parameters are universally higher than the kriged heads. In addition, model-predicted Grande Ronde heads show an anomalous mound where the formation is recharged in the northwest. Also, heads of the Wanapum Basalts in the Pasco Basin are hundreds of feet above the kriged surface. The closest match to the kriged heads occurs in the southwest corner of the model, where the model-predicted head surface for the Wanapum Basalts is controlled by the imposed boundary conditions. Model-predicted heads for the Saddle Mountain Basalts are also overestimated, with the most pronounced mismatch occurring in the Horse Heaven Hills basin. Heads within this basin are controlled by recharge, discharge to

the Columbia along the south, and leakage to the Wanapum basalts.

A series of parameter variations was then made in an attempt to reduce the universally high heads of the initial model. The heads could be reduced by either decreasing recharge or increasing conductivity. Therefore, changes in horizontal conductivity, leakance, and recharge were made. Some changes were made globally, others to individual layers. The model run having the lowest error index is shown in figures 7.46d-7.48d. These heads resulted from simply increasing every leakance by three orders of magnitude. Gradients in Pasco Basin have been reduced considerably, because of the increased connection to the highly conductive alluvium, and heads in all layers have decreased. Although this surface is an improvement on the initial heads, the Pasco Basin heads still show too steep a gradient. Also, because of the global increase in leakance, vertical gradients outside the Pasco Basin have been reduced, whereas the kriged data show large vertical gradients in portions of the Yakima and Horse Heaven Hills basins.

To solve the problems mentioned above, a series of simulations were made with conductivities varied separately in the portions of the model that contain interbeds. These simulations resulted in an improved match to the kriged heads. Results of the simulation having the lowest error index are shown in figures 7.46c-7.48c. Leakance values outside the region assumed to be influenced by interbeds were increased by 2 orders of magnitude

over the initial values. Leakance values within the interbed-affected region were increased by 3 orders. Horizontal conductivities in the interbed areas were increased by 2 orders of magnitude; conductivity in the alluvium was raised by 1 order of magnitude. The portion of the model where interbeds are included shows very little hydraulic gradient, as expected. Relatively large gradients remain outside the Pasco Basin.

7.2.LOCAL MODEL

The local model of BWIP is a more detailed representation of the flow field in the vicinity of the RRL. The increased resolution of the local model near the repository allows a more accurate estimation of the transport path in this area, as well as providing a way to represent stresses associated with the construction and operation of the repository. The grid and its position with respect to the regional model are shown in Figure 7.49. In addition to smaller node spacing near the RRL, the local model also has more layers, allowing the repository horizon and adjacent units to be represented individually. The local model layering is shown in Table 7.1

No-flow boundary conditions were used to represent the physical discontinuities of the modeled units (or the edge of the saturated zone for the alluvium). Remaining boundary conditions for the local model were the constant heads interpolated from

the results of the regional simulation. These boundary conditions should constrain the local flow field to be consistent with the results of the regional simulation.

Local scale model parameters are calculated from the values assumed for each stratigraphic unit. The conductivities of these units are the medians of the conductivities found in the literature, modified for consistency with the calibrated regional model.

Modifications made to regional parameter values during calibration reflect assumptions about the conductivities of the stratigraphic unit. As an example, increasing the vertical conductivity of a regional model layer to improve the match of the regional head surface implies that the initial vertical conductivity of the flow interiors was too low, since these low conductivity units control the effective vertical conductivity of the regional model layer. Decreasing the horizontal conductivity of a regional layer implies a decrease in the horizontal conductivity of the flow tops and interbeds; the conductivities of these relatively transmissive units dictate the effective horizontal conductivity.

An input file for a local model corresponding to the regional run with the lowest error index has been constructed. The simulation was not converging at the time work on it stopped. We feel that using a smaller timestep and larger storage

coefficient at the beginning of the simulation should produce a convergent head surface from which a steady-state solution can be obtained.

The local model is currently capable of performing the following simulations with minor input changes:

Disposal ponds - These waste-water ponds are used by DOE for disposing of mildly radioactive water. Their influence on local hydrology can be simulated by including source terms in the nodes representing the location of the ponds. The rate of injection would be the estimated rate of infiltration of pond water. Note, that while these ponds were included in the initial regional model, they were not needed in the revised model to achieve an adequate match with the kriged heads.

Shaft construction - The representation of the large-scale drilling and the resulting shaft depend on the proposed method of construction as well as assumptions about, for example, the duration of drilling, the influence of construction on the surrounding rock, and the integrity of the grout used to seal the shaft annulus. The local model is flexible enough to allow many scenarios to be simulated. Construction stresses may be represented as constant heads at the assumed elevation of the drilling fluid, or at an elevation within the formation simulating drainage into the

shaft. Assumed damage to the rock surrounding the shaft can be modeled as changes in the effective connection of the heads in the nodes representing the shaft to the surrounding nodes in the model. Grout seal failure can also be simulated by increasing the leakance in the nodes representing the shaft.

Aquifer tests - The local model could be used to reproduce existing aquifer test data in order to verify calibration of the model, or to help in designing proposed hydrologic tests.

Scenarios involving alterations to the regional model, such as a hypothetical change in the location of the Columbia River, can also be readily represented at the local scale. Boundary condition calculation for the local scale model is automated, so that only the changes required to represent the physical alterations to the system, such as the relocation of the constant heads representing the river, need to be made manually.

8. SUMMARY AND RECOMMENDATIONS

This report has provided

- 1) A brief presentation of the existing geologic, hydrologic, and geochemical data collected at BWIP;
- 2) A Conceptual model developed from this data;
- 3) A review of numerical models based on BWIP data; and
- 4) A discussion of Sandia's regional and local BWIP numerical models.

Due to the scarcity of data, the formulation of a unique conceptual flow model is not possible. However several generalizations can be made from existing information. The hydrologic data suggest that the basalt flow tops and sedimentary interbeds are the pathways for most lateral ground water movement. These units receive recharge from exposed areas along the Yakima, Umtanum, and Rattlesnake Ridges, and along Horse Heaven Hills, with a an unknown quantity of recharge from the deep basalts. Discharge is to the Columbia and Yakima rivers, either directly or through overlying units. The regularity of head measurements in the Paso Basin suggest that the hydrologic system is regionally connected, however the lack of stratigraphic correlation between boreholes, and the

responses seen in monitoring wells to construction activity at nearby holes, suggest locally intermittent connection.

No numerical model of BWIP to date has been successfully calibrated, so that inferences about the behavior of the system cannot be made from their results. Each model reviewed in this report treats different hydrostratigraphic units, generally identified with the major basalt sequences, a combination of major sequences, or the most conductive members of the sequences. Comparison of parameters is consequently impossible. All models rely to some extent on interpolated boundary conditions. We believe the disparity in flow paths predicted by these models to be due to the differences in boundary conditions, rather than to the selection of hydrostratigraphic units.

We found that a numerical implementation of the conceptual model presented here was better able to reproduce the measured water levels with separate sets of parameters inside and outside the Pasco Basin. Presently, these two regions are being treated as homogeneous. Our best regional simulation has an associated error index of 0.68, however the error index for the Saddle Mountains layer is 1.1. We believe that the calibration of the regional model should be improved so that the maximum error index in any layer is less than 0.5.

Modeling of the Pasco Basin has been hampered by the scarcity of hydrologic data for the Grande Ronde. Existing Grande Ronde data is inadequate for characterizing the hydrology of this sequence. Insufficient data are available for establishing boundary conditions, or for evaluating numerical simulation results.

There is also a need for more detailed hydrologic data near the RRL. The unexplained contrast in heads across the "Cold Creek barrier", as well as the hydrographs presented in this report, suggest local discontinuities in the flow system. While the scale of these discontinuities may allow the hydrostratigraphic units to be considered continuous on a regional scale, their effects must be included in estimates of transport paths.

SELECTED REFERENCES

- Clifton, P. M., Baca, R. G., and Arnett, R. C., 1983. Stochastic Analysis of Groundwater Travel time for Long-Term Repository Performance Assessment, RHO-BW-SA-323P, Rockwell Hanford Operations, Richland, Washington.
- Delfiner, P., 1976. Linear Estimation of Non-Stationary Spatial Phenomena, in Guarascio and others, Advanced Geostatistics in the Mining Industry, NATO Advanced Study Institute Series, Reidel Publishing Co., Boston.
- Deju, R. A., and Fecht, K. R., 1979. Preliminary description of hydrologic characteristics and contaminant transport potential of rocks in the Pasco Basin, south-central Washington. RHO-BWI-LD-20, Rockwell Hanford Operations, Richland, Washington.
- DOE, 1982, Site Characterization Report for the Basalt Waste Isolation Project: DOE/RL-82-3 (3 volumes).
- DOE (U.S. Department of Energy), 1984. Draft Environmental Assessment: Reference Repository Location, Hanford Site, Washington. DOE/RW-0017 Washington, D.C.
- Gephart, R. E., R. C. Arnett, R. G. Baca, L. S. Leonhart, and F. A. Spane, Jr., 1979. Hydrologic Studies Within the Columbia Plateau, Washington: An Integration of Current Knowledge, RHO-BWI-ST-5, Rockwell Hanford Operations, Richland, Washington.
- Gephart, R. E., S. M. Price, R. L. Jackson, 1983. Geohydrologic Factors and Current Concepts Relevant to Characterization of a Potential Nuclear Waste Repository Site in Columbia River Basalt, Hanford, Washington. RHO-BW-SA-326P, Rockwell Hanford Operations, Richland, Washington
- Guzowski, R. V., F. B. Nimick, A. B. Muller, 1982. Repository Site Definition in Basalt: Pasco Basin, Washington, 1982. NUREG/CR-1352 (SAND81-2088), Prepared for U.S. Regulatory Commission, Washington, D.C.
- Kafritsas, J. and Bras, R. L., 1984. The Practice of Kriging (Second Edition). Technical Report No. 263. Ralph M. Parsons Laboratory, Department of Civil Engineering, M.I.T.
- La Sala, A. M., Jr., and G. C. Doty, 1971. Preliminary Evaluation of Hydrologic Factors Related to Radioactive Waste Storage in Basaltic Rocks at the Hanford Reservation, Washington, Open-file Report, U.S. Geological Survey, Washington, D.C.
- La Sala, A. M., Jr., G. C. Doty, and E. J. Pearson, Jr., 1973. A Preliminary Evaluation of Regional Ground-Water Flow in

South-Central Washington, Open-file Report, U.S. Geological Survey, Washington, D.C.

- Lehman, L., 1983. Hanford Reservation: Analysis of Chemical Data Released by DOE on February 15, 1983: Unpublished Report, dated March 27, 1983.
- Lehman, L., and E. J. Quinn, 1982. Comparison of Model Studies: The Hanford Reservation: NRC Memorandum to Michael Bell and Hubert J. Miller, dated March 30, 1982.
- Leonhart, L. S., 1979. Surface Hydrologic Investigations of the Columbia Plateau Region, Washington, RHO-BWI-ST-6, Rockwell Hanford Operations, Richland, Washington
- Leonhart, L. S., R. L. Jackson, D. L. Graham, G. M. Thompson, and L. W. Gelhar, 1982. Groundwater Flow and Transport Characteristic of Flood Basalts as Determined from Tracer Experiments, RHO-BW-SA-220 P, Rockwell Hanford Operations, Richland, Washington.
- Leonhart, L. S., R. L. Jackson, D. L. Graham, L. W. Gelhar, G. M. Thompson, B. Y. Kauchiro, C. R. Wilson, 1984. Analysis and Interpretation of a Recirculating Tracer Experiment Performed on a Deep Basalt Flow Top, RHO-BW-SA-300 P, Rockwell Hanford Operations, Richland, Washington.
- Long, P. E., and R. D. Landon, 1981. Stratigraphy of Grande Ronde Basalt, in Subsurface Geology of the Cold Creek Syncline, C. W. Myers and S. M. Price (editors), RHO-BWI-ST-14, Rockwell Hanford Operations, Richland, Washington.
- Myers, C. W. and others, 1979. Geologic Studies of the Columbia Plateau: A Status Report, RHO-BWI-ST-4, Rockwell Hanford Operations, Richland, Washington
- Newcomb, R. C., 1959. Some Preliminary Notes on Ground Water in the Columbia River Basalt, Northwest Science, vol. 33, no. 1, pp. 1-18.
- Newcomb, R. C., Strand, J. R., and F. J. Frank, 1972. Geology and Ground-Water Characteristics of the Hanford Reservation of the U. S. Atomic Energy Commission, Washington, U. S. Geologic Survey Prof. Paper 717.
- NRC, 1983. Draft Site Characterization Analysis of the Site Characterization Report for the Basalt Waste Isolation Project (Volumes 1 and 2): NUREG-0960.
- Olson, O. L., Letter to Robert Wright, October, 1984. U.S. Nuclear Regulatory Commission, Washington, D.C.
- Quinn, E., J., 1982. Analysis of Boundary Conditions and Conductivity Ratios used in Pasco Basin Modelling, NRC Memorandum to Malcolm R. Knapp, dated August 27, 1982.

Spane, F. A., Jr., P. D. Thorne, and W. H. Chapman-Riggsbee, 1983. Results and Evaluation of Experimental Vertical Hydraulic Conductivity Testing at Borehole DC-4 and DC-5, SD-BWI-TI-136. Rockwell Hanford Operation, Richland, Washington.

Leonhart, L. S., 1979. Surface Hydrologic Investigations of the Columbia Plateau Region, Washington, RHO-BWI-ST-6, Rockwell Hanford Operations, Richland, Washington.

Swanson, D. A., T. L. Wright, P. R. Hooper, and R. D. Bently, 1979. Revisions in Stratigraphic Nomenclature of the Columbia River Basalt Group, U. S. Geological Survey Bulletin 1457-G, Washington, D. C.

USGS, 1983. Review Comments on Site Characterization Report for the Basalt Waste Isolation Project: Letter from J. B. Robertson (USGS) to L. O. Olson (DOE/RL), Dated May 6, 1983.

Waters, A. C., 1961. Stratigraphic and Lithologic Variations in the Columbia River Basalt, American Journal of Science, vol. 259, pp. 581-611.

Williams and Associates Inc., 1983. Statistical Evaluation of Hydrochemical Data from the Saddle Mountains, Wanapum and Grande Ronde Basalts - Basalt Waste Isolation Project - Hanford Site: Report to U.S. Nuclear Regulatory Commission under Contract No. NRC-02-82-044.

Williams and Associates Inc., 1985. Statistical Evaluation of Additional Hydrochemical Data from the Saddle Mountains, Wanapum and Grande Ronde Basalts - Basalt Waste Isolation project - Hanford Site: Report to U.S. Nuclear Regulatory Commission under Contract No. NRC-02-82-044.

Table 3.1 Representative Hydraulic Properties of the Unconfined Aquifer (Gephard and others, 1979)

<u>Stratigraphic Interval</u>	<u>Hydraulic Conductivity (K)</u> <u>(feet per day)</u>
Hanford formation	500 - 20,000
Undifferentiated Hanford and Middle Ringold unit	100 - 7,000
Middle Ringold unit	20 - 600
Lower Ringold unit	0.11 10
<u>Region</u>	<u>Transmissivity (T)</u> <u>(square feet per day)</u>
North of Gable Butte and Gable Mountain	4,000 - 25,000
On the flank of Gable Butte and Gable Mountain and along paleochannels	40,000 - 600,000
Other areas on the Hanford Site	2,000 - 40,000
	<u>Storage Coefficients (S)</u>
Throughout the unconfined aquifer	0.01 - 0.1

Table 3.2 Grande Ronde Conductivities at RRL-2
 from RHO Interval Reports
 (Strait and Spane, 1982a,b,c,d, and e and 1983)

<u>Interval</u> <u>(depth below casing in feet)</u>	<u>Conductivity (ft/d)</u>
Middle Sentinel Bluffs flow top (2981 to 3020)	2.2*10 ⁻³
Middle Sentinel Bluffs vesicular zone (3057 to 3172)	1.6*10 ⁻⁵
Middle Sentinel Bluffs collonade/entablature (3175 to 3224)	6.4*10 ⁻⁸
Middle Sentinel Bluffs flow bottom (3247-3344)	9.9
Composite Umtanum flow top (3568-3781)	3.1
Umtanum fracture zone (3781-3827)	147

Table 3.3 Pasco Basin Water Budget
(Leonhart , 1979)

Precipitation/Infiltration/Deep Percolation

<u>Parameter</u>	<u>AF/yr</u>
Precipitation (P)	756,000
Evapotranspiration (ET)	750,000
Runoff (RO)	0

$$PR = - ET - RO = 6000 \text{ AF/yr (Probable groundwater recharge from precipitation)}$$

Stream Reach Inventory

<u>Parameter</u>	<u>AF/yr</u>
Inflow (IF), Priest Rapids Dam	87,230,000
Tributaries (TR)	43,832,000
Return Flows (RF)	225,000
Outflow (OF), McNary Dam	134,200,000

$$PSL = IF + TR + RF - DW - OF = -2,913,000 \text{ AF/yr (Probable groundwater discharge to the Columbia River)}$$

Water Use Inventory

<u>Parameter</u>	<u>AF/yr</u>	
	<u>GW</u>	<u>SW</u>
Municipal (M)	8,961	20,372
Industrial (IN)	15,361	403,675
Irrigation (IR)	47,760	907,600

$$AR = 0.1 IN_{sw} + 0.3 IR_{sw} = 313,000 \text{ AF/yr}$$

$$WG = 0.35 M_{gw} + 0.8 IN_{gw} + IR_{gw} = 63,000 \text{ AF/yr}$$

$$RAM = AR - WG = 250,000 \text{ AF/yr (Probable groundwater recharge from artificial mechanisms)}$$

Net Exchange

<u>Recharge Parameter</u>	<u>AF/yr</u>
Precipitation (PR)	6,000
Stream loss (PSL)	-2,913,000
Artificial mechanisms (RAM)	250,000

$$NR = PR + PSL + RAM = -2,657,000 \text{ AF/yr (Probable groundwater discharge from basin)}$$

Table 3.4 Hydraulic Heads within Selected Stratigraphic Intervals in the Saddle Mountains Basalt (Modified from DOE, 1982, Gephart and others 1979)

<u>Borehole Identification*</u>	<u>Aquifer**</u>	<u>Year of Measurements</u>	<u>Hydraulic Head Elevation (feet)</u>
DB-1	Mabton	1979	385
DB-2	Mabton	1979	385
DB-4	Mabton	1979	419
DB-5	Mabton	1979	407
DB-7	Mabton	1979	404
DB-9	Mabton	1979	403
DB-10	Mabton	1979	405
DH-8	Mabton	1979	403
WPPSS-3	Rattlesnake Ridge	1979	380
699-14-EEQ	Rattlesnake Ridge	1969	389
199-H4-2	Rattlesnake Ridge	1968	414
DB-12	Selah interbed	1978	401.9
	Mabton interbed	1979	401.9
DB-13	Elephant Mountain	1978	417.0
	flow top		
	Rattlesnake Ridge	1978	418.0
	/ interbed		
	Cold Creek interbed	1978	419.9
	Mabton interbed	1979	420.9

Table 3.4 (continued)

<u>Borehole</u>		<u>Year of</u>	<u>Hydraulic</u>
<u>Identification*</u>	<u>Aquifer**</u>	<u>Measurements</u>	<u>Head</u>
			<u>Elevation</u>
			<u>(feet)</u>
DB-14	Rattlesnake Ridge	1978	448.8
	interbed		
	Selah interbed	1978	423.9
	Cold Creek interbed	1978	422.9
	Mabton interbed	1979	421.9
DC-1	Selah interbed	1969	407.2
	Cold Creek interbed	1969	409.1
	Mabton interbed	1969	~400
DC-16A*	Rattlesnake Ridge	1982	448.2
	interbed		
	Selah interbed	1982	438.6
	Cold Creed interbed	1982	418.3
	Mabton interbed	1982	420.3

Table 7.1 Hydrostratigraphic Units Represented
in the Local Model

<u>Layer No.</u>	<u>Unit Name</u>	<u>Thickness(ft)</u>
17	Hanford/Ringold	400
16	Elephant Mtn/ Rattlesnake Ridge	173
15	Saddle Mtn Upper Basalts	266
14	Cold Creek Interbed/ Umatilla	227
13	Mabton Interbed/ Priest Rapids Flow Top	107
12	Priest Rapids Interior/ Roza	370
11	Upper Frenchman Springs	350
10	Lower Frenchman Springs	331
9	Vantage Interbed	23
8	Upper Sentinel Bluffs Flow Top	42
7	Upper Sentinel Bluffs Interior	247
6	Cohasset Flow Top	30
5	Cohasset Interior	194
4	Lower Sentinel Bluffs	320
3	Umtanum	71
2	Upper Schwana	150
1	Lower Schwana	730

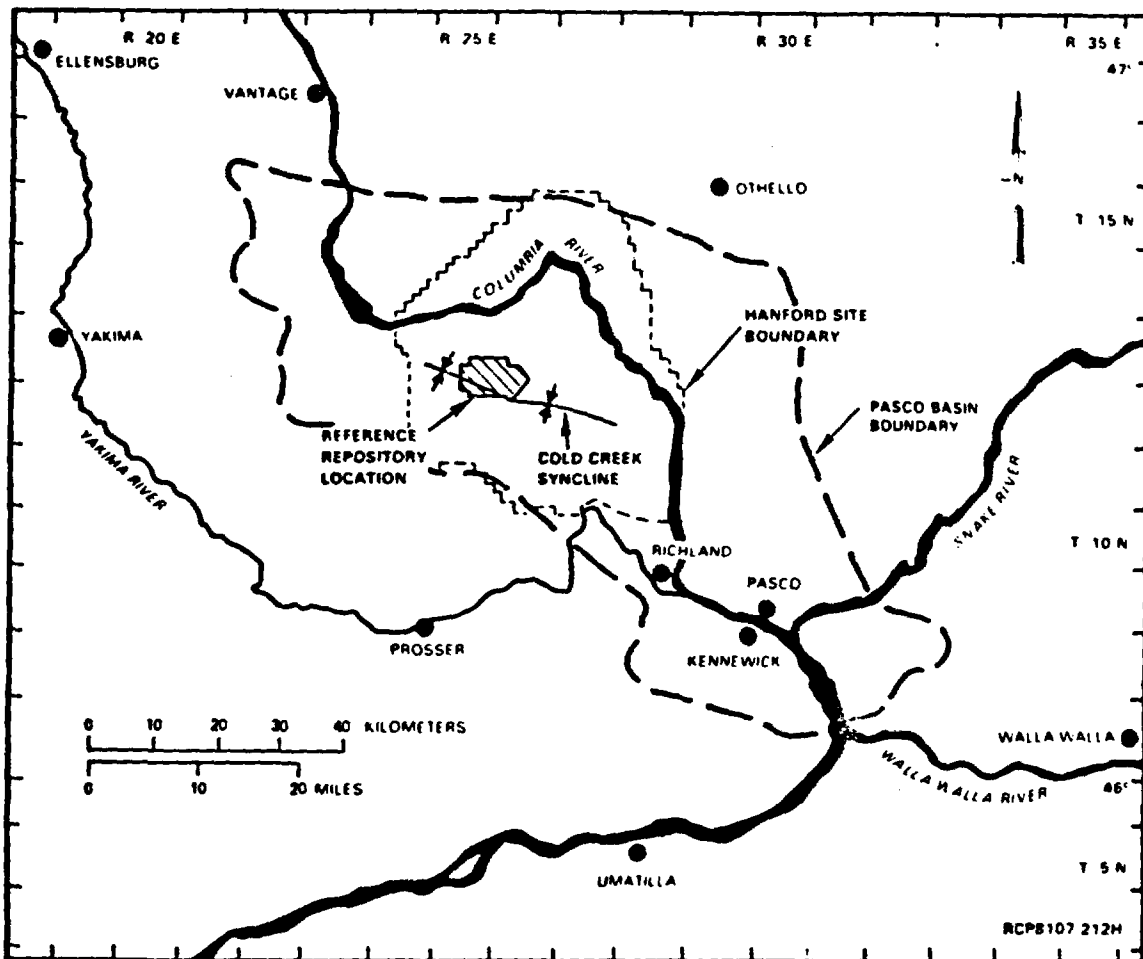
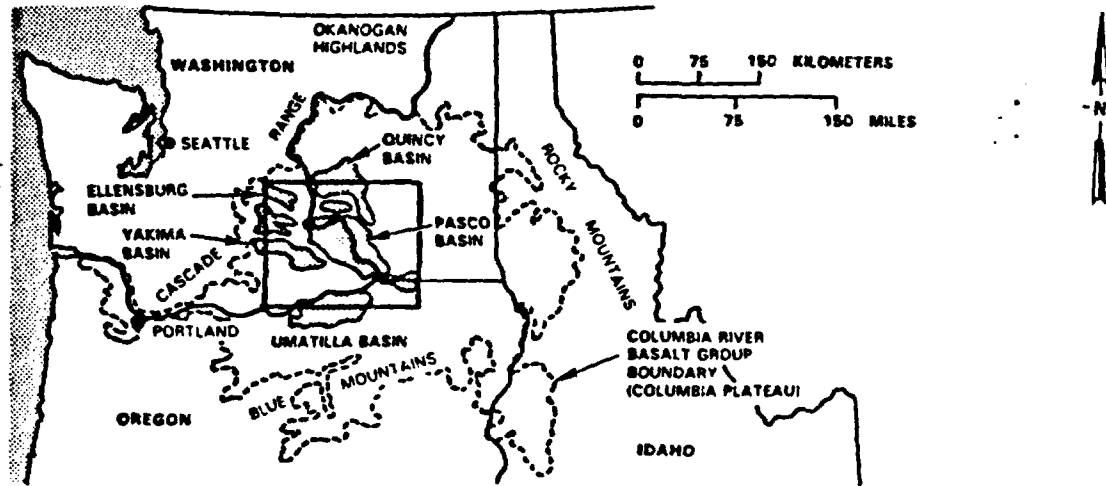


Figure 2.1 Location of the Hanford Site, Southeastern Washington State. (DOE, 1984)

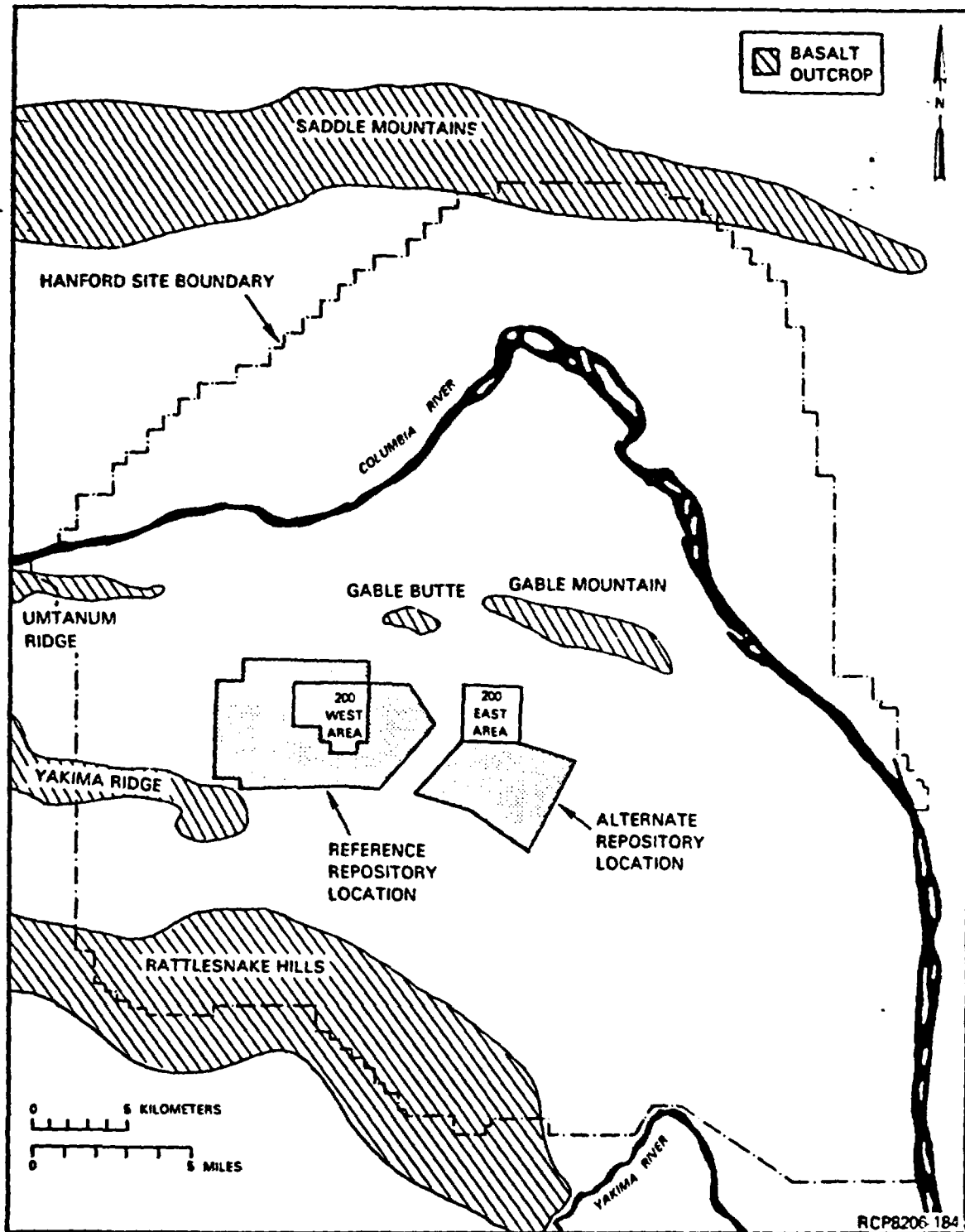


Figure 2.2 Reference Repository and Alternate Repository Locations. (DOE, 1984)

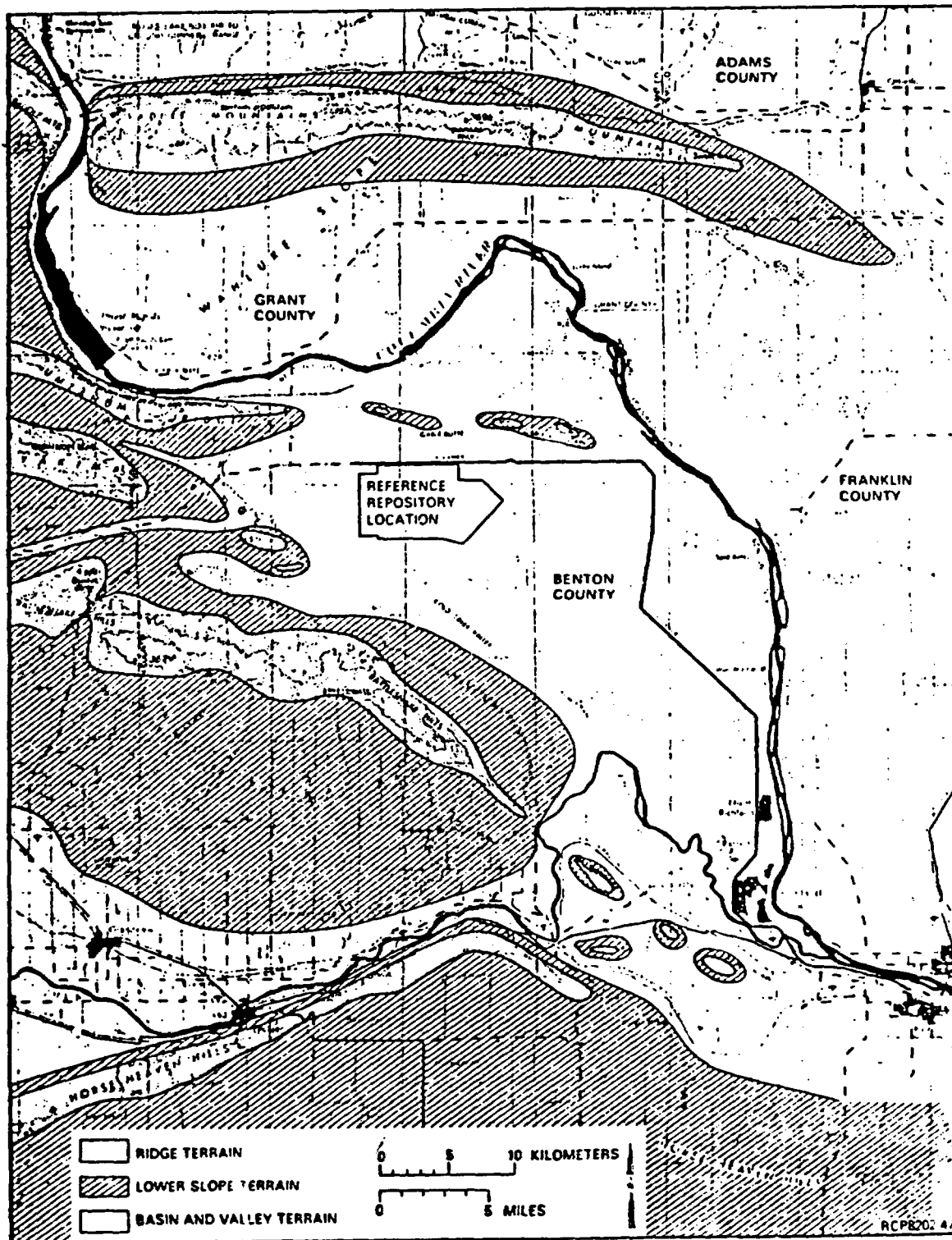


Figure 2.3 Map of Major Landform Systems of the Pasco Basin. (DOE, 1984)

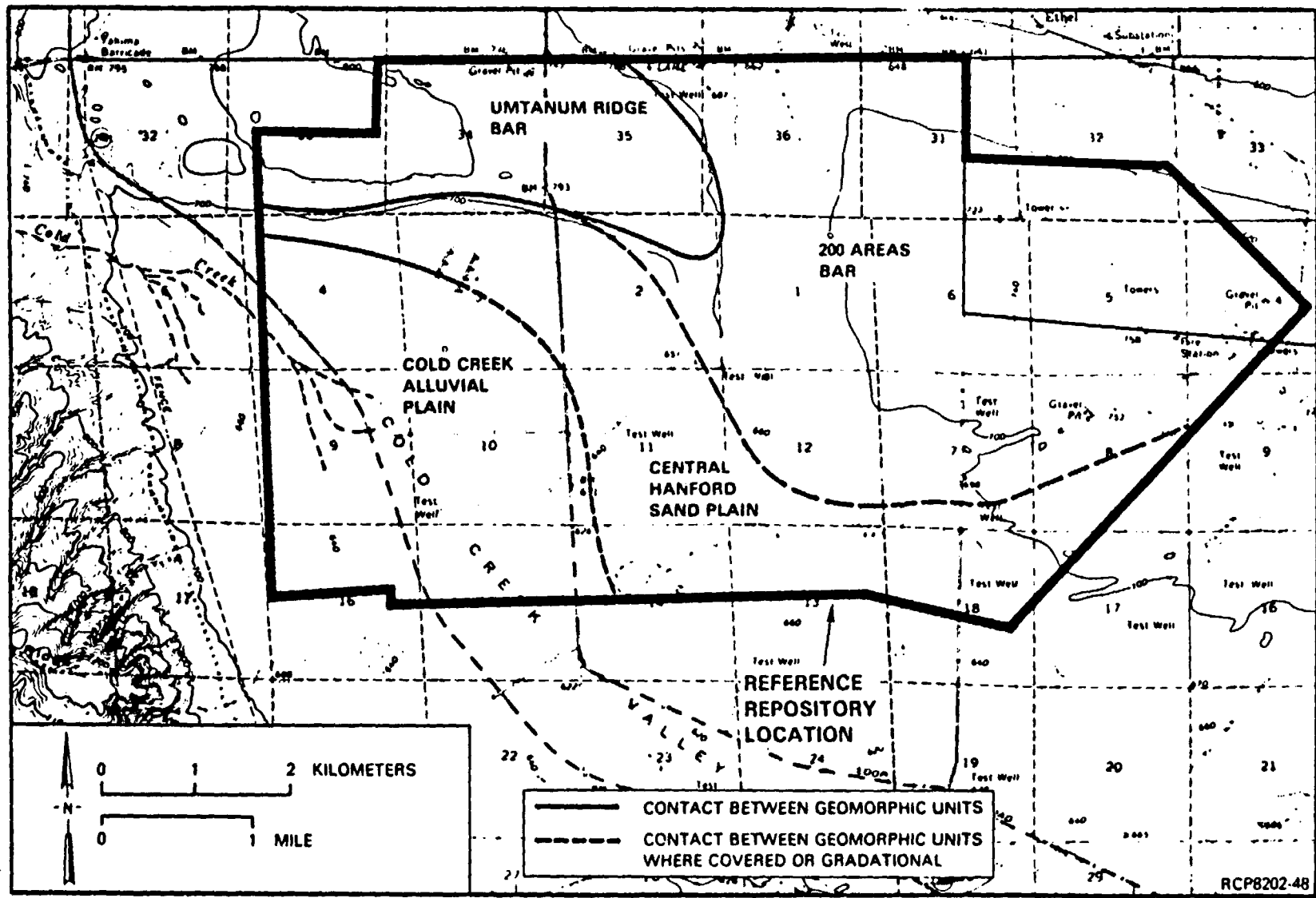


Figure 2.4 Geomorphic Map of the Reference Repository Location. (DOE, 1984)

SERIES	SUB-GROUP	GROUP	FORMATION	MEMBER	K-Ar AGE (10 ⁶ yr)	MAGNETIC POLARITY							
MIOCENE	Upper Miocene	COLUMBIA RIVER BASALT GROUP	YAKIMA BASALT SUBGROUP	LOWER MONUMENTAL MEMBER	6 ^a	N							
				// EROSIONAL UNCONFORMITY //									
				ICE HARBOR MEMBER									
				BASALT OF GOOSE ISLAND	8.5 ^b	N							
				BASALT OF MARTINDALE	8.5 ^b	R							
				BASALT OF BASIN CITY	8.5 ^b	N							
				// EROSIONAL UNCONFORMITY //									
				BUFORD MEMBER		R							
				ELEPHANT MOUNTAIN MEMBER	10.5 ^b	N.T							
				// EROSIONAL UNCONFORMITY //									
				Middle Miocene	COLUMBIA RIVER BASALT GROUP	YAKIMA BASALT SUBGROUP	Saddle Mountains Basalt	POMONA MEMBER	12 ^c	R			
								// EROSIONAL UNCONFORMITY //					
								ESQUATZEL MEMBER		N			
								// EROSIONAL UNCONFORMITY //					
								WEISSENFELS RIDGE MEMBER					
	BASALT OF SLIPPERY CREEK		N										
	BASALT OF LEWISTON ORCHARDS		N										
	ASOTIN MEMBER		N										
	// LOCAL EROSIONAL UNCONFORMITY //												
	WILBUR CREEK MEMBER		N										
	UMATILLA MEMBER		N										
	// LOCAL EROSIONAL UNCONFORMITY //												
	Lower Miocene	COLUMBIA RIVER BASALT GROUP	YAKIMA BASALT SUBGROUP					Wanapum Basalt	PRIEST RAPIDS MEMBER		R ₃		
									ROZA MEMBER		T, R ₃		
									FRENCHMAN SPRINGS MEMBER		N ₂		
				ECKLER MOUNTAIN MEMBER									
				BASALT OF SHUMAKER CREEK		N ₂							
				BASALT OF DODGE		N ₂							
				BASALT OF ROBINETTE MOUNTAIN		N ₂							
				Grande Ronde Basalt	17-15 ^d	N ₂							
Picture Gorge Basalt ^e				(15.8-14.6) ^{d,c}	N ₁								
Imnaha Basalt ^e					R ₁								

MEMBER	AGE	POLARITY
SWAMP CREEK MEMBER	?	?
CRAIGMONT MEMBER	?	?
GRANGEVILLE MEMBER	?	?
BASALT OF WEIPPE	?	?
BASALT OF LAPWAI	?	?
BASALT OF FEARY CREEK	?	?
ONAWAY MEMBER	?	?
BASALT OF POTLATCH	?	?

NEW MEMBERS AND INFORMAL BASALT UNITS CLEARWATER EMBAYMENT (CAMP. 1981)

ICICLE FLAT MEMBER

LEGEND
 N = NORMAL
 R = REVERSE
 T = TRANSITIONAL

^a DATA FROM McKEE et al. (1977)
^b DATA MOSTLY FROM WATKINS AND BAKSI (1974)
^c INFORMATION IN PARENTHESES REFERS TO PICTURE GORGE BASALT
^d THE IMNAHA AND PICTURE GORGE BASALTS ARE NOWHERE KNOWN TO BE IN CONTACT
 INTERPRETATION OF PRELIMINARY MAGNETOSTRATIGRAPHIC DATA SUGGESTS THAT THE IMNAHA IS OLDER

Figure 2.5 Stratigraphic Nomenclature for the Columbia River Basalt Group of the Columbia Plateau (after Swanson and others, 1979b in DOE, 1984)

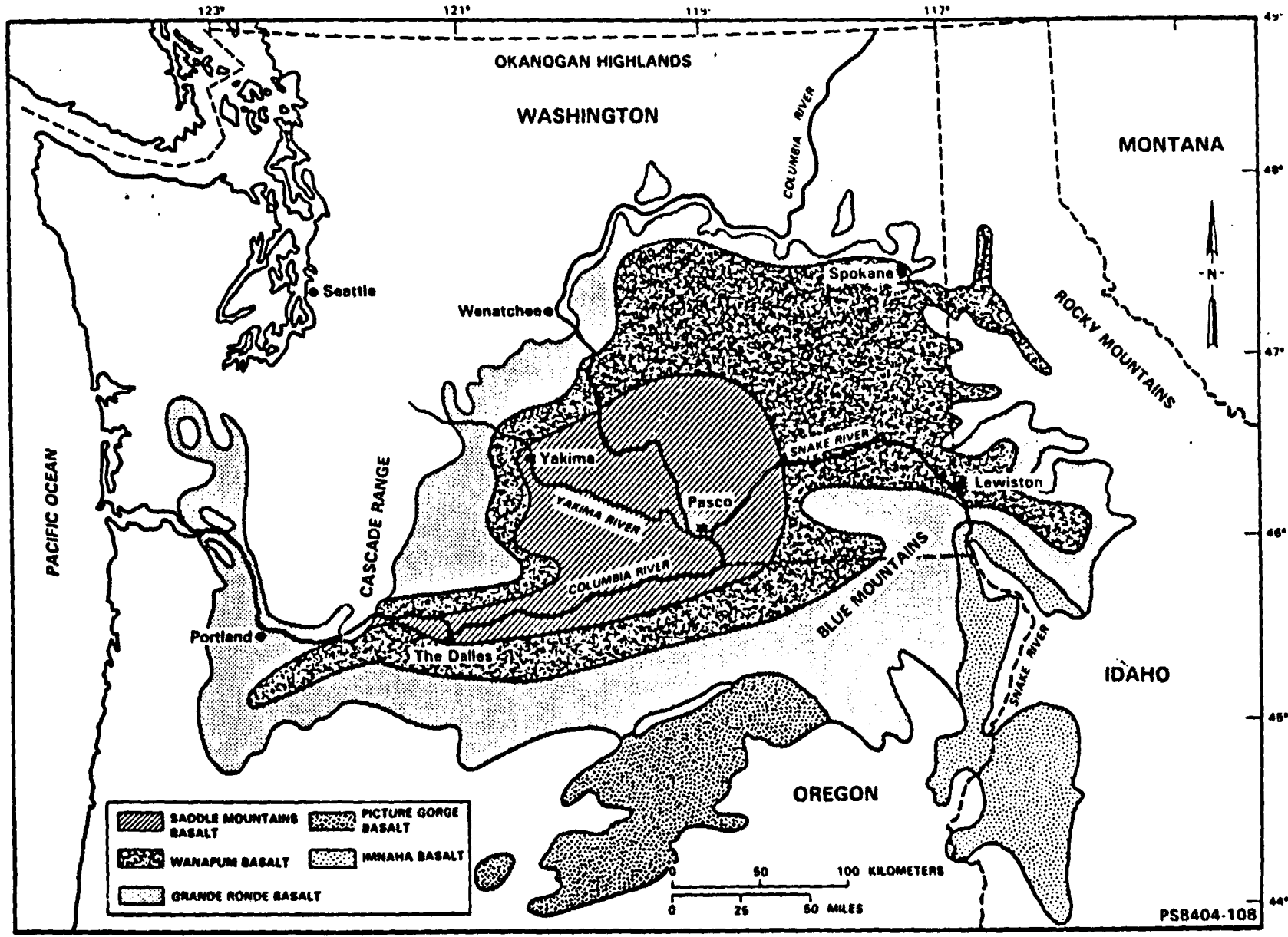


Figure 2.6 Distribution of Columbia River Basalt Group (after Wright and others, 1973 in DOE, 1984)

PSB404-108

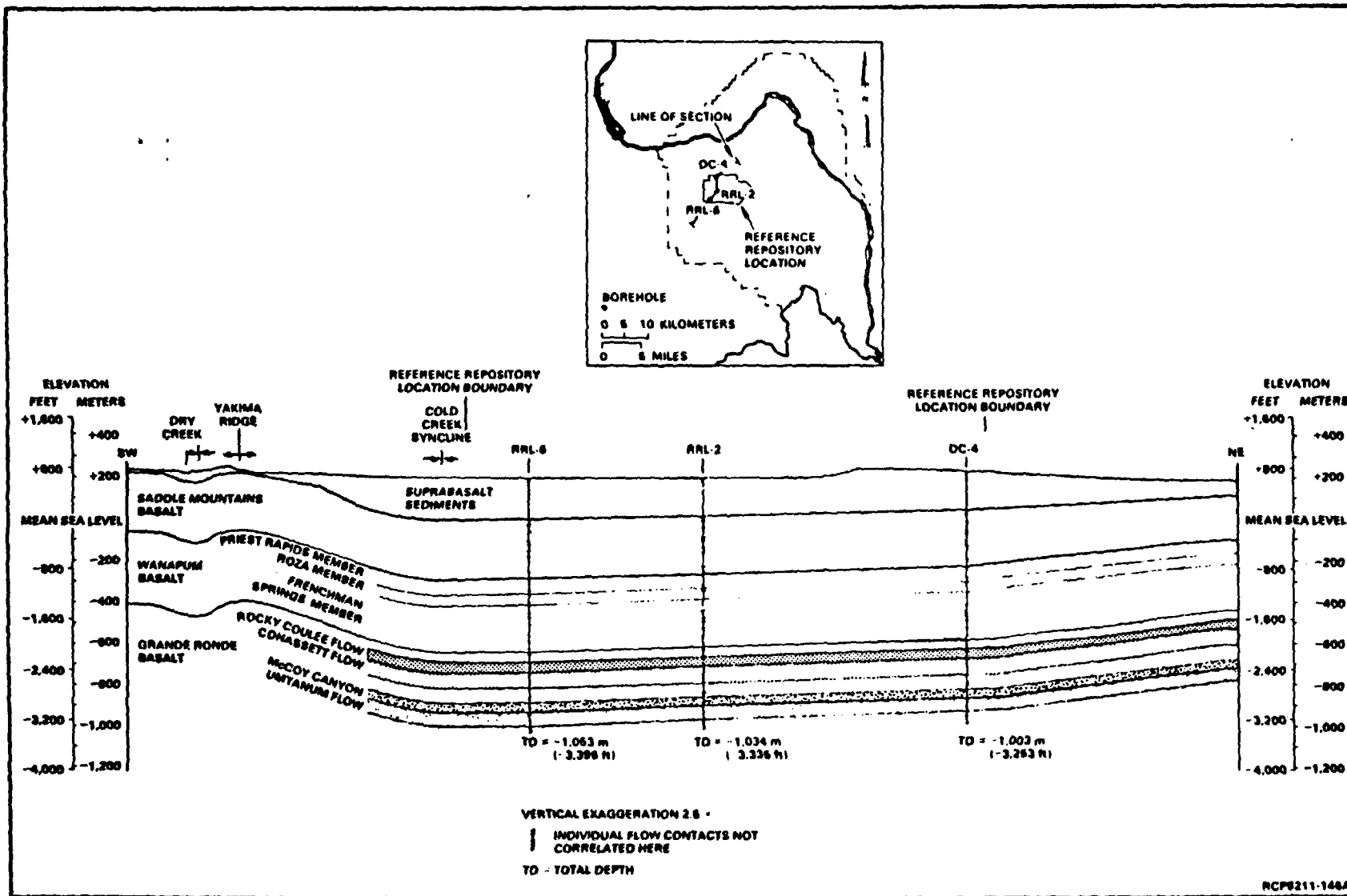


Figure 2.7 Geologic Cross Section Through the Reference Repository Location.
(DOE, 1984)

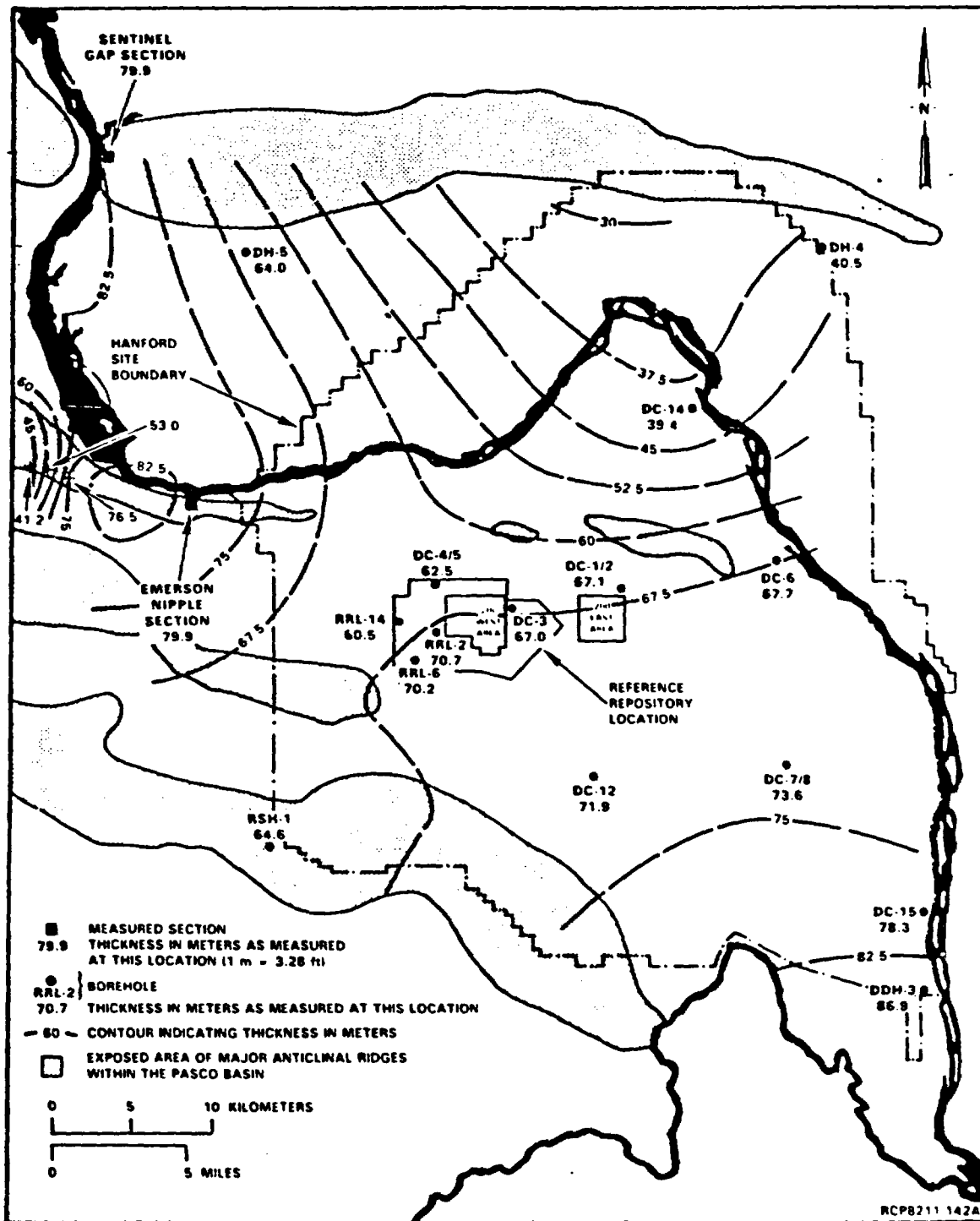


Figure 2.8 Umtanum Flow Isopach Map. (DOE, 1984)

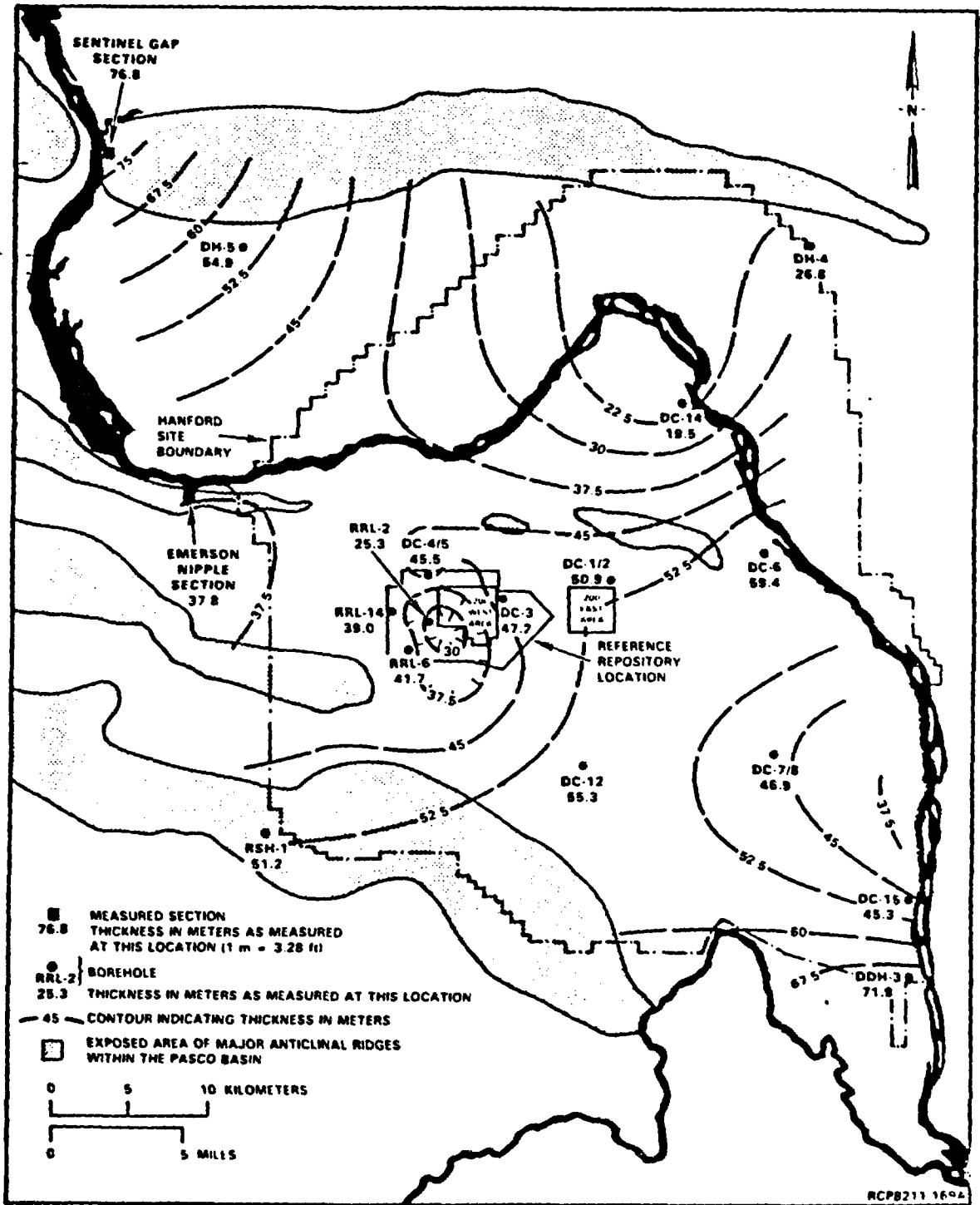


Figure 2.9 Isopach Map of the Dense Interior of the Umtanum Flow. (DOE, 1984)

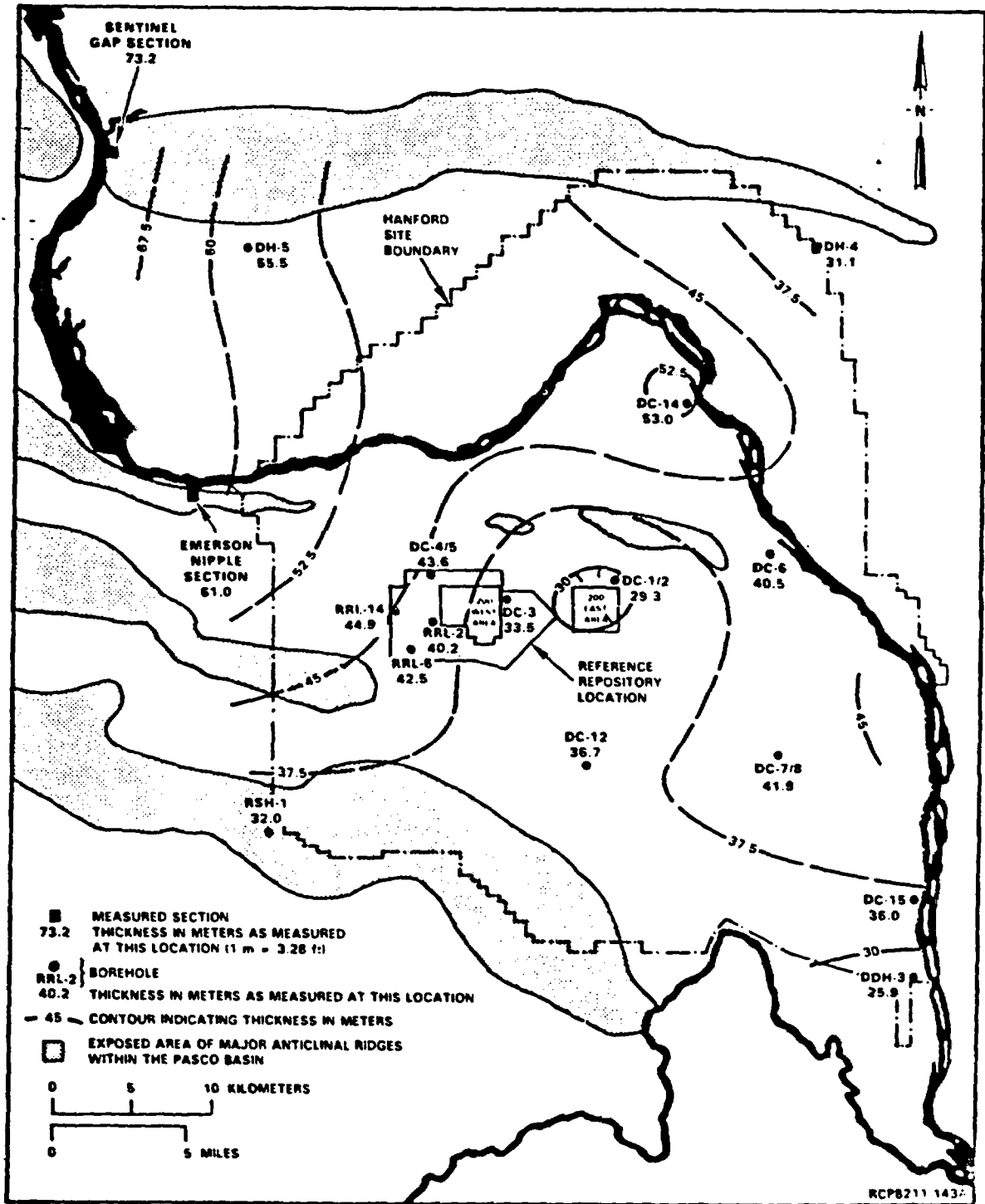


Figure 2.10 McCoy Canyon Flow Isopach Map. (DOE, 1984)

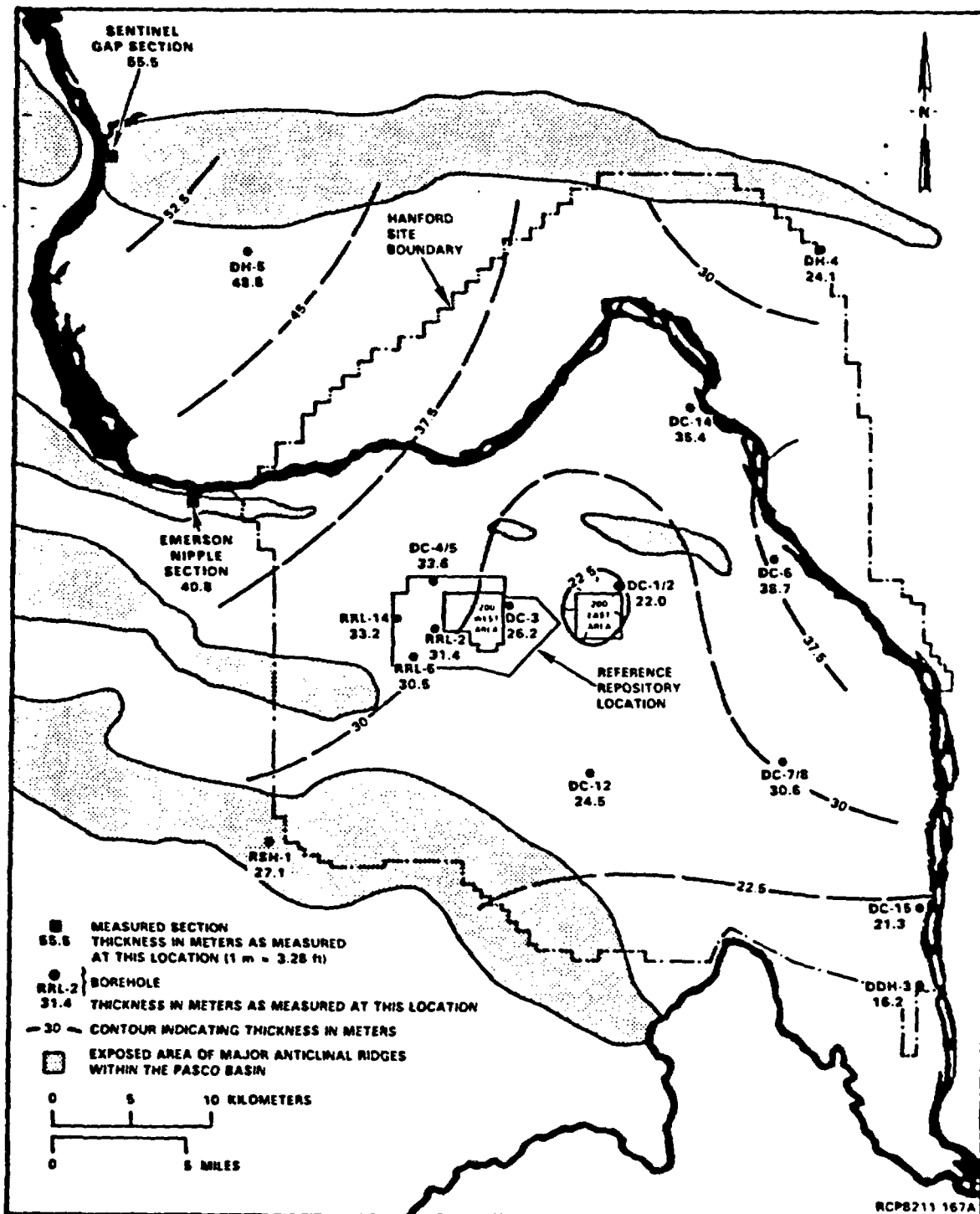


Figure 2.11 Isopach Map of the Dense Interior of the McCoy Canyon Flow. (DOE, 1984)

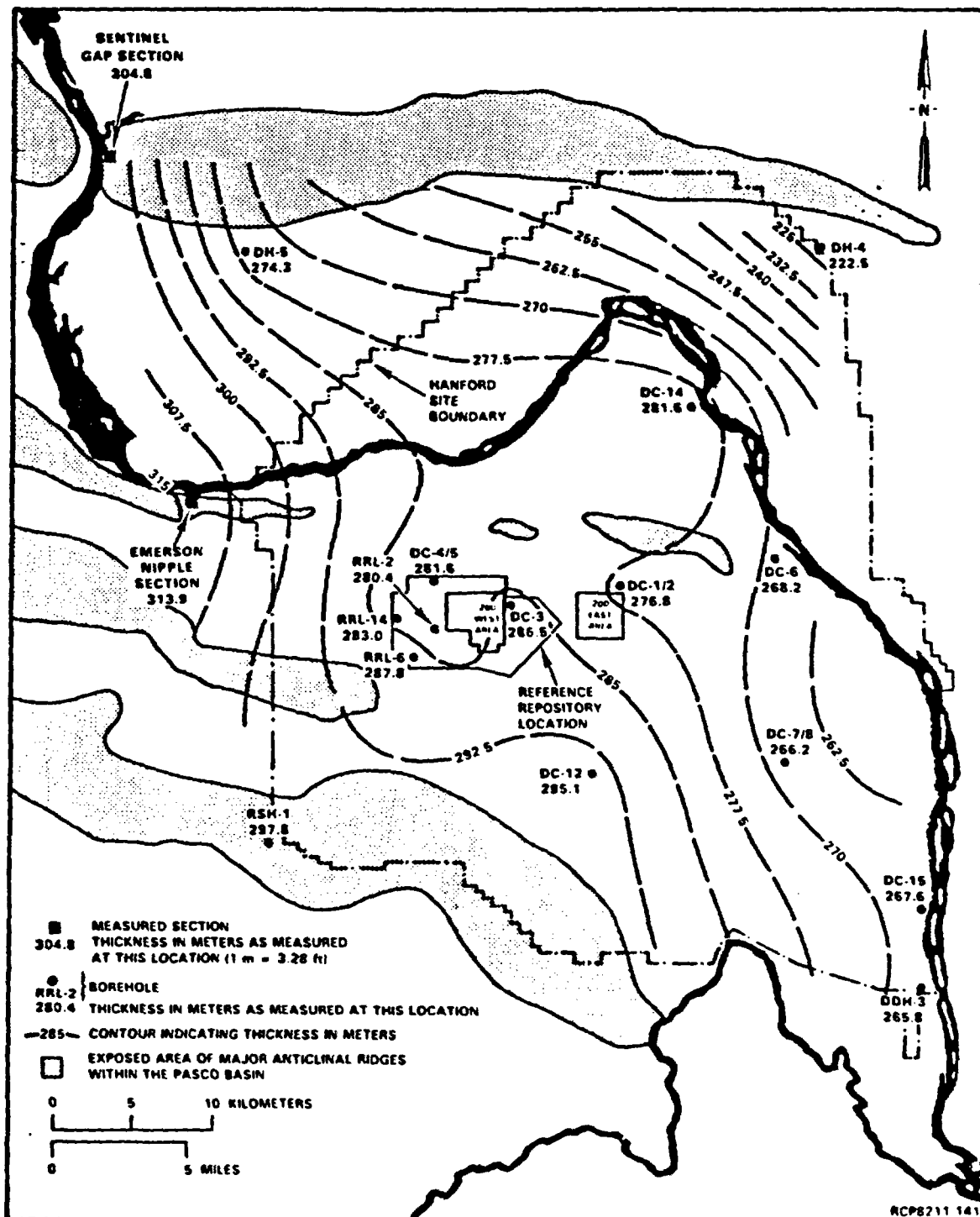


Figure 2.12 Sentinel Bluffs Sequence Isopach Map. (DOE, 1984)

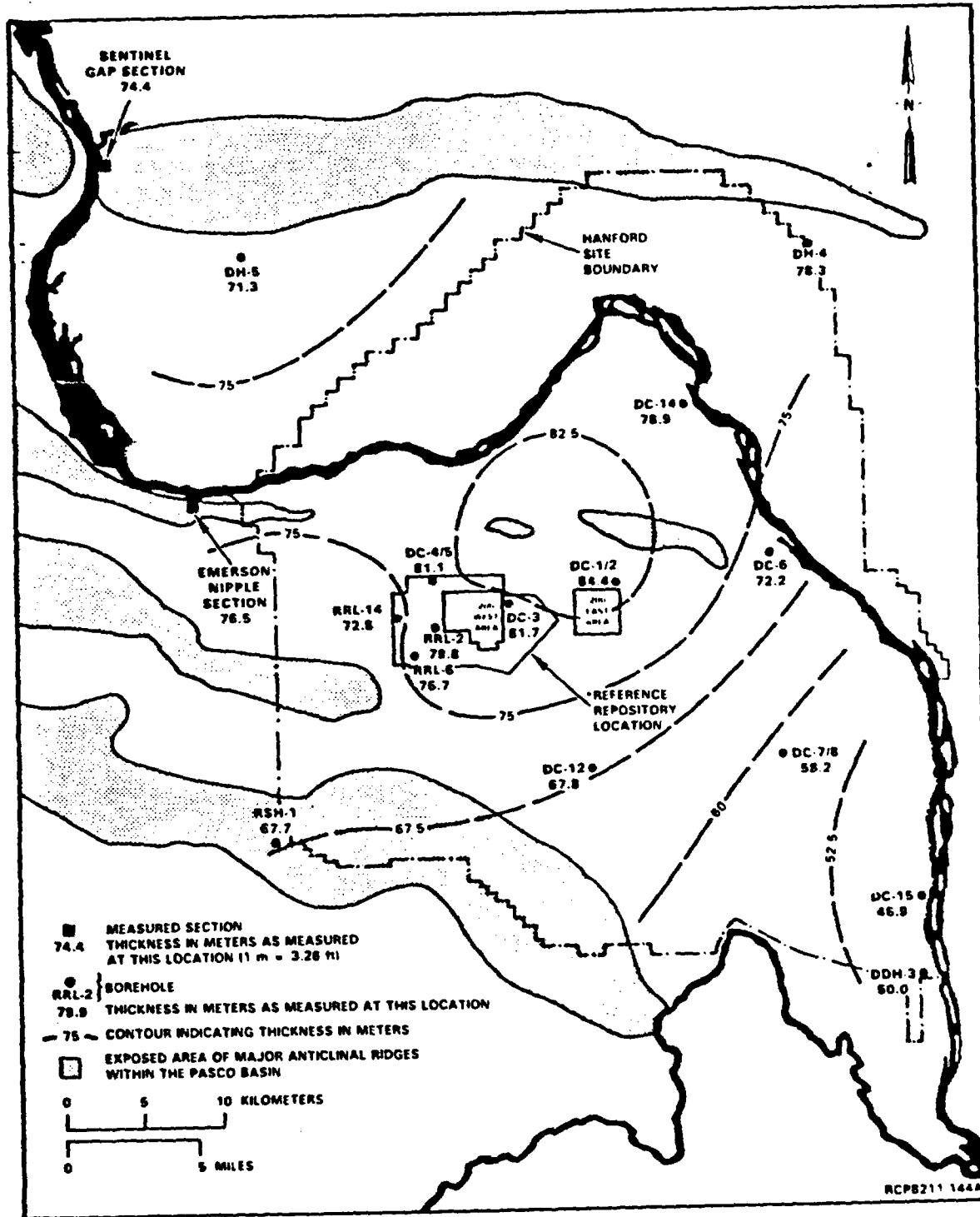


Figure 2.13 Cohasset Flow Isopach Map.

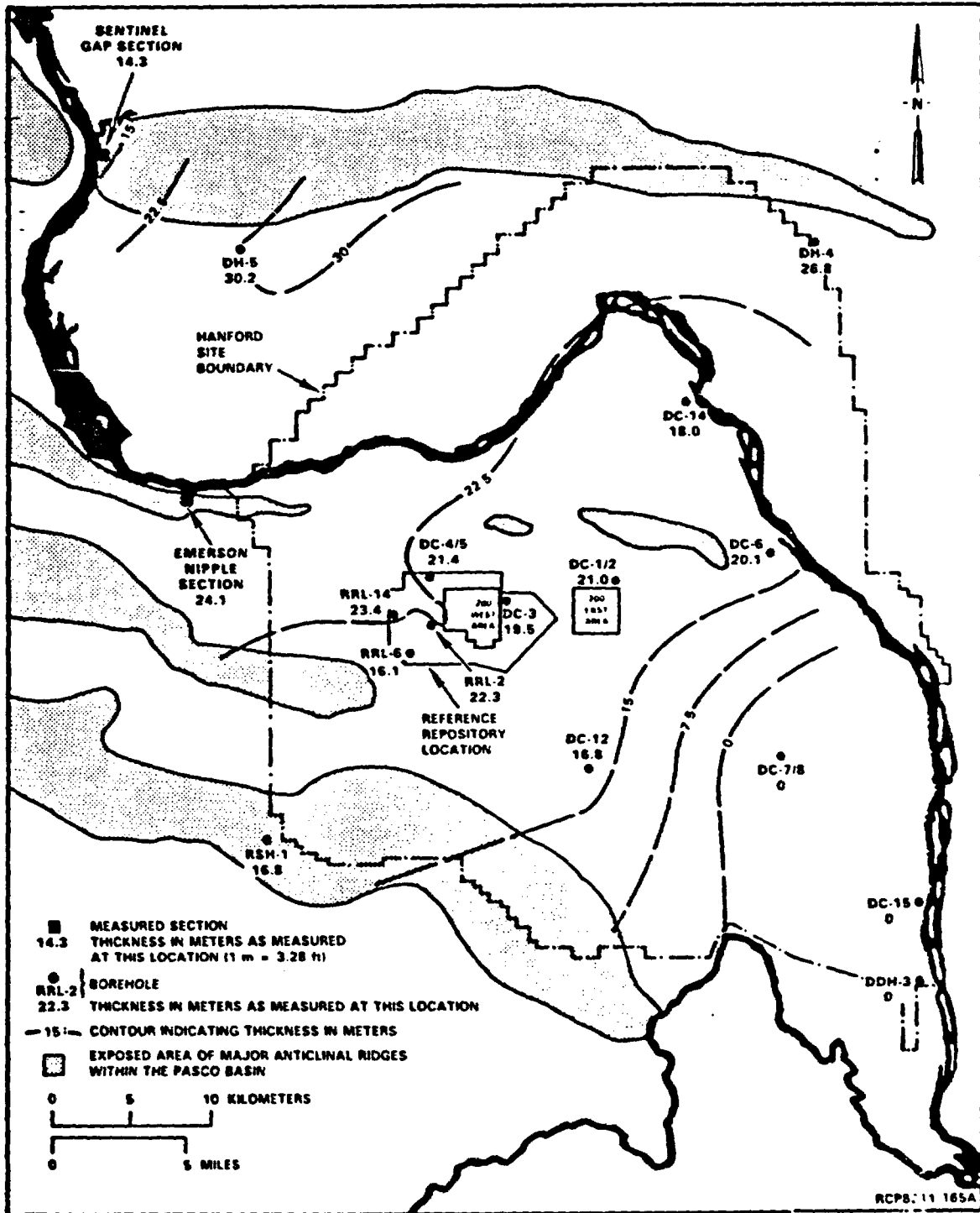


Figure 2.14 Isopach Map of the Dense Interior of the Cohasset Flow above the Vesicular Zone. (DOE, 1984)

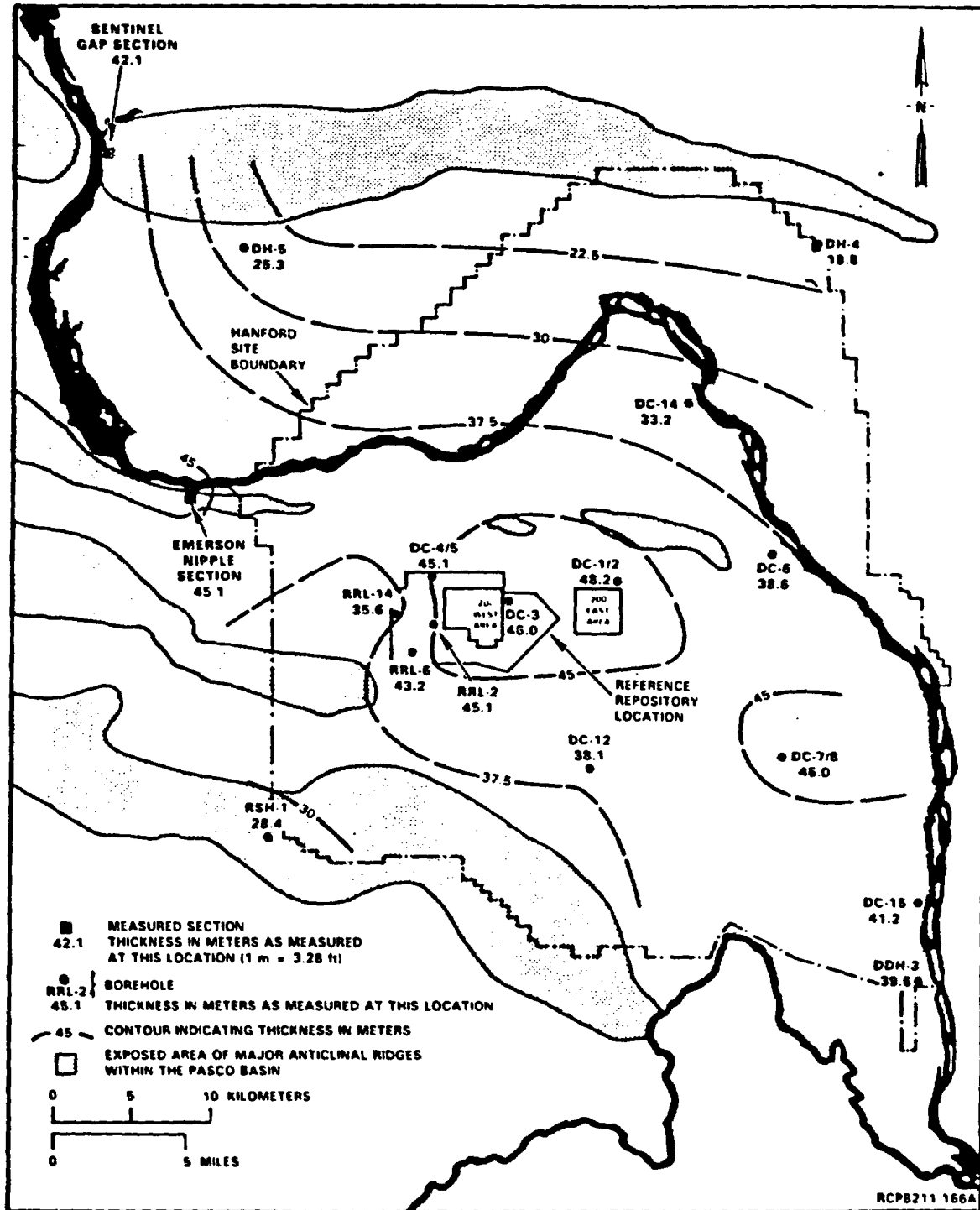


Figure 2.15 Isopach Map of the Dense Interior of the Cohasset Flow below the Vesicular Zone. (DOE, 1984)

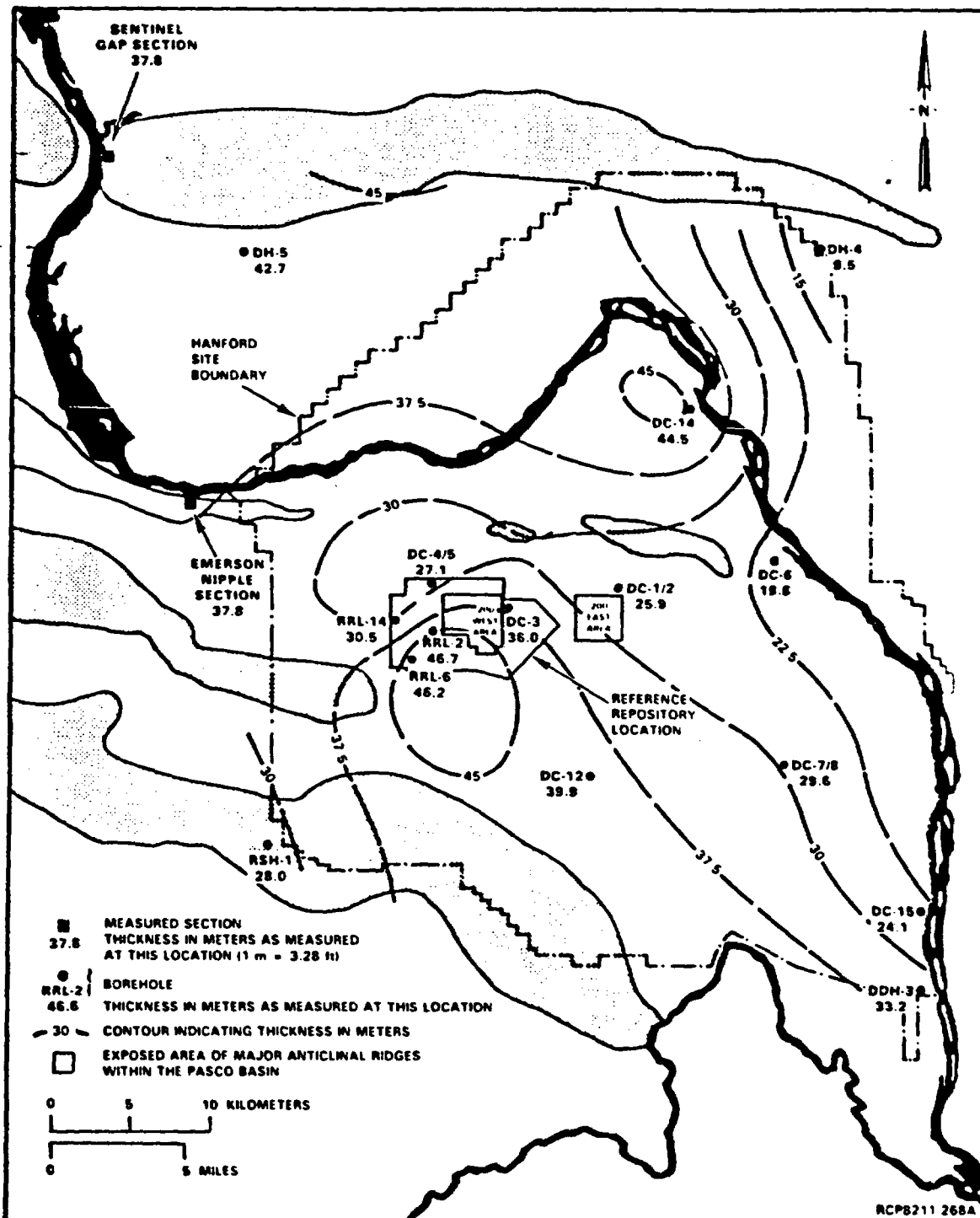


Figure 2.17 Isopach Map of the Dense Interior of the Rocky Coulee Flow. (DOE, 1984)

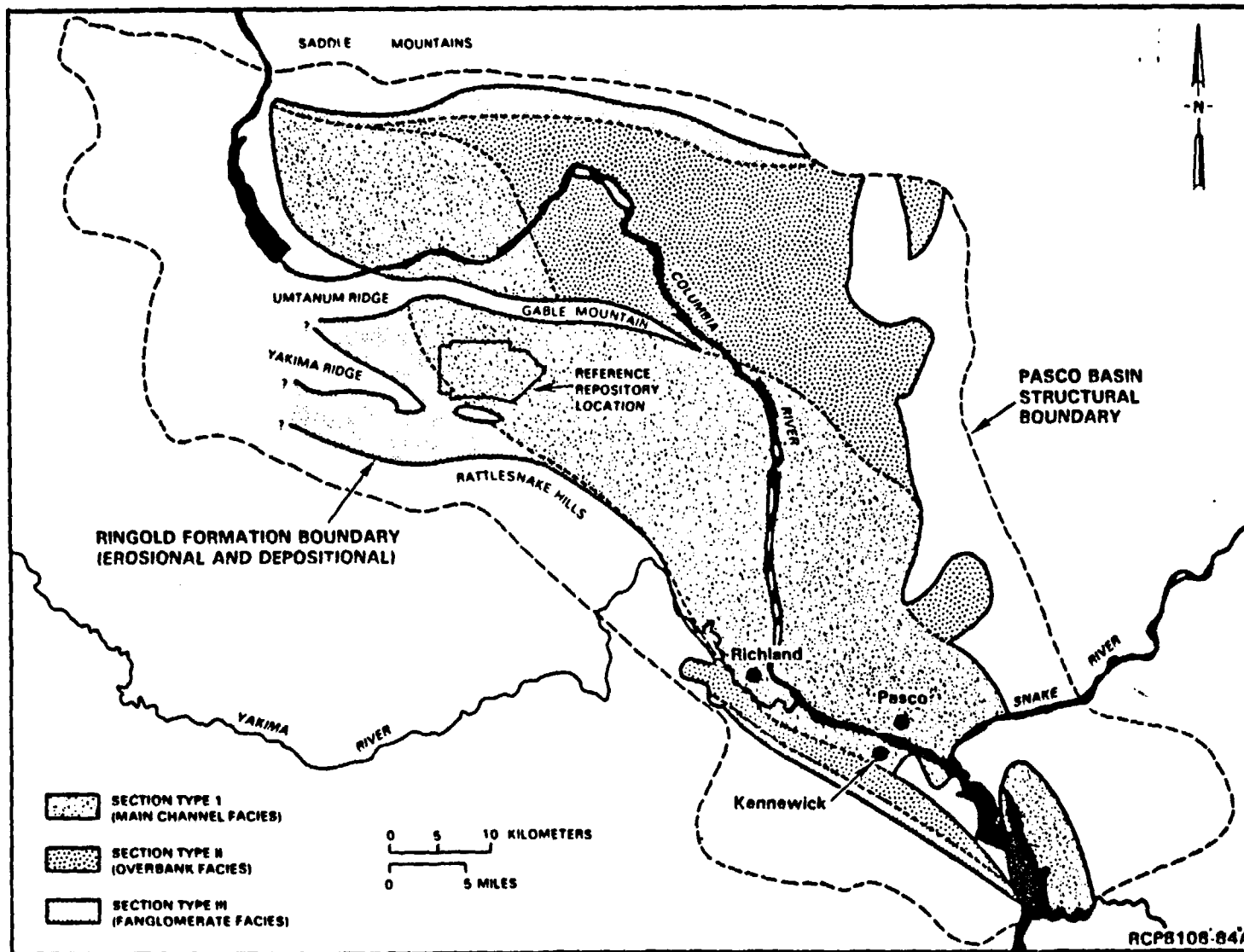


Figure 2.19 Distribution of Ringold Formation Section Types.

TERTIARY		QUATERNARY	PERIOD		
Miocene	Pliocene		Pleistocene		
Saddle Mountains Basalt	Ringold		Hanford		
UNIT/MEMBER	FORMATION	FORMATION	FORMATION		
ELEPHANT MOUNTAIN MEMBER	BASAL RINGOLD	Unconformity	TOUCHET BEDS (mud and sand facies)		
				Unconformity	PASCO GRAVELS? (sand and gravel facies)
MIDDLE RINGOLD	Local Unconformity	Unconformity	PALEOSOL		
				UPPER RINGOLD	FANGLOMERATE Unconformity
LOWER RINGOLD	Unconformity	Unconformity	Unconformity		
				Unconformity	
8.5	5.3	1.8	0.013		
10.5					

PS8406:150

Figure 2.18 Suprabasalt Stratigraphy in the Reference Repository Location. (DOE, 1984)

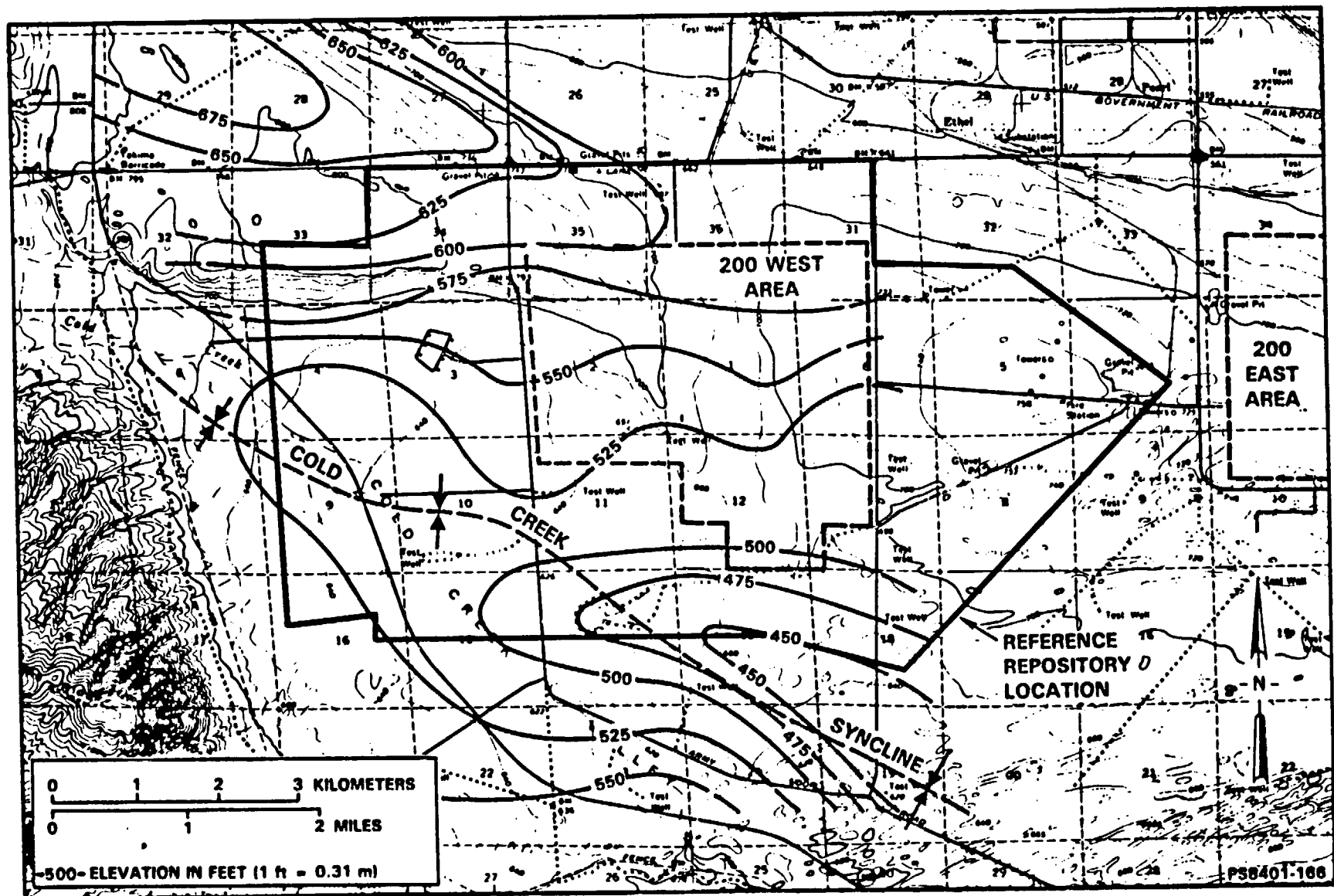


Figure 2.20 Top of the Ringold Formation. Contour Pattern Indicates Maximum Post-Ringold Incision Occurred near the Trend of the Present Cold Creek Valley. (DOE, 1984)

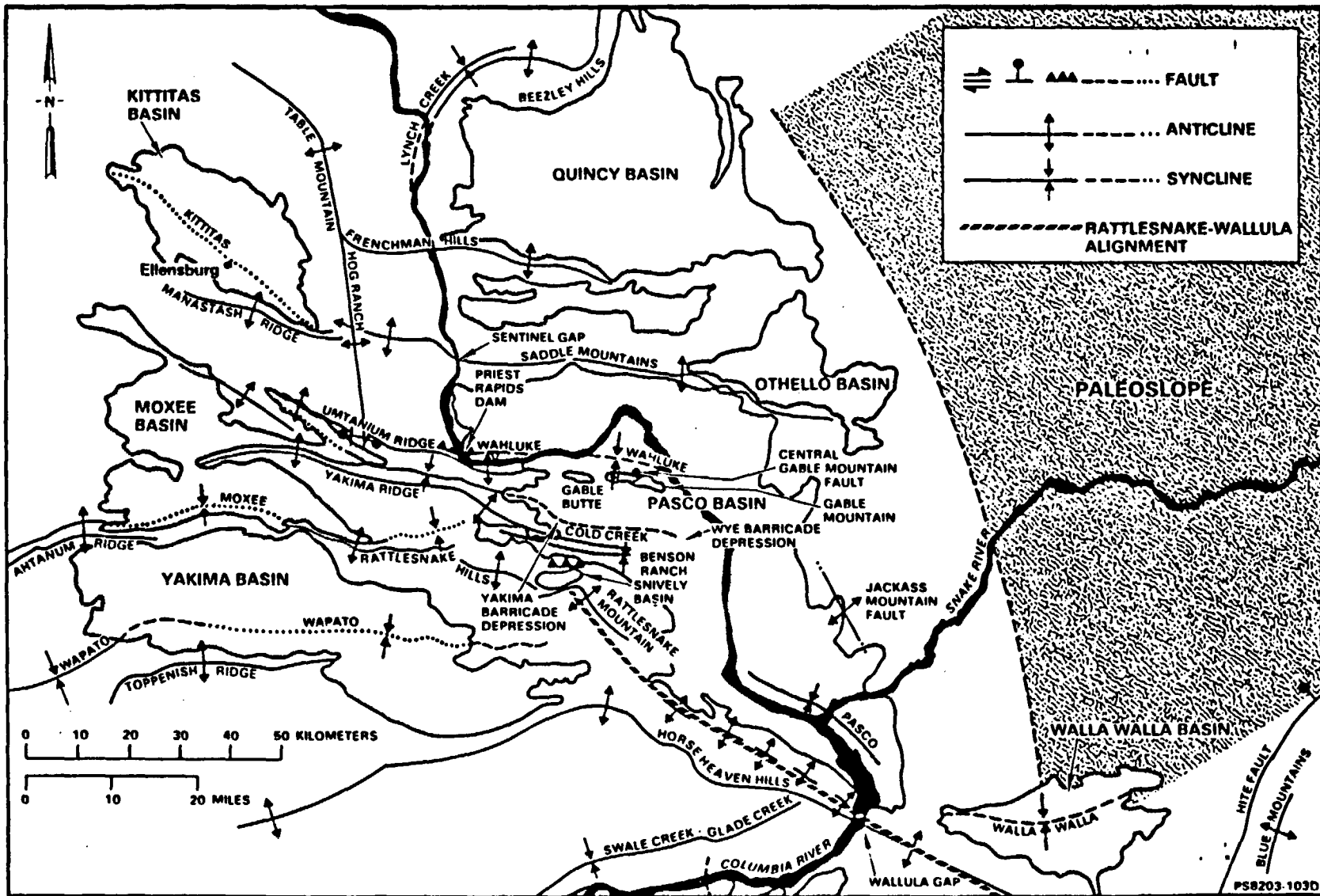
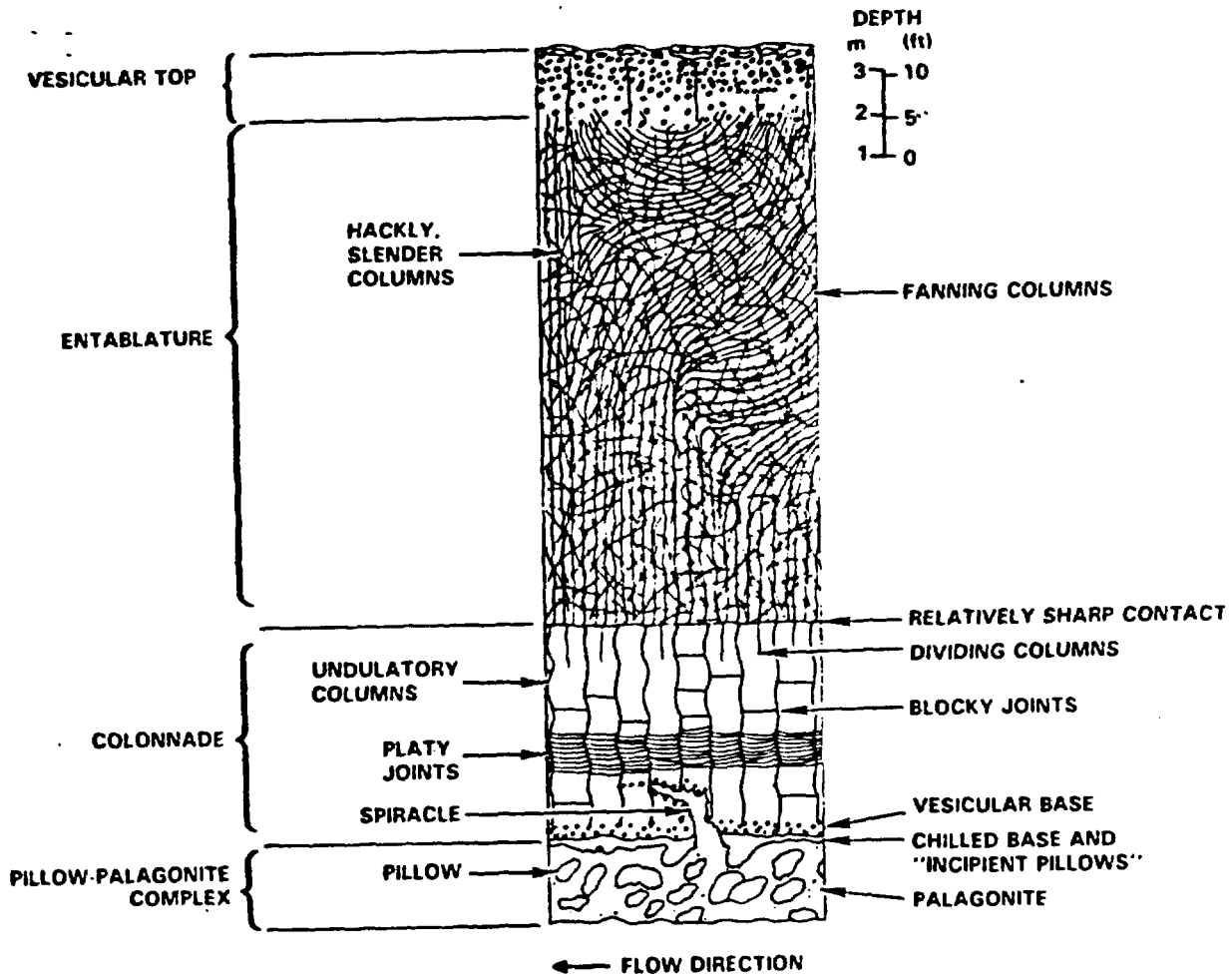


Figure 2.21 Generalized Geologic Structure Map of the Central Columbia Plateau. (DOE, 1984)



RCP8001-240B

Figure 2.22 Cross Section of a Typical Flow in the Columbia River Basalt Group Illustrating, in Idealized Form, Jointing Patterns and other Structures (from Swanson and Wright, 1976 in DOE, 1984)

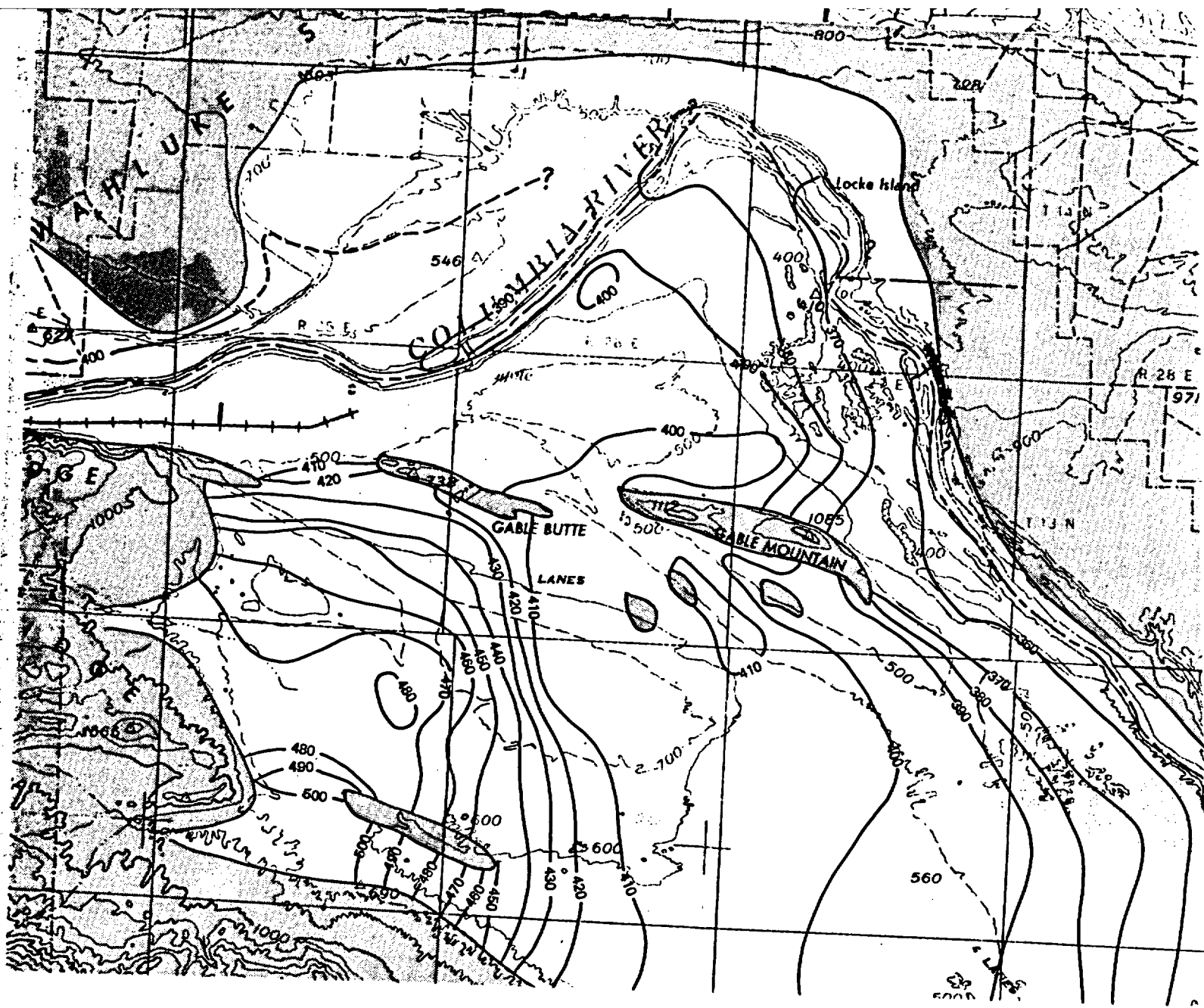


Figure 3.1 Water-Table Map within the Pasco Basin.
 (Gephart and others, 1979)

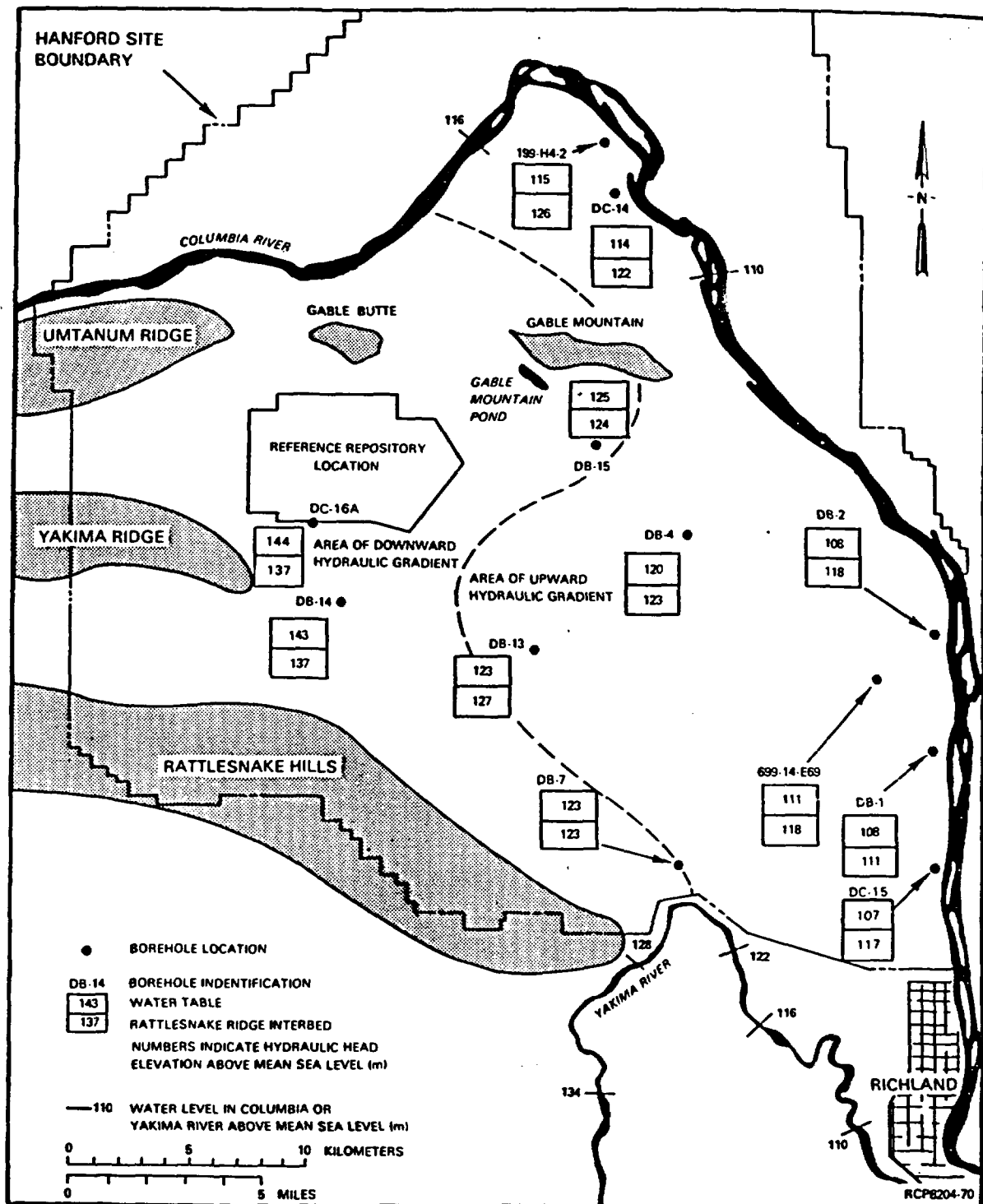


Figure 3.3 Comparison of Hydraulic Heads in the Rattlesnake Ridge Interbed to Water-Table Elevation (DOE, 1982)

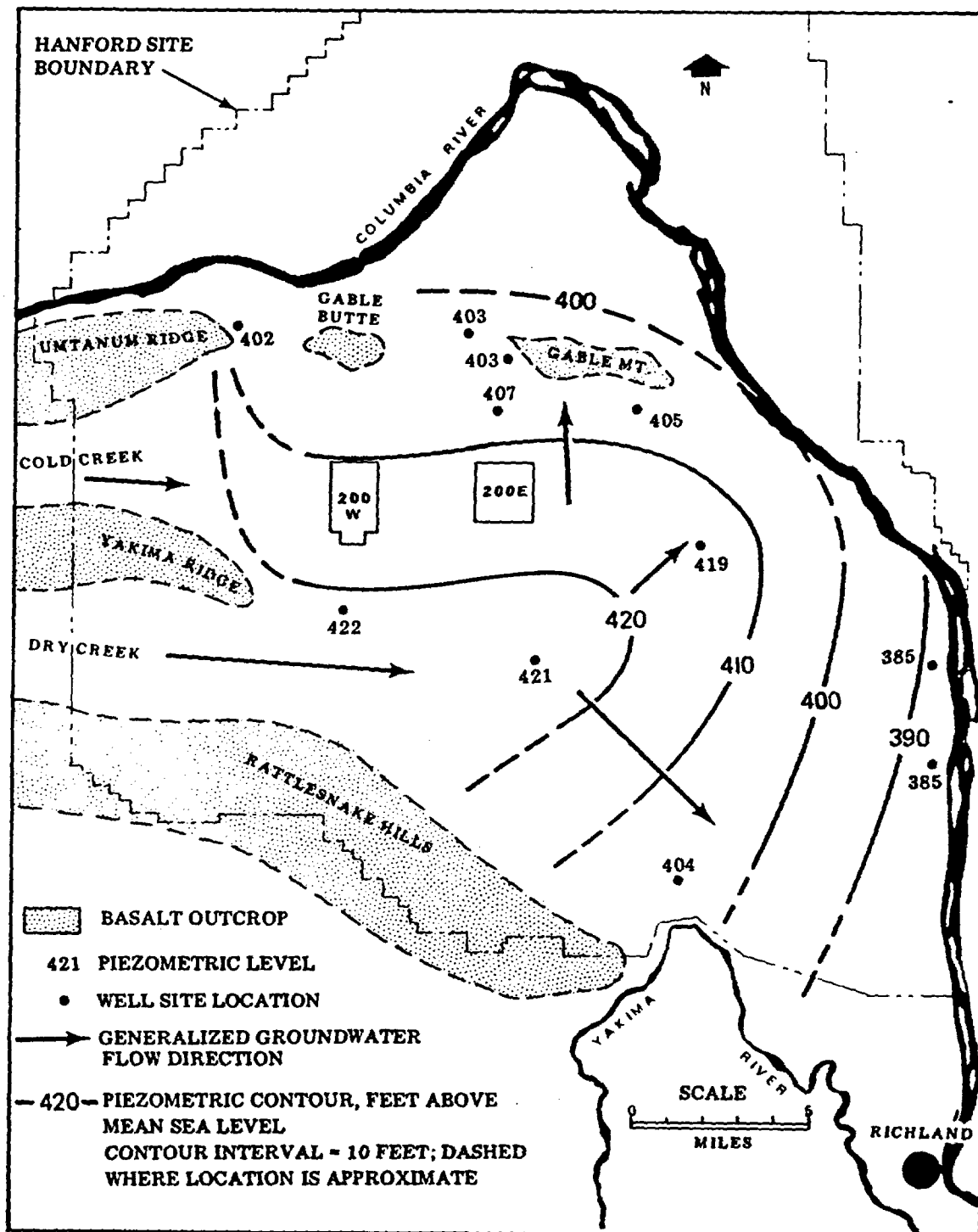
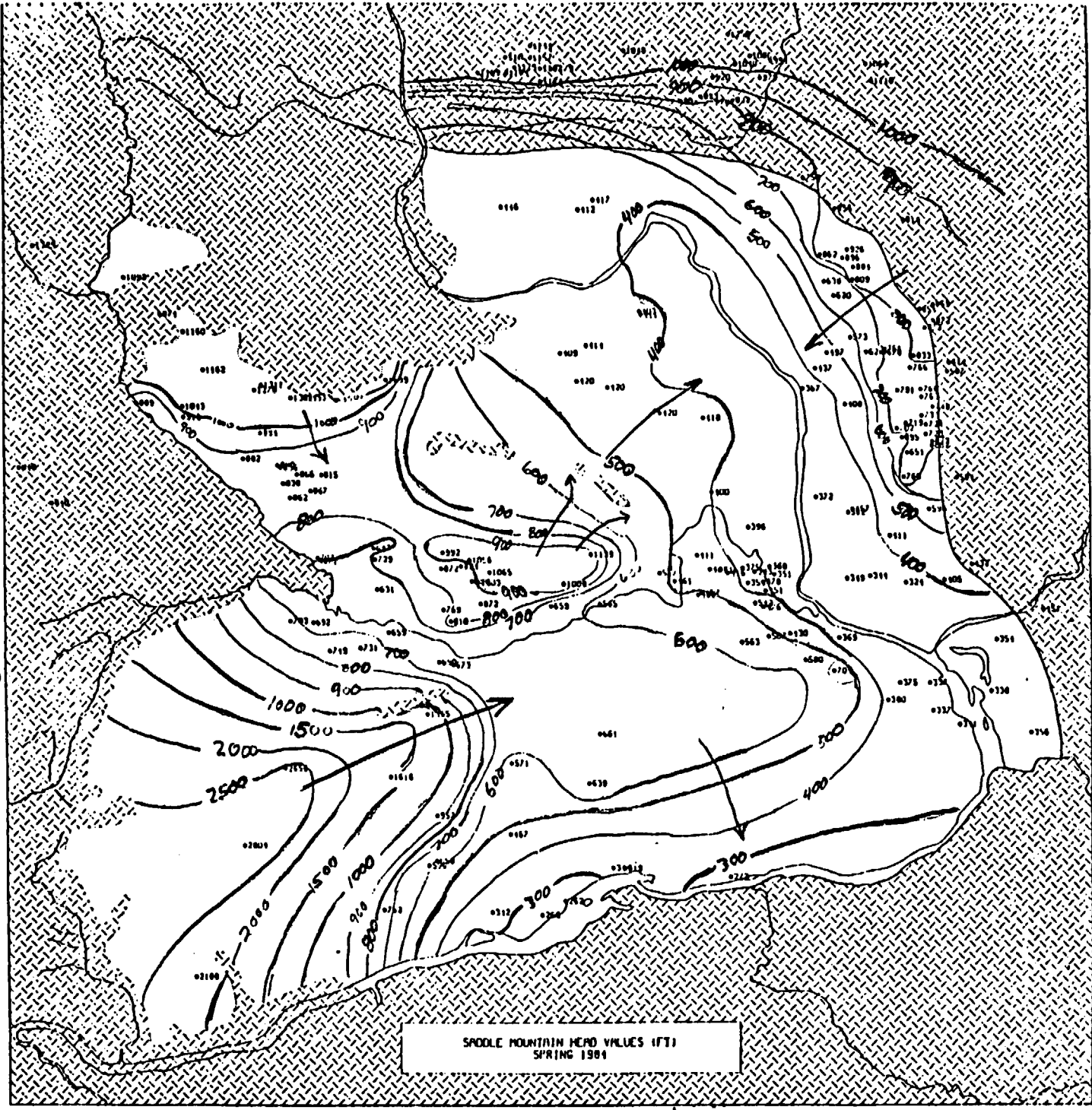


Figure 3.4 Potentiometric Map and Inferred Flow Directions for the Mabton Interbed beneath the Hanford Site. (Gephart and others, 1979)



We regret the poor quality of Figures 3.5-3.7. They are being redone and new ones will be forwarded ASAP.

Figure 3.5 Potentiometric Map of Saddle Mountains Basalts, Spring 1984.

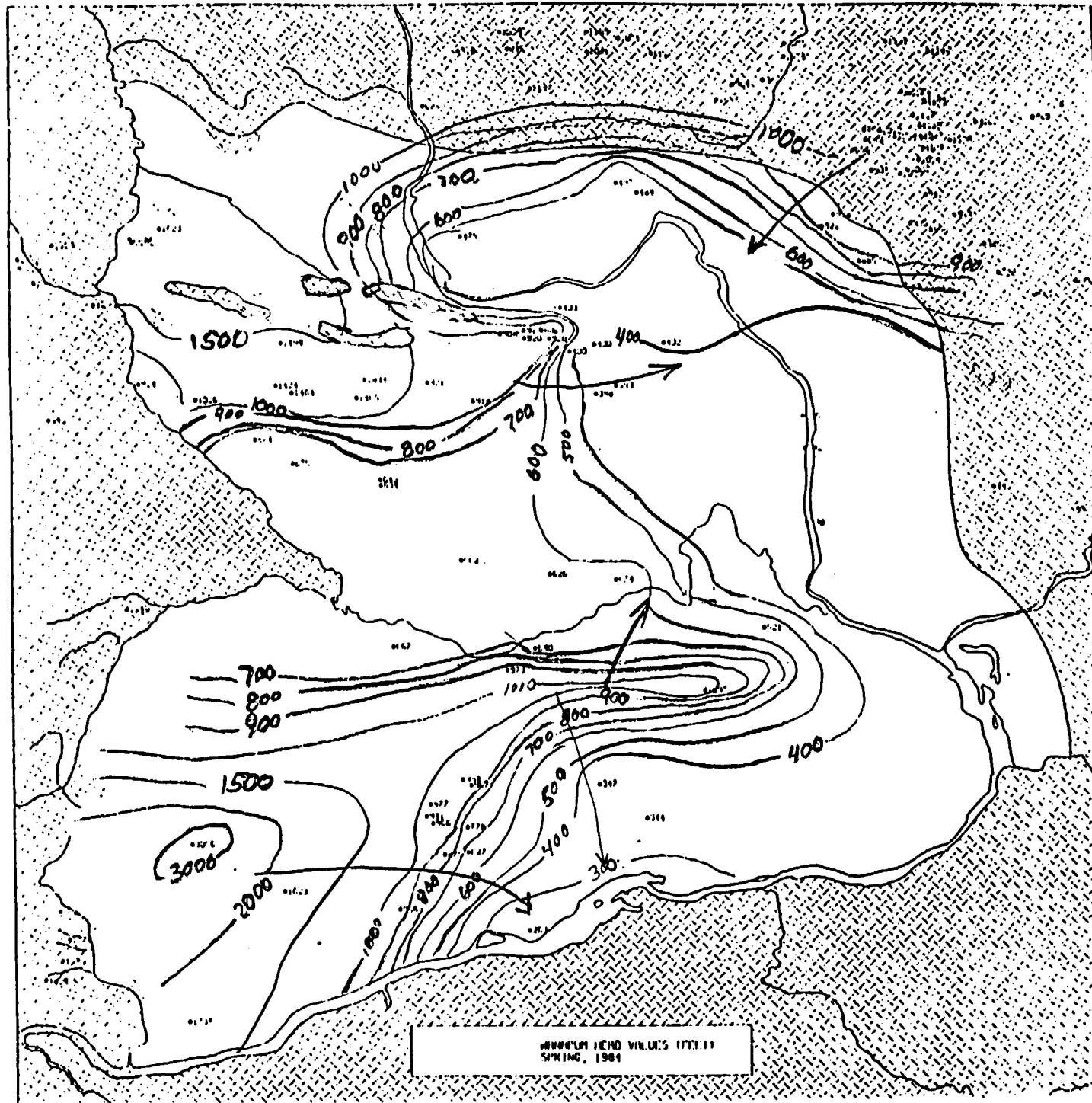


Figure 3.6 Potentiometric Map of Wanapum Basalts, Spring 1984.

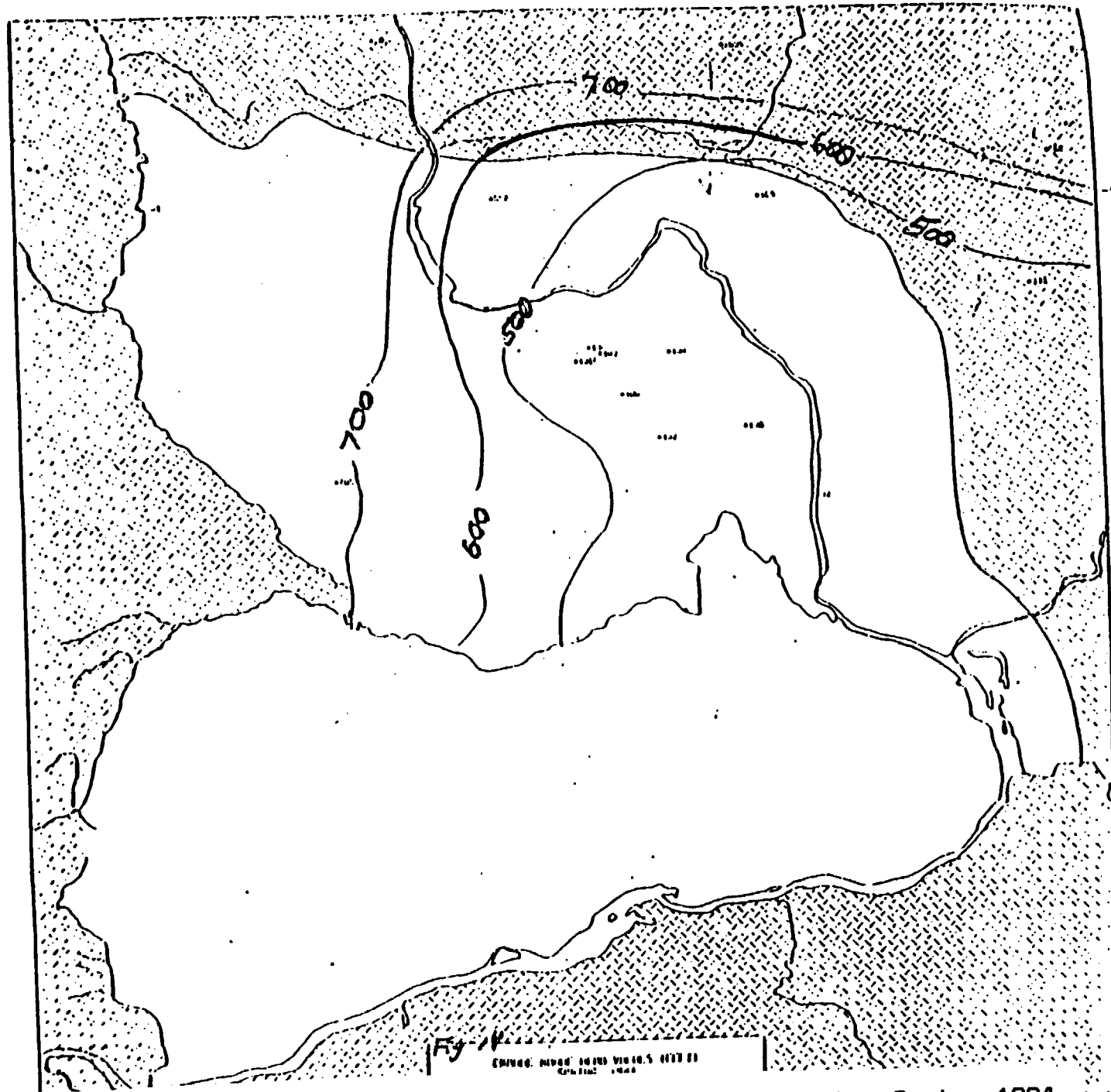


Figure 3.7 Potentiometric Map of Grande Ronde Basalts, Spring 1984.

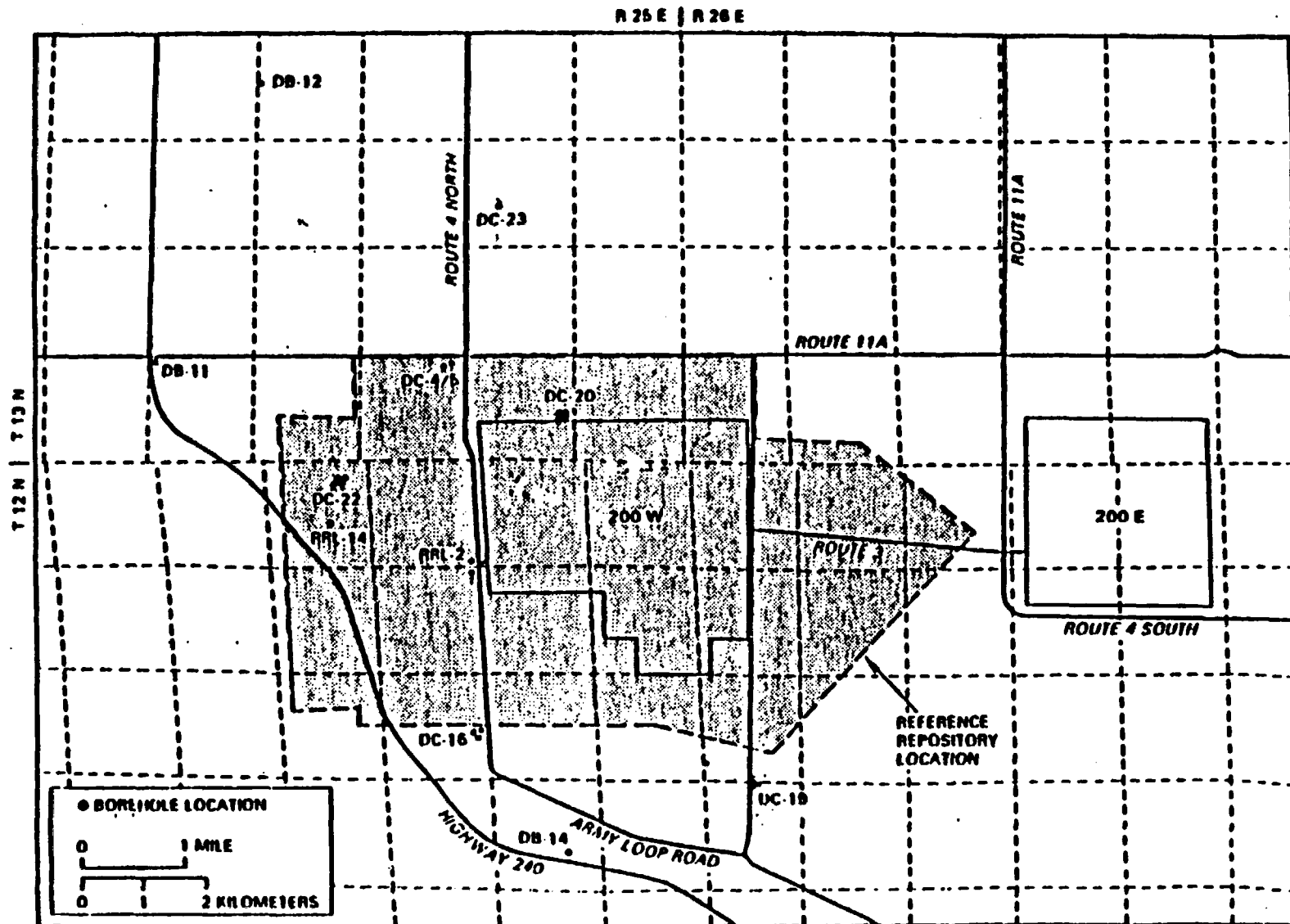


Figure 3.9 Location of Wells DC-19, DC-20, DC-22, DC-23W, and RRL-14
(Rockwell Hanford Operations, December 1985)

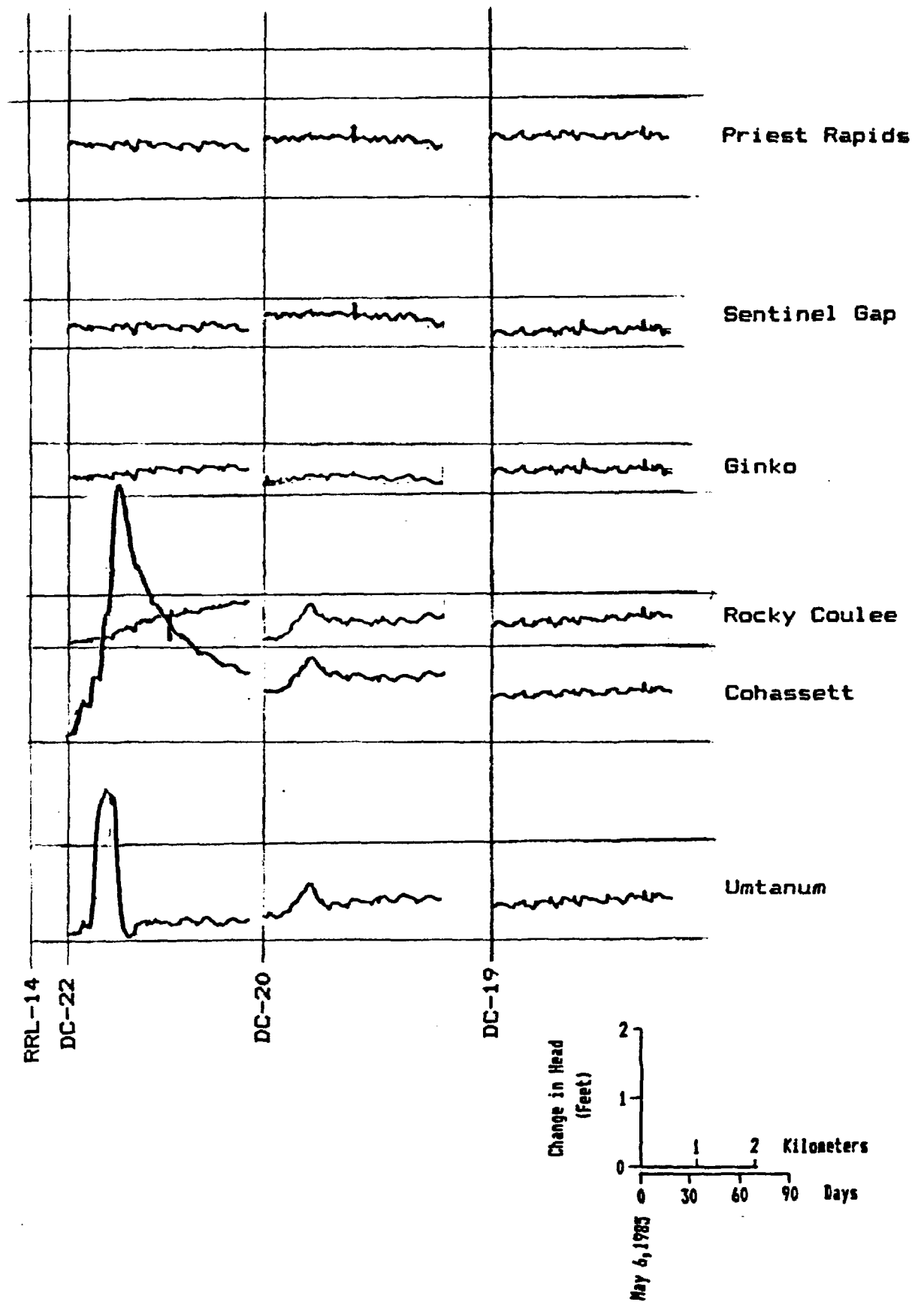


Figure 3.10 Response at DC-19, DC-20, and DC-22 to Bridge Plug Removal at RRL-14

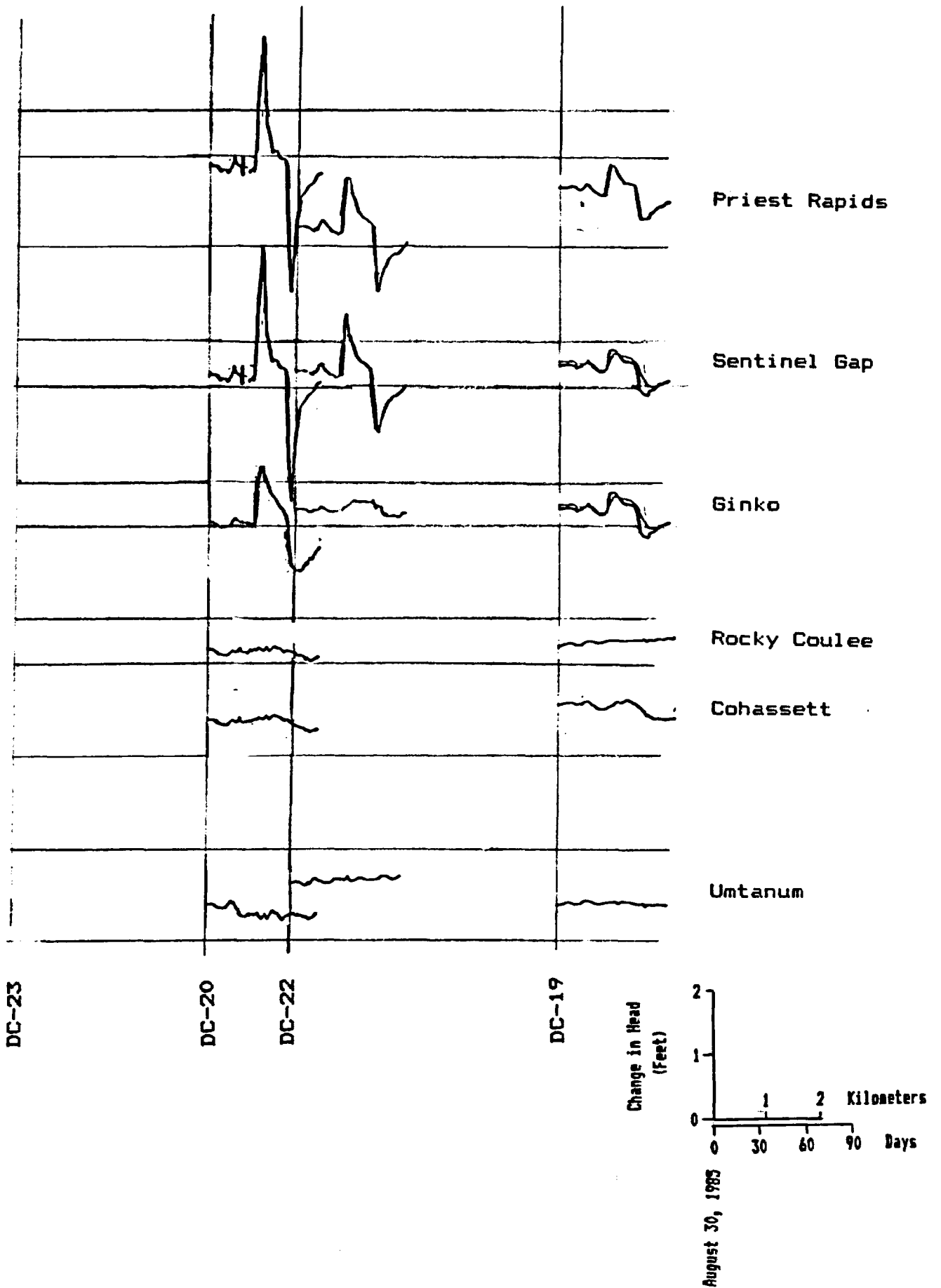


Figure 3.11 Response at DC-19, DC-20, and DC-22 to Drilling, Piezometer Installation, and Cleanup of DC-23W

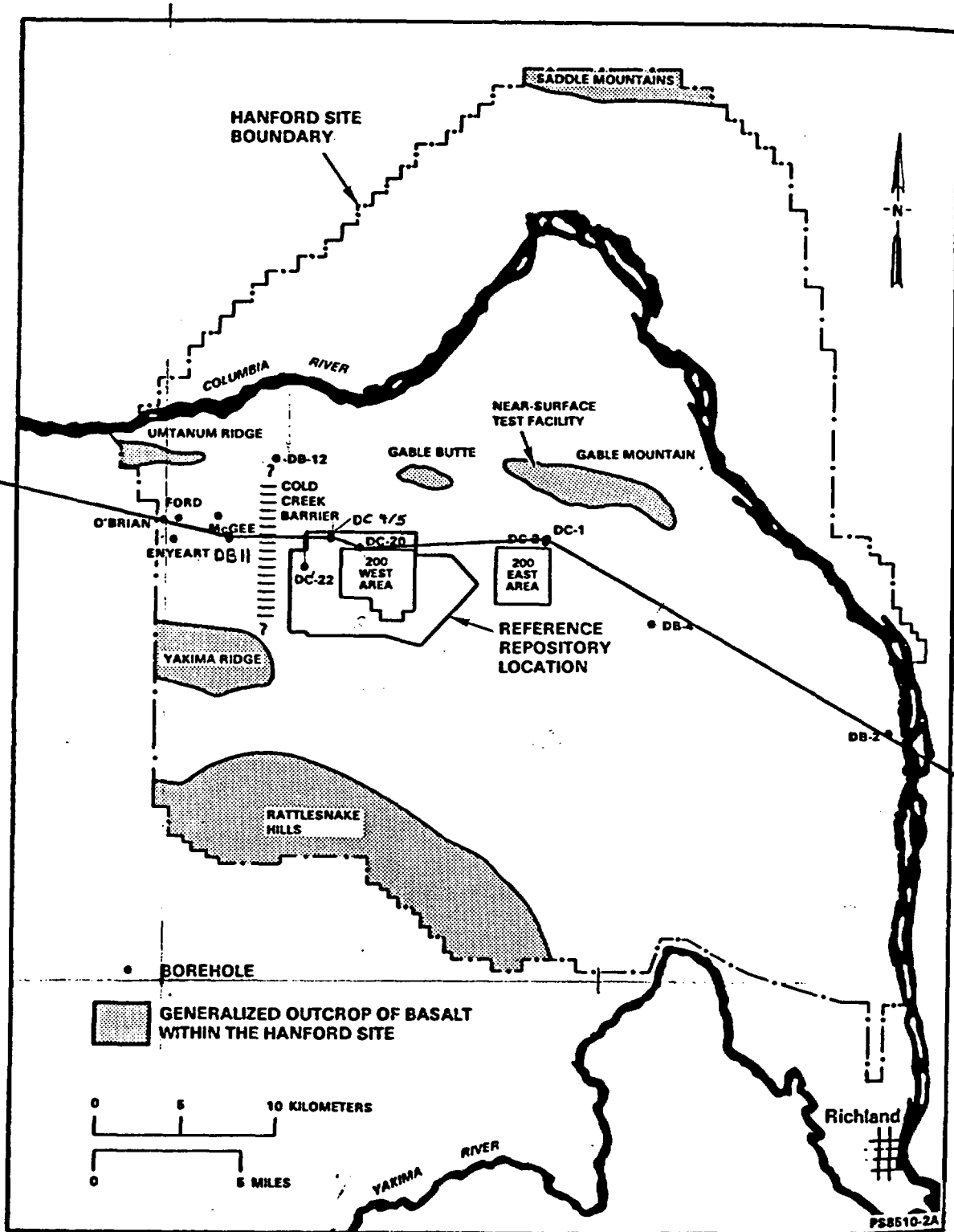


Figure 3.12 Location of Section A-A'

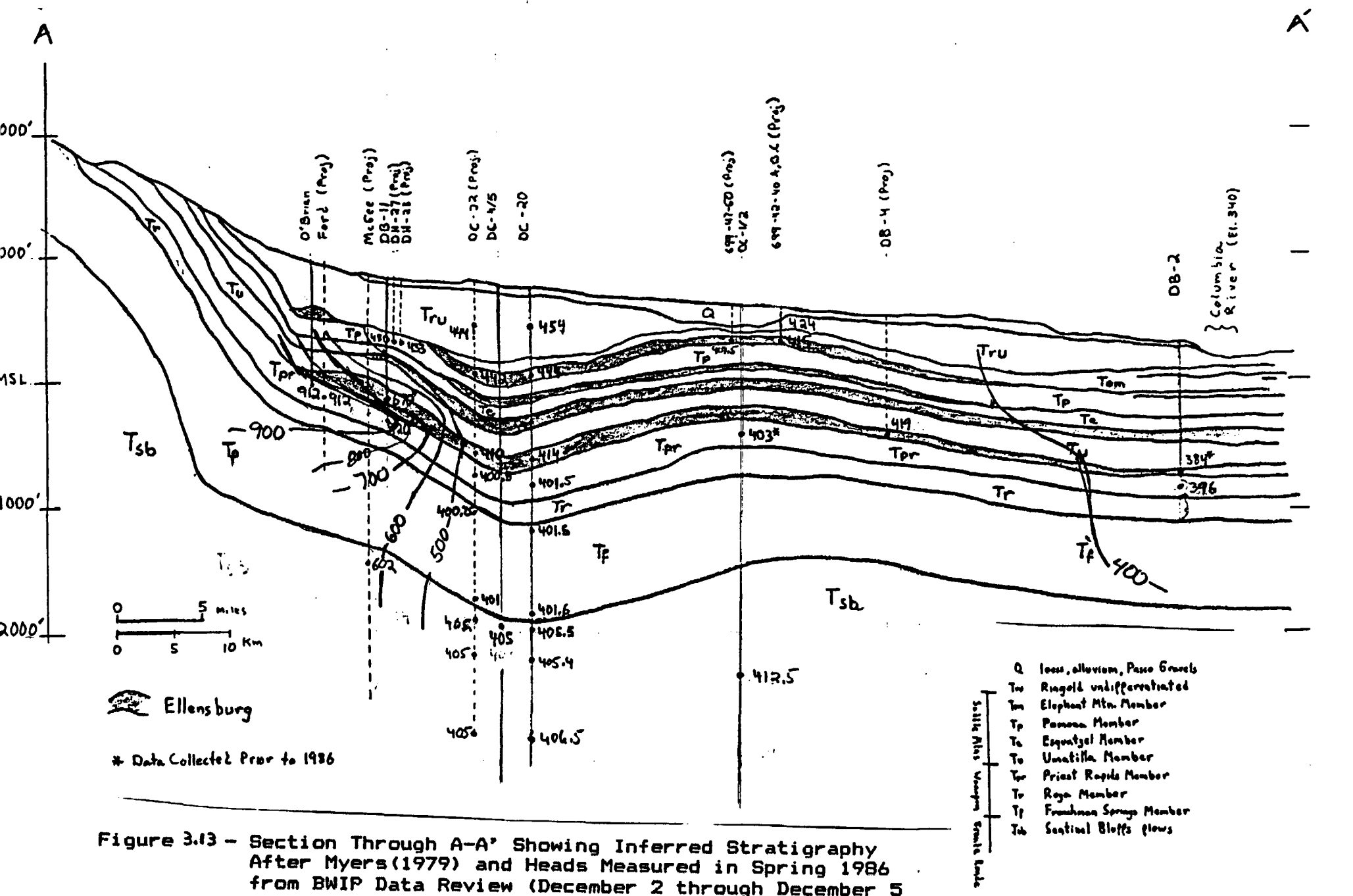


Figure 3.13 - Section Through A-A' Showing Inferred Stratigraphy After Myers (1979) and Heads Measured in Spring 1986 from BWIP Data Review (December 2 through December 5 1986, Richland, Washington)

400 - Contour of the potentiometric surface - number represents hydraulic head in feet above mean sea level

PIPER TRILINEAR DIAGRAM
 Ions expressed as percent of total
 milliequivalents per liter

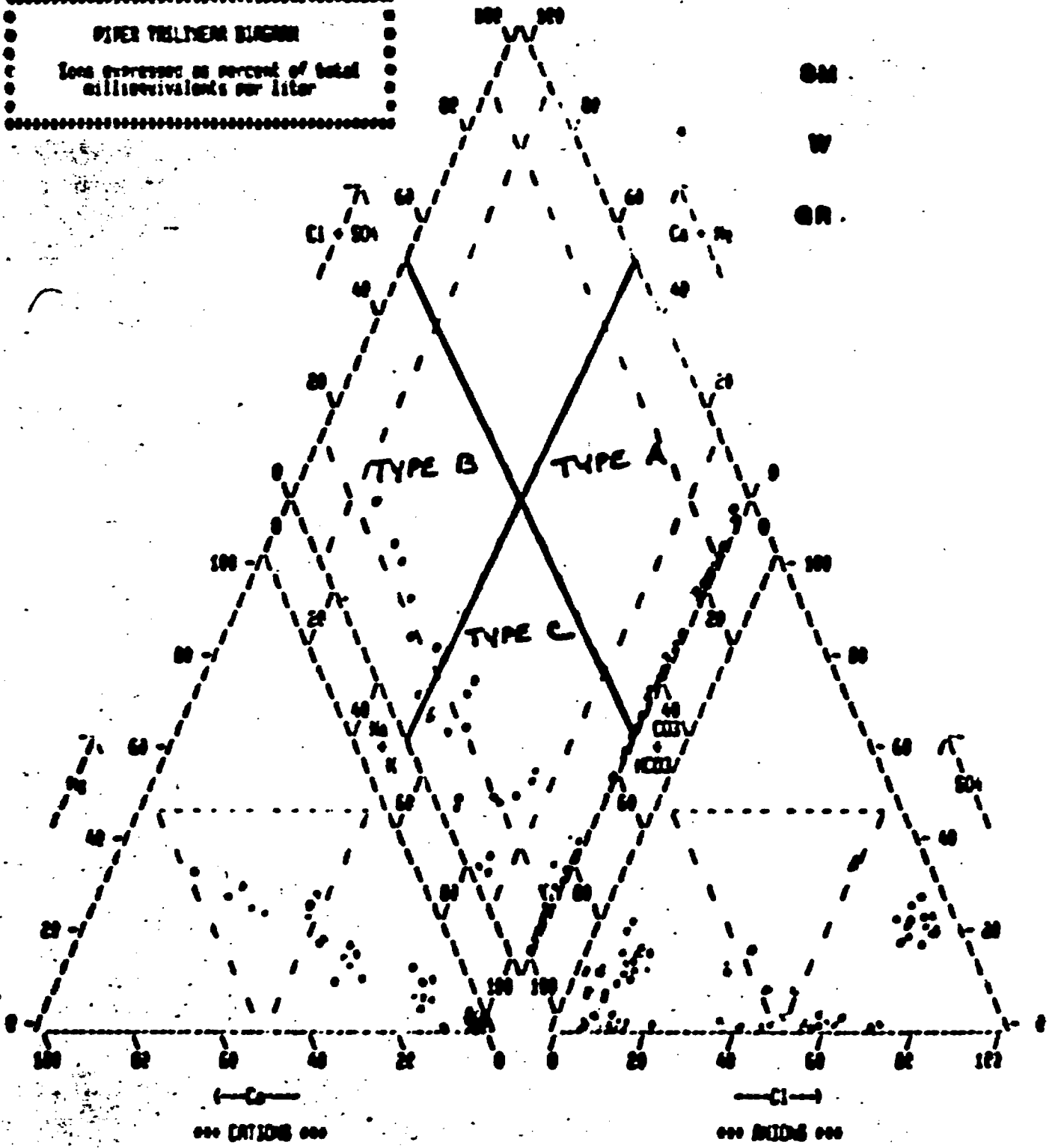


Figure 4.1 Piper Trilinear Plot of all Data Received from DOE
 Richland Office 2/15/83

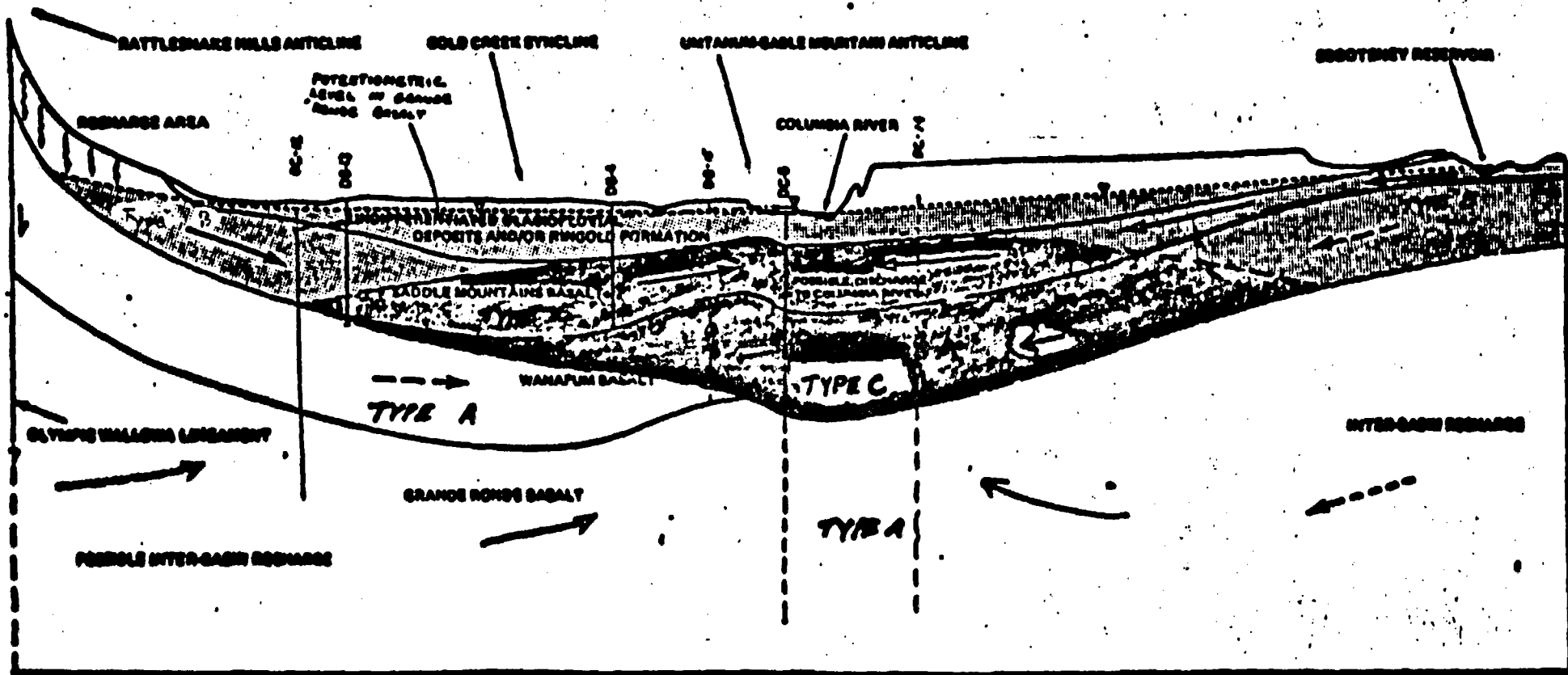


Figure 4.2 Distribution of Water Types within the Pasco Basin (Lehman, 1983)

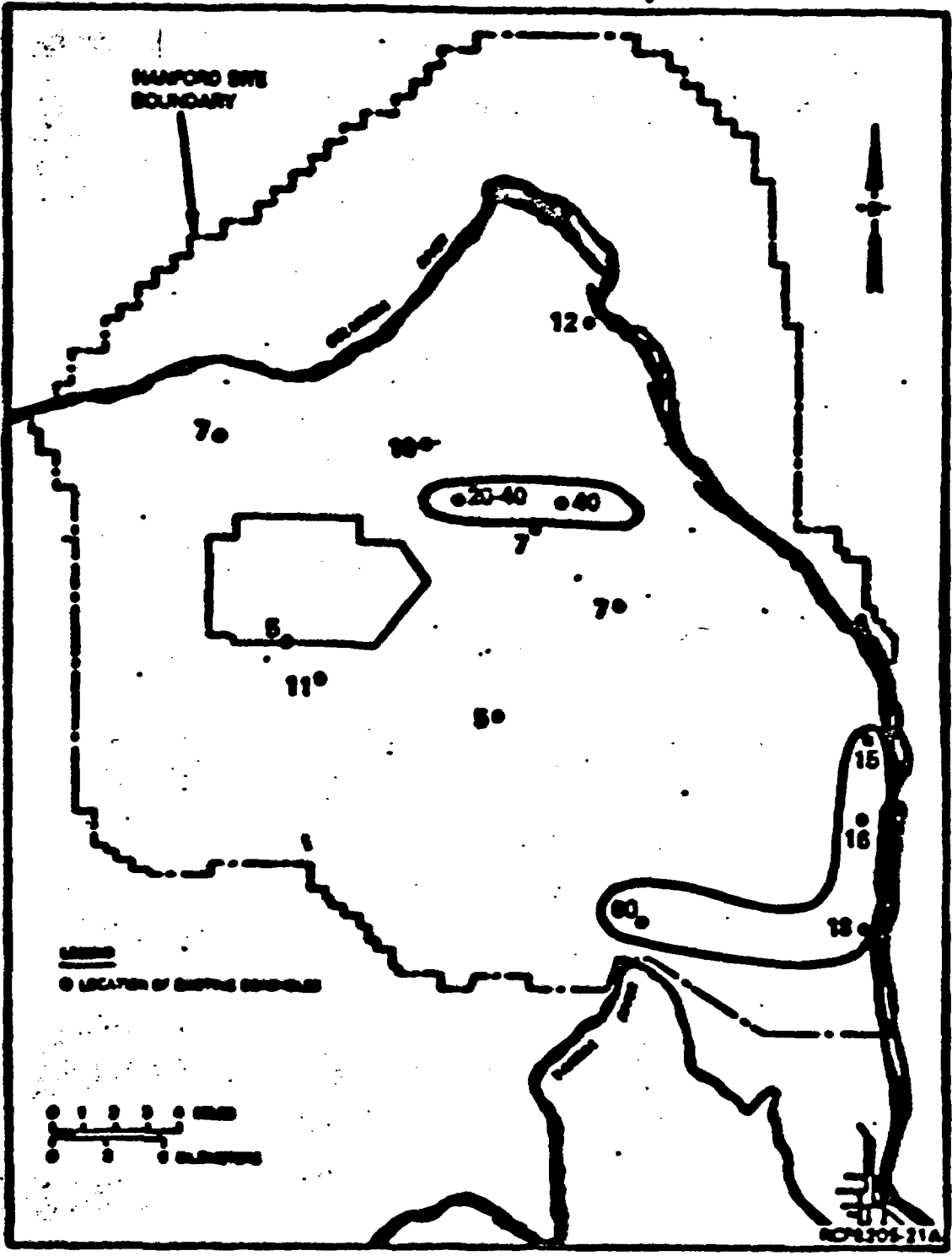


Figure 4.3 Chloride Concentrations (Mg/L) - Mabton Interbed (RHO, 1984)

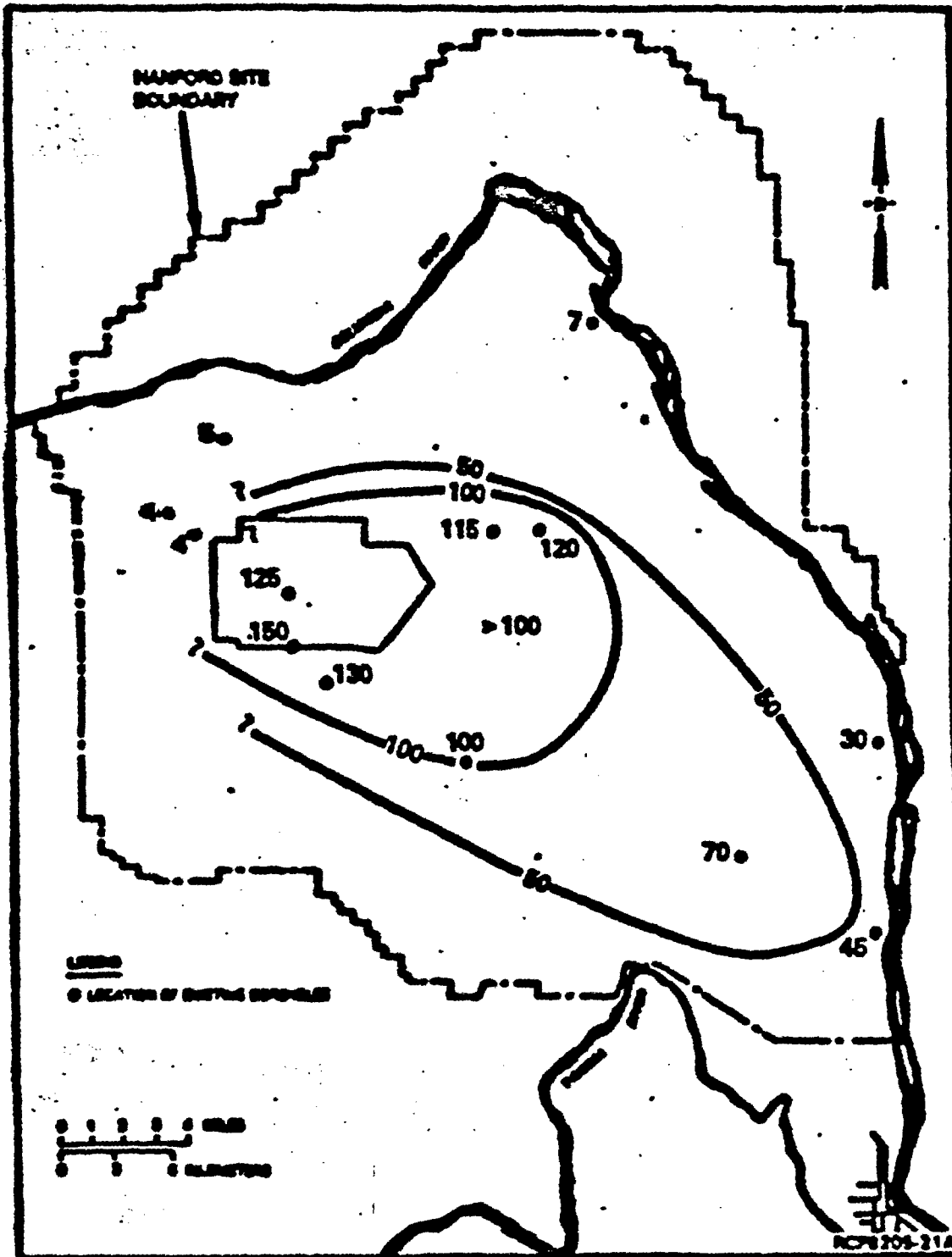


Figure 4.4 Chloride Contours (Mg/L) - U. Wanapum Groundwaters (RHD, 1984)

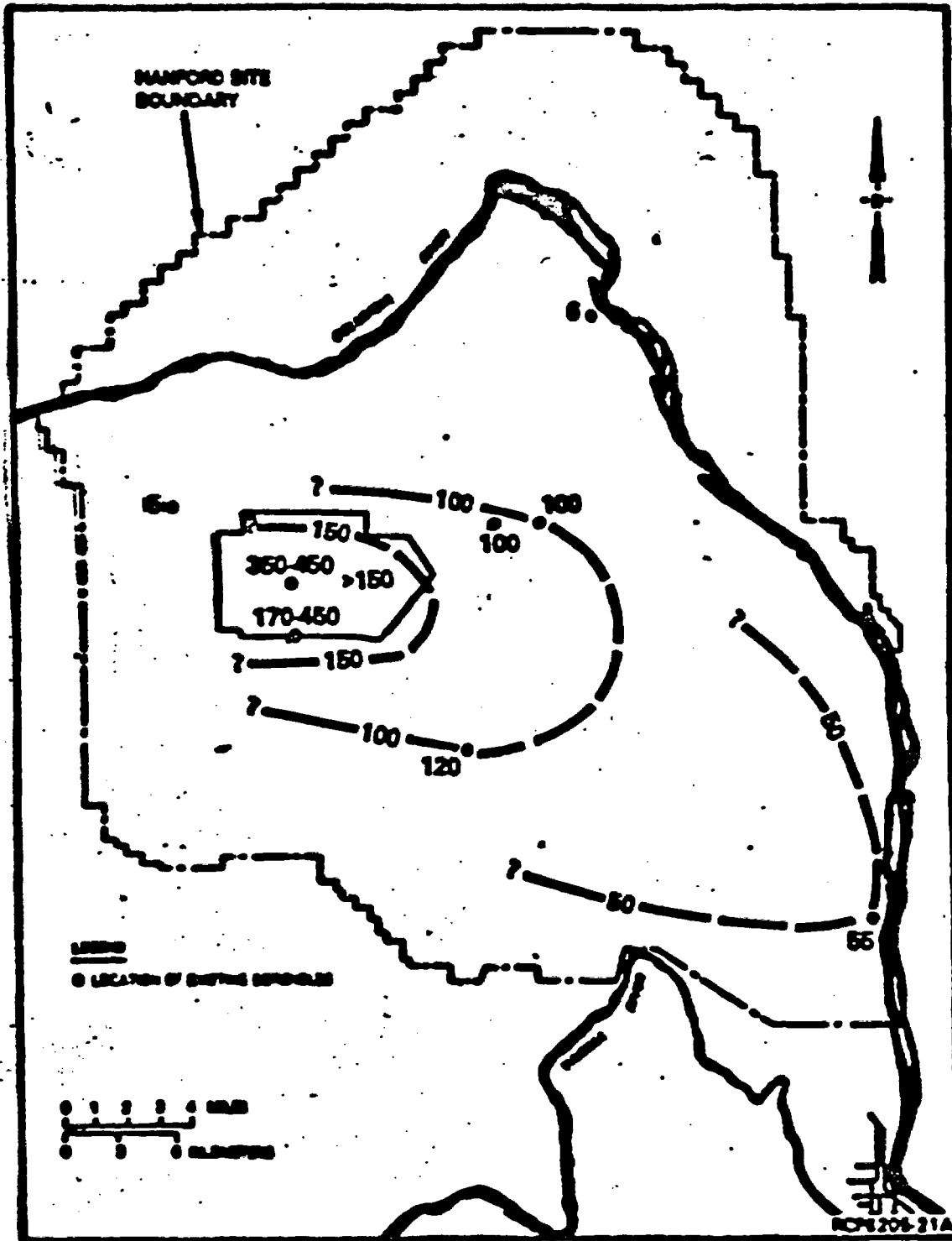


Figure 4.5 Chloride Contours (Mg/L) - L. Wanapum Groundwaters (RHO, 1984)

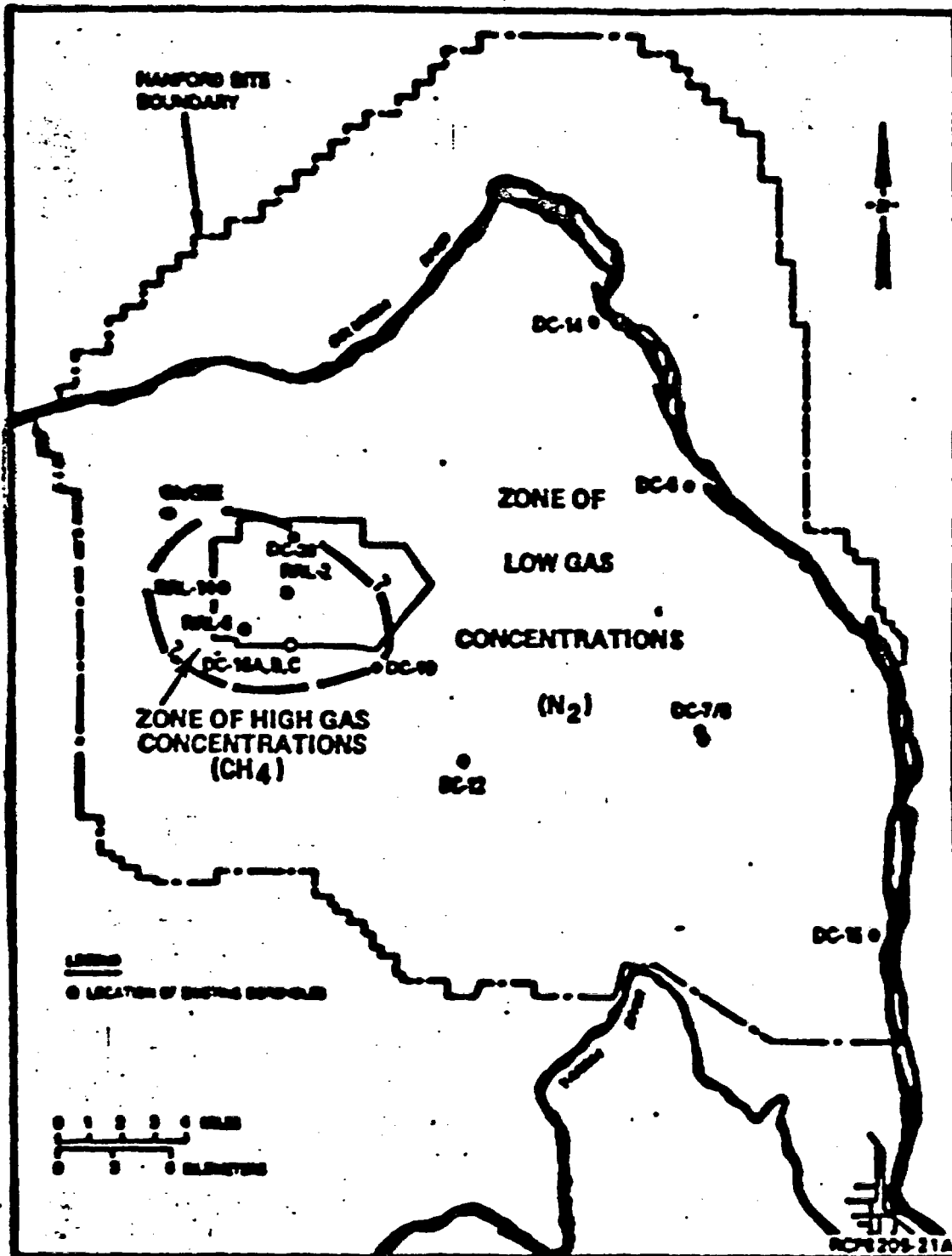


Figure 4.7 Dissolved Gases in the Grande Ronde Formation (RHO, 1984)

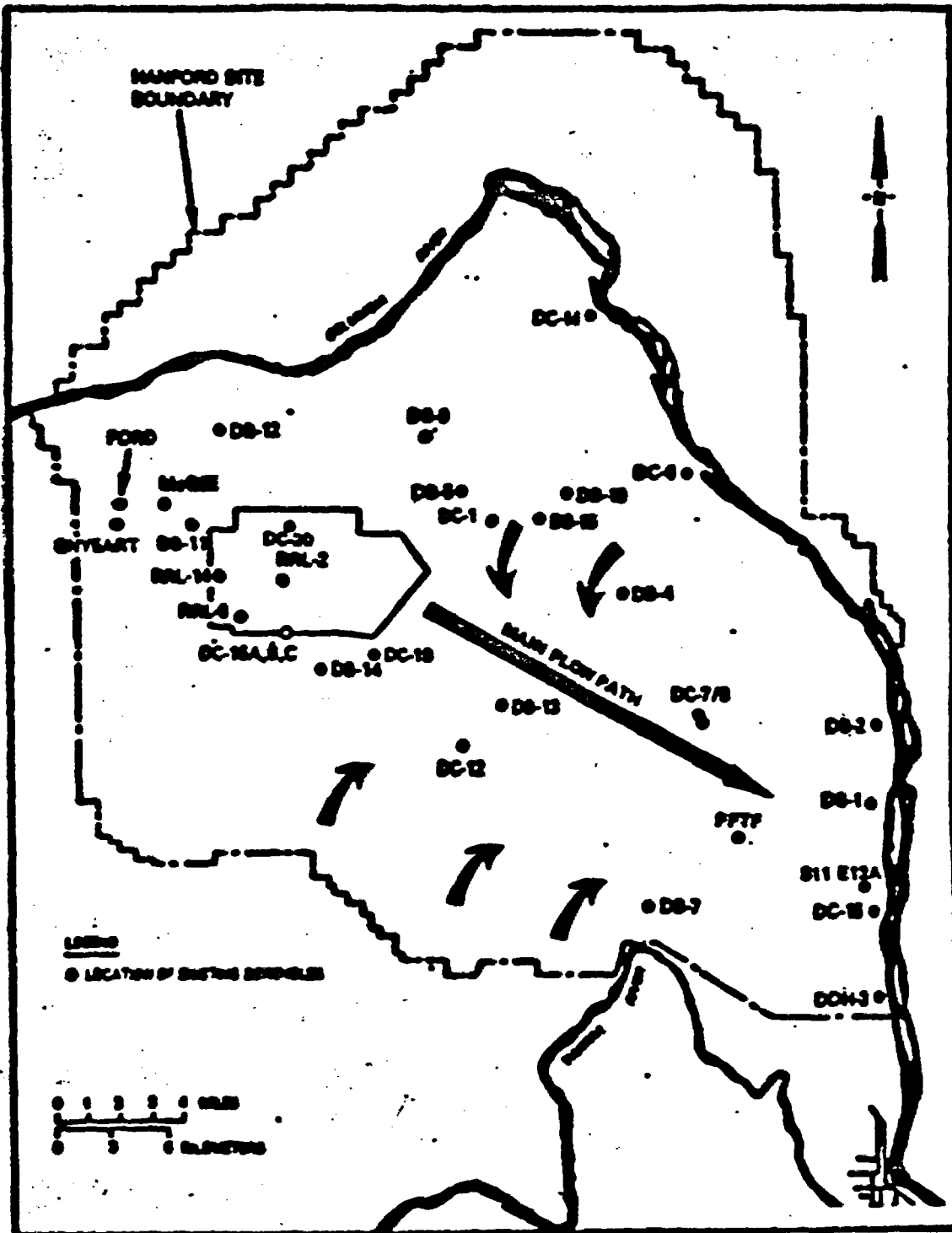


Figure 4.8 Tentative Flow Model Based on Hydrochemistry (RHO, 1984)

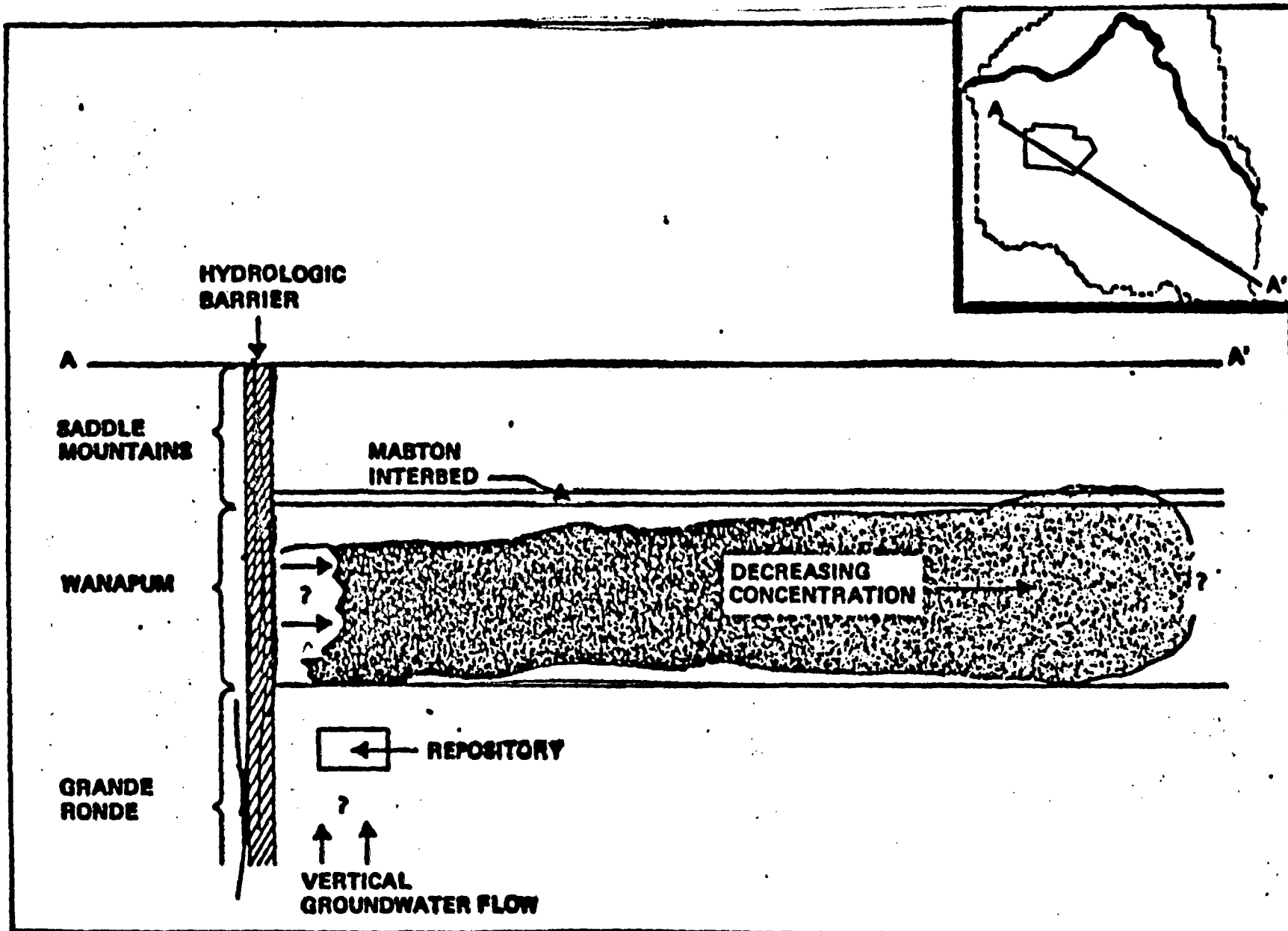


Figure 4.9 Schematic Cross Section AA' Showing Location of Hypothesized Mixing Plume (RUC 1992)

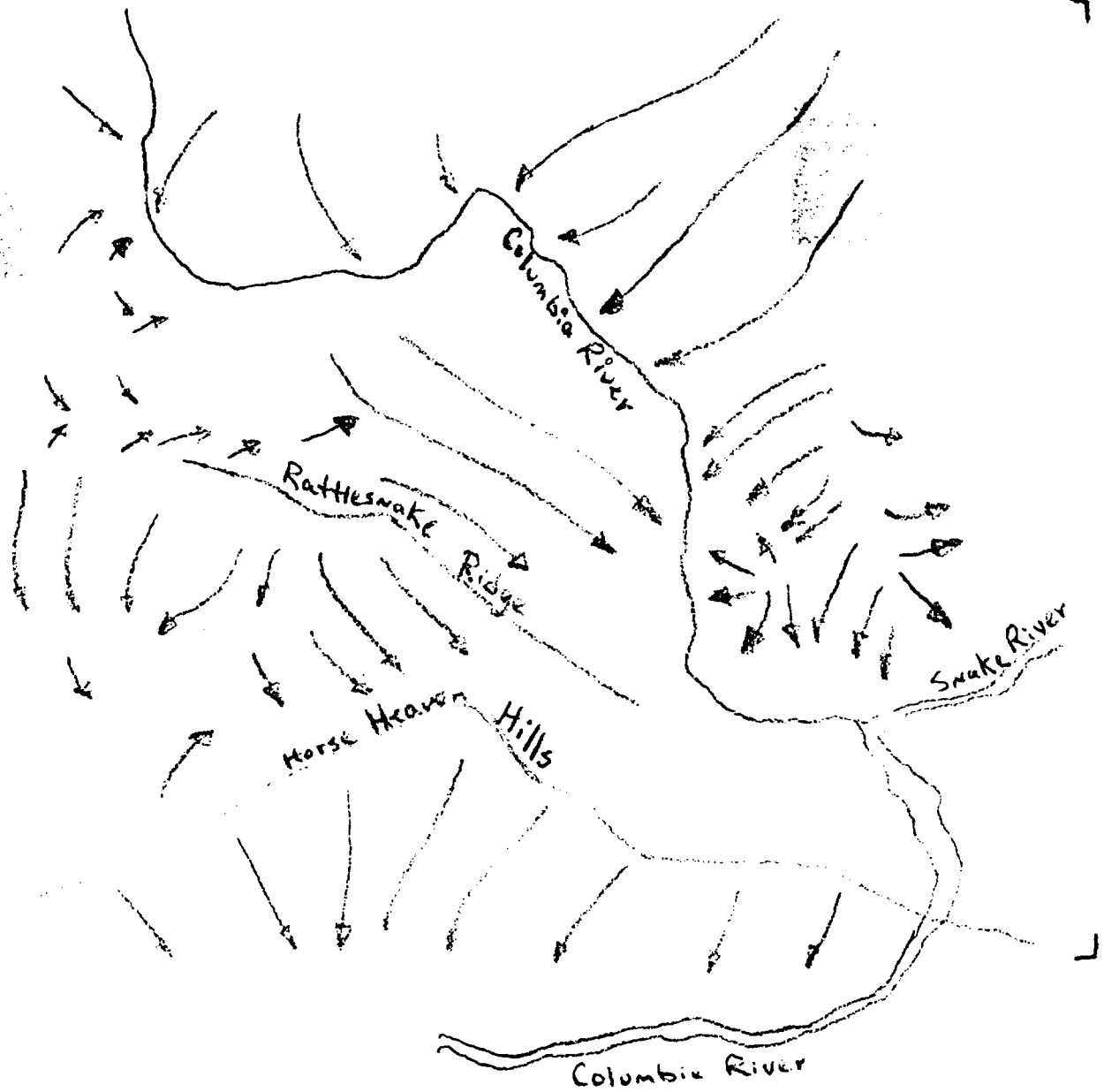


Figure 6.1 Ground-Water Flow Directions Postulated by LaSala and Doty, 1973

Figure 6.2 - Plan View of Streamlines from Hypothetical Repository to Boundary

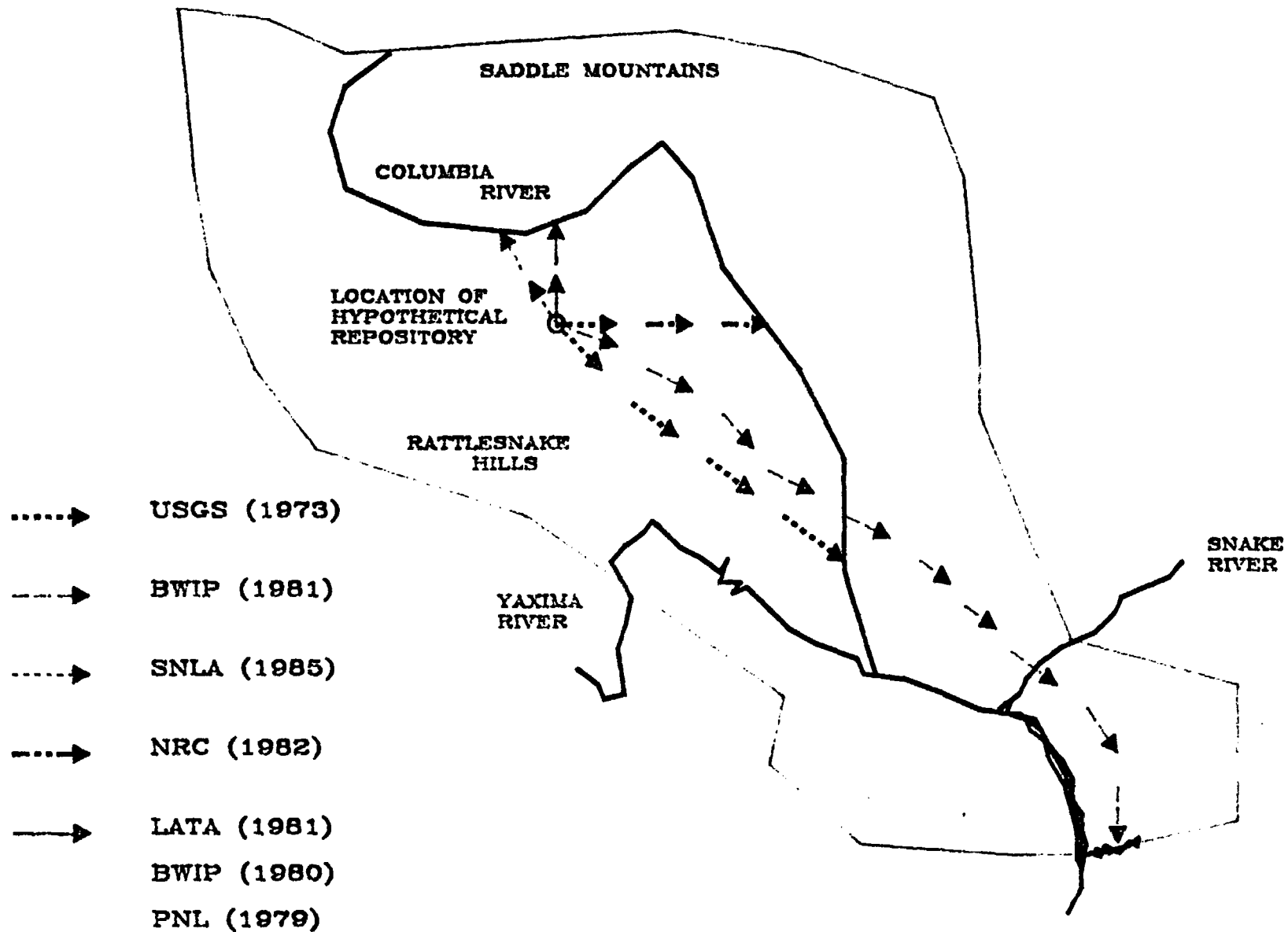
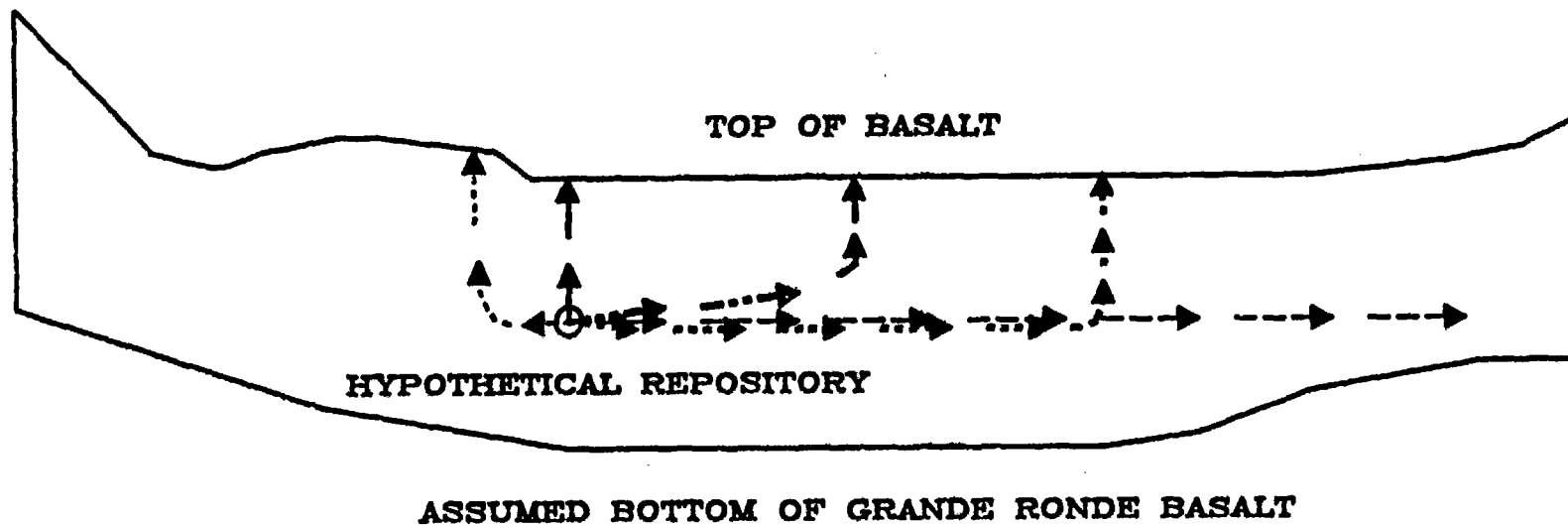


Figure 6.3 Cross section of Model-Calculated Streamlines



- | | | | |
|--------|-------------|--------|-------------|
| -----> | BWIP (1981) |> | NRC (1982) |
|> | SNLA (1985) |> | USGS (1973) |
| ————> | LATA (1981) | | |
| | BWIP (1980) | | |
| | PNL (1981) | | |

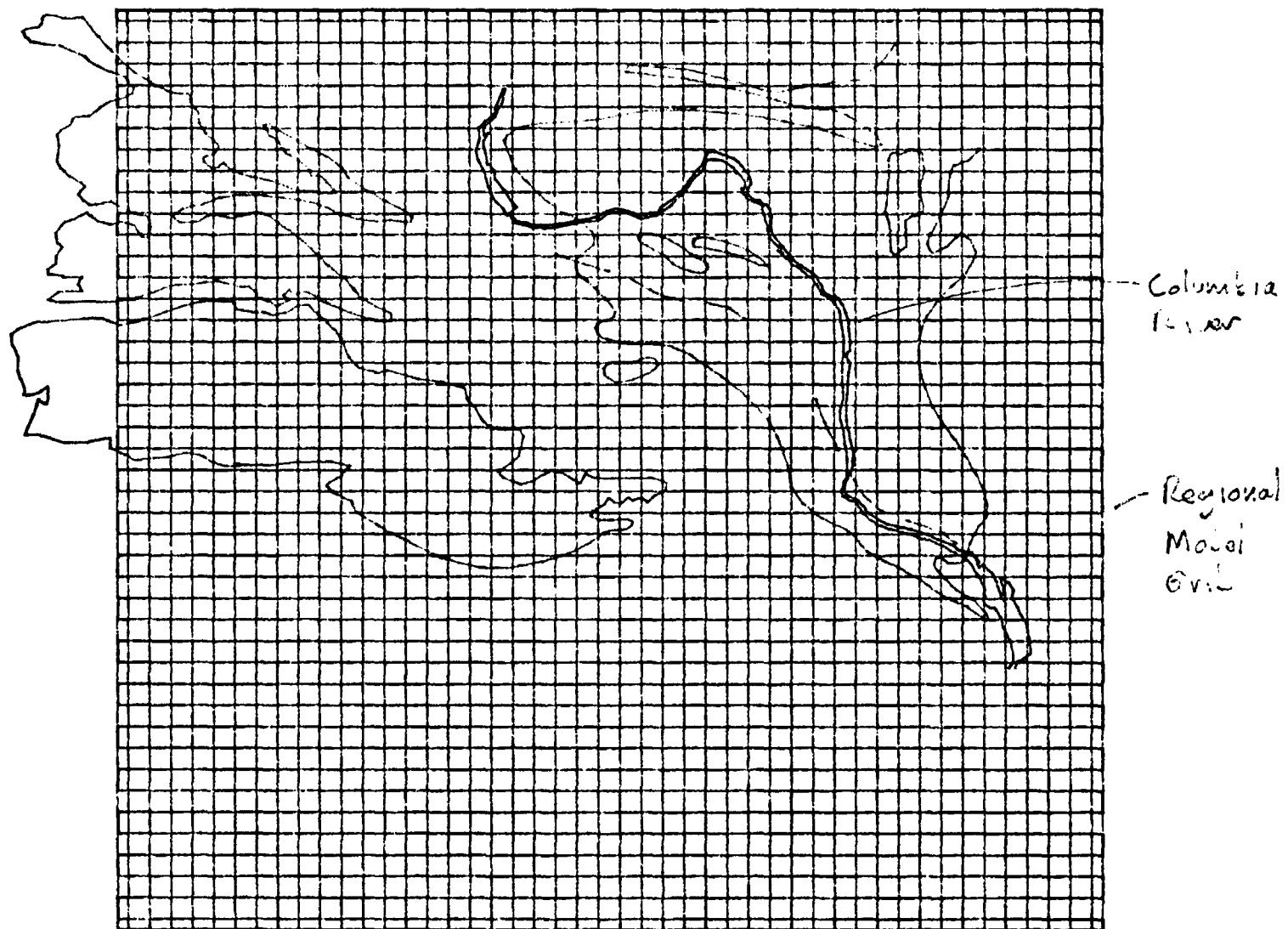


Figure 7.1 Regional Model Grid

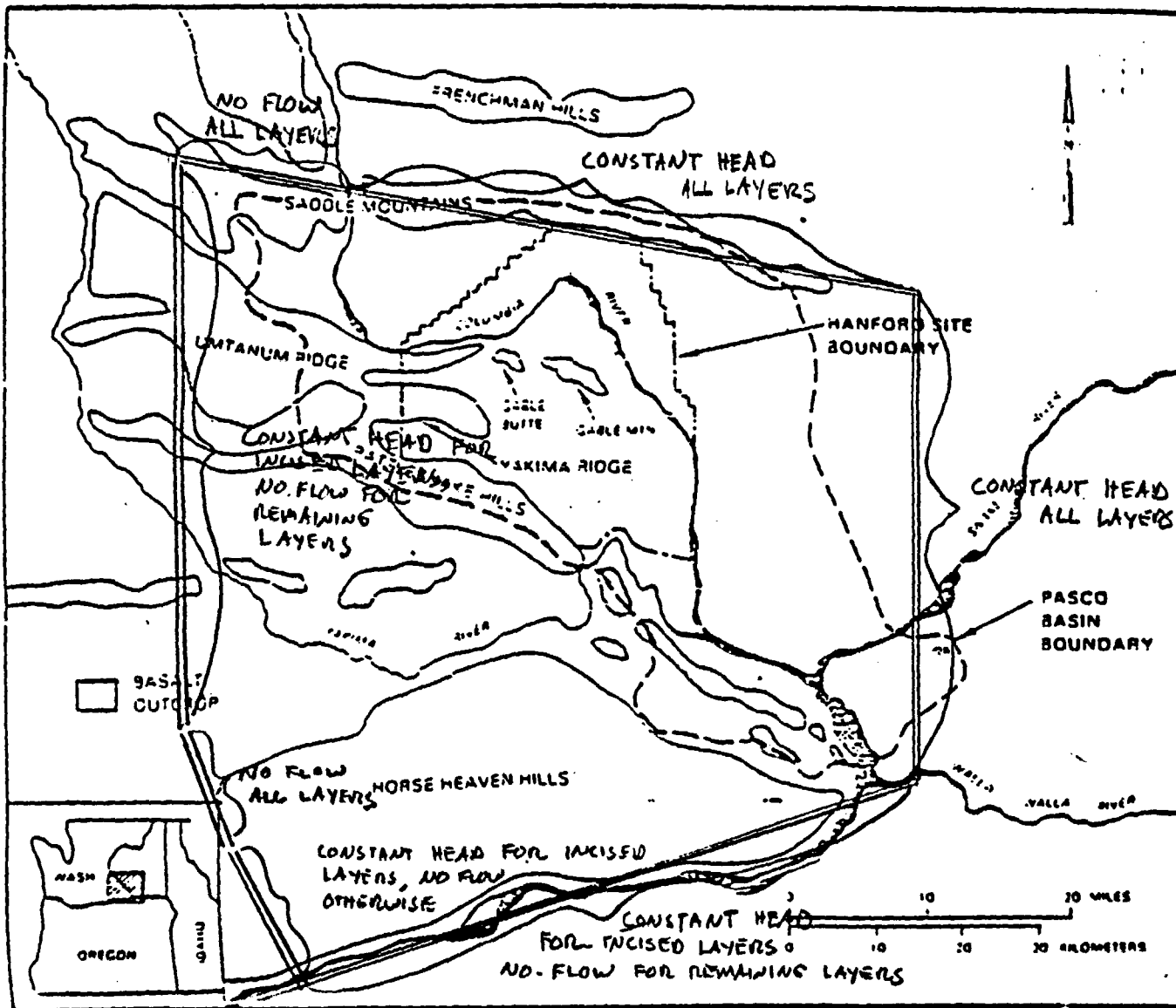
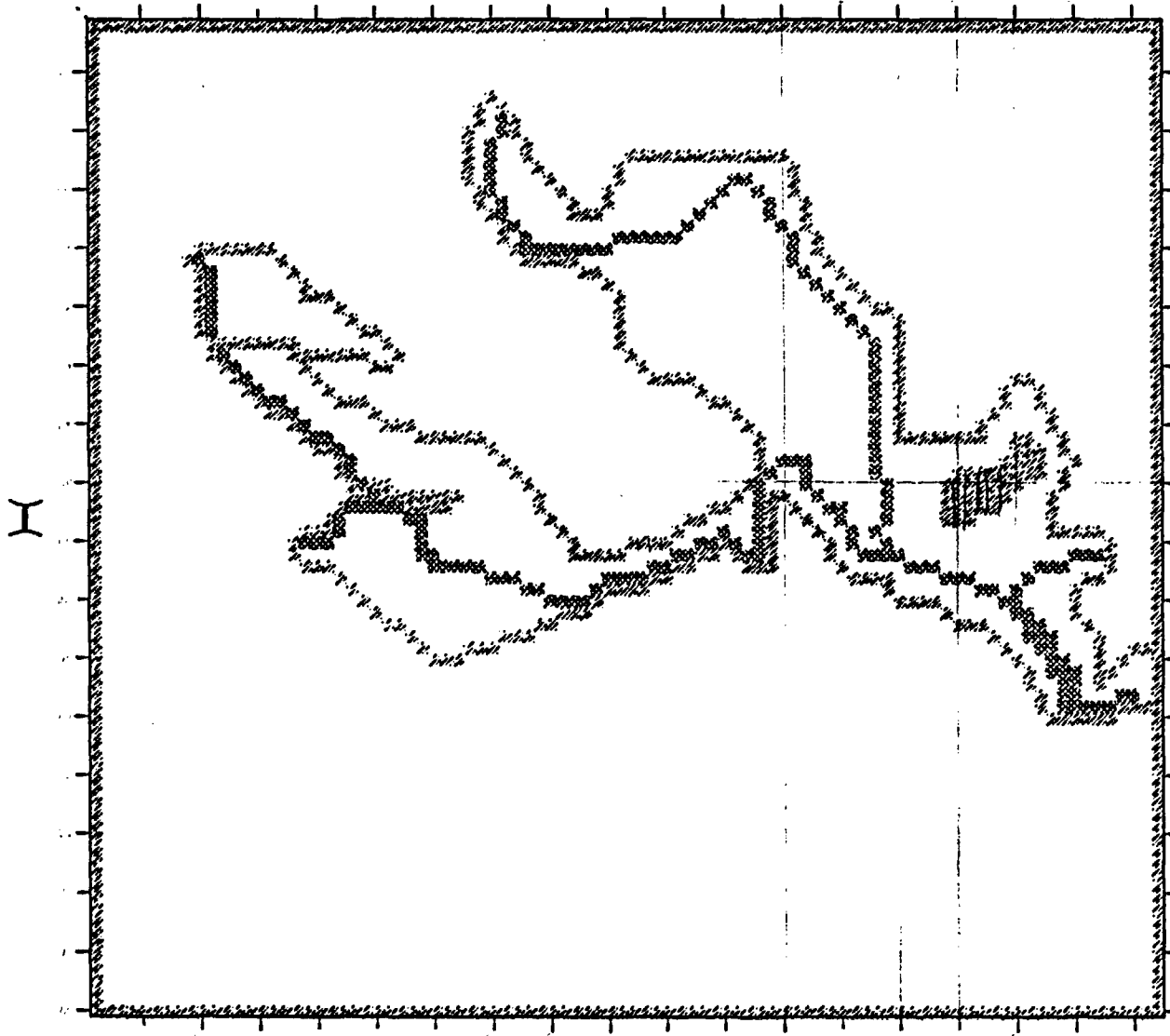


Figure 7.2 Boundary Conditions for the Regional Model

J



EXPLANATION

-  NO-FLOW BLOCKS
-  CONSTANT HEAD BLOCKS
- X - ROW INDEX
- J - COLUMN INDEX

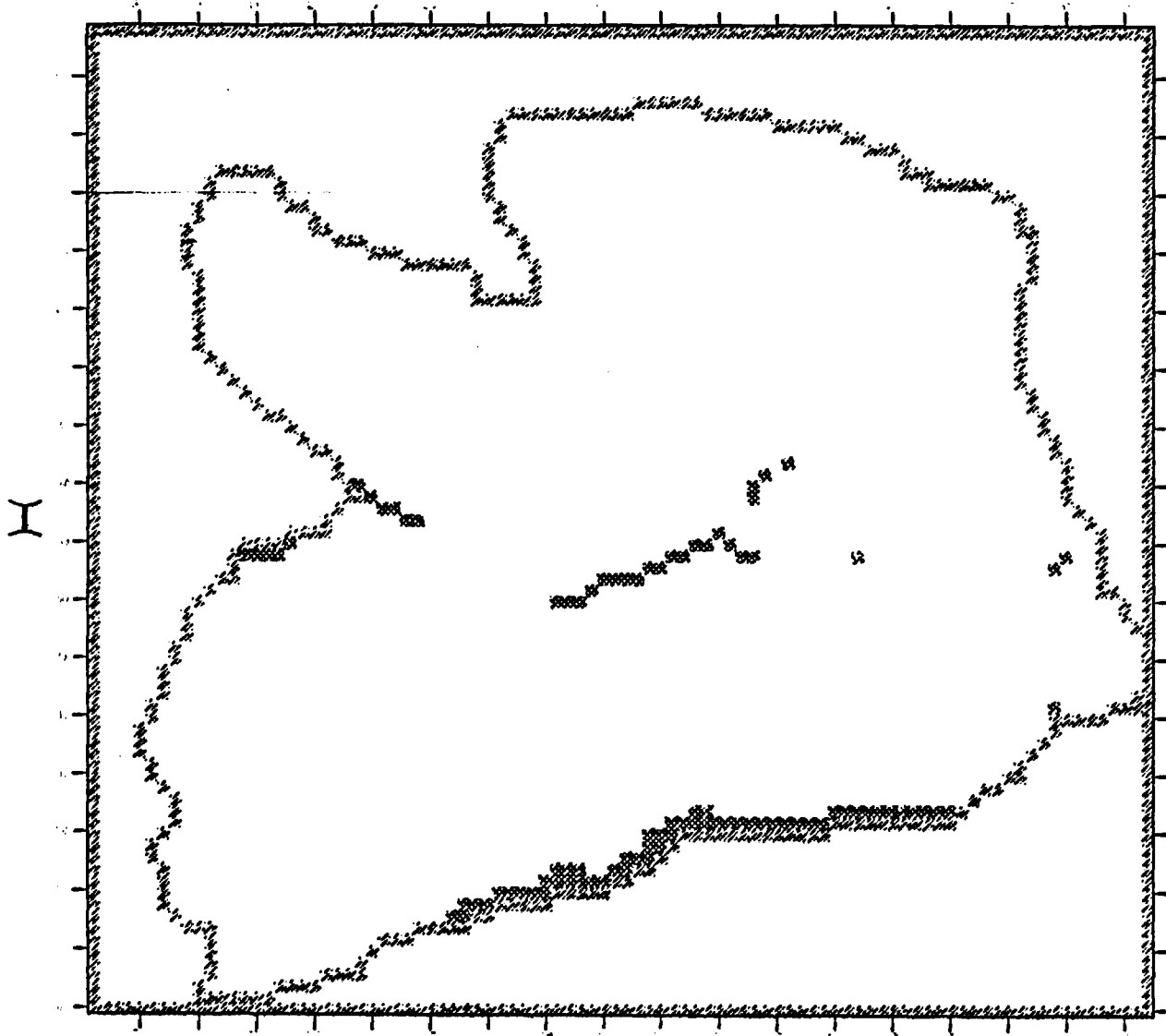
1 2 3 4 5 6 7 8 9 10 11 12 13 14 15 16 17 18 19 20 21 22 23 24 25 26 27 28 29 30 31 32 33 34 35 36 37 38 39 40 41 42 43 44 45 46 47 48 49 50 51 52 53 54 55 56 57 58 59 60 61 62 63 64 65 66 67 68 69 70 71 72 73 74 75 76 77 78 79 80 81 82 83 84 85 86 87 88 89 90 91 92 93 94 95 96 97 98 99 100

Figure 7.3 No-Flow and Constant Head Boundaries for Layer 4

PREPARED IN COOPERATION WITH
NUCLEAR REGULATORY COMMISSION

SANDIA NATIONAL LABORATORIES
ALBUQUERQUE, NEW MEXICO

J



EXPLANATION

- ☒ NO-FLOW BOUNDARY
- ☒ CONSTANT FLUX BOUNDARY
- X - ROW INDEX
- J - COLUMN INDEX

1 2 3 4 5 6 7 8 9 10 11 12 13 14 15 16 17 18 19 20 21 22 23 24 25 26 27 28 29 30 31 32 33 34 35 36 37 38 39 40 41 42 43 44 45 46 47 48 49 50 51 52 53 54 55 56 57 58 59 60 61 62 63 64 65 66 67 68 69 70 71 72 73 74 75 76 77 78 79 80 81 82 83 84 85 86 87 88 89 90 91 92 93 94 95 96 97 98 99 100

Figure 7.4 No-Flow and Constant Head Boundaries for Layer 3

PREPARED IN COOPERATION WITH
NUCLEAR REGULATORY COMMISSION

SANDIA NATIONAL LABORATORIES
ALBUQUERQUE, NEW MEXICO

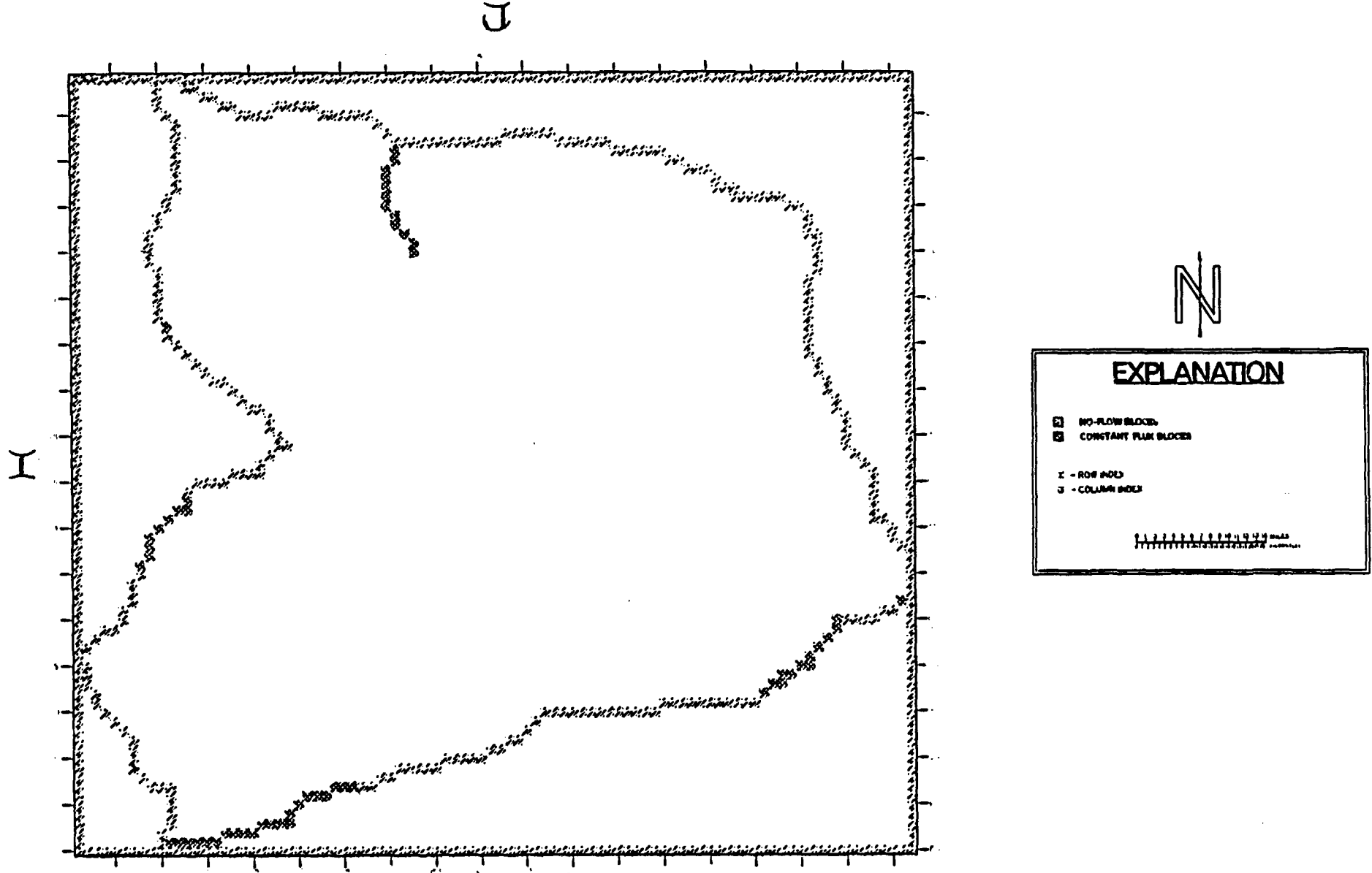


Figure 7.5 No-Flow and Constant Head Boundaries for Layer 2

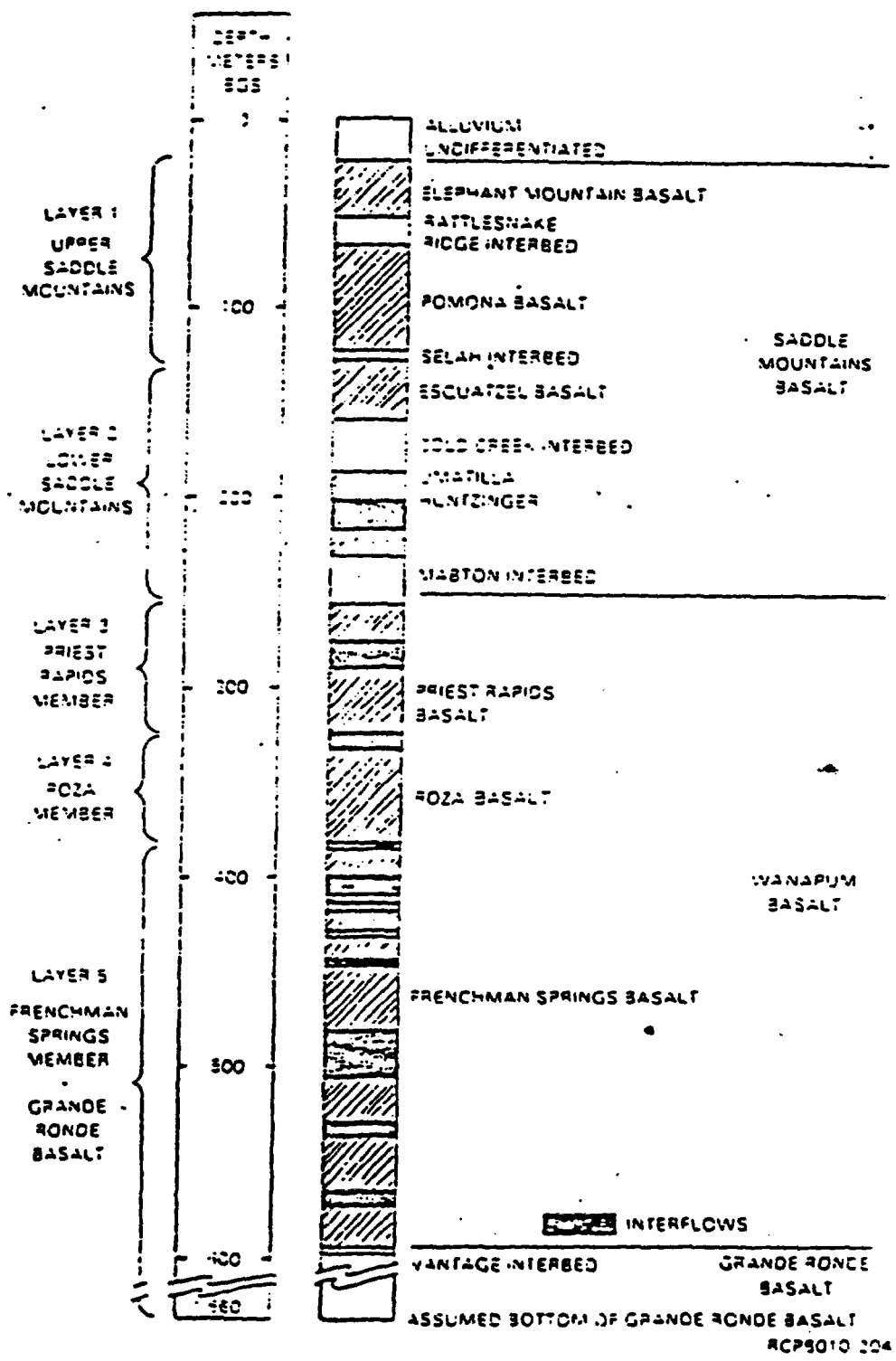


Figure 7.7 Generalized Stratigraphy of the Pasco Basin

CALCULATION OF HYDRAULIC CONDUCTIVITIES

REAL SYSTEM	MODEL LAYER
K, b	
K, b	K_h, K_v, b
K, b	
K, b	

HORIZONTAL HYDRAULIC CONDUCTIVITY

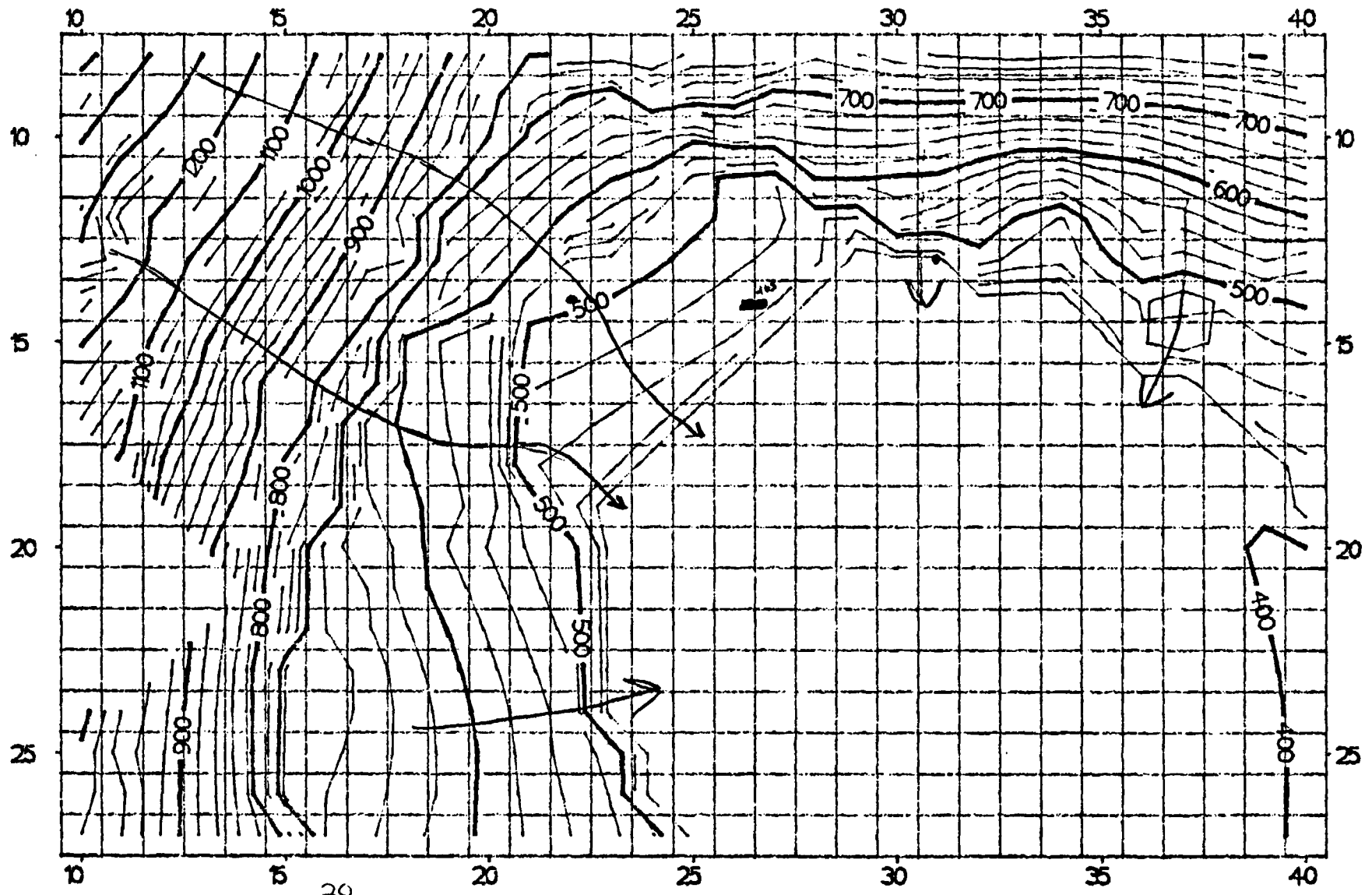
$$K_h = \frac{\sum_i K_i b_i}{\sum_i b_i}$$

VERTICAL HYDRAULIC CONDUCTIVITY

$$K_v = \frac{\sum_i b_i}{\sum_i \frac{b_i}{K_i}}$$

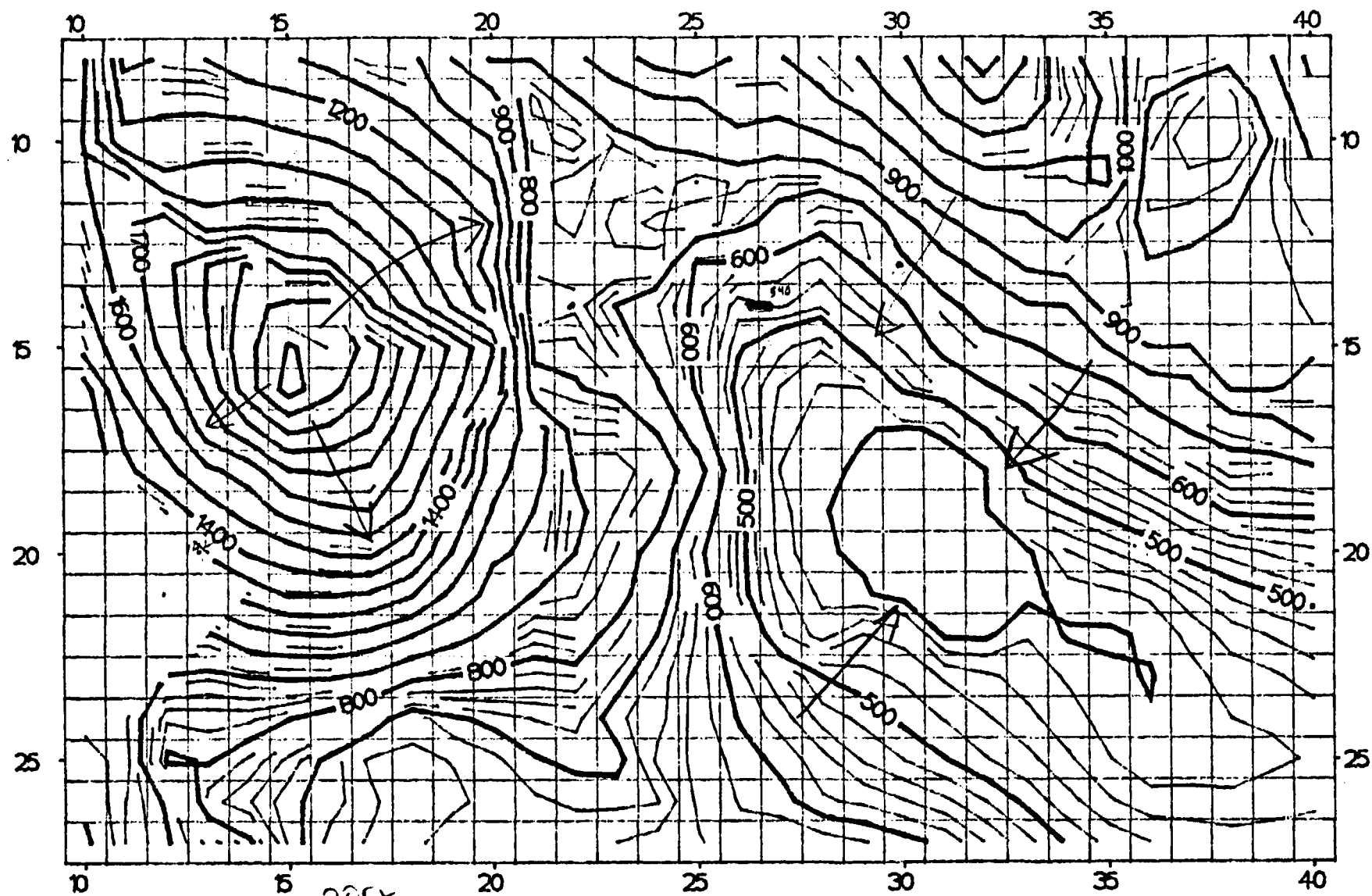
Figure 7.8 Calculation of Effective Conductivities for the Regional Model

These figures will
some points of
reference - rivers, RR, etc



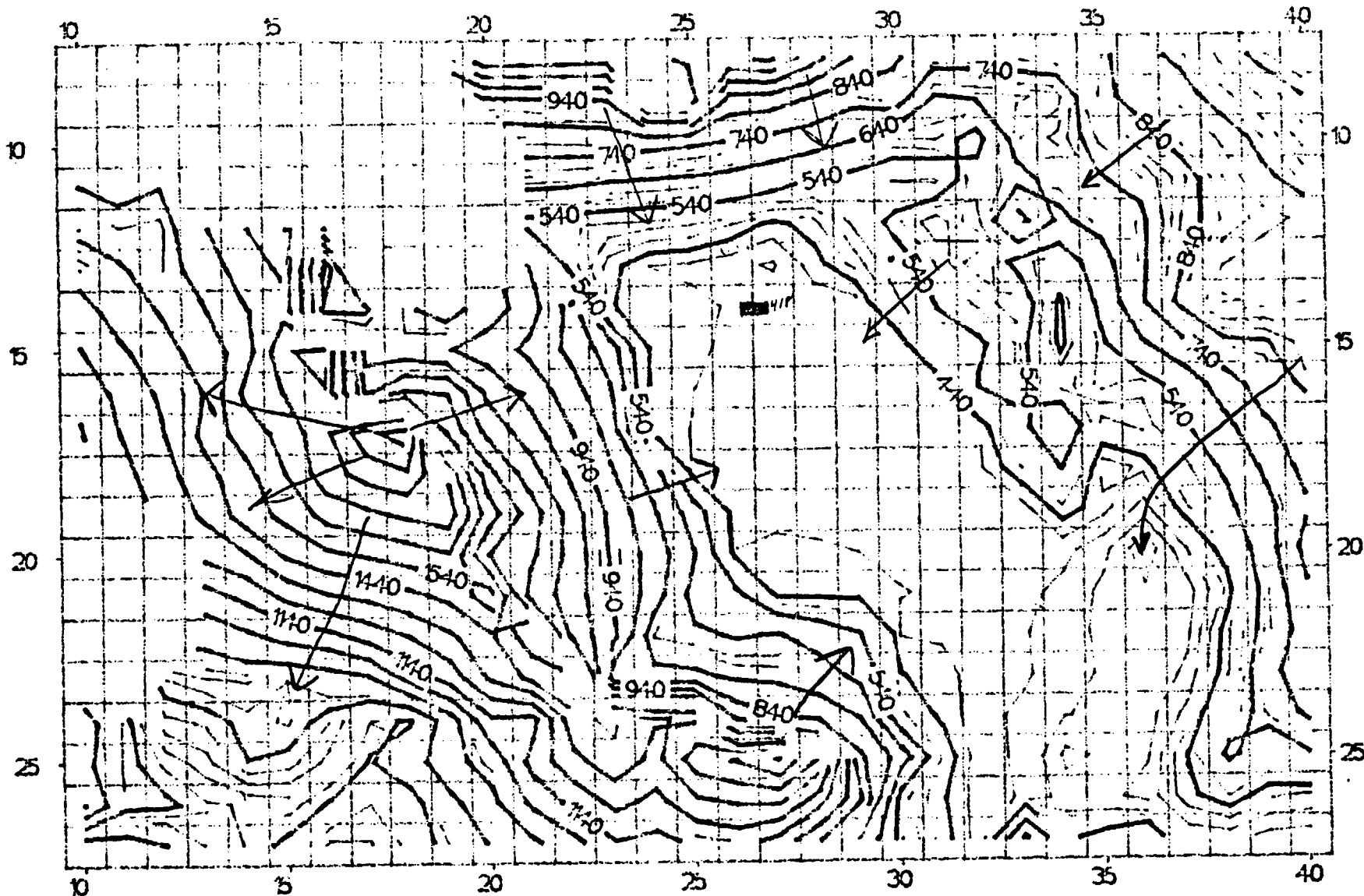
CONTOUR INTERVAL = 200×10^4
VERTICAL EXAGGERATION = 10
ELAPSED TIME = 0.0000 SECONDS

Figure 7.9 - KRIGED HEADS FOR THE
GRANDE RONDE BASALTS



CONTOUR INTERVAL = 200×10^1
 VERTICAL EXAGGERATION = 10
 ELAPSED TIME = 0.0000 SECONDS

Figure 7.10 - KRIGED HEADS FOR THE WANAPUM BASALTS



CONTOUR INTERVAL = 200' ±
 VERTICAL EXAGGERATION = 10
~~PLANNED TIME = 0.0000 SECONDS~~

Figure 7.11 - KRIGED HEADS FOR THE
 SADDLE MOUNTAINS BASALTS

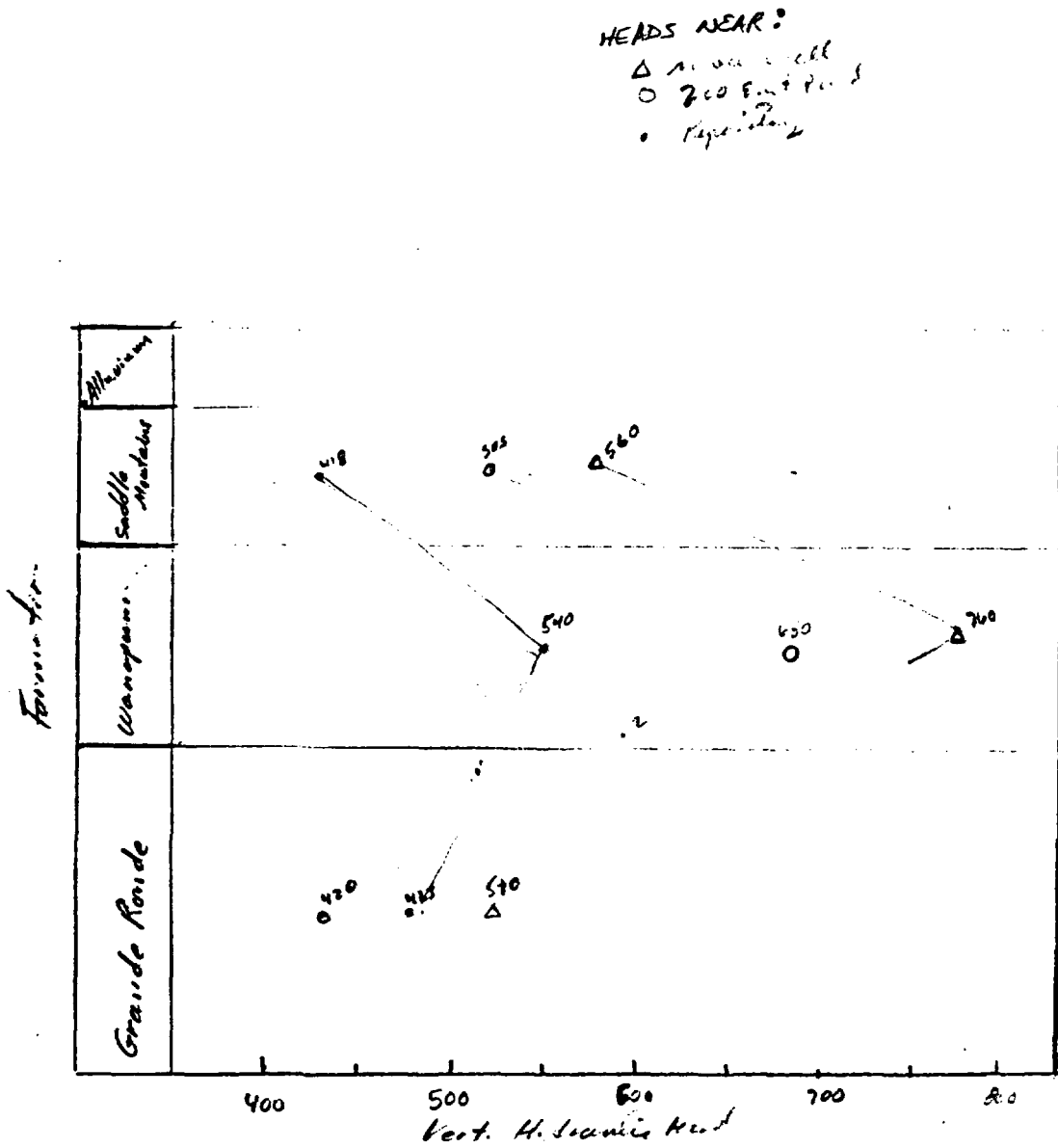
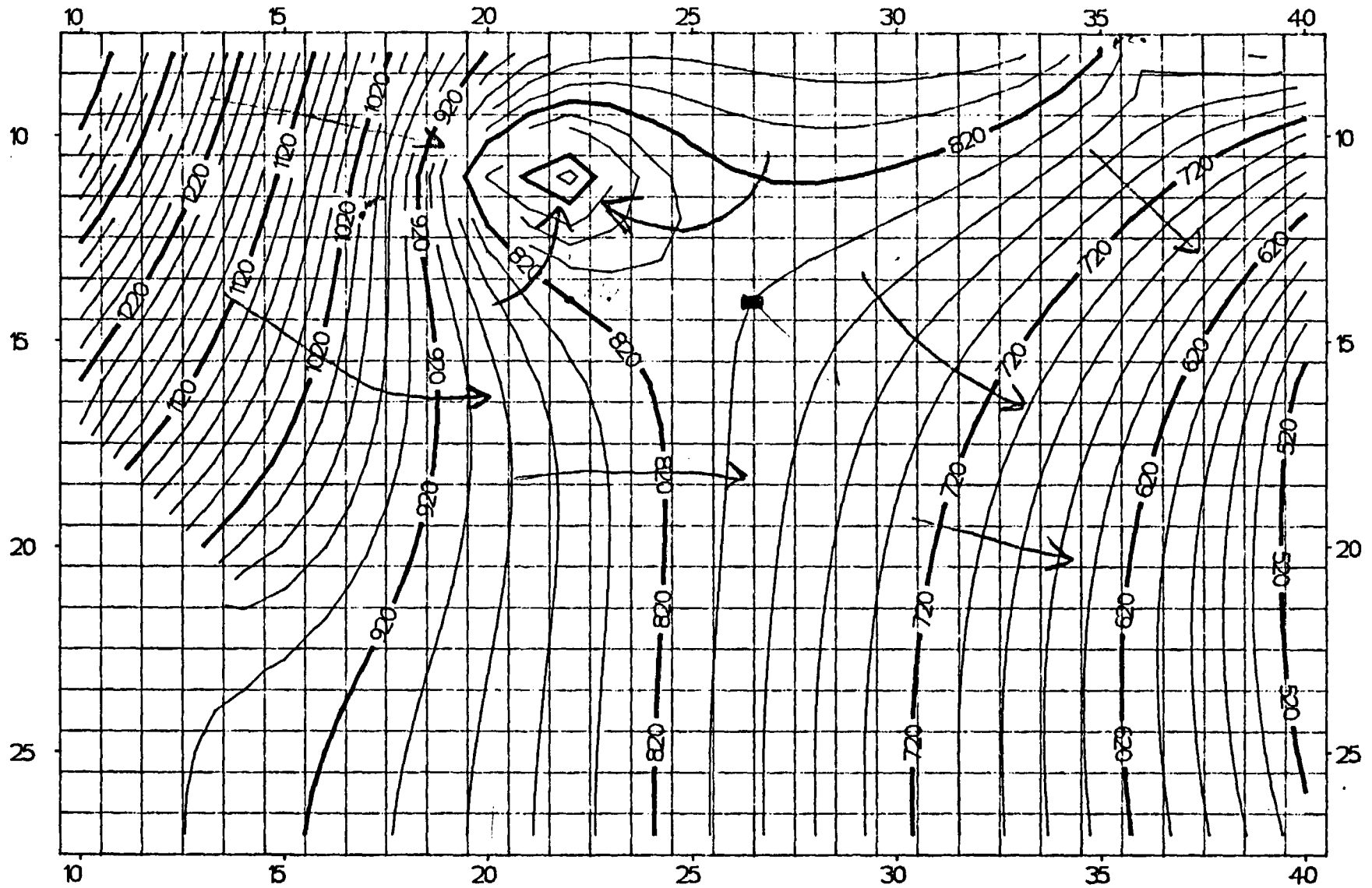
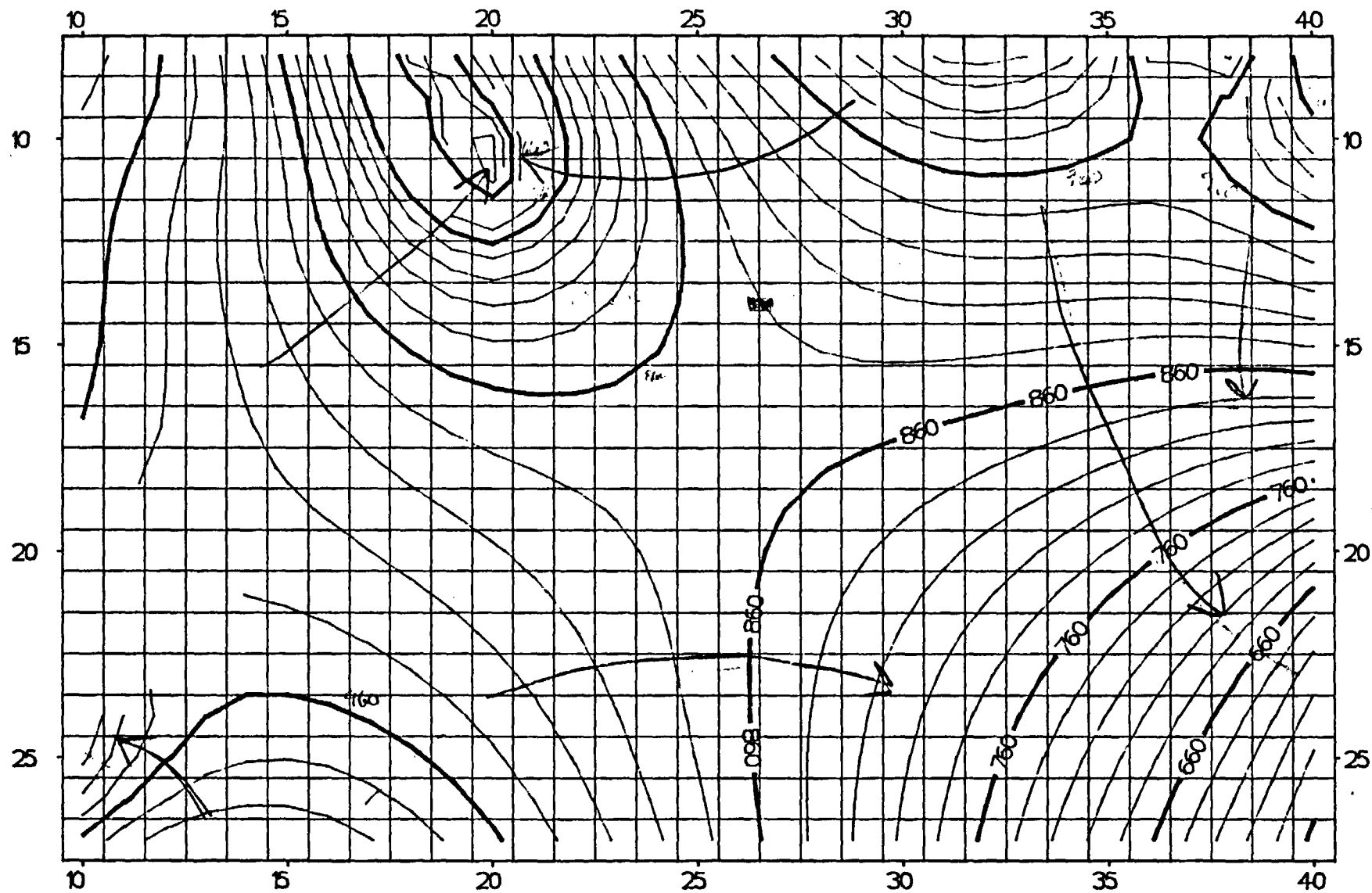


Figure 7.12 Composite Vertical Profile of Kriged Hydraulic Heads near the RRL, McGee Well, and 200 Ponds Areas



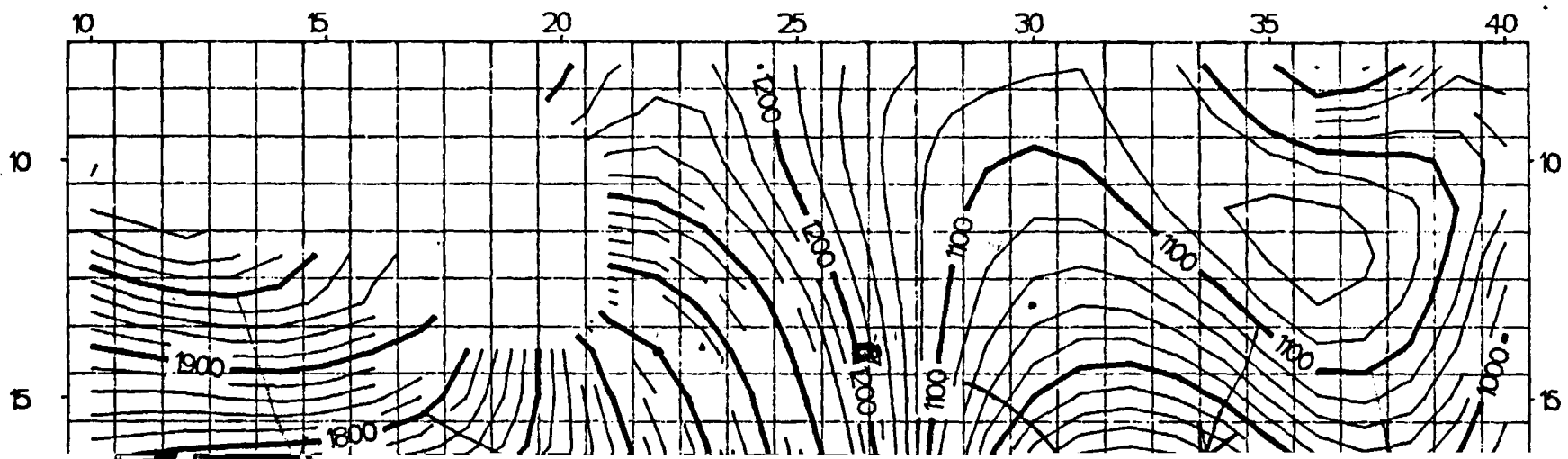
CONTOUR INTERVAL = 200 ~~ft~~
 VERTICAL EXAGGERATION = ~~10~~
 ELAPSED TIME = ~~7.8840 × 10⁶~~ SECONDS

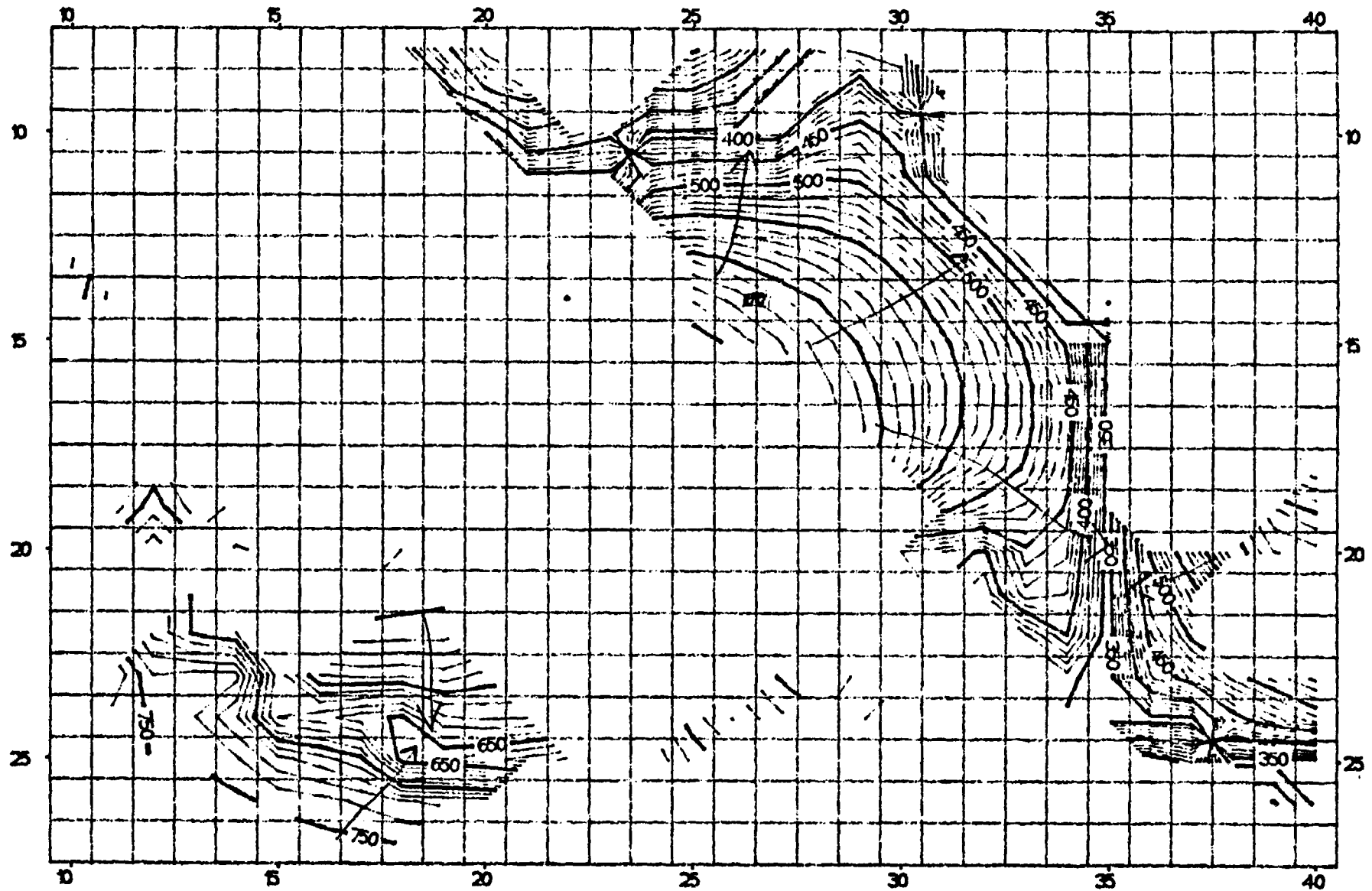
Figure 7.13 - Simulated Heads for the Grande Ronde Basalts



CONTOUR INTERVAL = 200 ft.
 VERTICAL EXAGGERATION = 10
 ELAPSED TIME = 71240 SECONDS

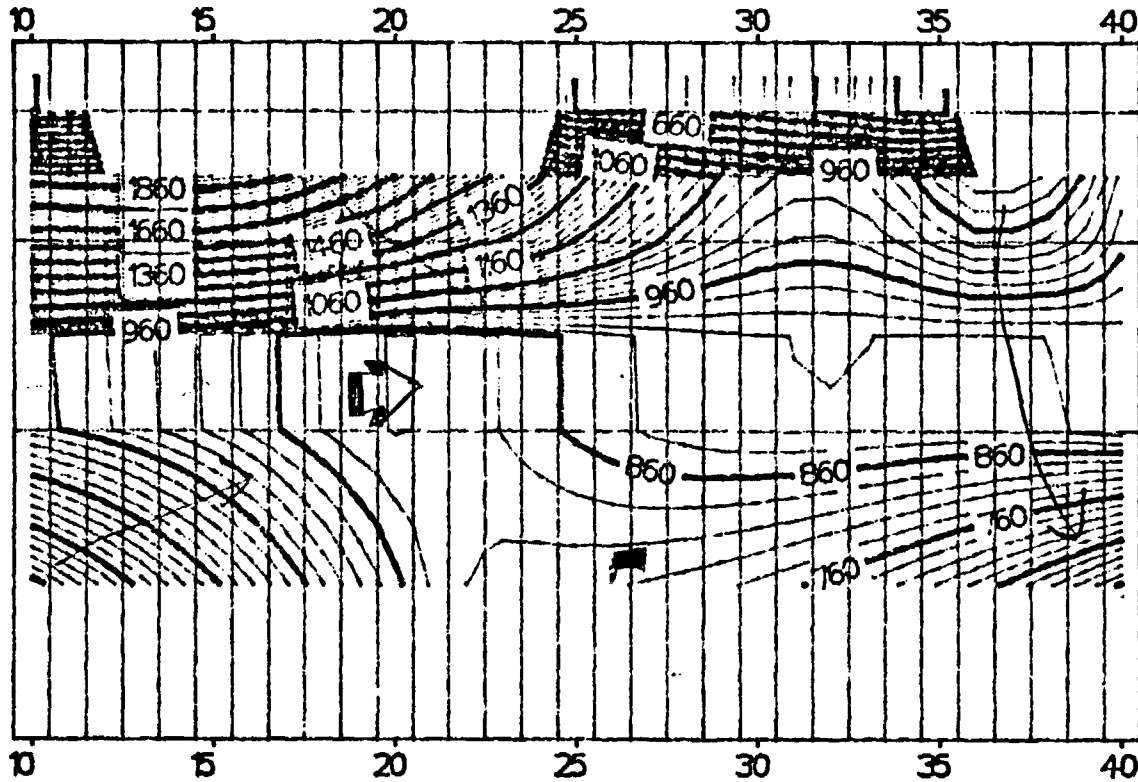
Figure 7.1/t - Simulated Heads for the Wanapum Basalts





CONTOUR INTERVAL = 100×10^1
 VERTICAL EXAGGERATION = -10
 ELAPSED TIME = 78840×10^6 SECONDS

Figure 7.1.6 - Simulated Heads for the Alluvium



CONTOUR INTERVAL = 200 ~~ft~~
 VERTICAL EXAGGERATION = 50.0
~~HEAD UNIT = 100 TO 100 SECONDS~~

Figure 7.17 - Simulated Heads
East-West Section through the RRL

Δ McGee Well
 ○ 200 East Area
 • Peperita

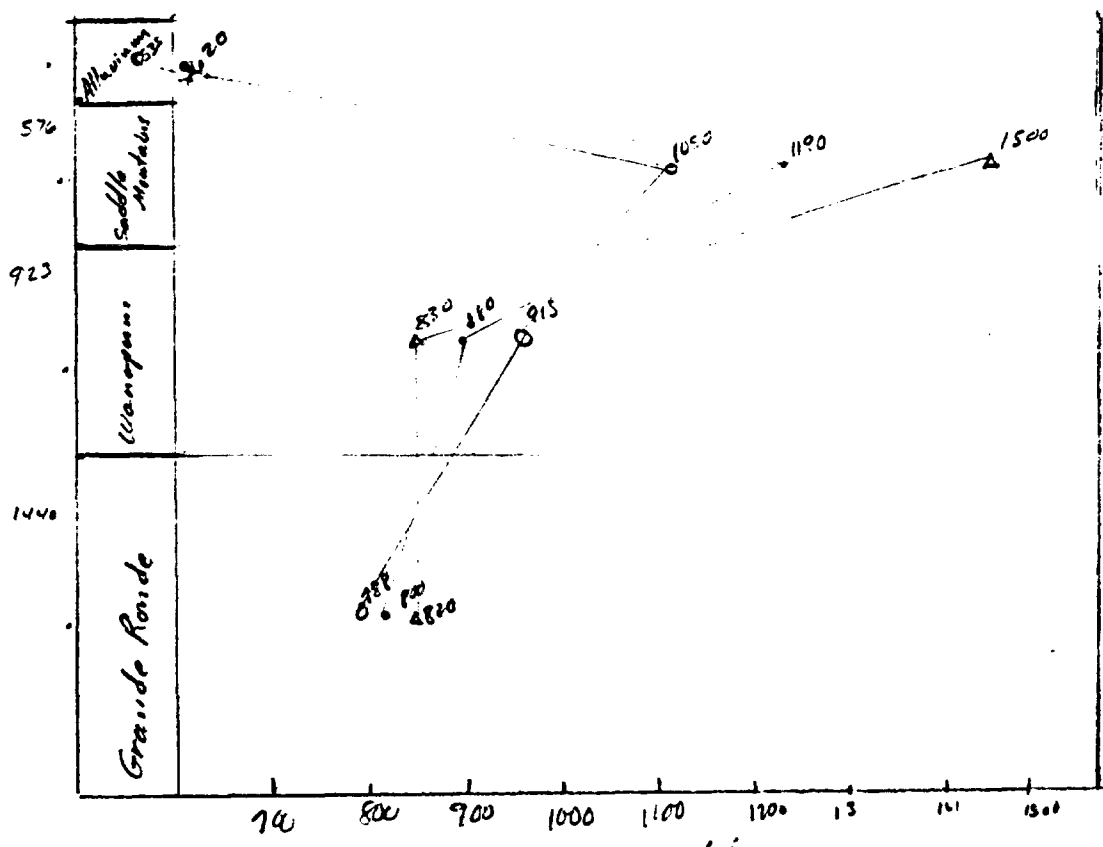
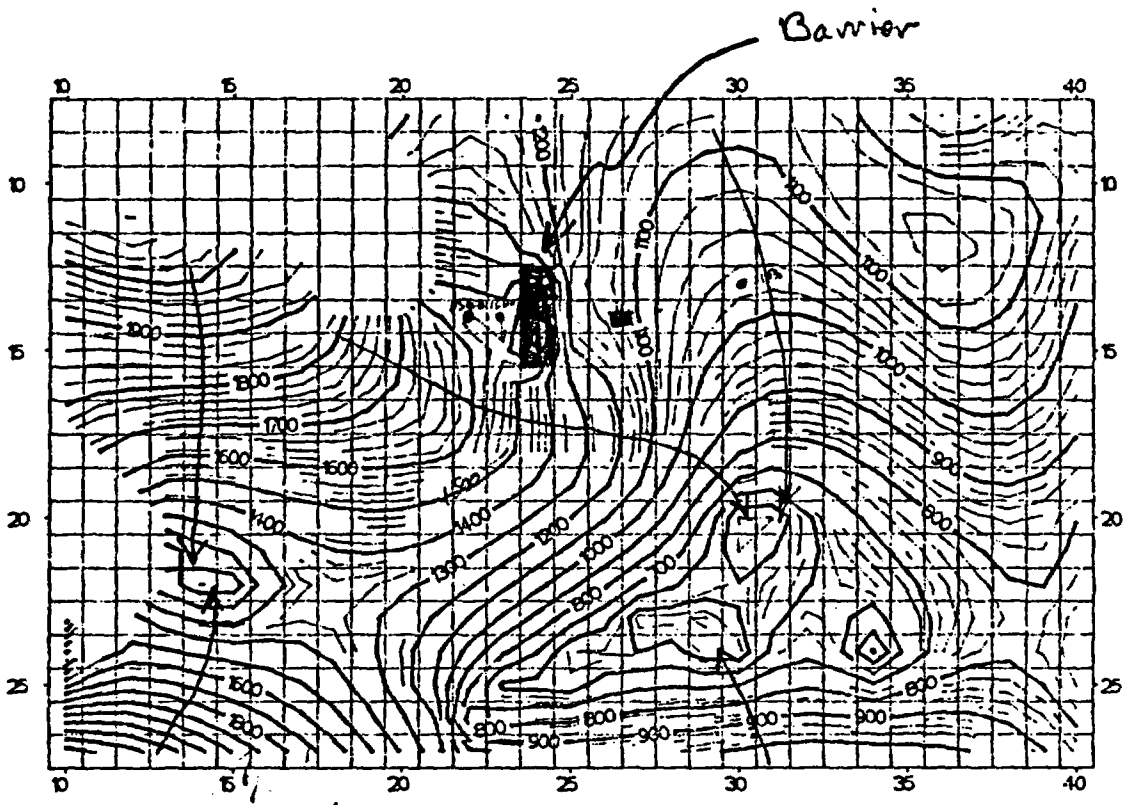


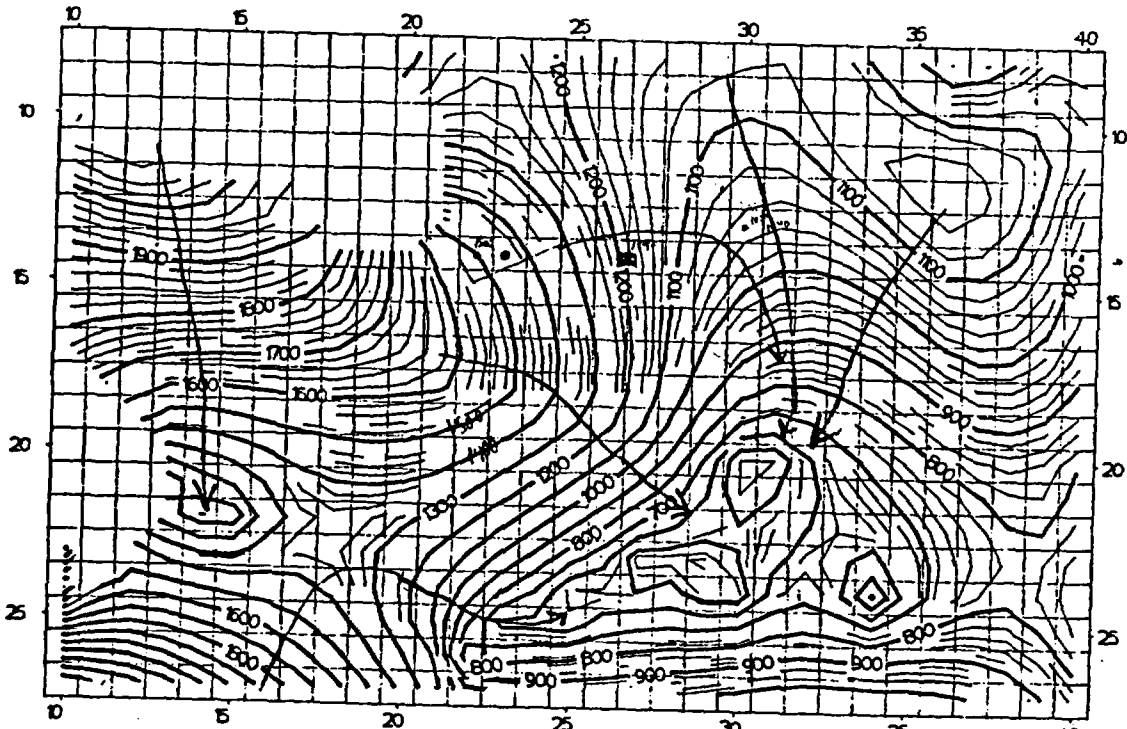
Figure 7.18 Composite Vertical Profile of Simulated Hydraulic Heads at the RRL, McGee Well, and 200 Ponds Areas



CONTOUR INTERVAL = 200×10^1
 VERTICAL EXAGGERATION = -10
 ELAPSED TIME = 7.8840×10^4 SECONDS

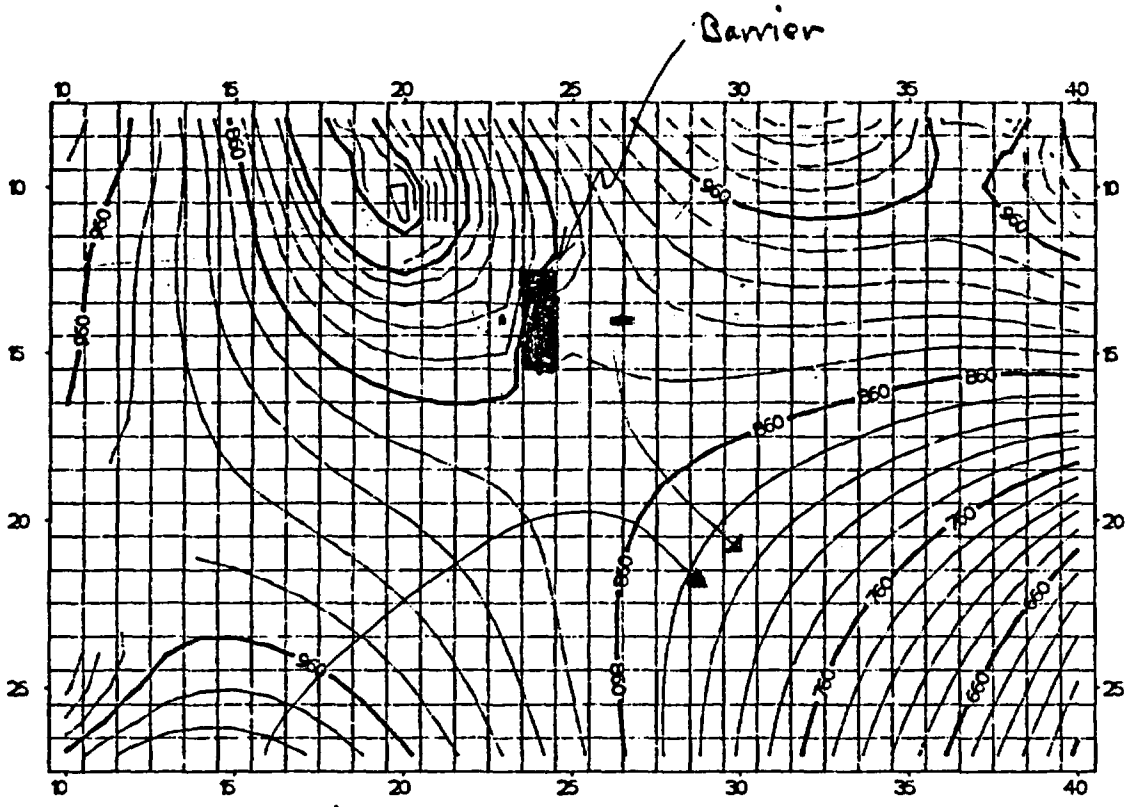
BARRIER INCLUDED

INITIAL RUN



CONTOUR INTERVAL = 200×10^1
 VERTICAL EXAGGERATION = -10
 ELAPSED TIME = 7.8840×10^4 SECONDS

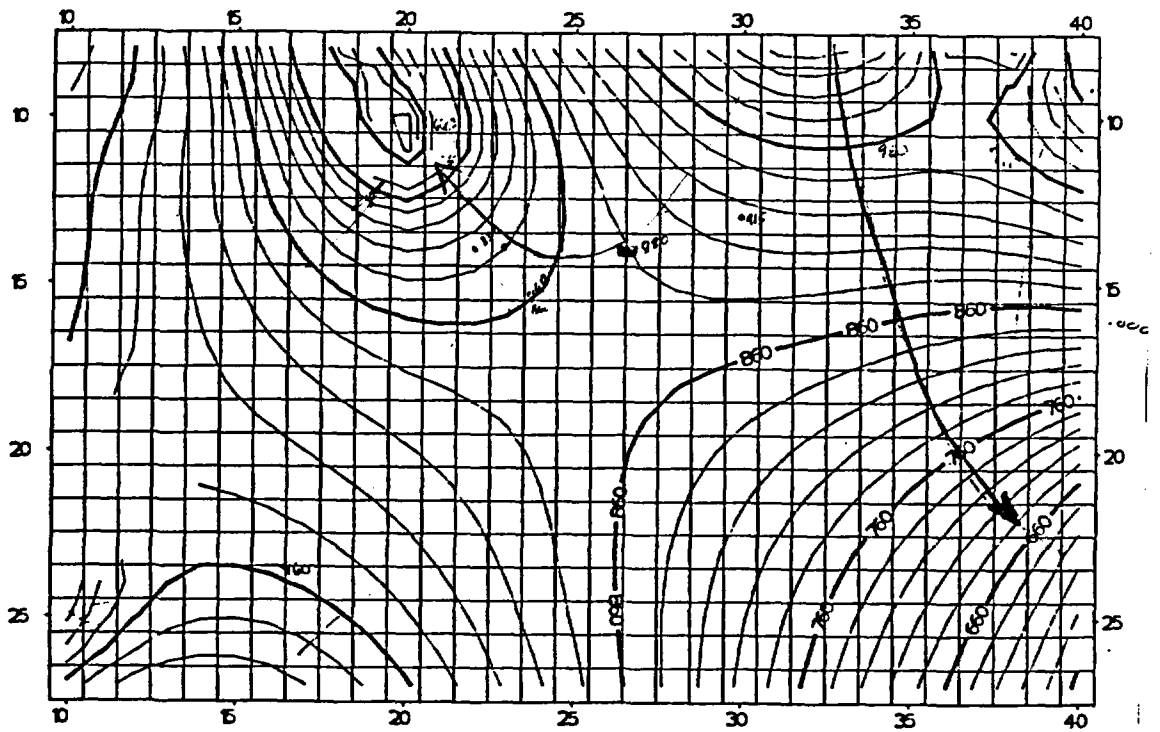
Figure 7.19 - Simulated Heads for the Saddle Mountains Basalts with and without the Cold Creek Barrier



CONTOUR INTERVAL = 200×10^1
 VERTICAL EXAGGERATION = -10
 ELAPSED TIME = 7.8840×10^8 SECONDS

BARRIER INCLUDED

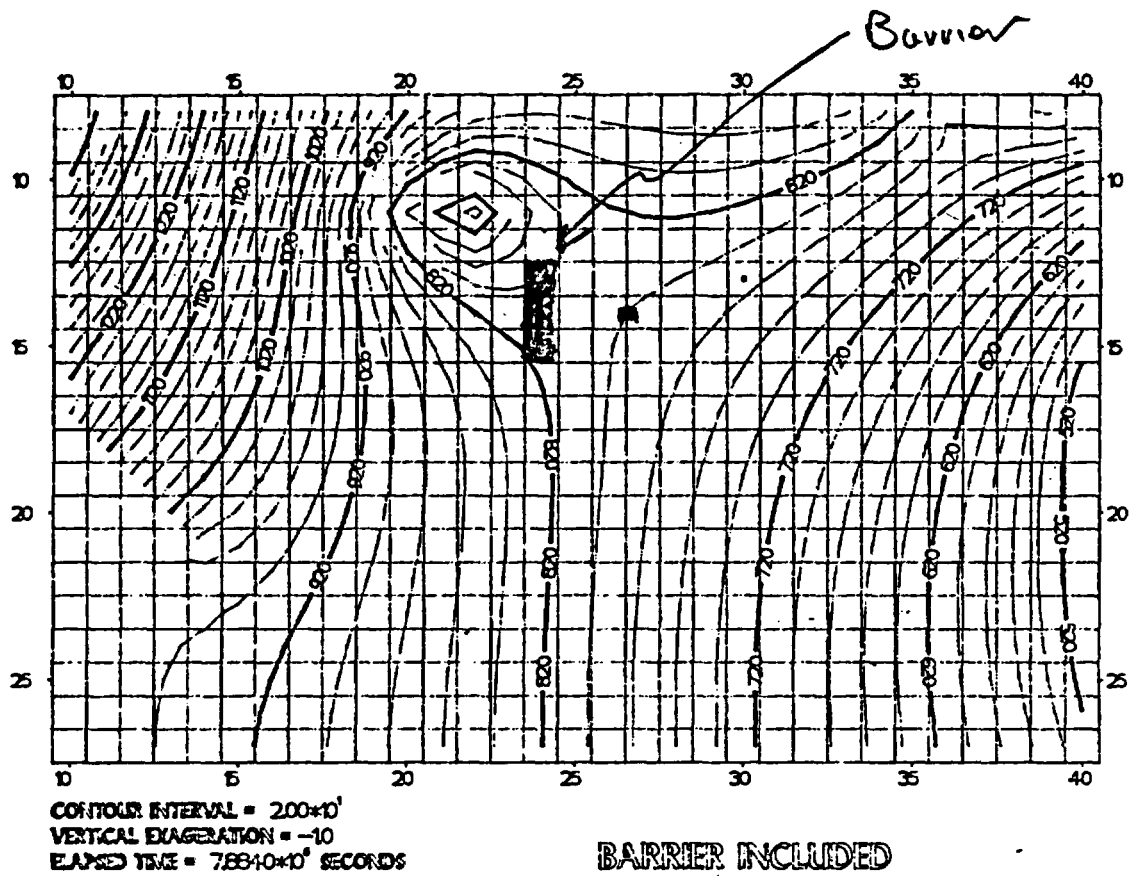
INITIAL RUN



CONTOUR INTERVAL = 200×10^1
 VERTICAL EXAGGERATION = -10
 ELAPSED TIME = 7.8840×10^8 SECONDS

Figure 7.20 - Simulated Heads for the Wanapum Basalts
 With and without the Cold Creek Barrier

24
 2/25



INITIAL RUN

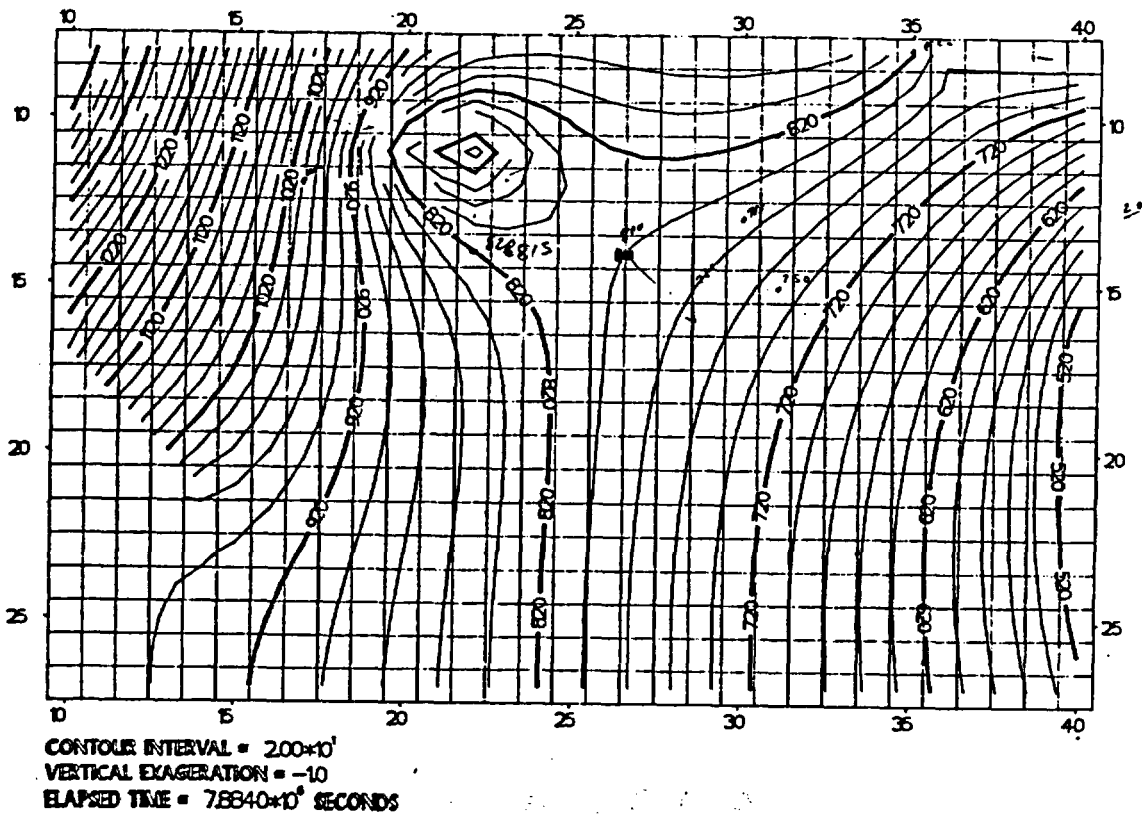


Figure 7.21 - Simulated Heights for the Grande Ronde Basalts with and without the Cold Creek Barrier

△ McGee
 • RRL
 ○ ~~at~~ 200 Yards area

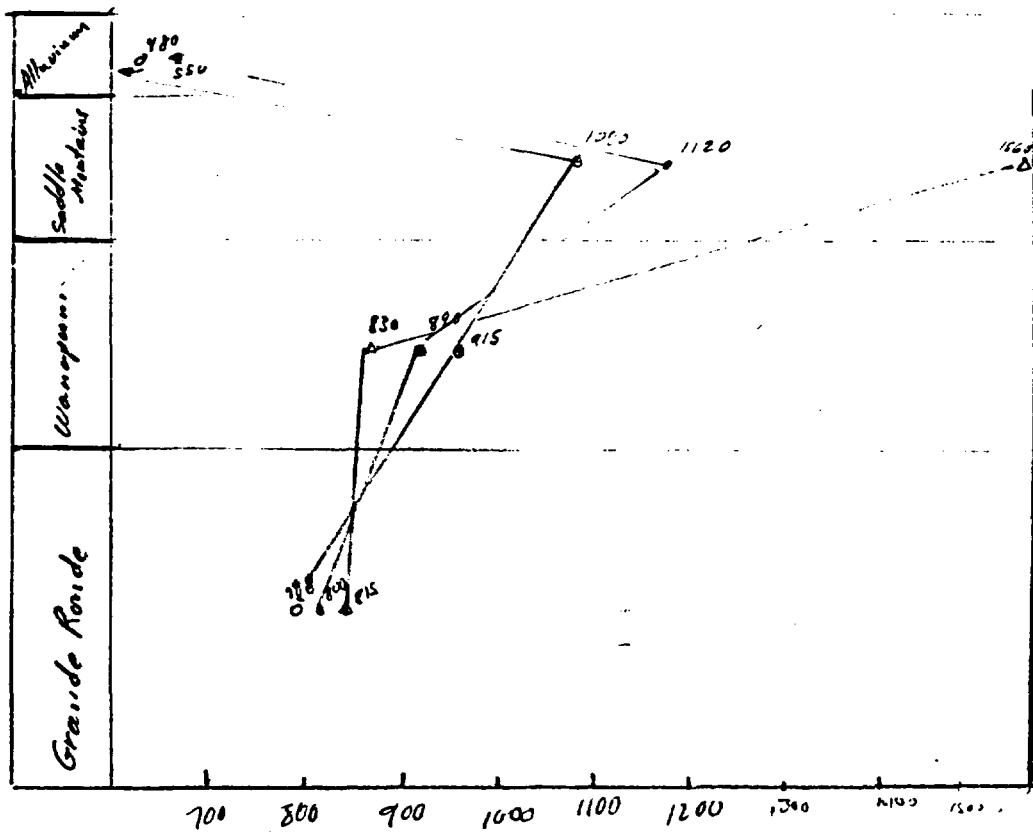
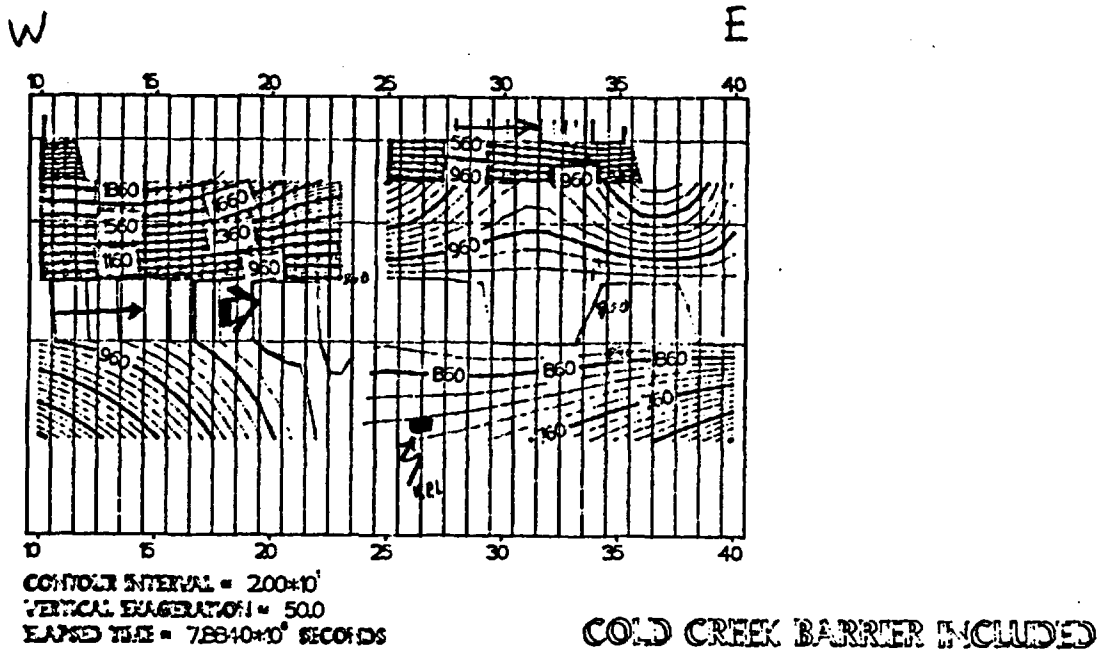


Figure 7.22 Vertical Profile of Simulated Heads with the Cold Creek Barrier Included



INITIAL RUN

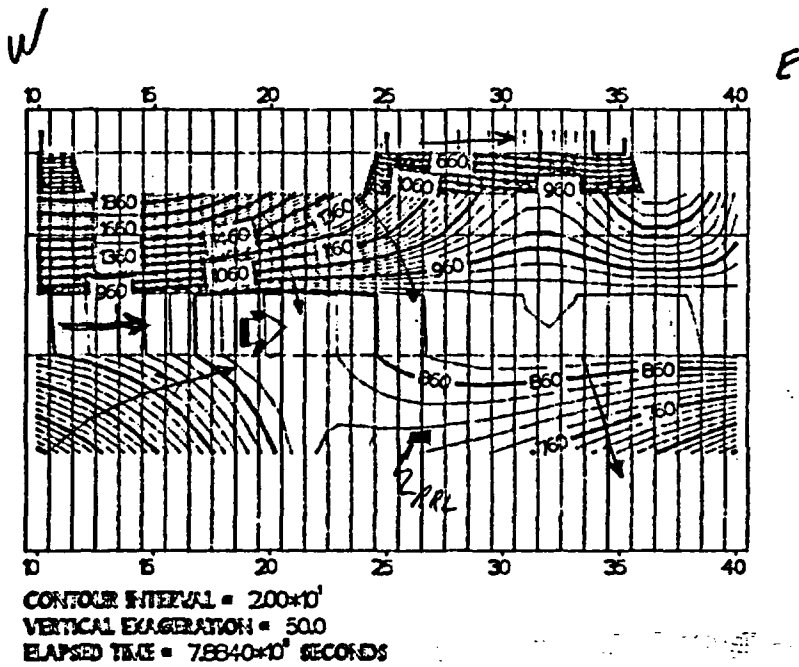
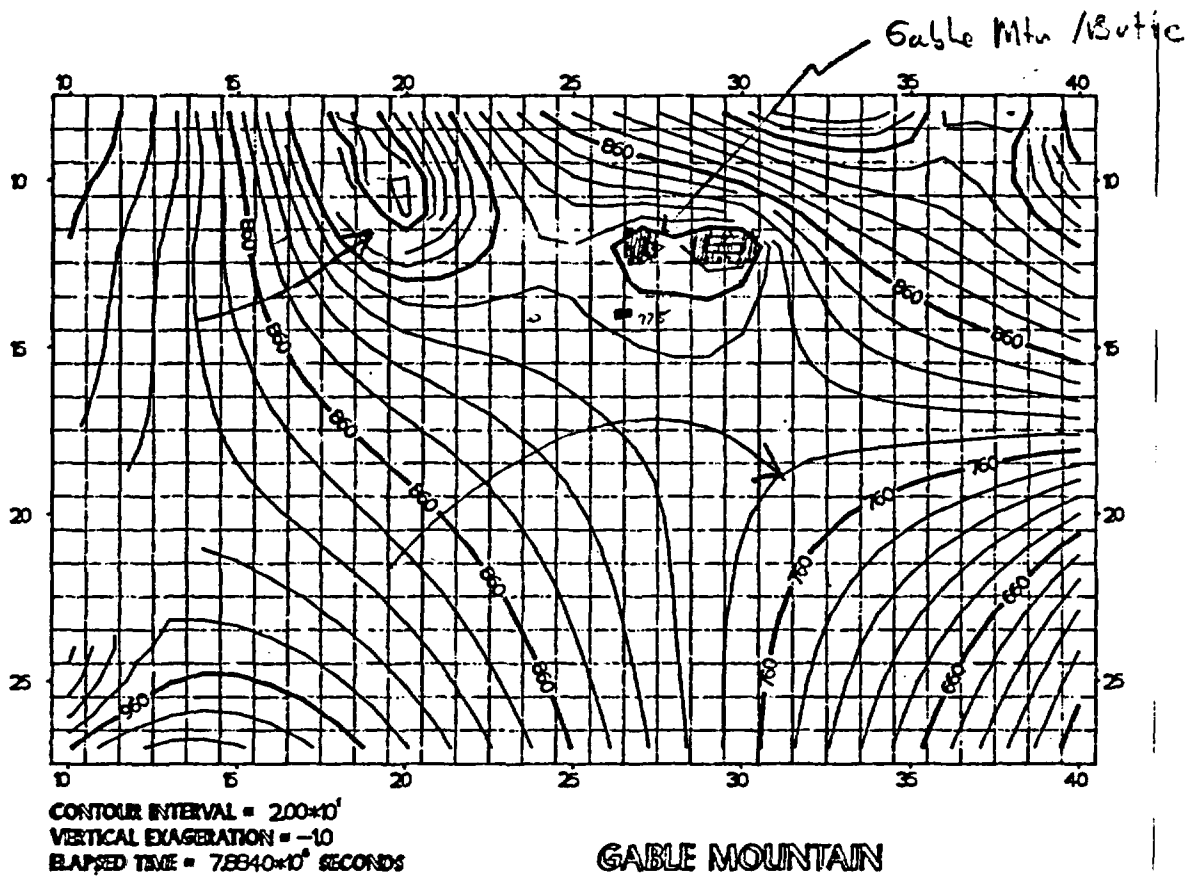


Figure 7.23 - Simulated Heads in an East-West Section through the RRL with and without the Cold Creek Barrier



GABLE MOUNTAIN

INITIAL RUN

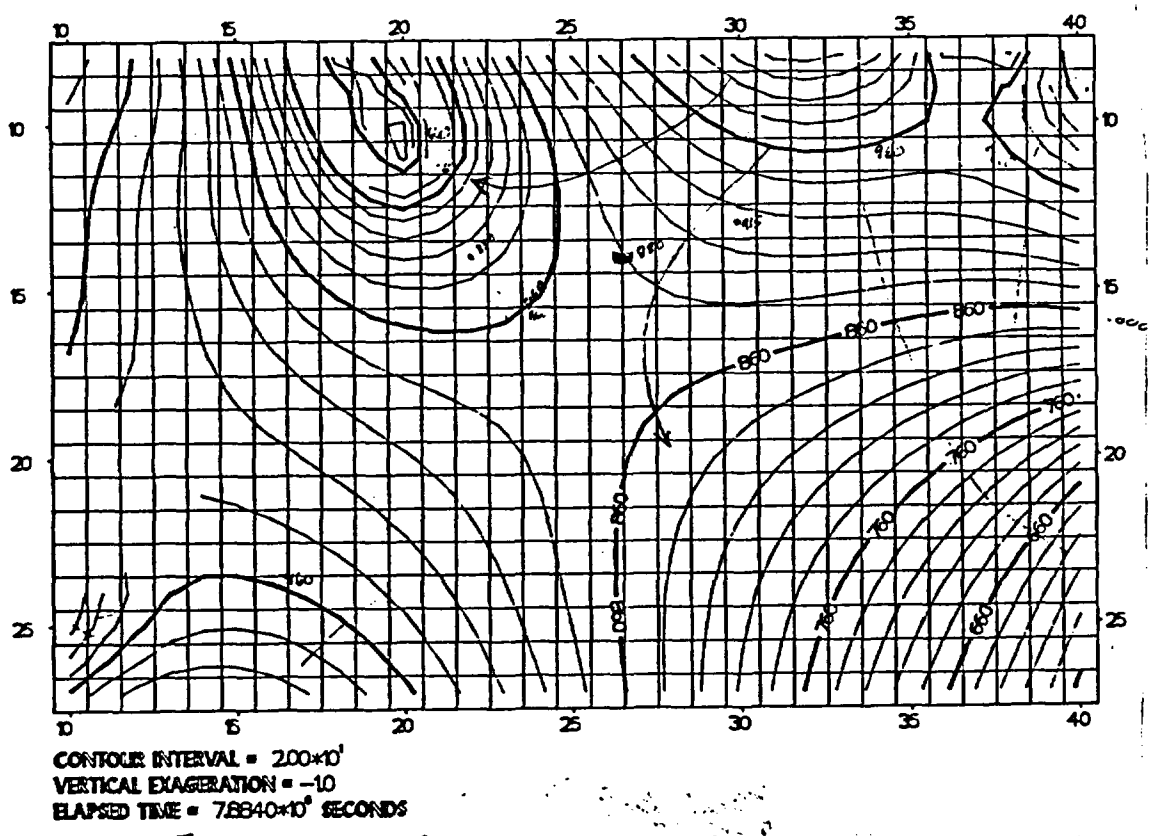
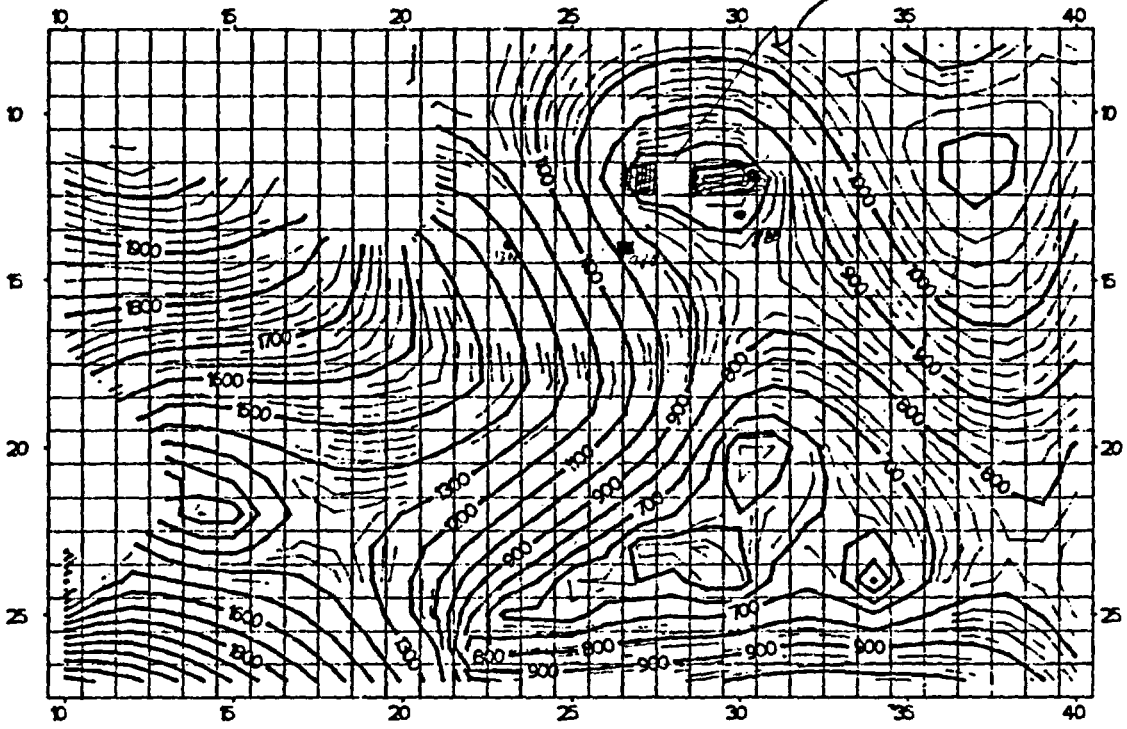


Figure 7.25 - Simulated Heads for the Wenapum Basalts with and without Gable Mtn / Butte

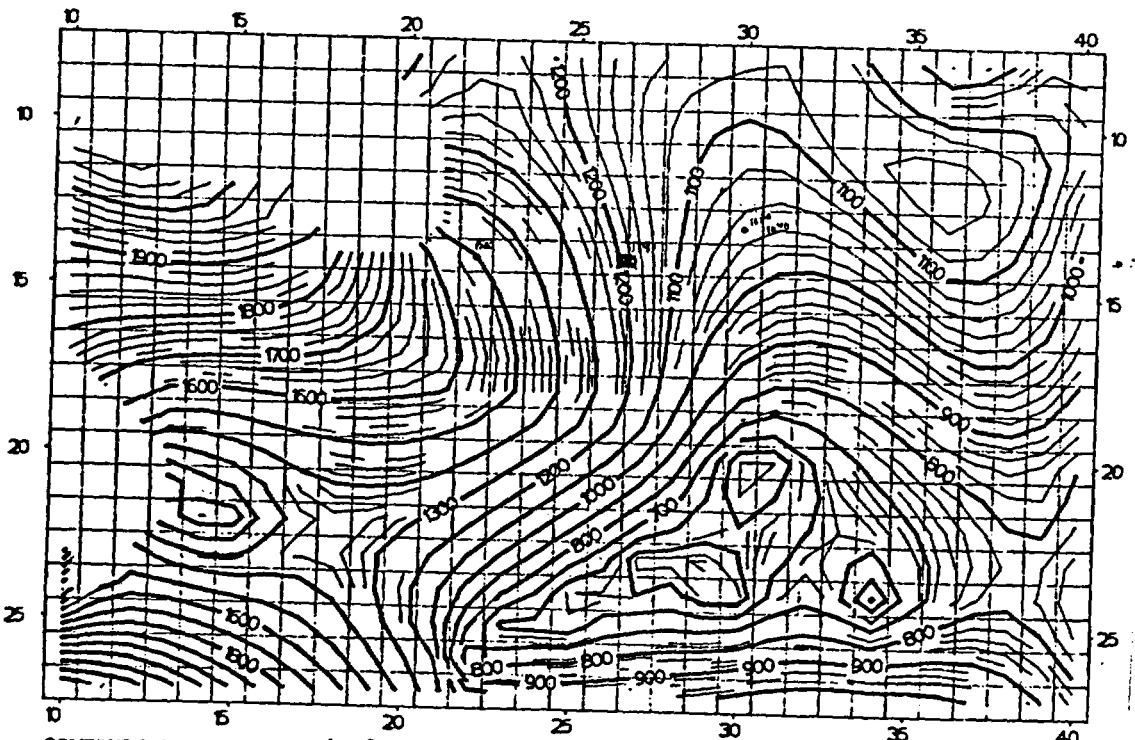
Gable Mtn / Butte



CONTOUR INTERVAL = 200×10^1
VERTICAL EXAGGERATION = $\times 10$
ELAPSED TIME = 7.8840×10^6 SECONDS

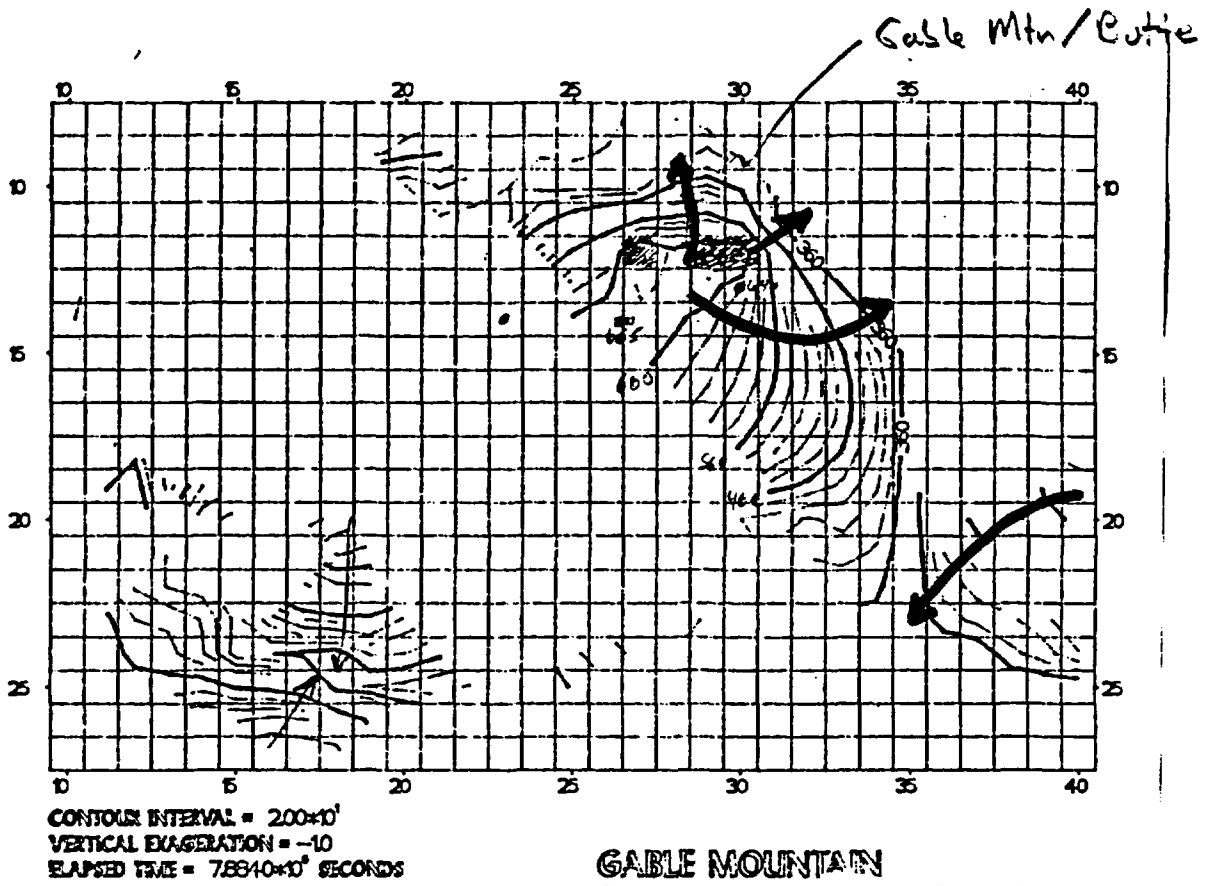
GABLE MOUNTAIN

INITIAL RUN



CONTOUR INTERVAL = 200×10^1 20
VERTICAL EXAGGERATION = $\times 10$
ELAPSED TIME = 7.8840×10^6 SECONDS

Figure 7.26 - Simulated Haze for the Saddle Mountain Escarpment with and without Gable Mtn / Butte



GABLE MOUNTAIN

INITIAL RUN

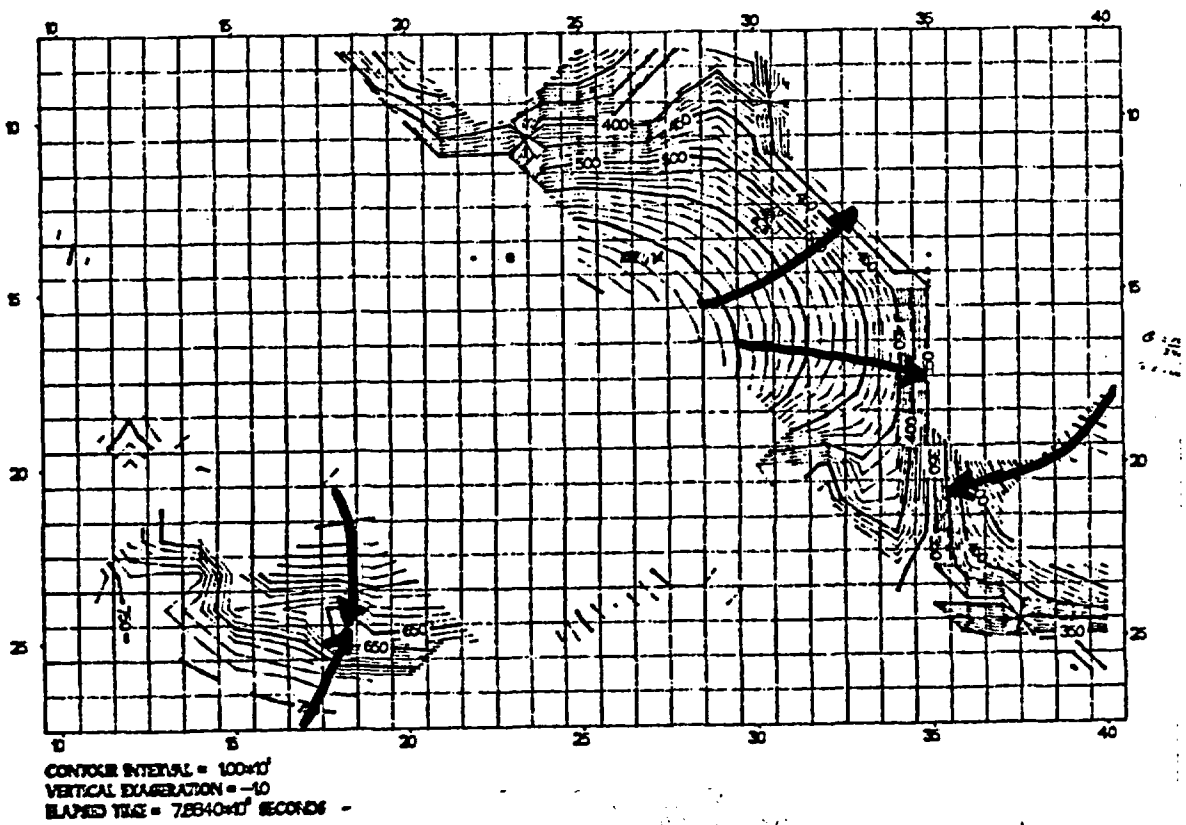
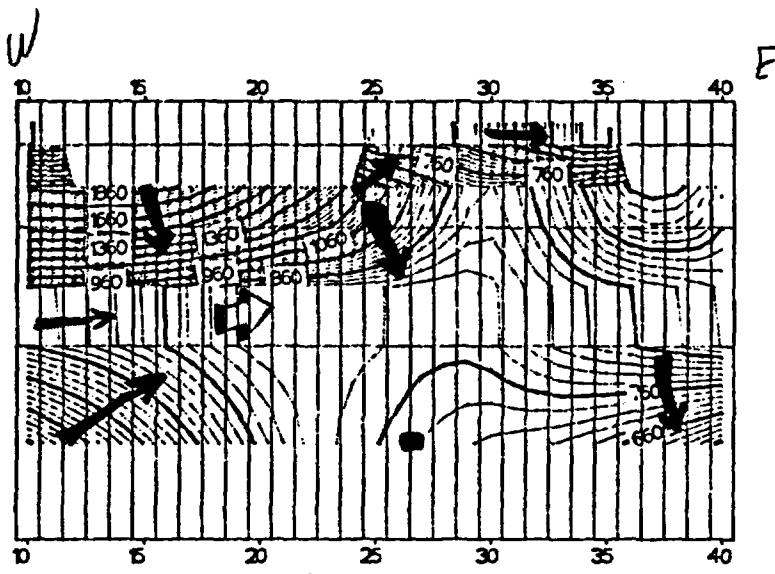


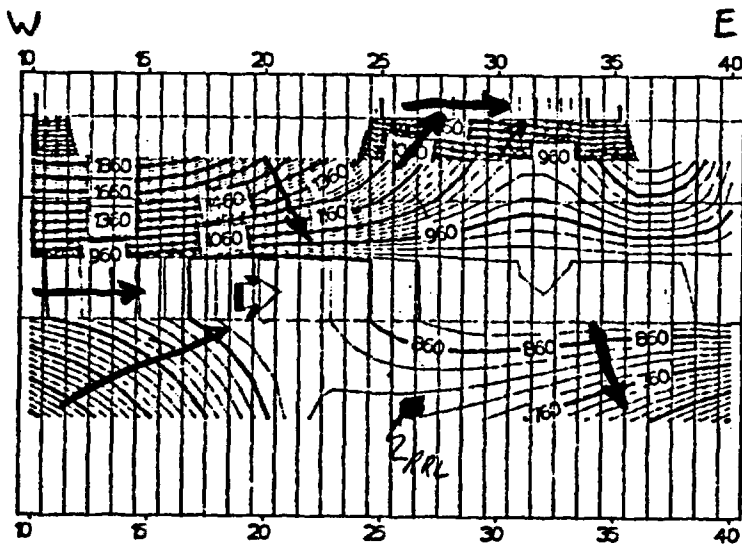
Figure 7.27 - Simulated Heads for the Alluvium with and without Gable Mtn / Butte



CONTOUR INTERVAL = 200×10^1
 VERTICAL EXAGGERATION = 50.0
 ELAPSED TIME = 7.8840×10^8 SECONDS

GABLE BUTTE REGION INCLUDED

INITIAL RUN



CONTOUR INTERVAL = 200×10^1
 VERTICAL EXAGGERATION = 50.0
 ELAPSED TIME = 7.8840×10^8 SECONDS

Figure 7.28 - Simulated Heads in an East-West Section through the RRL with and without Gable Mtn / Butte

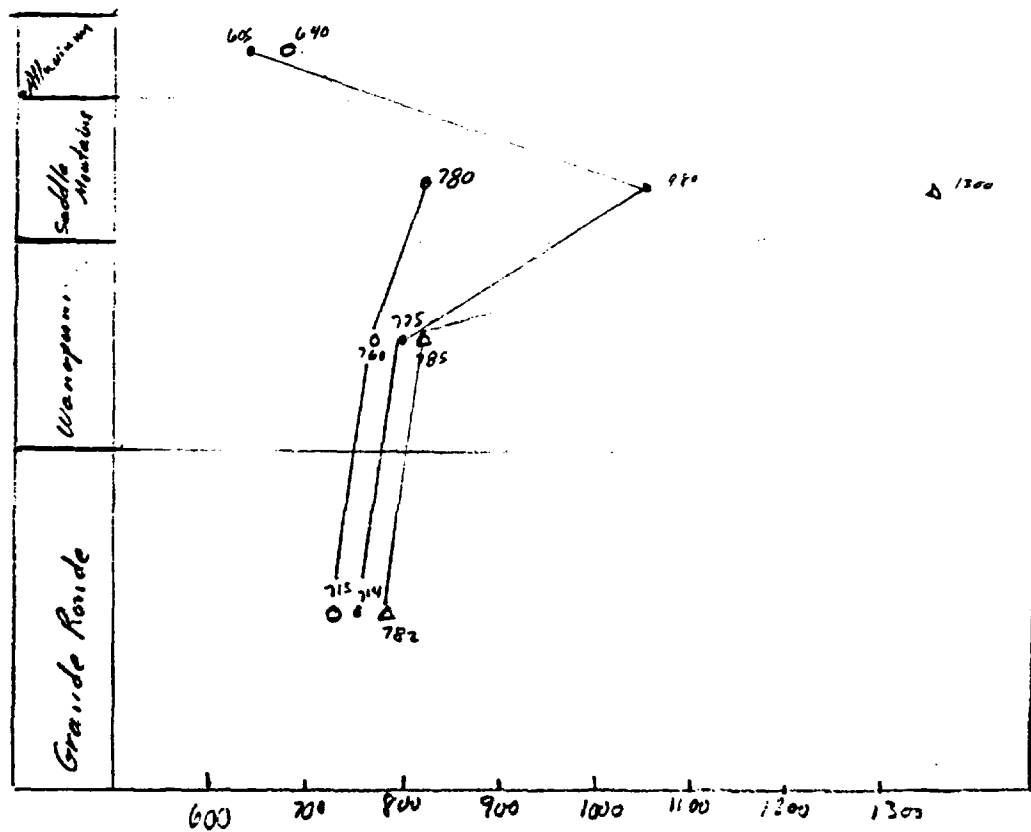
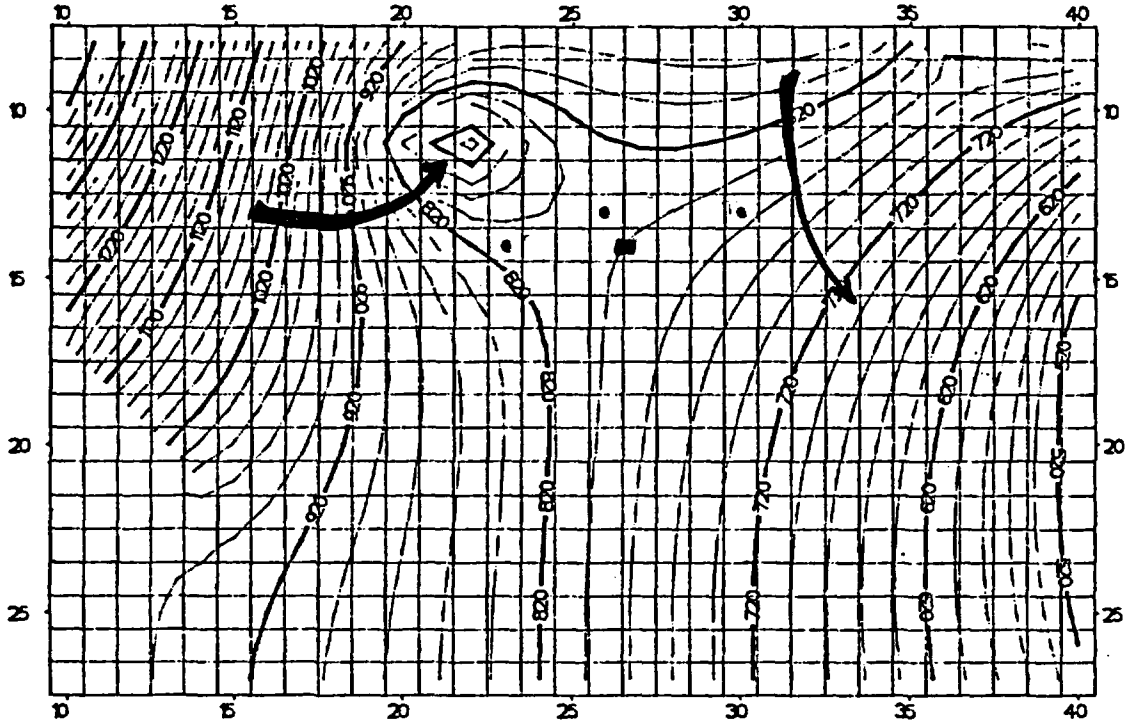


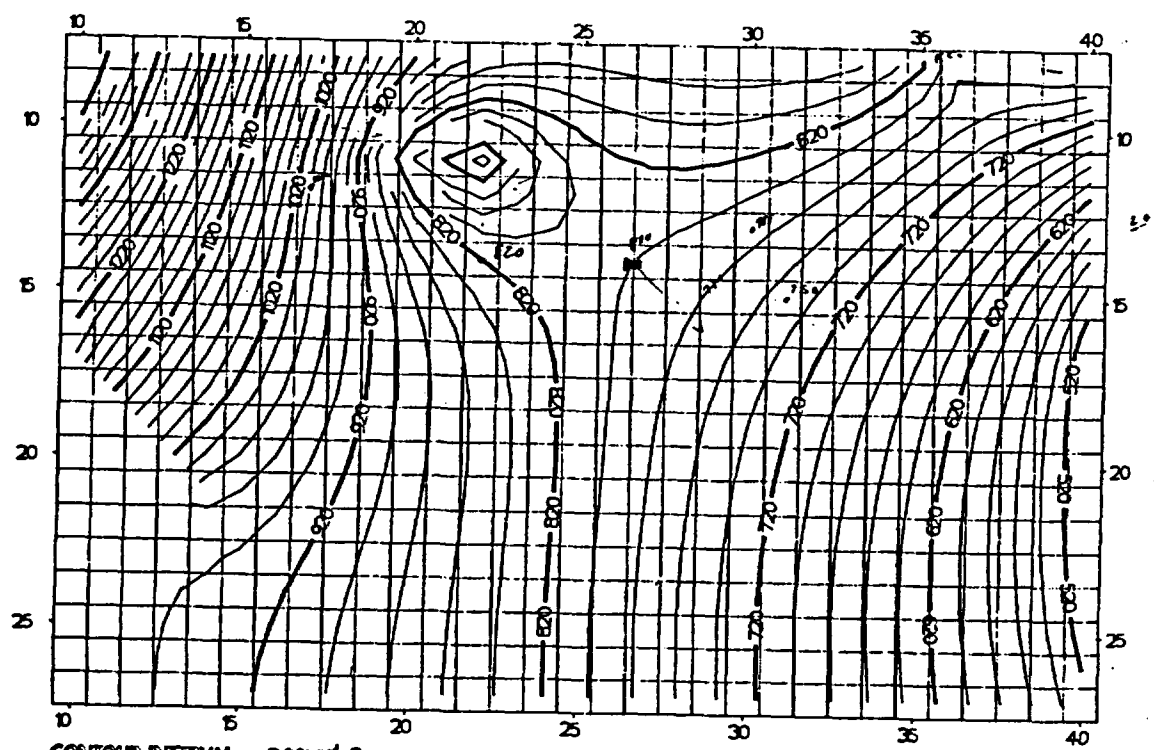
Figure 7.29 Vertical Profile of Simulated Heads with Gable Mountain/Gable Butte Included



CONTOUR INTERVAL = 200×10^1
 VERTICAL EXAGGERATION = -10
 ELAPSED TIME = 7.8840×10^6 SECONDS

W/PONDS - 30Y AVE.

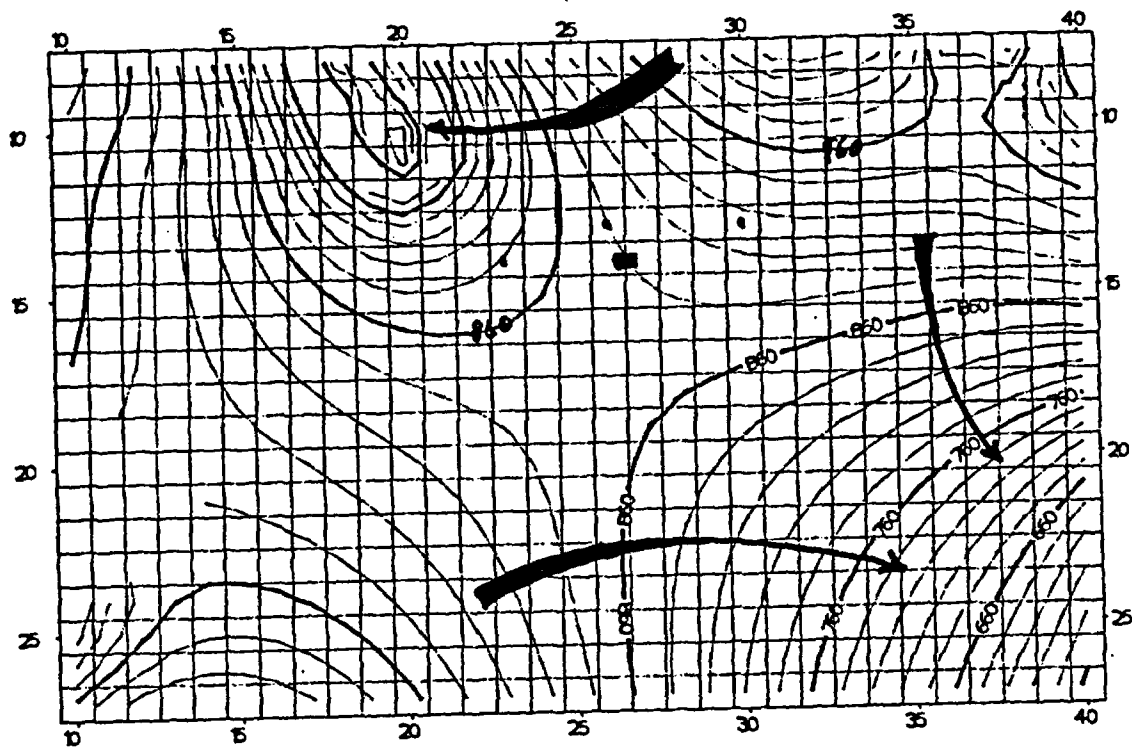
INITIAL RUN



CONTOUR INTERVAL = ~~200~~ 20
 VERTICAL EXAGGERATION = -10
 ELAPSED TIME = ~~7.8840~~ SECONDS

50.001

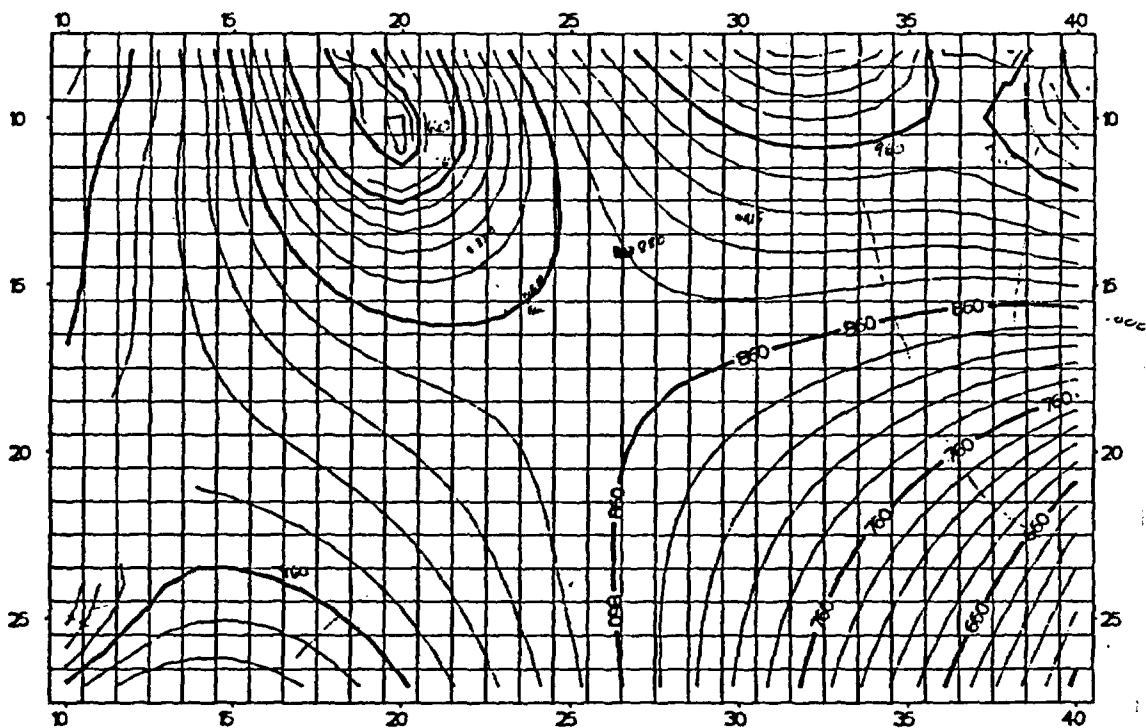
Figure 7.30 - Simulated Heads for the Granite Route Basalts with and without Ponds



CONTOUR INTERVAL = 200×10^1
 VERTICAL EXAGGERATION = -10
 ELAPSED TIME = 7.8840×10^5 SECONDS

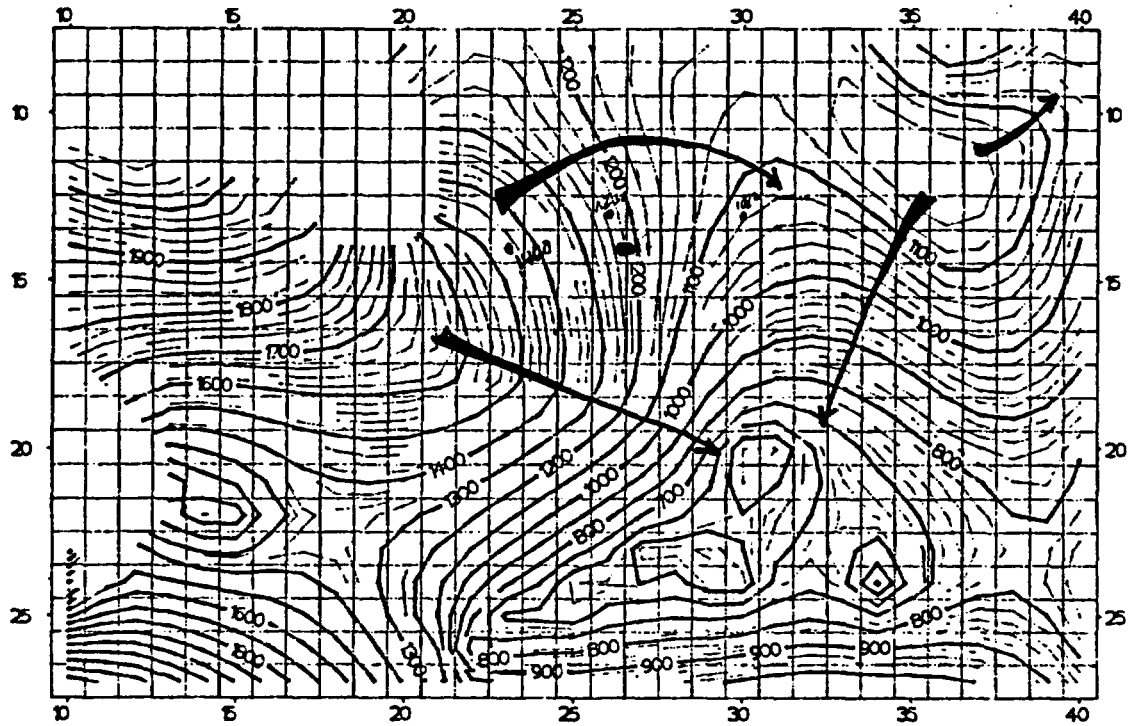
W/PONDS - 30Y AVE

INITIAL RUN



CONTOUR INTERVAL = 200×10^1
 VERTICAL EXAGGERATION = -10
 ELAPSED TIME = 7.8840×10^5 SECONDS

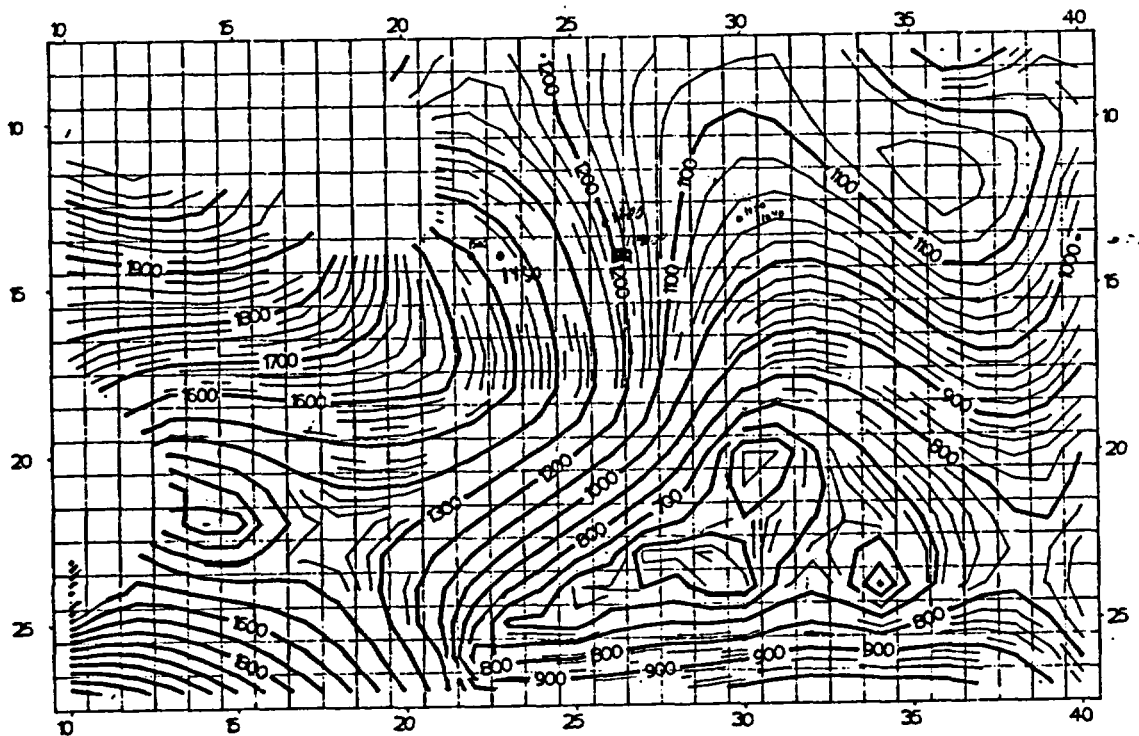
Figure 7.31 - Simulated Heads for the Wanapum Escalite with and without Ponds



CONTOUR INTERVAL = 200×10^1
 VERTICAL EXAGGERATION = -10
 ELAPSED TIME = 7.6840×10^6 SECONDS

W/ PONDS - 30Y AVE

INITIAL RUN



CONTOUR INTERVAL = 200×10^1
 VERTICAL EXAGGERATION = -10
 ELAPSED TIME = 7.6840×10^6 SECONDS

Figure 7.32 Simulated Heads for the Saddle Mountains Basalts with and without Ponds

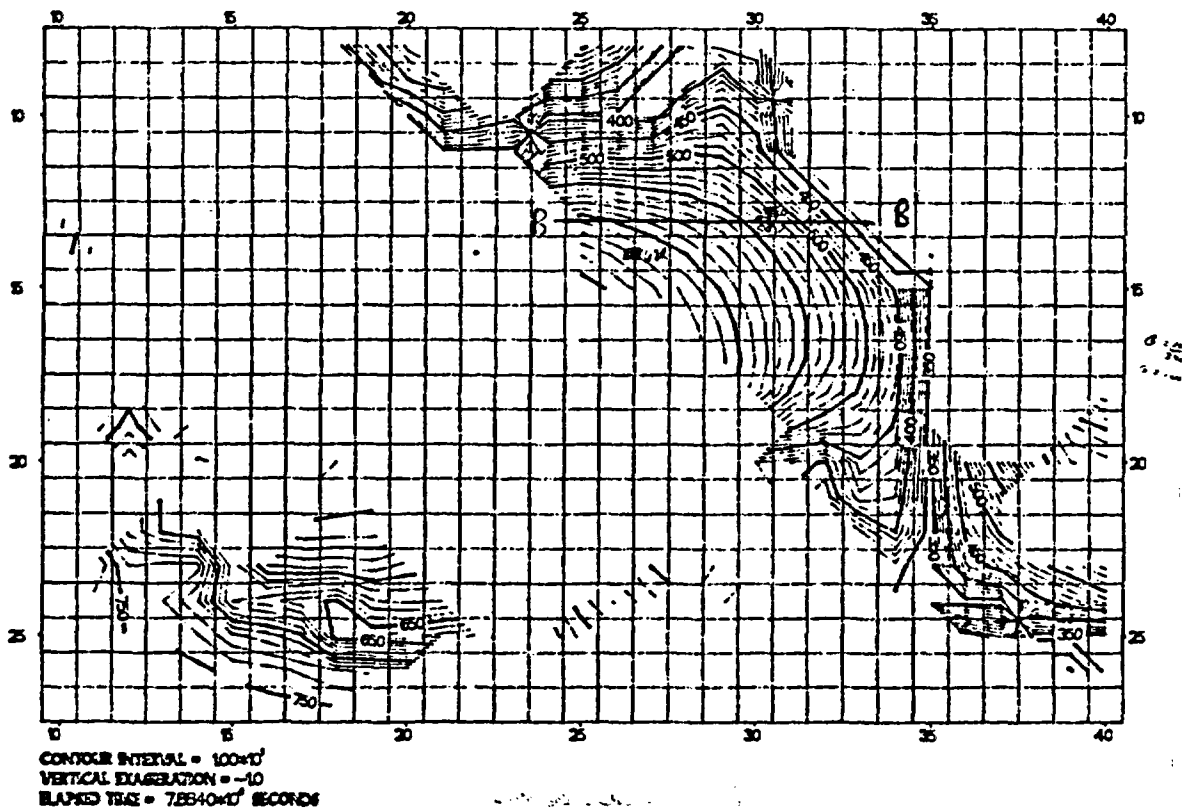
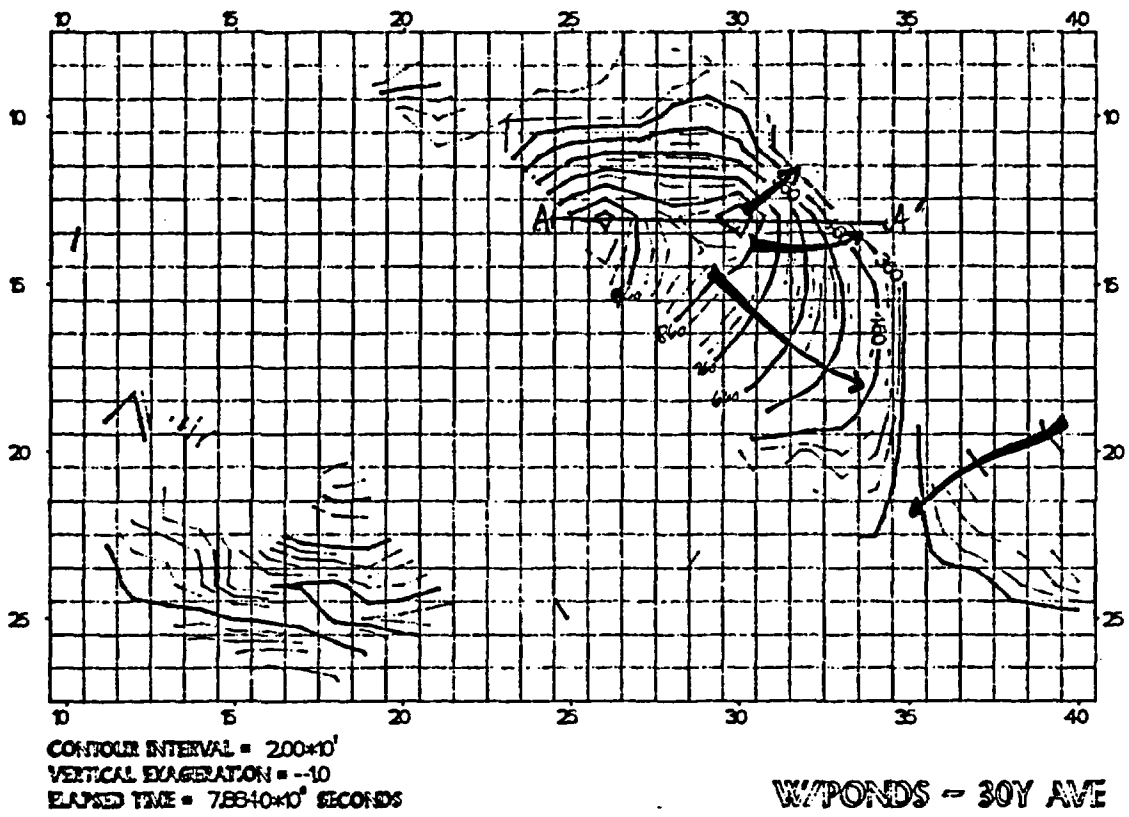
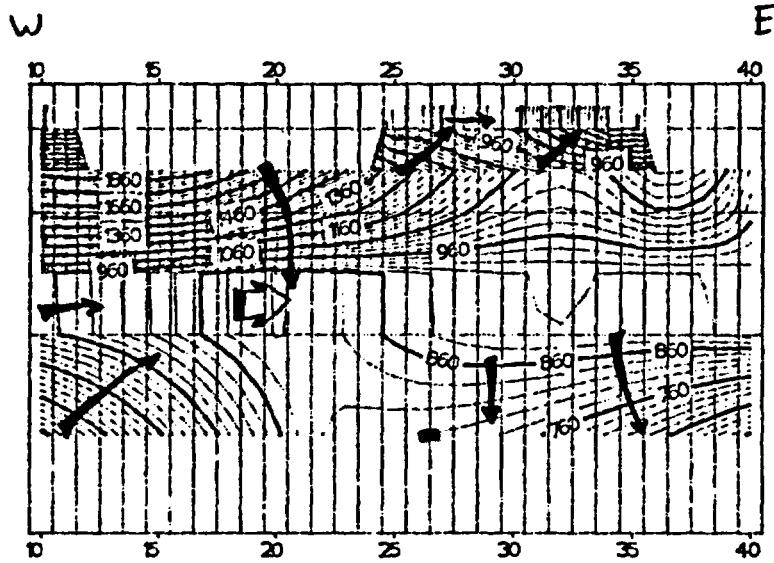


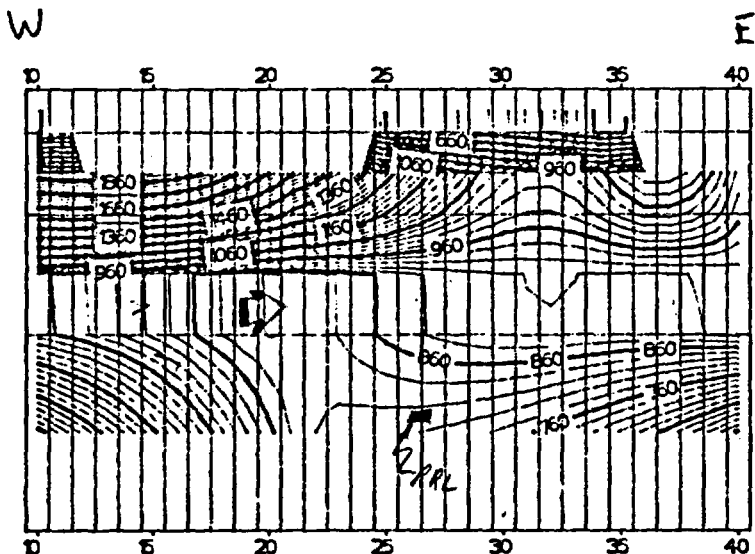
Figure 9.38 - Simulated Heads for the Alluvium with and without Ponds



CONTOUR INTERVAL = 200×10^1
 VERTICAL EXAGGERATION = 50.0
 ELAPSED TIME = 7.88×10^6 SECONDS

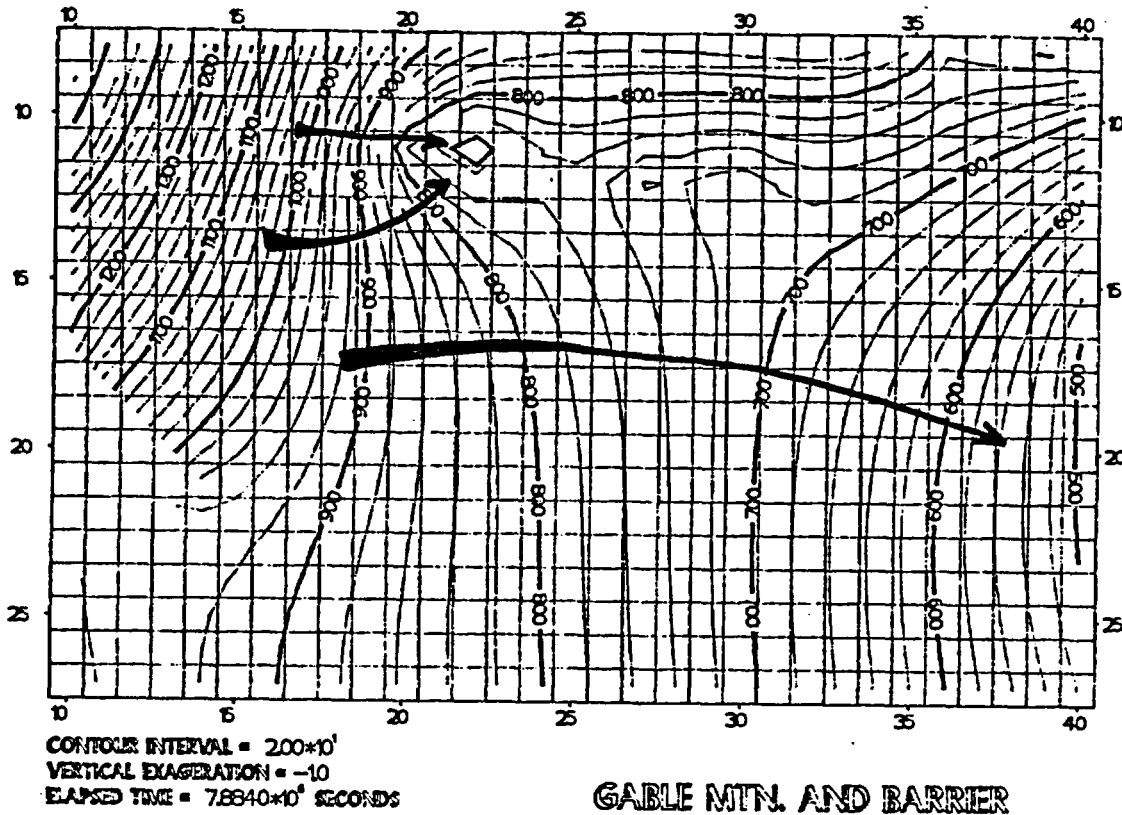
PONDS INCLUDED USING 30 YEAR AVERAGE

INITIAL RUN



CONTOUR INTERVAL = 200×10^1
 VERTICAL EXAGGERATION = 50.0
 ELAPSED TIME = 7.88×10^6 SECONDS

Figure 7.34- Simulated Heads in an East-West Section through the RRL with and without Ponds



GABLE MTN. AND BARRIER

INITIAL RUN

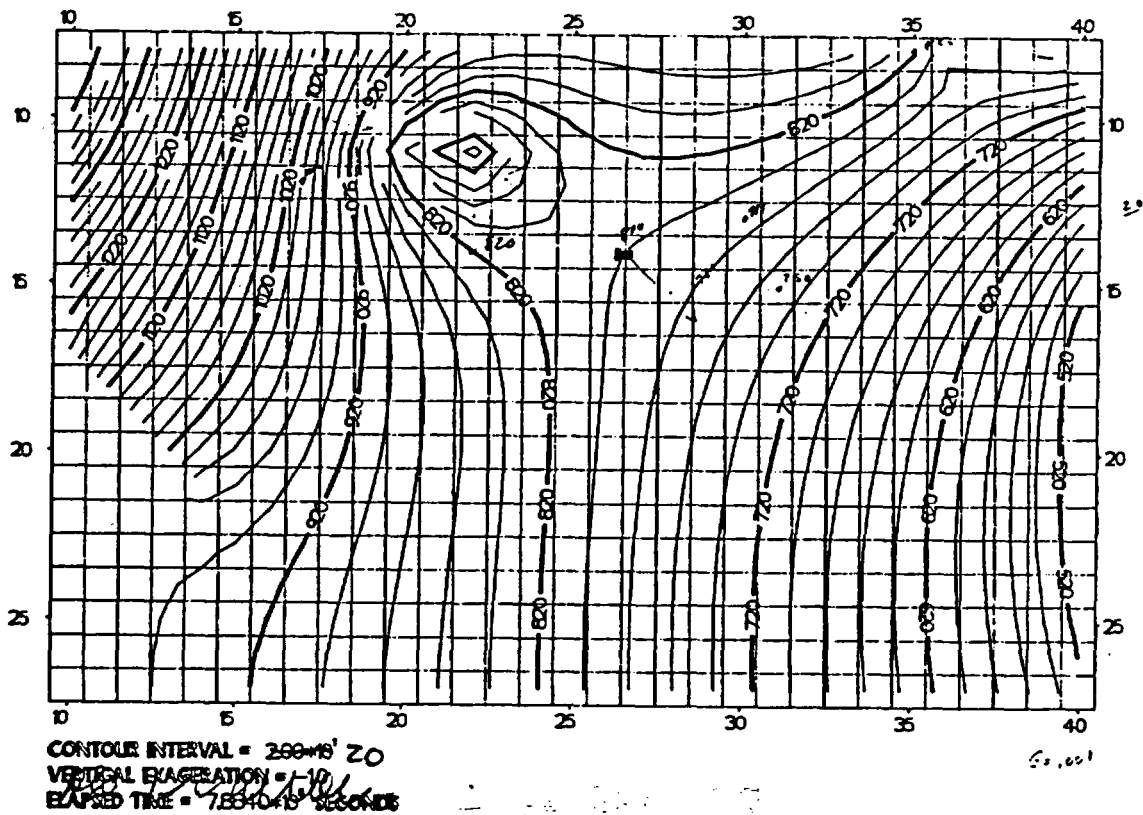
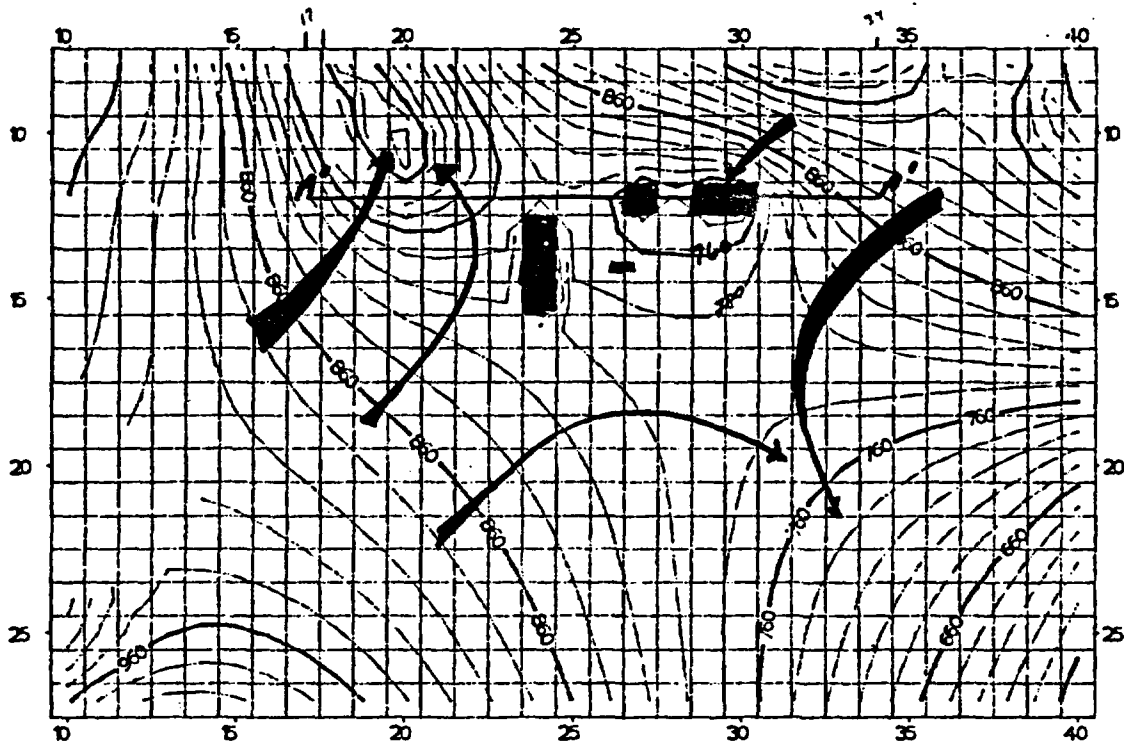


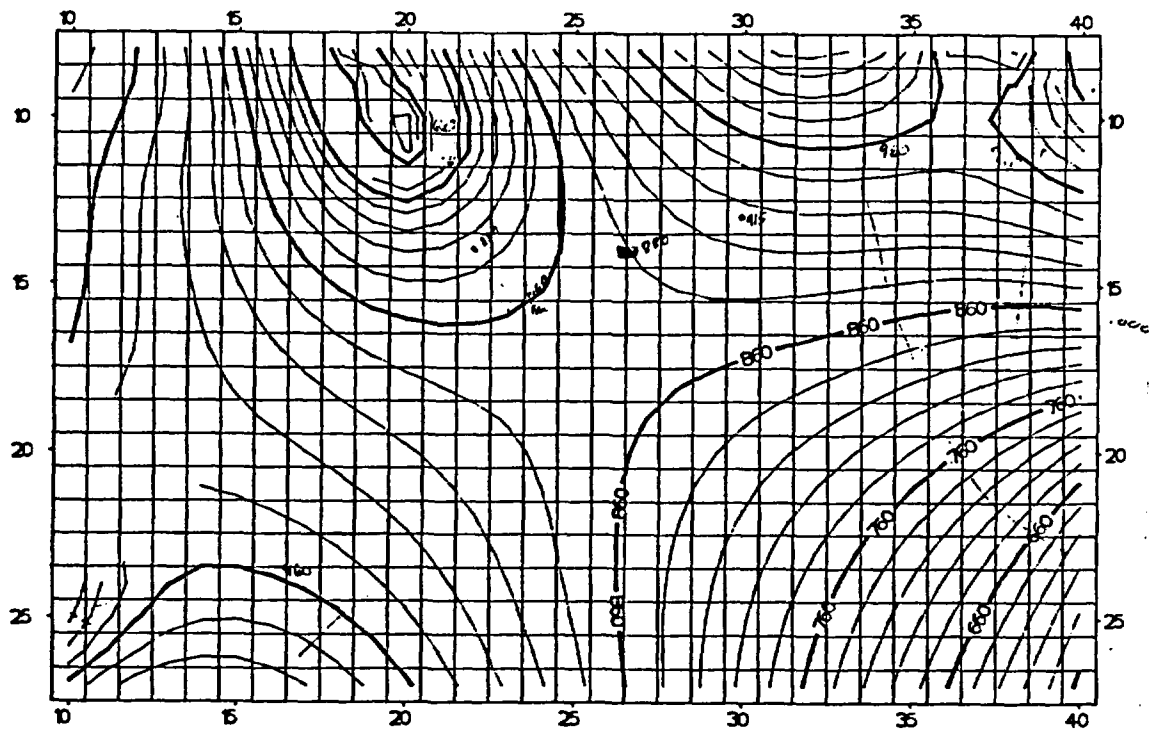
Figure 7.35 - Simulated Heads for the Grande Ronde Basin with and without Gable Mtn / Butte + Cold Creek Barrier



CONTOUR INTERVAL = 200'±10'
 VERTICAL EXAGGERATION = -10
 ELAPSED TIME = 7.8840×10⁶ SECONDS

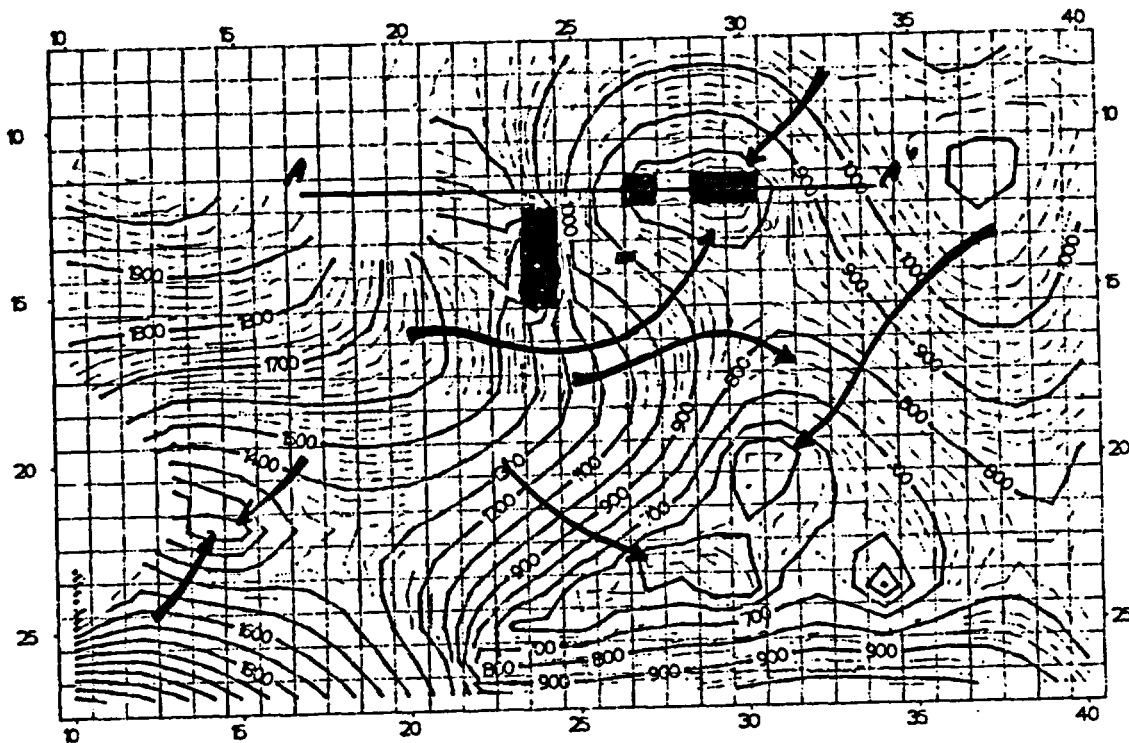
GABLE MTN. AND BARRIER

INITIAL RUN



CONTOUR INTERVAL = 200'±20'
 VERTICAL EXAGGERATION = -10
 ELAPSED TIME = 7.8846×10⁶ SECONDS

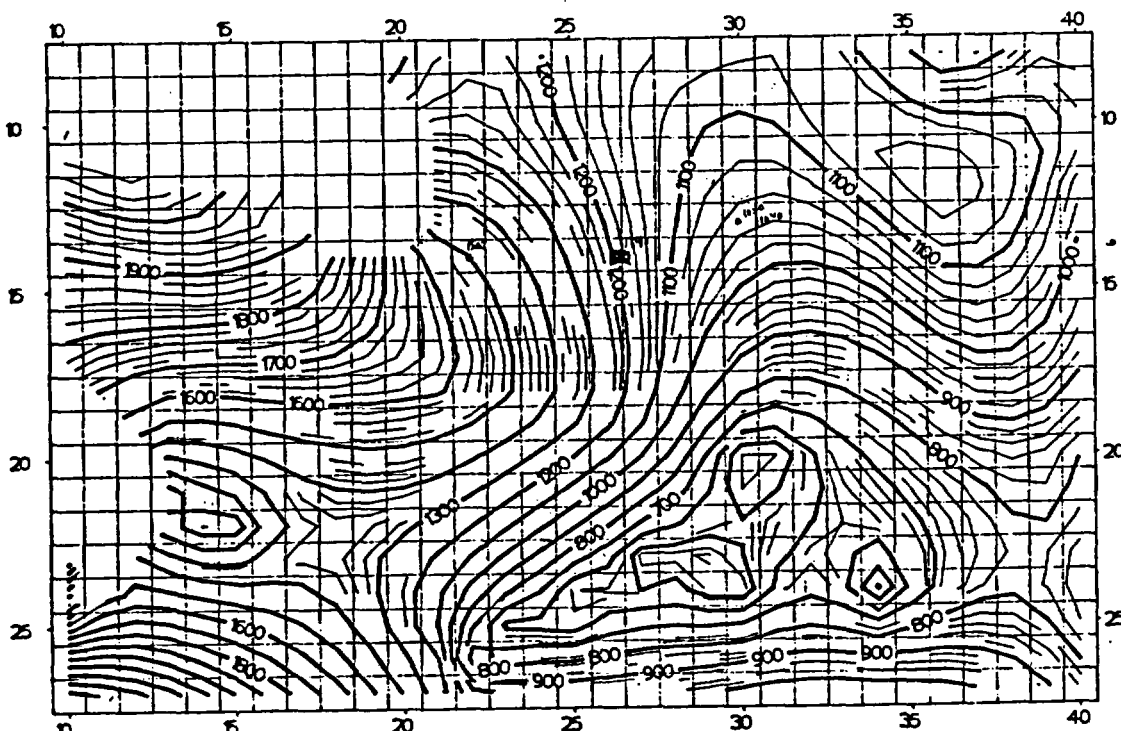
Figure 7.36 Simulated Heads for the Wampum Results
 with and without Gable Mtn /Butte + Cold Creek Barrier



CONTOUR INTERVAL = 200×10^1
 VERTICAL EXAGGERATION = 10
 ELAPSED TIME = 78810×10^6 SECONDS

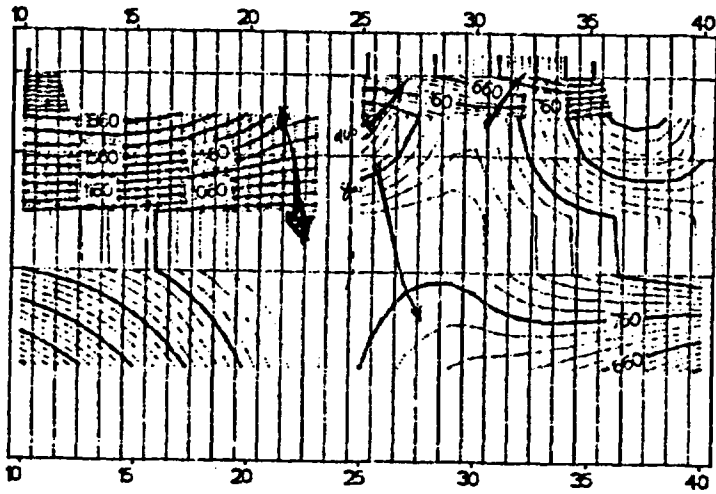
GABLE MTN. AND BARRIER

INITIAL RUN



CONTOUR INTERVAL = 200×10^1 20
 VERTICAL EXAGGERATION = 10
 ELAPSED TIME = 78840×10^6 SECONDS

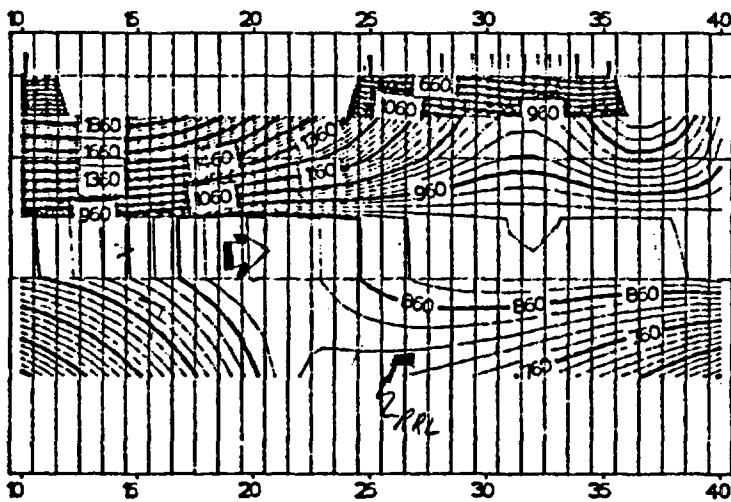
Figure 7.37 - Simulated Heads for the Saddle Mountains Basalts with and without Gable Mtn./Butte + Colic Crests Barrier.

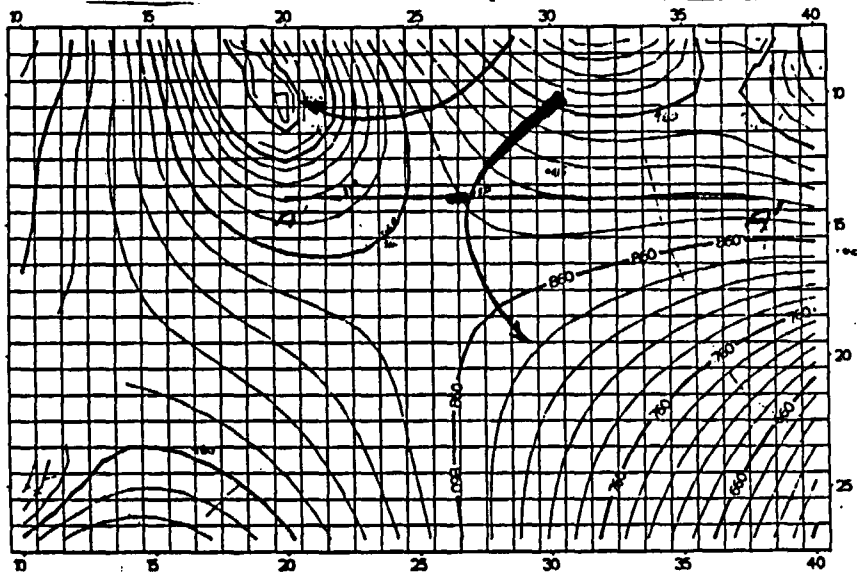


CONTOUR INTERVAL = 200±10'
 VERTICAL EXAGGERATION = 50.0
 ELAPSED TIME = 78840±10³ SECONDS

COLD CREEK BARRIER AND GABLE

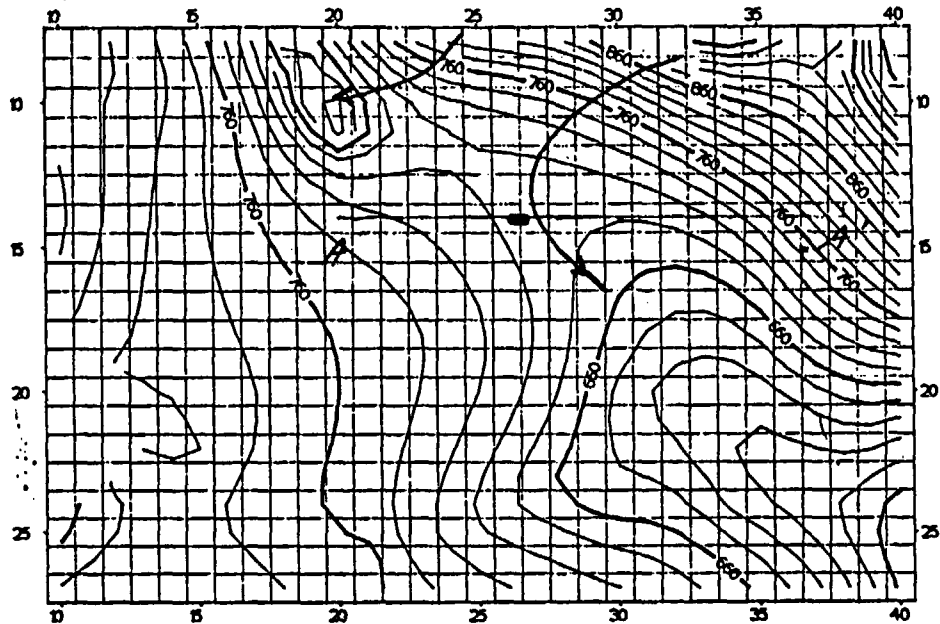
INITIAL RUN





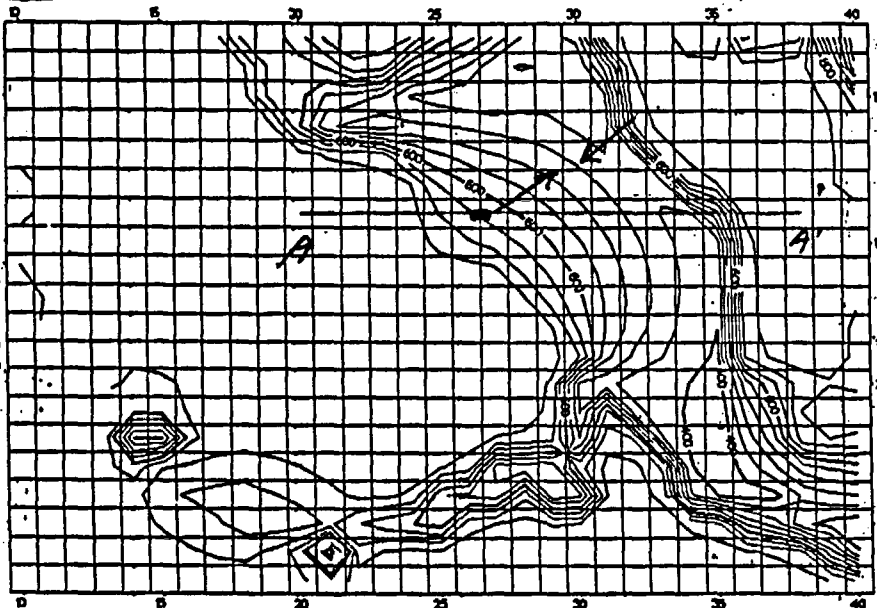
CONTOUR INTERVAL = 200'±
 VERTICAL EXAGGERATION = -10
 ELAPSED TIME = 78940×10³ SECONDS

INITIAL VALUES
 WANAPUM BASALTS



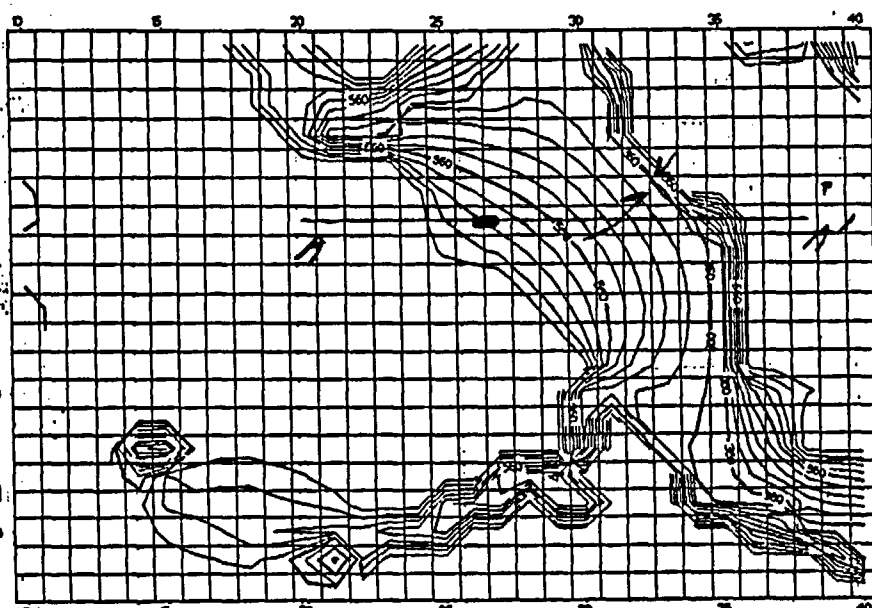
CONTOUR INTERVAL = 200'±
 VERTICAL EXAGGERATION = -10
 ELAPSED TIME = 78940×10³ SECONDS

LEAKAGE INCREASED 2 ORDERS
 WANAPUM BASALTS



CONTOUR INTERVAL = 400'±
 VERTICAL EXAGGERATION = -10
 ELAPSED TIME = 78940×10³ SECONDS

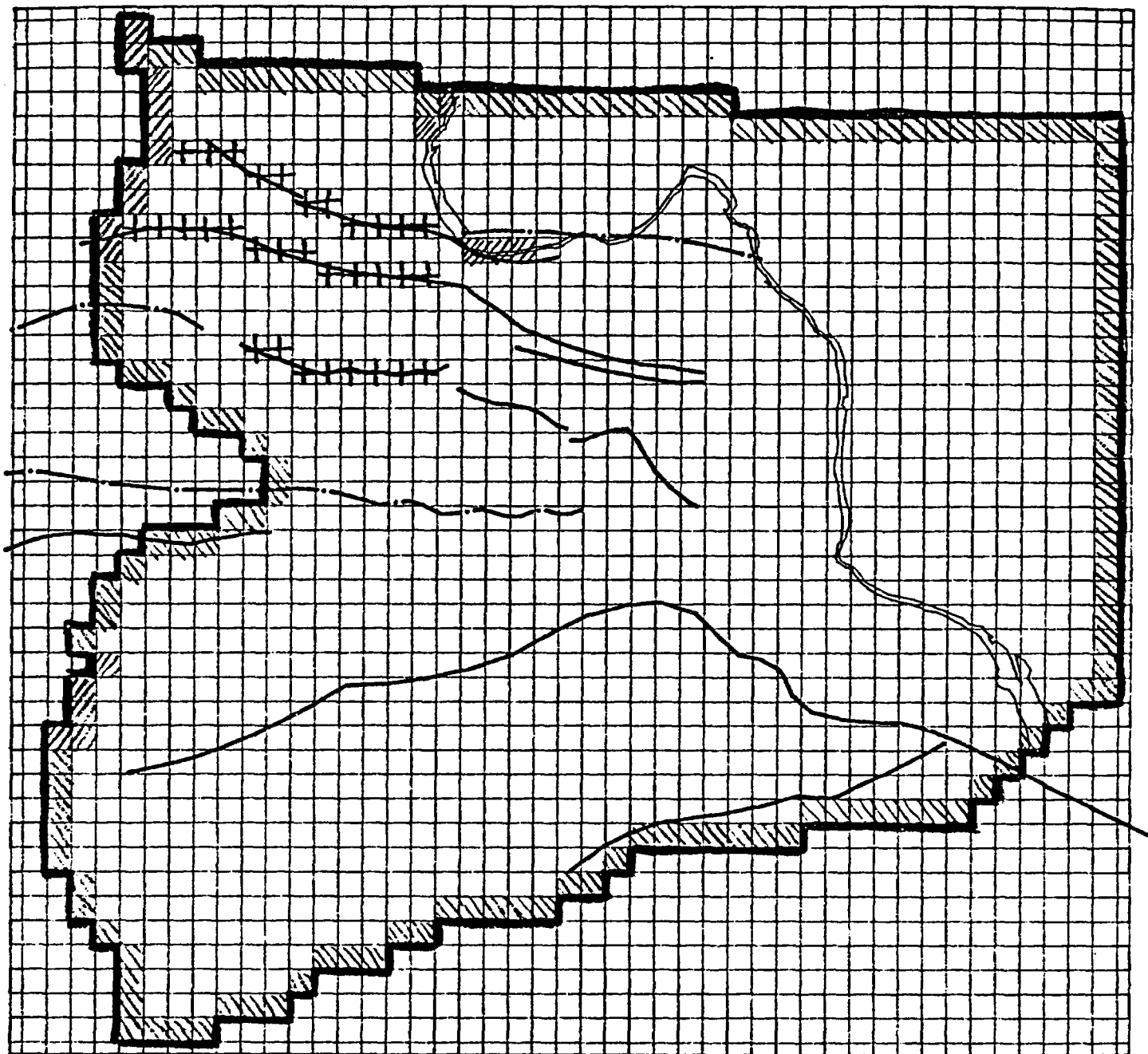
HEADS FOR WANAPUM BASALTS
 LEAKAGE INCREASED 4 ORD. OF MAG



CONTOUR INTERVAL = 400'±
 VERTICAL EXAGGERATION = -10
 ELAPSED TIME = 78940×10³ SECONDS

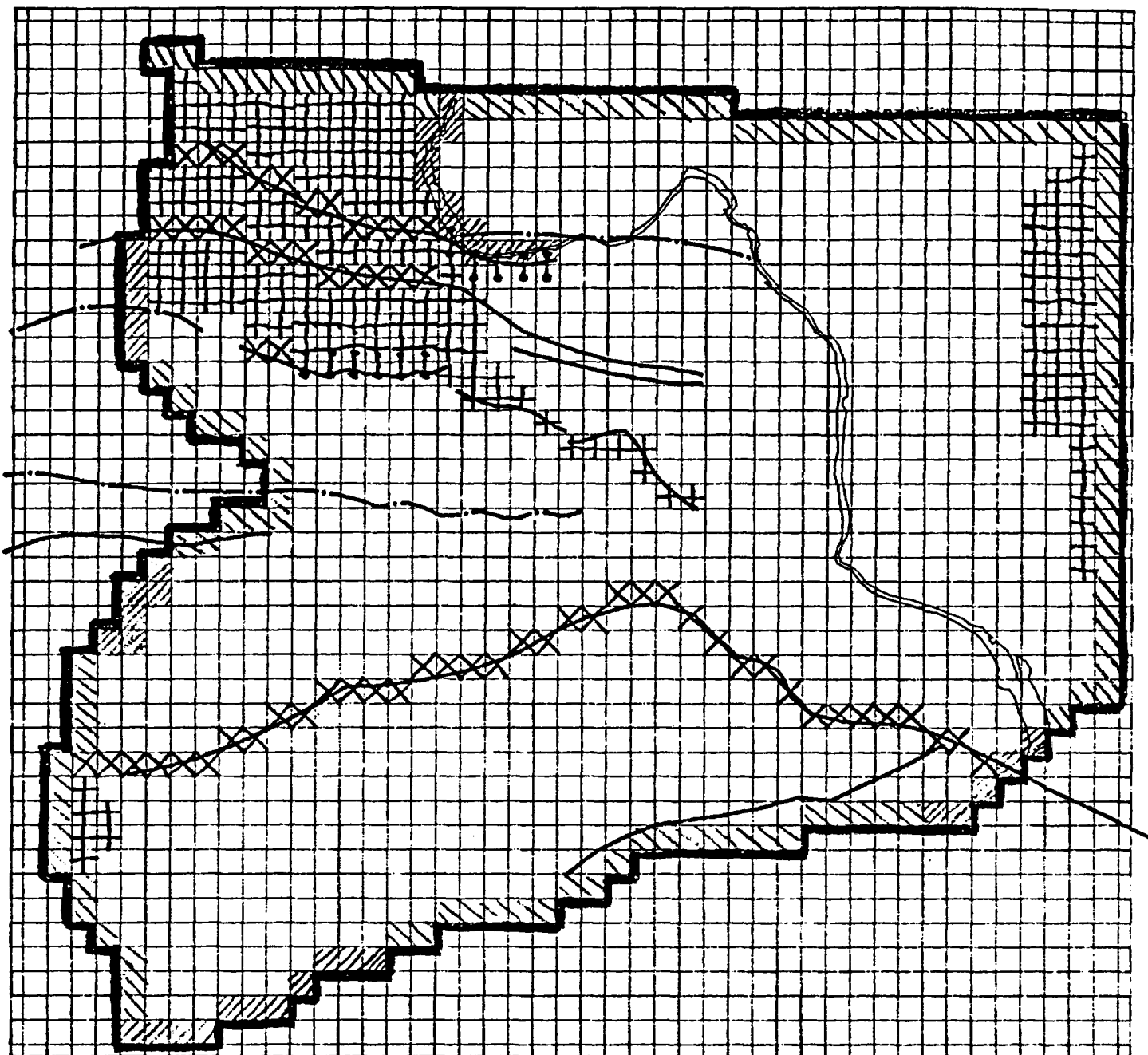
HEADS FOR WANAPUM BASALTS
 LEAKAGE INCREASED 6 ORD. OF MAG

Figure 7.39 Simulator Heads in the Wanapum for various values of Leakage



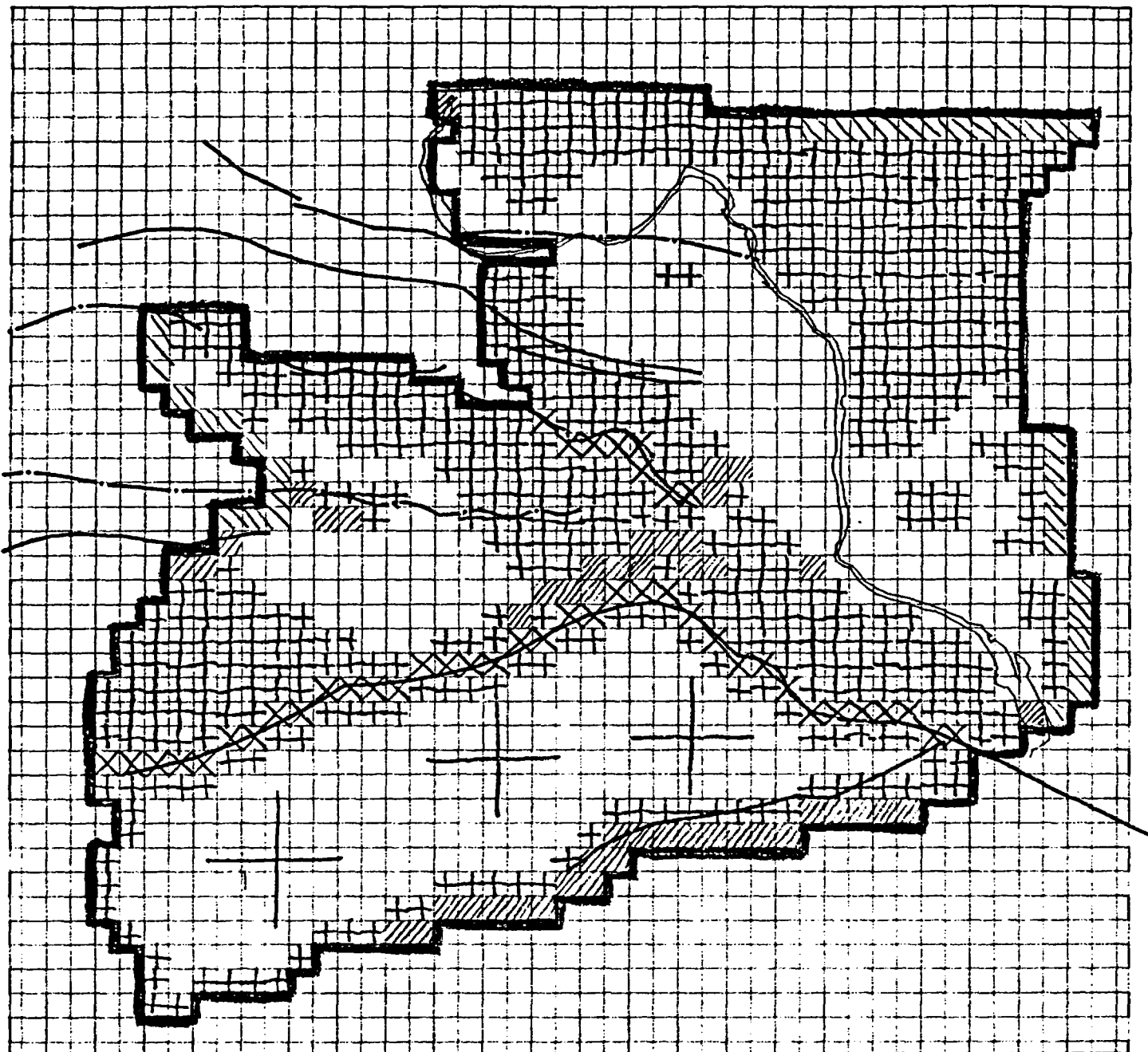
- Model Boundary
- ▨ Constant Head from River Elevation
- ▩ Constant Head from Kriged Heads
- ⊠ No-Flow
- ⊞ Recharge from Precipitation
- Anticline
- - - Syncline

Figure 7.40 Boundary Conditions for the Revised BWIP Regional Flow Model - Layer 1: Grande Ronde Basalts



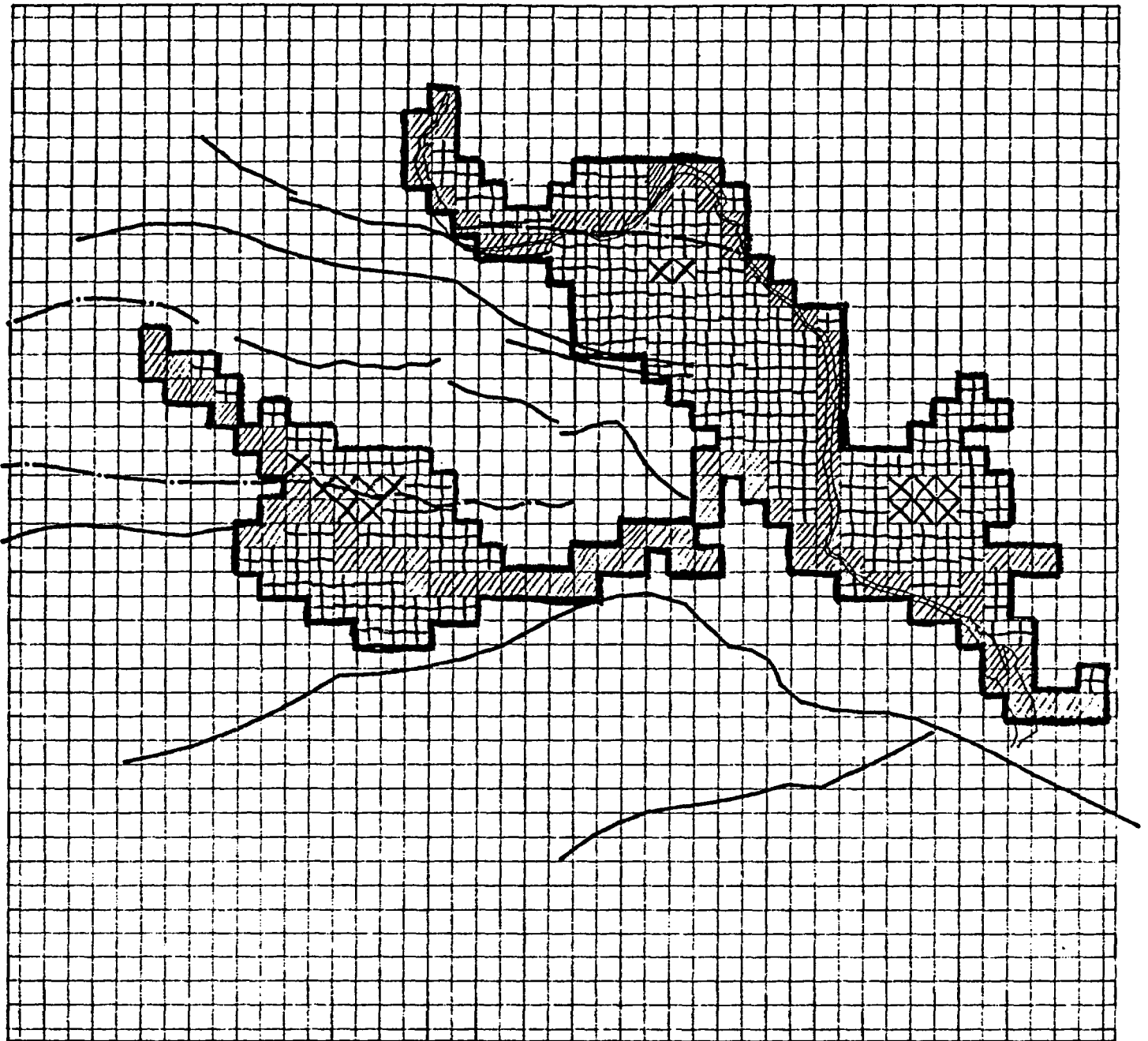
- Model Boundary
- ▨ Constant Head from River Elevation
- ▧ Constant Head from Kriged Heads
- ⊠ No-Flow
- ⊞ Recharge from Precipitation
- Anticline
- Syncline

Figure 7.41 Boundary Conditions for the Revised BWIP Regional Flow Model - Layer 2: Wanapum Basalts



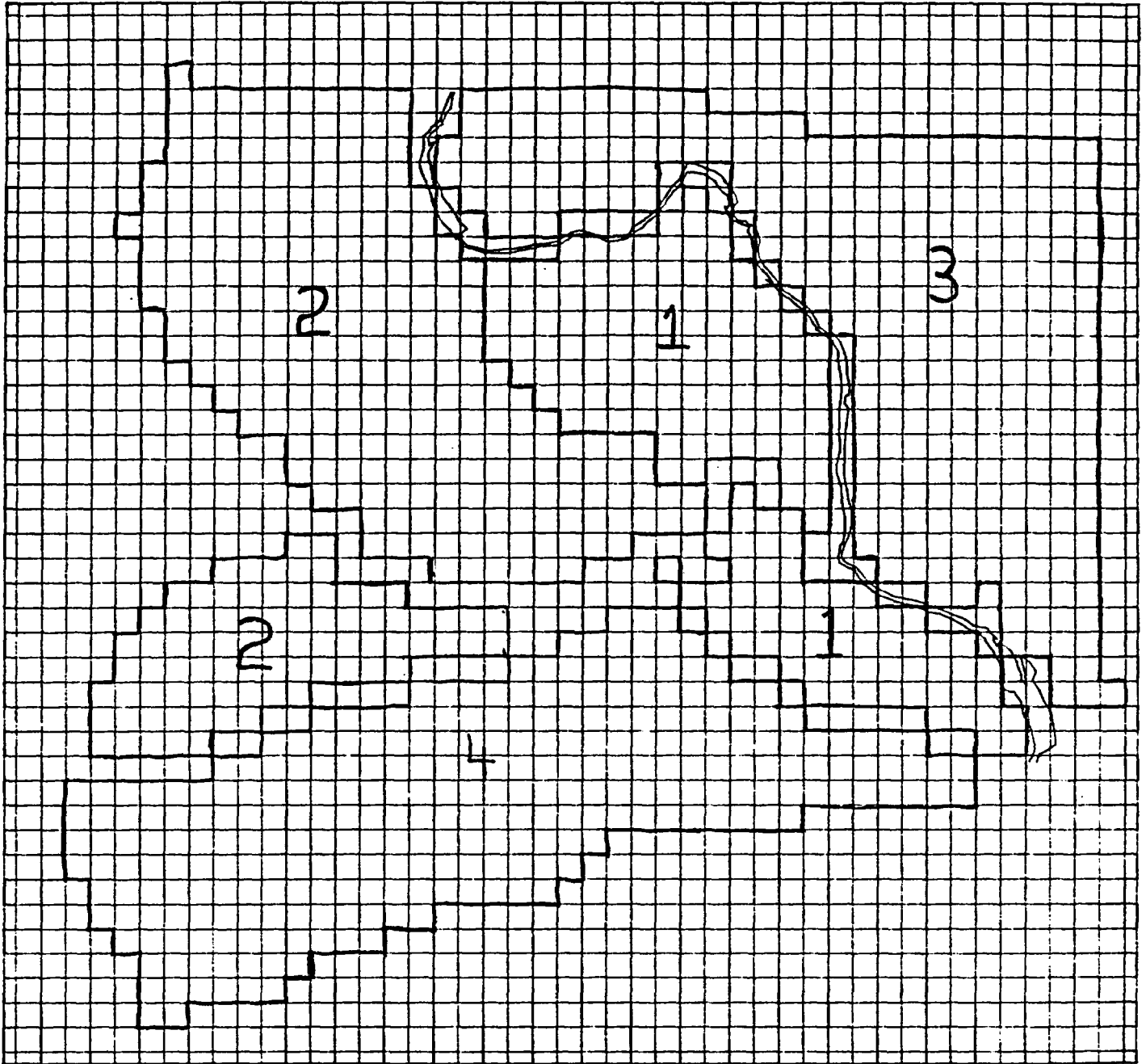
- Model Boundary
- ▨ Constant Head from River Elevation
- ▩ Constant Head from Kriged Heads
- ⊗ No-Flow
- ⊕ Recharge from Precipitation
- Anticline
- Syncline

Figure 7.42 Boundary Conditions for the Revised BWIP Regional Flow Model - Layer 3: Saddle Mountains Basalts



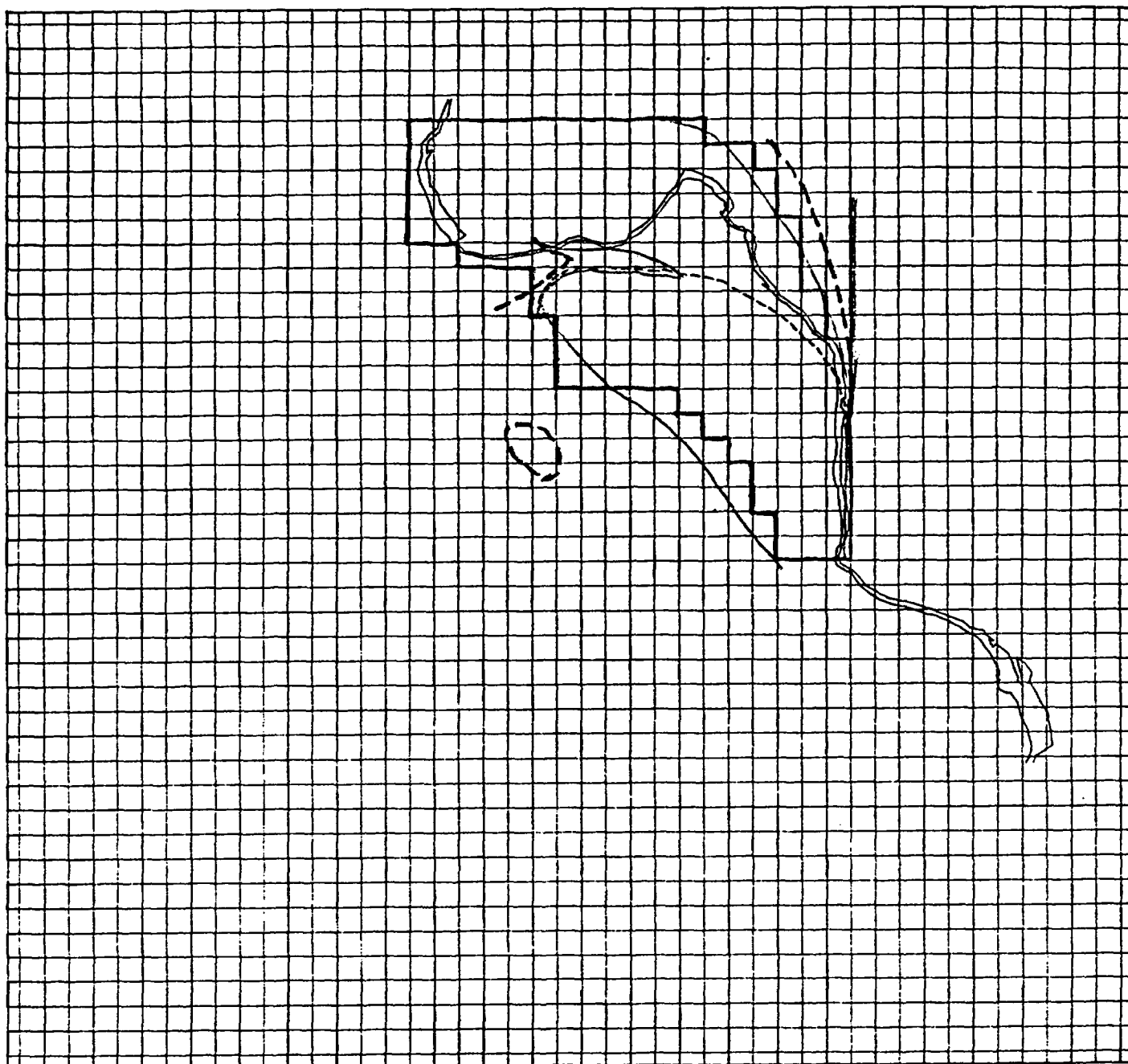
- Model Boundary
- ▨ Constant Head from River Elevation
- ▩ Constant Head from Kriged Heads
- ⊠ No-Flow
- ⊞ Recharge from Precipitation
- Anticline
- - - Syncline

Figure 7.43 Boundary Conditions for the Revised BWIP Regional Flow Model - Layer 4: Saturated Ringold, Hanford, and Alluvium



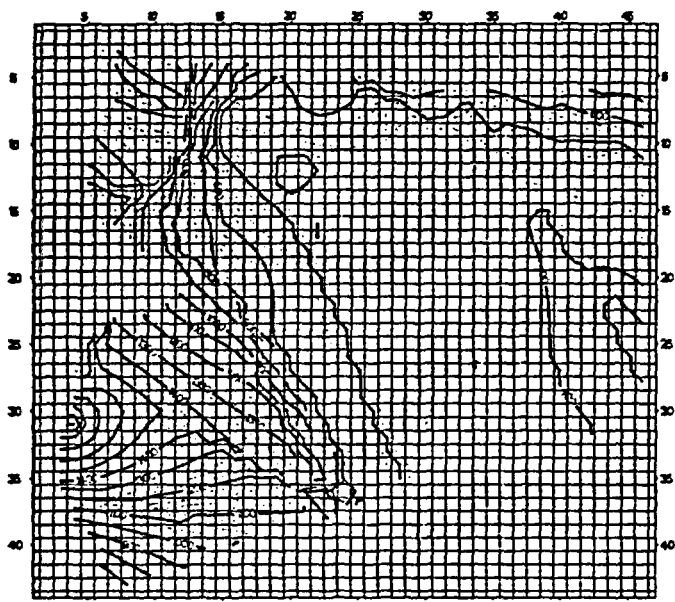
Area	Percent of Rainfall Recharging Groundwater
1	1
2	3
3	1
4	6

Figure 7.44 Percentage of Rainfall Assumed to Recharge Groundwater

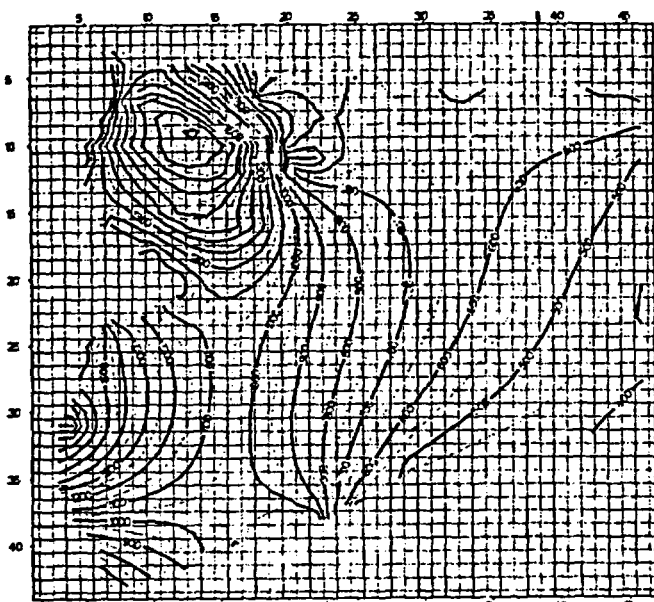


- Rattlesnake Ridge
- Selah
- Cold Creek
- Vantage

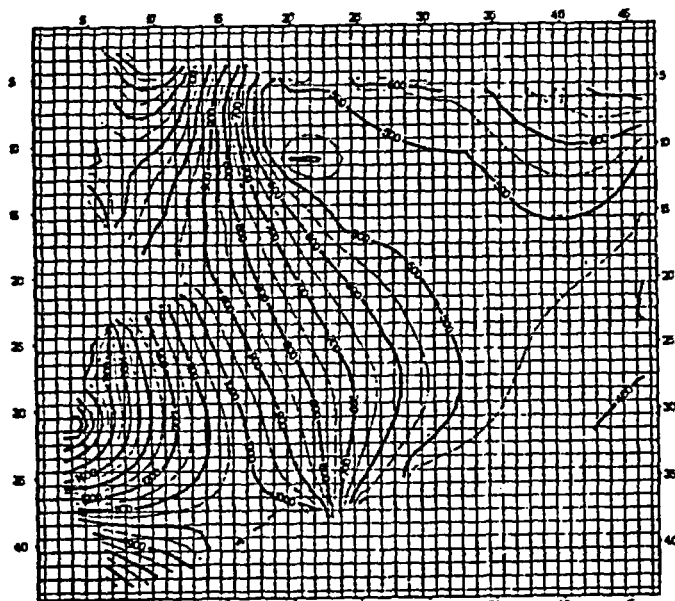
Figure 7.45 Inferred Interbed Boundaries from Myers (1979) and the Model Blocks Modified to Reflect Interbed Influence



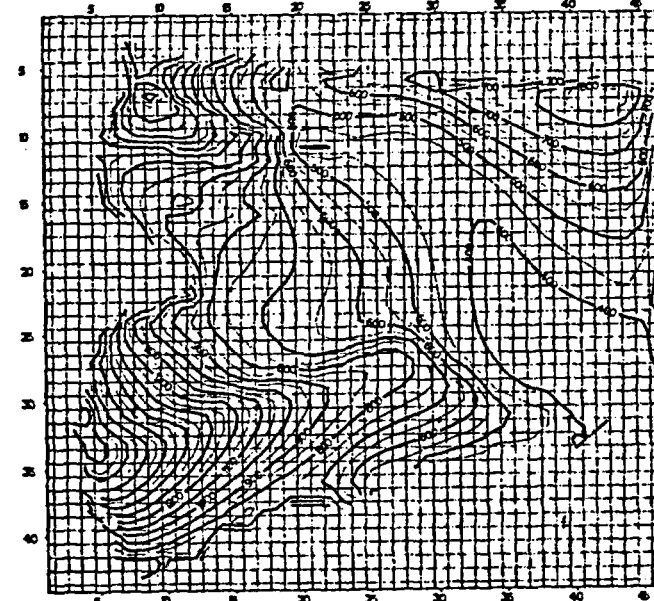
a. Kriged Heads



b. Initial Simulation of Revised Model
EI = 1.37

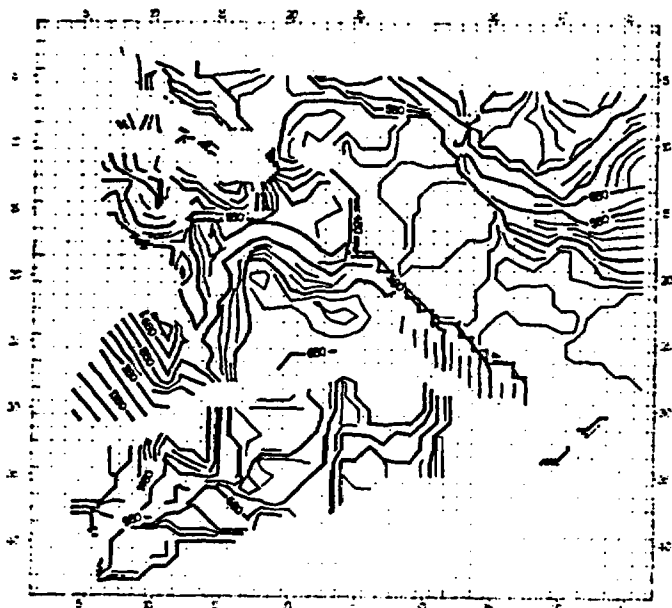


c. Lowest Error Index with
Interbeds Included
EI = 0.44

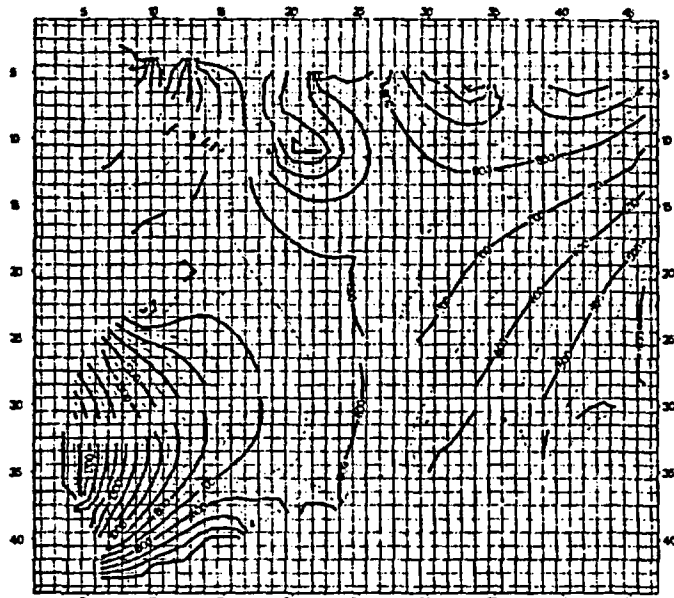


d. Lowest Error Index
with No Interbeds
EI = 0.66

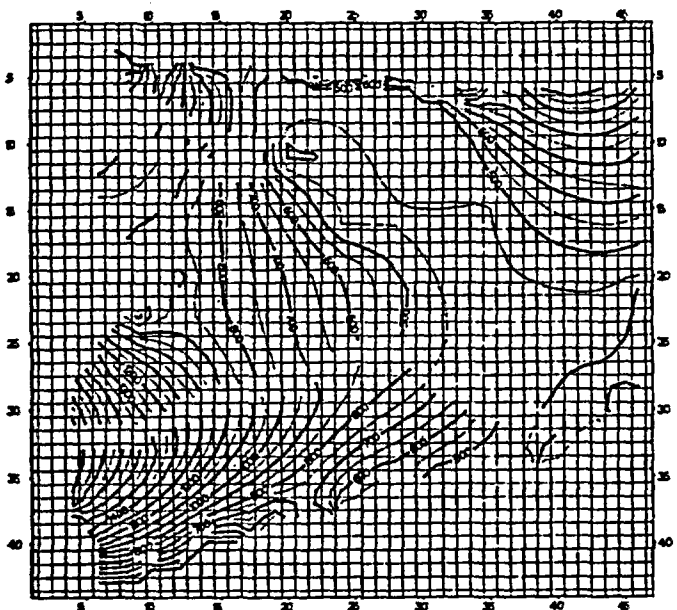
Figure 7.46 Potentiometric Maps for the Grande Ronde Basalts showing Kriged Heads and Model-Predicted Heads for the Initial Simulation of the Revised Model and for the Revised Regional Simulations with and without Interbeds



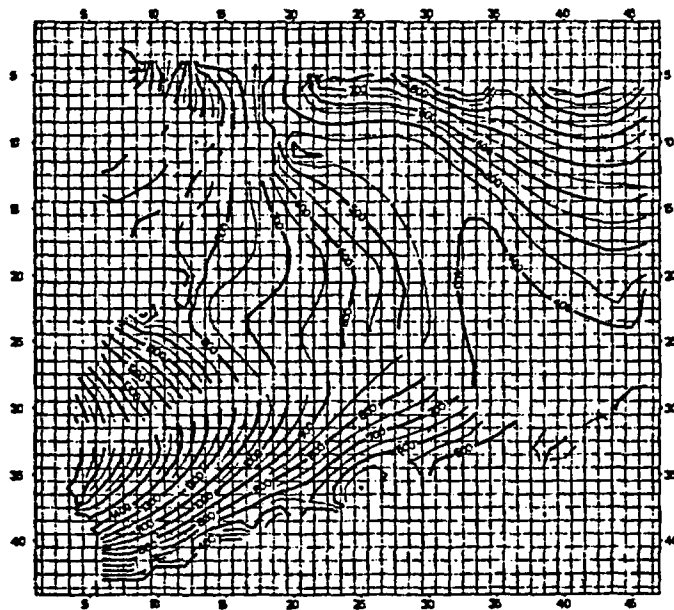
a. Kriged Heads



b. ~~Revised Base Case~~
Initial Simulation of Revised Model
EI = 1.22

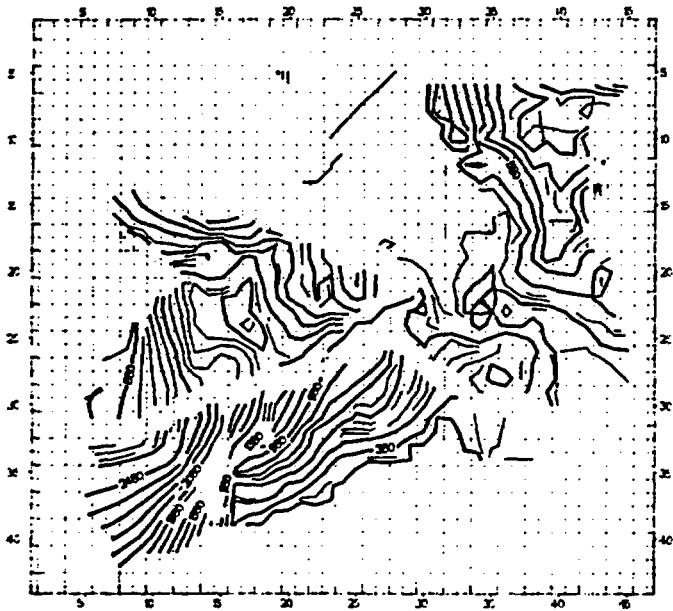


c. Lowest Error Index with
Interbeds Included
EI = 0.61

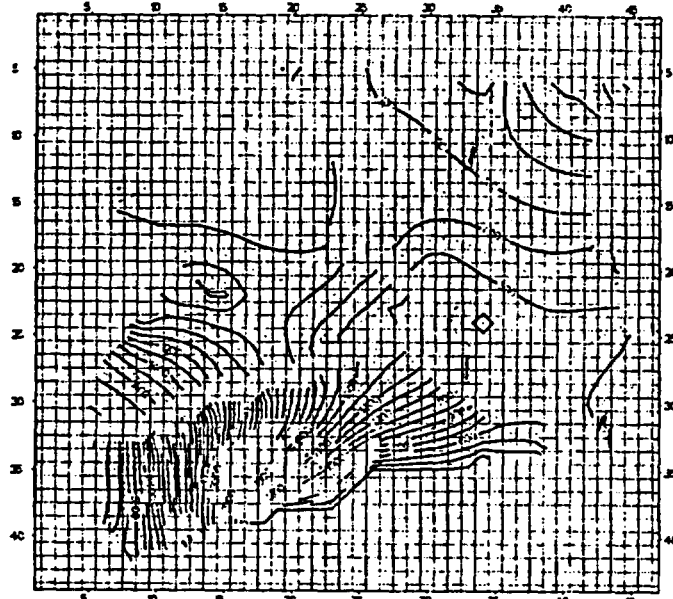


d. Lowest Error Index
with No Interbeds
EI = 0.59

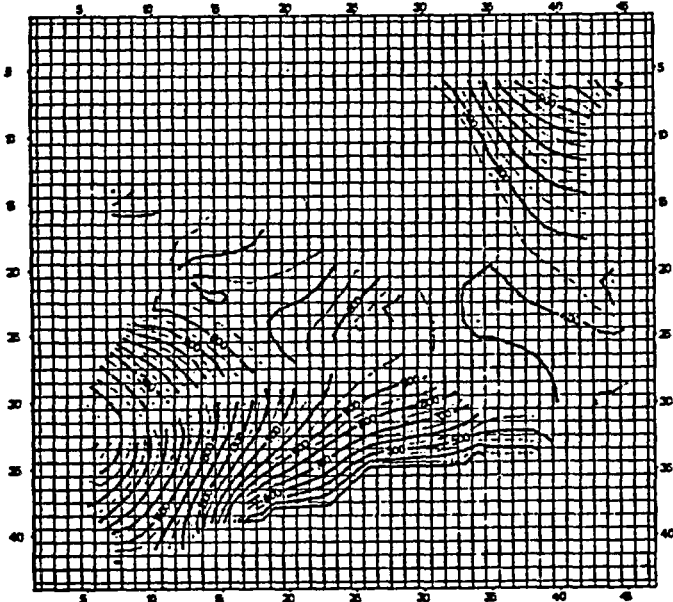
Figure 7.47 Potentiometric Maps for the Wanapum Basalts showing Kriged Heads and Model-Predicted Heads for the Initial Simulation of the Revised Model and for the Revised Regional Simulations with and without Interbeds



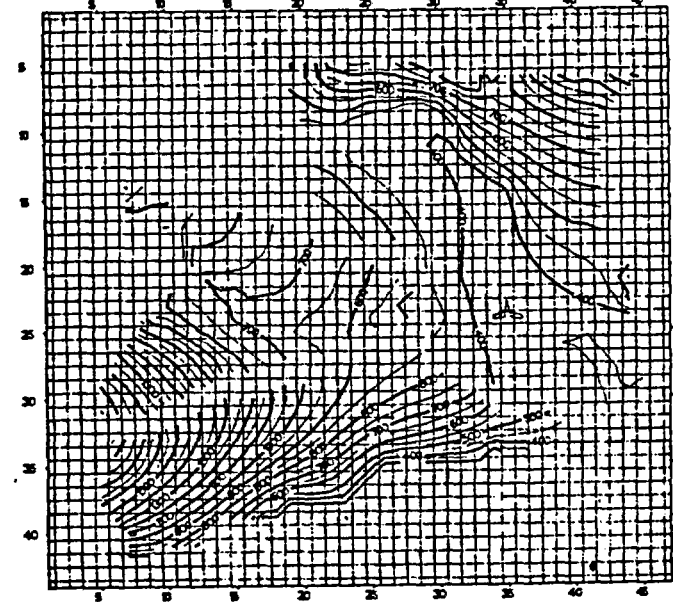
a. Kriged Heads



b. *Initial Simulation of Revised Model*
 EI = 3.10



c. Lowest Error Index with Interbeds Included
 EI = 1.10



d. Lowest Error Index with No Interbeds
 EI = 1.44

Figure 7.48 Potentiometric Maps for the Saddle Mountains Basalts showing Kriged Heads and Model-Predicted Heads for the Initial Simulation of the Revised Model and for the Revised Regional Simulations with and without Interbeds

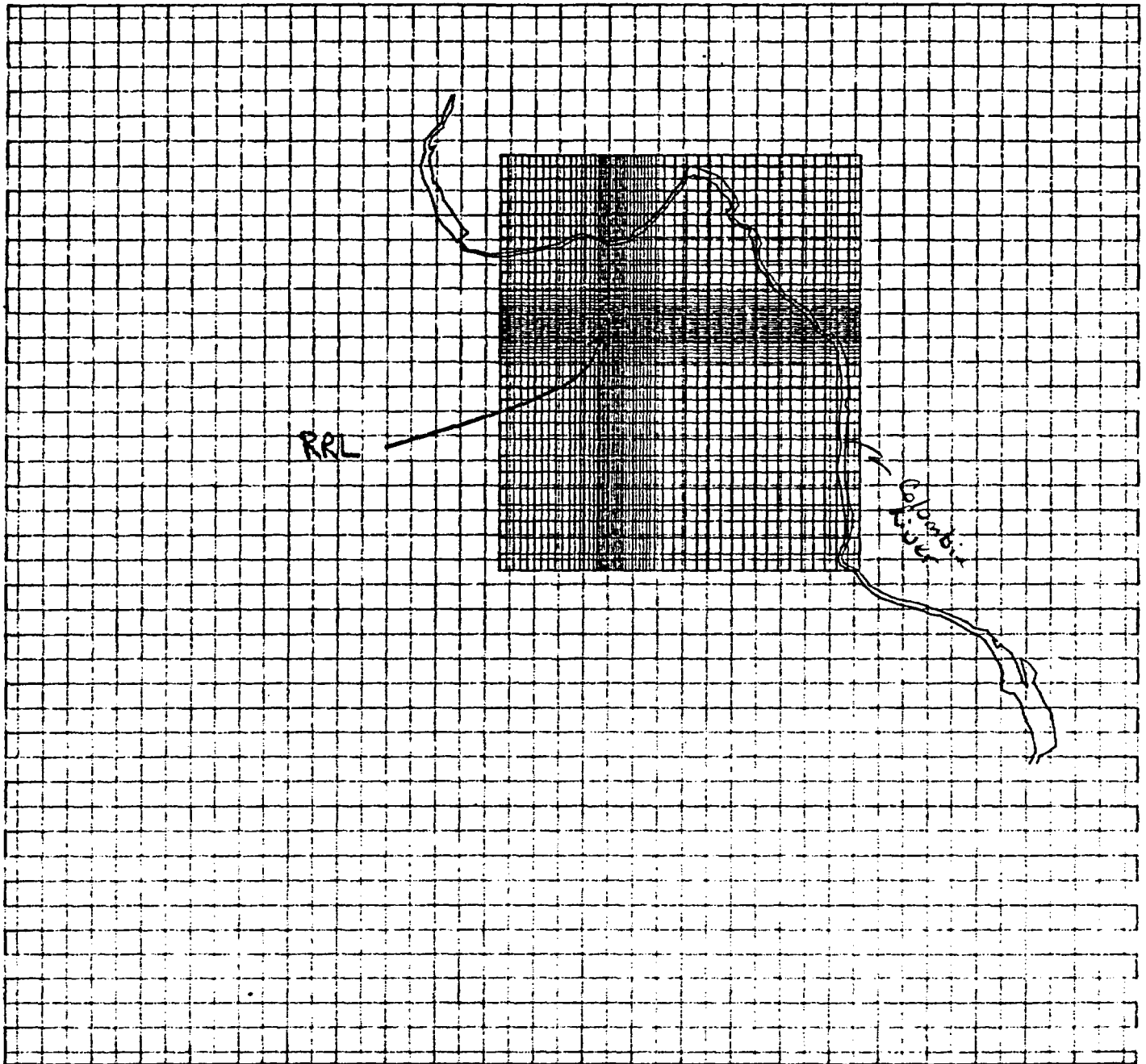


Figure 7.49 Location of the Local Scale Model Grid Within the Regional Scale Model Grid

Appendix A
Review of Ground-Water Flow Models of the Hanford Site

This section contains reviews of available ground-water flow models of the Hanford site. The reviews provide a brief description of each model, its limitations and assumptions, and its relevance to NRC licensing rules.

A.1 ARNETT, 1980

A.1.1 REFERENCE

Arnett, R. C., 1980; "Far-Field Modeling: Simulation of the Natural Groundwater System in the Pasco Basin," in Basalt Waste Isolation Project Annual Report - Fiscal Year 1980; RHO-BWI-80-100

A.1.2 PURPOSE OF THE STUDY

Understanding the ground-water flow systems in the Pasco Basin, identifying data and conceptual model limitations and calculating preliminary travel times.

A.1.3 SOURCES OF DATA

Spane, F. A. Jr., 1980, Groundwater hydrology of the Columbia River Basalts beneath the Hanford Site, in Basalt Waste Isolation Project: Annual Rept. - 1980, RHO-BWI-80-100.

A.1.4 GEOHYDROLOGIC FRAMEWORK

Hydrostratigraphic Units

The selection of hydrostratigraphic units was based on "groundwater head and chemistry measurements." That is, a reversal of hydraulic head gradient with depth and abrupt changes in chemical composition with depth (Figure A.1.2). Note that the layers shown in Figure A.1.1 do not correspond with the model reported in this study which includes only the Grande Ronde, Wanapum, and Saddle Mountains basalt along with, possibly, the alluvium as an upper boundary condition.

Hydraulic Parameters

Listed in Table A.1.1 are the parameters and their starting values. Table A.1.2 lists the parameter values used in the calibrated model.

A.1.5 BOUNDARY CONDITIONS

The location of the model boundaries is shown in Figure A.1.3. These boundaries correspond to the surface-water drainage boundaries of the Pasco Basin. The type of boundary condition imposed at these locations is not discussed but the report indicates that they are fixed potential boundaries. We could not ascertain whether the top boundary was a recharge boundary or fixed potentials representing the elevation of the rivers and the water table in the sediments.

A.1.6 NUMERICAL IMPLEMENTATION

Code Name: RHAFE - Rockwell Hanford Finite - Element Model

Reference: Gupta, S. K., Tanji, K. K., and on Luthin; 1975; A Three-dimensional Finite Element Groundwater Model; Contribution Number 152, California Water Resource Center, University of California. (possibly version of FE3DGW)

Dimensions: 3

Equations Solved: Steady-state and transient isothermal ground-water flow equations

Method of Solution: Finite element

Discretization: (see Figure A.1.4)

Layer discretization corresponds to the hydrostratigraphic units shown in Figure A.1.1

Implementation of Boundary Conditions: Not described.

A.1.7 MODEL CALIBRATION

Data Set Used for Comparison

See Spane (1980), RHO-BWI-80-100 and Figure A.1.5. Note: only Mabton heads were used for comparison.

Type of Calibration Procedure: Trial and error

Type of Statistics Relating Model to Measured Heads: None

Accuracy of Calibrated Model:

All calculated heads are substantially above the measured heads

A.1.8 SENSITIVITY ANALYSIS

None performed

A.1.9 MODEL RESULTS

The authors state the following results:

Hydraulic Heads

Only the heads for the top of the Wanapum Basalt are reported

1) A composite ratio of vertical to horizontal hydraulic conductivity 10^{-4} to 10^{-5} provides a better match of the "relative pattern" of the hydraulic head surface than a ratio of 10^{-2} .

2) With a composite hydraulic conductivity of 10^{-4} to 10^{-5} , the vertical pathway from a potential candidate site is a significant portion of the total path in terms of overall travel time to the biosphere.

3) The problem of the model-calculated heads being "significantly" higher than the measured heads is attributed to absence of the "Cold Creek Syncline Barrier" in the model.

Fluxes

Information on model-calculated fluxes was not provided.

Travel Times

No travel times were reported. However, Figures A.1.6 and A.1.7 reveal significantly different flow directions from the location of a hypothetical repository. For anisotropy ratios of 10^{-2} to 10^{-3} (Figure A.1.6), the inferred direction of flow is to the north/northeast toward the Columbia River. Anisotropy ratios of 10^{-4} to 10^{-5} produce flow toward the north, then vertically upward (Figure A.1.7). This latter path would probably result in longer travel times to the accessible environment (that is,

a given distance from the repository) because of the additional time spent in low permeability dense flow interiors.

Significance to Licensing

The travel path corresponding to what the authors feel to be the ratio best representing the system shows a significant vertical component through dense basalt interiors. This path would presumably have a large associated travel time.

A.1.10 EVALUATION

Conceptual Model

The most important aspects of a steady-state model are the boundary conditions and the choice of layering. Little information was provided about the boundary conditions and the discussion of layering is internally inconsistent (see discussion below).

Boundary Conditions

Bottom

There is no explicit description of the bottom boundary. We assume, however, that it has been treated as a no-flow boundary. The exact nature of this boundary has not been determined as there is an extreme paucity of data in units below the Wanapum Basalts. There is a possibility that the Pasco Basin is a discharge area for regional flow in the flood basalts. If this is the case, then treating this boundary as impermeable could produce unrealistically low vertical gradients, and inaccurate travel times.

Top and Lateral Boundaries

The treatment of these boundaries is not described by the authors. Possibly they were treated as constant hydraulic head boundaries with heads being equal to the water-table elevation for the top boundary and equal to heads measured from wells completed in the appropriate units for the lateral boundaries. This would be consistent with other modeling studies of the Pasco Basin. However, the document seems to make contradictory statements

with regards to the lateral boundaries. On page III-51, the authors state that the boundary conditions may need adjustment but appear to be in the proper range. This statement suggests that the boundaries were treated as constant heads. However, on Figures A.1.6 and A.1.7 (this report) the model-calculated heads are different at the boundary for the two cases. This would not be possible if the boundaries were constant heads. In a steady-state simulation, held potentials will dominate the model results. The uncertainty in the model results depends on the uncertainty in the boundary heads. If hydraulic head data are sparse, as they are for most basalts within the Pasco Basin, then a large uncertainty is introduced by interpolating or extrapolating values to the boundary. Since no information exists on the real flux crossing the boundary, there is no possibility of cross-checking the accuracy of the boundary conditions.

In summary, the lack of a description of the type and values of flux or head assigned to the model makes the evaluation of the boundary conditions impossible. Also, because the boundary conditions dominate steady state simulations, the ability to evaluate the overall modeling effort is severely limited.

Hydrostratigraphic Units

Several questions arise in evaluating the hydrostratigraphic units simulated in this study: 1) Which units were simulated?, 2) How were the units chosen?, and 3) How are model results affected by this choice?

Figure A.1.1 shows the five layers the authors state have been simulated. However, in their "SUMMARY OF RESULTS," they indicate that four layers were simulated. One possible resolution of this discrepancy is that the top layer was held as a constant-head boundary. If this were true, then the model would have five layers of which only the lower four were simulated. However only three layers are mentioned. This could mean that the three basalts were simulated and the top layer was held at a constant head.

Due to the complexity of the flood basalts, no pervasive set of hydrostratigraphic units

exists. In addition, even if every zone of different hydraulic properties could be identified and characterized, sufficient computer resources do not exist to simulate all of them. The units were chosen on the basis of changes in the geochemistry and hydraulic heads with depth which may or may not be indicators of distinct hydrostratigraphic units. However because some lumping of smaller units will always be necessary, a more important consideration is the effect the choice of units has on model results. One effect is to lose detail of the hydraulic-head distribution but perhaps less notable is the incorrect travel path that would be predicted by a grid which does not individually represent each hydrologically distinct zone. In addition, any comparison of model results to measured values requires some interpolation or lumping procedure for the measured parameters. This introduces additional uncertainty into model calibration.

Numerical Implementation

No details of numerical implementation are provided in the document.

Model Calibration

The only calibration that was performed involved adjusting the ratio of vertical to horizontal hydraulic conductivity for the three basalt layers. The resulting hydraulic-head surface for the top of the Wanapum was then subjectively compared to the measured surface. All simulations resulted in heads that are significantly higher (at least 100 ft. in some places) than the measured values. However, the authors believe the simulations with lower ratios of vertical to horizontal conductivities produced a "relative pattern" of hydraulic heads that more closely resembles the measured heads.

Following is an evaluation of the model calibration:

- 1) Insufficient data, in terms of input parameters, boundary conditions, and data used for model comparison are provided to allow for a complete evaluation of the model calibration.
- 2) The fact that all model calculations produce heads that are too high is indicative of a

systematic error in either the model setup or the model parameters. If the top and lateral boundaries of the model are held at constant hydraulic heads interpolated from measured values, then the most likely cause of the high heads is that the model hydraulic conductivities are too low. If the top boundary is a recharge condition, then the amount of assumed recharge could be too large.

- 3) Assuming that: a) the shape of the potentiometric surface presented in Figure A.1.5 is accurate; b) the model boundary conditions are held potentials with values being close to the real values; and c) the shape of the model-predicted potentiometric surface would not change as a more accurate calibration is achieved; then the fact that lower conductivity ratios produce a more realistic pattern of hydraulic heads indicates that the lower units are controlled more by the shape of the basin and perhaps a more regional flow system, than they are by the Columbia River.
- 4) The authors of the report under review believe that if the Cold Creek barrier were included in the model the overall calibration would improve. This is unlikely as heads in all regions, even far to the south, are too high.
- 5) Even though the lower hydraulic conductivity ratios appear to produce more realistic patterns of hydraulic heads, the absolute values of heads for the higher ratios are closer to the measured values.

Sensitivity Analysis

None performed

Model Results

The fact that this model could not be calibrated makes any results suspect. The lack of information on boundary conditions makes evaluation of the effort impossible.

Fluxes

Information on model-calculated fluxes was not provided.

A.2 ARNETT AND OTHERS, 1981

A.2.1 REFERENCE

Arnett, R. C., Mudd, R. D., Baca, R. G., Martin, M. D., Norton, W. R., and McLaughlin, D. B., 1981: Pasco Basin Hydrologic Modeling and Far-Field Radionuclide Migration Potential, RHO-BWI-LD-44.

A.2.2 PURPOSE OF THE STUDY

The study is a first attempt by BWIP to integrate hydrologic data, a conceptual model, and numerical modeling for far-field analysis. The results were supposed to aid in the evaluation of the hydrologic systems identified by ground water flow paths (streamlines), estimate ground water travel times derived from 2D and 3D simulations, predict a range of velocities, and provide input to biotic transport and dosimetry models.

A.2.3 SOURCES OF DATA

Gephart, R. E. and others, Hydrologic studies within the Columbia Plateau, Washington: An integration of current knowledge: Rockwell Hanford Operations, 1979, RHO-BWI-ST-5, 1537 p.

Myers, C. W., 1979, Geologic Studies of the Columbia Plateau: A Status Report: Rockwell Hanford Operations, Rept., RHO-BWI-ST-4, 502 p.

Spane, F. A., Jr., 1980, Groundwater hydrology of the Columbia River Basalts Beneath the Hanford Site, in Basalt Waste Isolation Project, Annual Report - Fiscal Year 1980, RHO-BWI-80-100.

A.2.4 GEOHYDROLOGIC FRAMEWORK

Hydrostratigraphic Units

The report presents a discussion of the geologic setting and stratigraphic nomenclature including treatment of the intraflow structures of basalts and discussion of the prevalence of sedimentary interbeds of high hydraulic conductivity in the Saddle Mountains and Wanapum Basalts. However, the conceptual model that is used in the three-dimensional modeling includes only four layers, based primarily on geologic characteristics (Figure A.2.1). Of these four layers, the uppermost ("undifferentiated glaciofluvial deposits and/or Ringold Formation") is used only to define the upper boundary of the modeled system.

In the two-dimensional modeling of a vertical section reported in the second half of the report, the three basalt formations are divided into 8 units, (Figure A.2.2). The planar section is oriented approximately NW - SE, from the Saddle Mountains north of the Columbia River to an area east of the Columbia and north of Wallula Gap, a total distance of about 100 km. The orientation of the section is based on estimated flow directions, not on the streamlines that resulted from the 3-D simulations. The vertical layering of the two-dimensional model accounts for changes in dip due to folding, but there is no accommodation for faulting or fracturing.

Hydraulic Parameters

The hydraulic parameters used in the 3D model are presented in Table A.2.1. The distribution of material types in the 2D simulations is shown in Figure A.2.3. The material properties used for the material distribution are shown in Table A.2.2.

In both cases, RHO uses composite hydraulic conductivity values for the model layers. Although the method of calculation is not presented, a reference to Freeze and Cherry (1979) suggests that the series/parallel electrical analogies were used. The report does not provide the data that were used, so it is not possible to check the calculation of hydraulic conductivities. It appears that vertical hydraulic conductivities are based on assumed anisotropy ratios only. (This is explicitly stated in the discussion of the 3D model; for the 2D model the K_v values may reflect modifications introduced in the calibration process.)

The data used for hydraulic conductivity appear to have come from Spane (1980) and from Gephart (1979). The report does not provide any data to support the values of effective porosity that were used.

A.2.5 BOUNDARY CONDITIONS

3-D

The plan view of the Pasco Basin finite element (FE) network, including the head boundary conditions and major rivers is shown in Figure A.2.4. The notations on the figure indicate where RHO assumed hydrostatic conditions, vertical variations between layers, and surface-only boundary conditions. In areas where basalt extends above the water table, surface nodes are assumed to lie on a no-flux boundary. The major source of data for all heads is Gephart and others (1979).

Heads for the upper boundary nodes lying below the major rivers (Columbia, Yakima, Snake) are taken to be equal to the average stage; therefore, heads in the unconfined system between the rivers and the basalts are assumed to be hydrostatic.

Heads for upper boundary nodes below the unconfined sedimentary aquifer are assumed to be equal to the hydrostatic unconfined heads.

Heads for boundary nodes on the vertical sides of the domain are estimated from borehole measurements, though the locations are not given. The upper portions of the Rattlesnake Hills and Saddle Mountains anticlines are assumed to be no-flux boundaries. In most areas, the heads are assumed to be hydrostatic.

Illustrated in Figure A.2.5 are the recharge and pumping areas that were modeled. The surface fluxes for the upper boundary elements lying below recharge areas were assumed to be proportional to annual rainfall. RHO assumed that one-fifth of the average annual rainfall (i.e., 3.7 cm/yr) reaches the basalt ground-water system. Pumping rates that were used in the MAGNUM3D simulations are shown in Table A.2.3.

The lower boundary was assumed to be a no-flux boundary, about 1,000 m below the top of the Grande Ronde. RHO assumed that this depth is beyond the influence of recharge and pumping and asserts that "At this depth vertical head profile should be hydrostatic and vertical flow should be negligible."

2-D

The geometry of the two-dimensional model is shown in Figures A.2.6 and A.2.7. Boundary conditions were stipulated as follows:

- a. The bottom of the model is assumed to be a no-flow boundary.
- b. The "upper" portion (not defined in the paper) of the left lateral boundary is also considered to be a no-flow boundary corresponding to a ground-water divide at a topographic ridge. The "lower" portion (also undefined) appears to have been modeled as a "specified head" (apparently hydrostatic conditions), the value of which was estimated in the absence of any measured values. Note that this approach is not consistent with the results of the three dimensional model. The entire discussion of the left lateral boundary conditions is vague.

- c. The right lateral boundary is defined to be a "constant" (i.e., fixed for each layer) head boundary. Data was used from DC-15 and modified to mimic the shallow data from well 9/30-18H.
- d. The upper boundary of the 2-D model corresponds with the top of the basalt. This is taken to be a no-flow boundary where the basalt is exposed and a constant-head boundary (set equal to the head value for the unconfined aquifer) where the basalt is overlain by the unconfined sedimentary aquifer.

A.2.6 NUMERICAL IMPLEMENTATION

3-D:

Code Name: MAGNUM-3D

Reference: No citation, "... Rockwell Hanford Operations (Rockwell) MAGNUM-3D program. This program, initially developed by RMA ..."

Dimensions: 3

Equations Solved: Steady-state (used in this study) and transient ground-water flow.

Method of Solution: Isoparametric finite element

Discretization: See Figures A.2.4 and A.2.8

Implementation of Boundary Conditions:

See Figure A.2.4 and discussion of boundary conditions, above.

2-D:

Code Name: MAGNUM

Reference: Baca, R. G. and Arnett, R. C., 1981, Analysis of Fracture Flow and Transport in the Near Field of a Nuclear Waste Repository, RHO-BWI-SA-81.

Baca, R. G., and Arnett R. C., and King, I. P., 1981, Numerical Modeling of Flow and Transport Processes in a Fractured-Porous Rock System, RHO-BWI-SA-113.

Dimensions: 2

Equations Solved: Coupled heat and porous/fracture ground-water flow. For the purposes of this analysis, the modeling was isothermal, steady-state flow of ground water in a porous medium.

Method of Solution: Finite element

Discretization: See Figure A.2.7. See also Figures A.2.2 and A.2.3 for the relationship of the grid to the hydrostratigraphic units and the distribution of material properties.

Implementation of Boundary Conditions: Not discussed

A.2.7 MODEL CALIBRATION

3-D:

Data Set Used for Comparison

Table A.2.4; data appear to be from Spane (1980)

Type of Calibration Procedure

Trial and error (may have been only one trial)

Types of Statistics Relating Model to Measured Heads: None

Accuracy of Calibrated Model

All calculated heads are substantially (5-20 m) above measured heads.

2-D:

Data Set Used for Comparison

See Table A.2.4. Probably from Spane (1980)

Type of Calibration: Trial and error

Type of Statistics Relating Model to Measured Heads

Absolute value of largest difference between measured and model-calculated heads; root-mean-square error (RMSE) of head differences.

Accuracy of Calibrated Model

Calculated heads at internal match points used by RHO are 5.5 - 11.3 m higher than measured heads.

A.2.8 SENSITIVITY ANALYSIS

There was no sensitivity analysis performed for the 3-D modeling.

For the 2-D model, several runs were made to test the sensitivity of calculated internal head distribution to different values of head held at the left lateral boundary. The results are presented in Table A.2.5.

A.2.9 MODEL RESULTS

3-D: The authors state the following results:

Hydraulic Heads

"Plotted head contours appear to be physically reasonable and generally consistent with available borehole measurements." (See Figures A.2.9 to A.2.12)

Flow Directions

"All three layers indicate a dominant flow direction from the basin boundaries toward the Columbia River and down the axis of the basin."

Pathlines

"Particles move predominantly west to east, under the Columbia River, and slowly upward. This trajectory does not reflect the possibility of transport within more conductive sedimentary interbeds which are not included in the three-layer model network." (Emphasis added by reviewer.) (See Figures A.2.13 and A.2.14).

Travel Time

" . . . we believe that the calculated travel time from the hypothetical repository location to the edges of the Pasco Basin of >100,000 yr is a useful, and in several ways conservative, guide."

Fluxes: Not addressed.

Significance to Licensing

If these results were "correct" or even "conservative," then the flow paths and travel times would support DOE assertions of site suitability in terms of ground-water travel time and (by inference) radionuclide flux to the accessible environment, including "major sources of ground water."

2-D

Hydraulic Heads

"The results . . . clearly demonstrate the sensitivity of ground water flow (head distribution) to the boundary conditions We believe the bias of the data set . . . is causing distortions in the results of the 'best fit' procedure." (See Figure A.2.16 and Table A.2.5)

Streamlines

"The initial path is downward followed by movement to the right (specified head boundary). It is recalled that this analysis does not consider potential temperature effects" (See Figure A.2.17)

Travel Time

"The total calculated travel time from the hypothetical repository location to the edge of the model was 2×10^6 yr . . . the travel time reported . . . in the 3-D modeling may be more credible."

Fluxes: Not addressed.

Significance to Licensing: Same as the 3-D case.

A.2.10 EVALUATION

Conceptual model

The choices of boundary conditions and modeling layers dominates the results of steady-state models. The following comments evaluate the treatment in this study of these aspects of the conceptual model.

Boundary Conditions

No evidence is presented in the paper to support the assumption of the bottom boundary as a no-flow boundary. There is some evidence, both hydrologic and geochemical, that the Pasco Basin could be a regional discharge area. If this were true, then a no-flow boundary at the base of the model would produce unrealistic vertical gradients and consequently distorted pathlines and travel times.

The paucity of reliable data on hydraulic heads in the Columbia River Basalts, particularly the Grande Ronde, limits the reliability of extrapolated or interpolated data along the lateral boundaries. However, only slight (in many cases, <1 m) errors in head values could reverse the apparent vertical gradient in single boreholes. The scarcity of data may preclude calculation of boundary conditions accurate enough to preserve observed vertical gradients.

The use of hydrostatic heads for the basalt sequence along the left lateral boundary appears to have little or no justification. As mentioned above, this type of boundary condition is not consistent with the results of the 3-D modeling; the flow path (and, consequently, the calculated travel time through low-conductivity materials) is dominated by the choice of head profile from DC-4/5 along the center line of the hypothetical repository. Despite RHO's contention that the model is highly sensitive to boundary conditions, it appears (in terms of absolute difference in head or RMSE of head) the model is insensitive over the range of 105 m to 135 m in specified head values along the left-lateral boundary. These results may be dominated by the assumptions for the upper and lower boundaries and the use of hydrostatic head conditions along the left-lateral boundary. Perhaps the most significant result is that for no feasible value of head at the left boundary do the simulation heads match the measured values at the right boundary.

Hydrostratigraphic Units

Although the basis for choosing the units is not described in the paper, it appears that the modeling layers were taken to be coincident with major geologic units, rather than being based on hydrologic or hydrochemical data. There is no particular reason to believe that the geologic distinctions coincide with the hydrologic behavior of the basalts. Even more importantly, the omission of the sedimentary interbeds

and the inclusion of the basalt interflows with the dense interiors is likely to significantly affect the predicted flow paths from the repository to the edge of the modeled domain. This uncertainty in conceptualization will enhance the uncertainties in flow path calculations and, ultimately calculations of radionuclide flux.

Numerical Implementation

Except for the FE grids and the statement that heads were represented by quadratic basis functions, no details of model implementation were presented in the document.

Model Calibration

There is very little documentation on model calibration. Subjective evaluations of the relative similarity of the calculated and measured values are made in some places. The consistently higher calculated values suggest that there are some systematic flaws in the modeling. Because most of the heads along the lateral and upper boundaries are fixed, the most likely explanation (assuming that the boundary conditions are approximately correct) for the anomalously high heads is that the hydraulic conductivity values used are too low, the recharge is too high, or a combination of both.

Sensitivity Analysis

The only sensitivity runs conducted were discussed above.

Model Results

The results show a calculated head distribution that does not accurately reproduce the measured head values. This may be due to the reliance of this model on limited amounts of virtually point-scale hydraulic data and uncertain head measurements to establish boundary conditions. The uncertainties in the conceptualization, the boundary conditions, and the hydraulic parameters are too great to lend credibility to the estimates of either flow path or travel time that result from the simulations.

A.3 RIGDON AND OTHERS, 1981 (LATA)

A.3.1 REFERENCE

Rigdon, L. D., S. E. Logan, H. Sing, and K. J. Hong, 1981, Preliminary Risk Assessment Results for a Nuclear Waste Repository in Basalt; LATA-RHO-04-02-A

A.3.2 PURPOSE OF STUDY

This study was conducted to simulate ground-water conditions in the Pasco Basin and to estimate ground-water and radionuclide transport away from the vicinity of a hypothetical repository in basalt. Three scenarios were analyzed: (1) natural conditions, (2) fault connecting repository with upper aquifers, and (3) borehole seal degradation or failure.

A.3.3 SOURCES OF DATA

Gephart, R. E., and others, 1979, RHO-BWI-ST-5

A.3.4 GEOHYDROLOGIC FRAMEWORK

Hydrostratigraphic Units

1. Upper and unconfined layers
2. Composite Saddle Mountains interbeds (Except Mabton)
3. Mabton Interbed
4. Vantage Interbed
5. Umtanum Flow Top

Note: Layers 3, 4, and 5 vertical connection terms reflect properties of aquitards between each layer. Also, the vertical conductivity of layer 2 included intervening basalt layers. See Figure A.3.1.

Parameter Values

Table A.3.1 lists the parameter values used in the model

A.3.5 BOUNDARY CONDITIONS

Lateral - held potentiometric levels (constant heads) were applied to each layer at the edge of the model (i.e. edge of the Pasco Basin)

Top - Not discussed

Bottom - Not discussed but probably impermeable

A.3.6 NUMERICAL IMPLEMENTATION

Code Name: Although the code name is not mentioned, enough description is provided to conclude that SWIFT was used.

Reference: Dillon, R. T., R. B. Lantz, and S. B. Pahwa, 1978; Risk Methodology for Geologic Disposal of Radioactive Waste: The Sandia Waste-Isolation Flow and Transport (SWIFT) Model; SAND78-1267.

Dimensions: 3

Equations Solved: Coupled energy, fluid flow, brine and radionuclide transport

Method of Solution: Finite difference

Discretization: Spatial - the only information provided indicated that 240 nodes were used in each layer.

Temporal - None (steady state)

Implementation of boundary conditions - not discussed

A.3.7 MODEL CALIBRATION

Data Set used for Comparison:

Regional matching of heads was performed but the data set used for comparison is not provided. The only data mentioned are the transient test data from well DC-2.

Type of Calibration Procedure:

Trial and Error. Two calibrations were mentioned. They involved adjusting hydraulic conductivities in an attempt to match; 1) transient hydraulic heads during a test in well DC-2 and 2) steady-state hydraulic heads over the entire region.

Type of Statistics Relating Model to Measured Heads: None

Accuracy of Calibrated Model: Not described.

A.3.8 SENSITIVITY ANALYSIS

None performed

A.3.9 MODEL RESULTS

Hydraulic Heads

Not described

Fluxes

Not described

Travel Times

33,600 years from the repository horizontally northward in the Umtanum and vertically upward to the Columbia River. Approximately 70% of the time is spent in the vertical portion.

Significance to Licensing

Although the authors report a calculated travel time to the Columbia River, the travel time to the EPA define accessible environment can be estimated from other information provided. Given that the total travel time to the Columbia River was calculated to be 33,600 years and 70% of that was in the vertical leg of the path, then about 10,000 years was spent in the horizontal leg. The horizontal distance to the Columbia River is about 7.5 Km. Therefore, the average horizontal particle velocity is about $7E-4$ Km/yr. For the EPA specified distance of 5 Km to the accessible environment, the travel time would be about 7000 years, assuming that the horizontal velocity is constant, and the NRC criterion would be met.

A.3.10 EVALUATION

Conceptual Model

The factors that dominate the conceptual and in turn the numerical model are the lateral boundaries and the assumed vertical pathway in the vicinity of the Columbia River.

Limiting the lateral boundaries to the Pasco Basin results in the confidence in the model being dependent on the confidence in the fixed hydraulic heads along the boundaries. These heads were obtained by interpolation and extrapolation from the few measured heads. Because of the lack of data and the lack of quality control on the existing data, very little confidence can be put into the boundary conditions and therefore the model results.

The authors have assumed that the vertical hydraulic conductivity is larger below the Columbia River than

elsewhere in the Pasco Basin. This contrast in conductivity, along with the imposed boundary conditions, results in a flow system where water moves in laterally from the edges of the model and then upward to the Columbia River. Apparently, the evidence that supports this concept is the potentiometric map of the Mabton which indicates flow toward the vicinity of the Columbia River. In addition, the assumption of an upward vertical component of flow below the river would have to be made. The authors cannot support this assumption or the assumption of larger vertical hydraulic conductivities. This is because insufficient data are available to determine the vertical hydraulic gradient and no data are available concerning the vertical hydraulic conductivity near the Columbia River. Their concepts would be indirectly supported if this was the only model that could reproduce the measured hydraulic heads. However, no evaluation of this type can be made because the authors have failed to provide any quantitative description of how well their modeled heads match the measured heads.

Numerical Implementation

Not enough information is provided to evaluate this aspect of the modeling.

Model Calibration:

Insufficient data, both in terms of the data set used for comparison and the ability of the model to reproduce that data, are provided to evaluate the model calibration.

Sensitivity Analysis

No sensitivity analysis was performed.

Model Results

While the study produces results that are consistent with the conceptual model (i.e. particles are predicted to travel from the repository to the Columbia River). However, the data are too sparse and unreliable to support the boundary conditions. No data exists to support the assumption of large vertical conductivities below the river.

These problems result in such a high degree of uncertainty that no judgment can be made as to how well the model represents the real system.

A.4 DOVE AND OTHERS, 1982

A.4.1 REFERENCE

Dove, F. H., Cole, C. R., Foley, M. G., Boad, F. W., Brown, R. E. Deutsch, W. J., Freshly, M. D., Gupta, S. K., Gutknecht, P. J., Kuhn, W. L., Lundbert, J. W., Rice, W. A., Schalla, R., Washburn, J. F., ZEMMER, J. T., 1982; "AEGIS Technology Demonstration for a Nuclear Waste Repository in Basalt;" PNL-3632/UC-70.

A.4.2 PURPOSE OF THE STUDY

This study was performed to demonstrate the performance assessment methodology developed at Pacific Northwest Laboratories and documented in Petrie and others, 1981 and Foley and others, 1982. This methodology was developed for the Department of Energy to assess the performance of a mined geologic repository in basalt.

A.4.3 SOURCES OF DATA

"Published hydrologic and geologic data . . . gathered in 1979 or earlier."

A.4.4 GEOHYDROLOGIC FRAMEWORK

Hydrostratigraphic Units

The PNL regional model consisted of three layers, one of which was used only to maintain a specified hydraulic-head upper boundary condition. The two simulated layers represented a combined Saddle Mountains/Wanapum basalts layer and a layer for the Grande Ronde basalts. The upper layer was used to specify fixed hydraulic heads which were held equal to the elevations of rivers, lakes, and the water-table of the alluvial aquifer.

Three layers were simulated in the local (Pasco Basin) model: the Saddle Mountains basalts, the Wanapum basalts, and the Grande Ronde basalts. As in the regional model, a top layer was used to apply boundary conditions.

Hydraulic Parameters

Hydraulic parameters used in the regional model are listed in Table A.4.1. For the Saddle Mountains/Wanapum basalts (layer 1), transmissivities varied over the modeled region whereas a constant value was assumed for the Grande Ronde basalts (layer 2). Table A.4.1 lists the average of the

parameter values used in the Saddle Mountains. The Grande Ronde basalts were assumed to act hydraulically like the Wanapum basalts. The authors state that this assumption was made mainly because of the lack of data on the Grande Ronde basalts.

In the local model values of horizontal hydraulic conductivity were spatially distributed for each layer. The average initial values for the Saddle Mountains, Wanapum, and Grande Ronde basalts were 2.96, 1.73, and .75 ft/d respectively. A uniform ratio of vertical to horizontal hydraulic conductivity of 0.1 in the alluvium and 0.01 in all other layers was used initially. These values were changed areally within each basalt layer during calibration. The authors adjusted the ratio based on the assumption that vertical conductivities increased in areas of structural deformation (see Figure A.4.1).

The authors state the "the porosity distribution was set as shown [in Table A.4.2] and maintained throughout the model calibration process," presumably referring to the average values. The value of porosity does not affect the calculated heads, as the model simulated steady-state conditions, but is used in calculating ground-water travel times.

A.4.5 BOUNDARY CONDITIONS

The boundary of the regional model is shown in Figure A.4.2. A combination of rivers, seepage faces, alluvial water tables, lakes and impermeable boundaries are applied to the two layers. No-flow (impermeable) boundaries were imposed in the appropriate layer but constant head boundaries (rivers, lakes, etc.) were applied to the top layer and then hydraulically connected to the appropriate layer. For example, a constant head boundary is established in the top layer where the Columbia River incises the Grande Ronde basalts (Layer 2). The top layer is then hydraulically connected to the Grande Ronde layer, the effect being that the head in the Grande Ronde layer is always approximately equal to the constant head in the alluvium. No-flow boundaries were imposed at the southwestern and eastern edges of the model. The application of no-flow conditions was based on assumptions of the effects of geologic structures, ground-water divides and in some cases, the edge of the basalts. Distributions and types of boundary conditions are displayed on Figures A.4.3 and A.4.4. In addition, 2300 ft³/s were input as recharge and 280 ft³/s were taken out of the model as pumpage.

Figure A.4.5 shows the location of the boundaries in the Pasco Basin model along with the regional model boundaries. Fixed values of hydraulic head were held along the northern and eastern boundaries of the model. The head values were obtained from the regional scale model. No-flow conditions

zero outside of the active areas. Constant hydraulic-head boundaries which represent rivers, lakes, seepage faces, and the alluvial water table were implemented by holding the hydraulic head constant in a layer which is above the two active layers and then by increasing the vertical conductivity between the constant head node and the node in the lower layer. In addition, recharge from precipitation and irrigation was input to the top active layer.

Pasco Basin Model

Code Name: FE3DGW - Finite Element Three-Dimensional Ground-Water Model

Reference: Gupta, S. K., and others; 1980; Finite-element three-dimensional groundwater FE3DGW flow model formulation, program listing and user's manual; PNL-2939, Pacific Northwest Laboratory, Richland, Washington.

Dimensions: 3

Equations Solved: Transient and steady-state isothermal ground-water flow equations

Method of Solution: Finite element

Discretization: The model grid is shown in Figure A.4.6. This grid represents the total areal extent of all of the layers. The upper layers do not extend to the edge of this grid. Where the layers do not exist the thickness of the elements has been reduced to near zero.

Implementation of Boundary Conditions

In contrast to the regional model, almost all of the rivers and lakes are located in the top (alluvium) layer. No-flow and constant-head boundaries (along the north and east) are applied directly to the basalt layers.

A.4.7 MODEL CALIBRATION

REGIONAL MODEL

Data Set Used for Comparison

A potentiometric map was constructed for the Saddle Mountains/Wanapum Basalt layer and compared to well data from 1958, 1959, and 1978. No information is provided about the source of data used to construct the map. Model simulations were compared to this interpreted potentiometric map, not to measured head values. In comparing their map to the data, Dove and others (1982) noted that the least average error was 79.2 feet. Their criterion of calibration was that the difference between the model values and the well data be less than this error of interpolation. Comparisons between the model-simulated heads of the Grande Ronde layer and field data or potentiometric maps were not done due to lack of field data.

Type of Calibration Procedure: Trial and error

Type of statistics Relating Model to Measured Heads:

Average, maximum positive and negative, and root mean square errors were used to describe the differences between model and measured heads for the Saddle Mountains/Wanapum basalt layer. No comparisons between model and measured heads were made for the Grande Ronde basalt layer.

Accuracy of the Calibrated Model:

Table A.4.3 lists the average, root mean square (rms) and maximum positive and negative errors (difference between model and measured head) for the Saddle Mountains/Wanapum basalt layer for the three years for which well data are available.

The main difference between the three data sets used for comparison is the number of data for each. The number of measurements for the years 1958, 1959, and 1978 are 162, 439 and 360, respectively. The reason for using three data sets for comparison is not clear. The authors may be emphasizing the difficulty of identifying steady state conditions. In any event, the fact that three different time periods are being compared does not indicate that a transient simulation was performed.

Without knowing the procedure and data used in generating the interpreted potentiometric map, comparing the model results to that map is meaningless. Therefore, the only comparison that can be made here is that of the model

results to the well data. Any qualitative evaluation of the accuracy of a model is subjective, however, this particular model displays significant differences with observed data. Namely, average differences between modeled and measured heads are on the order of 100 feet with maximum differences of up to 761 feet. These differences appear to be too large to allow the model to be termed "calibrated." This is especially true if one considers that a larger number of nodes in the comparison layer (the Saddle Mountains/Wanapum basalts) are directly connected to constant head nodes in the overlying layer. That connection effectively constrains the heads in the Saddle Mountains/ Wanapum basalts layer to be fairly close to the measured values.

LOCAL MODEL

Data Set Used for Comparison:

Potentiometric maps from Gephart and others (1979) were used for model comparison. The model results were therefore compared to interpretations of the data instead of to the measured data.

Type of Calibration Procedure: Trial and error

Type of Statistics Relating Model to Measured Heads:

Maximum positive and negative differences, average difference, and root mean square errors were used to relate the simulated heads to the interpreted heads taken from potentiometric maps.

Accuracy of Calibrated Model:

Table A.4.4 lists the calibration statistics for both the "preman" and "current conditions" simulations.

A.4.8 SENSITIVITY ANALYSIS:

No sensitivity analysis was performed for either model.

A.4.9 MODEL RESULTS:

REGIONAL MODEL

Hydraulic Heads:

Figures A.4.7 and A.4.8 are contour maps of the model-predicted hydraulic heads for both layers. The

authors believe that the predicted flow directions show general agreement with those derived from available data. Flow directions indicated from the available are displayed on Figure A.4.9. Model-predicted flow paths do show some agreement with this data. The flow paths shown in figure A.4.9 were obtained through discussions between the USGS and PNL. The data used to arrive at these paths is not available for review.

Fluxes:

Table A.4.5 lists the fluxes predicted by the calibrated model. The authors believe that these values are reasonable but provide little data for comparison.

Travel Times:

No ground water travel times from the RRL to the accessible environment were calculated using these model results, however travel times were calculated using the Pasco Basin model. Boundary conditions for the Pasco Basin model were interpolated from the results of the regional model.

Travel times from recharge areas to selected wells were used to compare model results with ages of ground waters estimated from isotopic dating. These ages compare favorably, however the authors admit to a large uncertainty ($\pm 100\%$) in the calculated ground-water ages.

LOCAL MODEL

Hydraulic Heads:

Figures A.4.10 and A.4.11 show the simulated heads for the Grande Ronde basalt for both the "preman" and "current" conditions. Note that the model-predicted heads for the Grande Ronde are larger than those for the overlying units. The vertical component of flow is therefore upward in the vicinity of the proposed repository.

Fluxes:

Model predicted fluxes for the Pasco Basin simulation were not discussed.

Travel Times:

The model predicts that particles leaving the proposed repository location would travel up to the alluvium and then

north to the Columbia River. A travel time of 15000 years from the location of a hypothetical repository to the Columbia River was calculated from the calibrated model results. Using the ground-water velocity associated with this calculation results in a travel time of about 5500 years from the location of the hypothetical repository to the 5 kilometer accessible environment defined by the EPA.

Significance to Licensing:

The predicted travel time of 5500 years would indicate that the site meets the NRC 1000 year ground-water travel time requirement. This predicted travel time also indicate that for any radionuclide which has a retardation factor of at least 2, the EPA standard for integrated discharge over 10,000 years would also be met.

A.4.10 EVALUATION

Boundary Conditions

The overall approach of using a large scale, less complex model to set boundary conditions for a local scale, more complex model represents a significant improvement over the other BWIP modeling efforts. This is because, in some areas, the regional model was extended to the physical edge of the modeled units, reducing the uncertainty in the boundary conditions. The regional model was not extended everywhere to correspond with the physical extent of the units. The interpolated boundary conditions result in a large uncertainty in boundary conditions, especially for the Grande Ronde layer, for which little hydraulic head data exist. The uncertainty in boundary condition values contributes to the uncertainty in travel time.

A second major source of uncertainty is the assumption that the Grande Ronde basalts behave hydraulically like the Wanapum basalts. Considering the paucity of data on the Grande Ronde, no judgement as to the accuracy of this assumption can be made. However, several facts about the site conflict with this assumption. First, the Grande Ronde basalts crop out in different areas than do the Wanapum basalts. Recharge from precipitation and river leakage will therefore occur in different areas for the Grande Ronde than for the Wanapum. In addition, the elevation where recharge occurs may also be different, which may result in a larger driving force for flow in the Grande Ronde. Both of these factors could result in a different flow path in the Grande Ronde basalts. Second, geologic structures within the modeled region affect the two units differently. For example, at some anticlines the Grande Ronde is exposed and the Wanapum basalts are not

continuous across the anticline. Therefore, the hydraulic system in the Grande Ronde may be continuous while the anticline acts as a no-flow barrier for the Wanapum flow system.

Hydrostratigraphic Units

Both regional and local models use a fairly coarse layering. The regional model simulates flow in the Grande Ronde basalts and in a combined Saddle Mountains/ Wanapum basalts layer while the local model simulates each of the three main basalt sequences. Although the report states that the flow in the sediments above the basalts is being simulated in both of the models, this layer is really only represented as a source or sink for the basalt layers. Flow laterally within this unit is not simulated in either model.

The coarse layering of the regional model may be adequate for establishing boundary conditions for the local scale model, however the authors did not estimate the uncertainty in these boundary conditions. One unusual aspect of the regional model layering is that the Wanapum basalts were lumped with the Saddle Mountains basalts instead of with the Grande Ronde basalts, considering the authors assumption that the Grande Ronde basalts behave hydraulically like the Wanapum basalts

For the local scale (Pasco Basin) model simulation the three basalt layers may be sufficient to investigate the overall hydraulic behavior. However, the path followed by a particle leaving the repository would be governed by the properties of individual layers and structures within each major basalt unit, which are not explicitly represented in the model. Therefore, model predicted ground-water travel times should be considered very uncertain.

Numerical Implementation

Insufficient information is provided to allow for the evaluation of this aspect of the study.

Model Calibration

Two major problems are evident in the model calibration. The first, which is independent of this study, is the lack of an adequate data set on the measured hydraulic heads. This is especially true for the Grande Ronde basalts. The result of an inadequate data base for comparison is that no matter how well the model reproduces the existing data, there is no assurance that the model is accurately

simulating the real system. In this case, however, the second major problem is that the models do not appear to be simulating the measured heads accurately. The regional model over-predicts the measured hydraulic heads by up to 761 feet and under-predicts them by as much as 649 feet. The local model has similar problems, with over-predictions of up to 948 feet and model-predicted heads as much as 666 feet below the measured heads.

Sensitivity Analysis

None performed

Model Results

Two questions can be asked about the results of this study: first, do they represent an accurate enough picture of the real system to be useful in predicting repository behavior; and second, what does this modeling effort tell us about the system behavior and the remaining uncertainties of the system ?

The answer to the first question seems to be no. The primary reasons for this are:

- 1) the data set used to construct the model and used for comparison of model results was inadequate, this is especially true for the Grande Ronde basalts;
- 2) the inaccuracy of the calibrated model with respect to the measured hydraulic heads;
- 3) the unjustified assumption that the Grande Ronde basalts act hydrologically like the Wanapum basalts; and
- 4) the large uncertainties associated with the constant-head boundaries and the recharge estimates.

On the other hand, this modeling effort is the only one reviewed in the report that is sufficiently documented to allow us to address the second question of what the model indicates about the real flow system. These implications are listed below. Note that due to the concerns raised above, they may not be completely accurate statements about the real system.

- 1) The regional basalt system receives almost all of its recharge from within the model region of the Columbia Plateau.

- 2) The Pasco Basin is a regional discharge area for the Columbia Plateau.
- 3) Model transmissivities had to be much larger than measured transmissivities. The authors believe the reported values were not measured over the entire thickness of a unit.
- 4) In order to match measured heads, vertical permeabilities which were larger than most used in previous models had to be used.
- 5) Rattlesnake anticline and Hog Ranch Axis form a local ground-water divide.

A.5 BONANO AND OTHERS (1986)

A.5.1 REFERENCE

Bonano, E. J., Davis, P. A., Brinster, K. F., Beyeler, W. B., Shippers, L. R., Updegraff, C. D., Shepherd, E. R., Tilton, L. M., Cranwell, R., M., 1986: Demonstration of a Performance Assessment Methodology for High-Level Waste Disposal in Basalt Formations, SAND86-2325 (NUREG/RW-4759).

A.5.2 PURPOSE OF STUDY

To demonstrate a methodology for analyzing performance of a repository located in basalt. A hypothetical site is analyzed, however the geometry of the site follows BWIP and parameter ranges were taken from interpretations of BWIP test results.

A.5.3 SOURCES OF DATA

DOE (U.S. Department of Energy), 1982. Site Characterization Report for the Basalt Waste Isolation Project, DOE/RL 82-3, 3 vols., Rockwell Hanford Operations for the U. S. Department of Energy, Washington, D.C.

DOE (U.S. Department of Energy), 1984, Draft Environmental Assessment: Reference Repository Location, Hanford Site, Washington. DOE/RW-0017.

Gephart, R. E., R. C. Arnett, R. G. Baca, L. S. Leonhart, and F. A. Spane Jr., 1979. Hydrologic Studies Within the Columbia Plateau, Washington: An Integration of Current Knowledge, RHO-BWI-ST-S, Rockwell Hanford Operations, Richland, Washington.

Guzowski, R. V., F. B. Nimick, A. B. Muller, 1982.
Repository Site Definition in Basalt: Pasco Basin,
Washington. NUREG/CR-2352, SAND81-2088.

Myers, C. W., S. M. Price and others, 1979. Geologic
Studies of the Columbia Plateau: A Status Report,
R40-BWI-St-4, Rockwell Hanford Operations, Richland,
Washington.

A.5.4 GEOHYDROLOGIC FRAMEWORK

Hydrostratigraphic Units

Two separate models were constructed in this analysis: one was a regional model including the Pasco, Yakima, and Horse Heaven Hills basins, the other simulated an area within the Pasco Basin near the RRL. The first model used 4 layers corresponding to the Grande Ronde basalts, the Wanapum basalts, the Saddle Mountains basalts, and the Ringold/Hanford formations and alluvial deposits. The local scale model used 28 layers with individual flow tops and interiors represented near the proposed repository elevation.

Hydraulic Parameters

Samples of conductivity, porosity, geochemical parameters (retardation coefficients, solubility limits, exchange coefficients) and a universal recharge multiplier were generated by a latin hypercube sampling technique from ranges of values found in the literature. Seventy sets of these parameter samples were generated. Conductivities were sampled for each flow top, flow interior, and interbed in an idealized system consisting of homogeneous layers of uniform thickness. These thicknesses were calculated by averaging reported unit thicknesses. Equivalent transmissivities and leakances for the model layers were calculated by lumping the sampled conductivities. Single values for fracture porosity, immobile phase porosity, and exchange coefficient were generated in each set. Retardation coefficients and solubility limits were generated for each isotope in each set. Separate regional and local models were run for each set of parameter values.

A.5.5 BOUNDARY CONDITIONS

The regional model boundaries correspond to the physical limits of the basalts in many areas of the model. These areas are treated as no-flow boundaries. Constant head boundaries are used to represent contact with rivers.

Constant heads are also used where the represented basalt sequences extend beyond the model boundaries.

Constant head boundary conditions were used along all edges of the local scale model. Heads values for these nodes were interpolated from the results of the corresponding regional simulation. The bottom boundaries for both models were impermeable.

A.5.6 NUMERICAL IMPLEMENTATION

Code Name: NMF3D -- New Mexico Finite Difference three dimensions

Reference: Posson, D. R., G. A. Hearne, J. U. Tracy, and P. F. Frenzel; A computer program for simulating geohydrologic systems in three dimensions; U. S. geological Survey, Open File Report, 80-421

Dimensions: 3

Equations Solved: Steady-state and transient ground-water flow equations

Method of Solution: Finite difference using the strongly implicit procedure (SIP) numerical method

Regional Scale Discretization:

Spatial: 47 columns by 44 rows by 4 layers. Each active node was 2 miles on each side. Layer thicknesses were :

Grande Ronde -- 1784 ft
Wanapum -- 1096 ft
Saddle Mtns. -- 752 ft
Alluvium -- 400 ft

Temporal: None

Local Scale Discretization:

Spatial: 24 columns by 26 rows by 28 layers. Figure A.5.1a shows the local scale layering. Figure A.5.1b shows the relationship between the regional and local grids.

Temporal: None

Implementation of boundary conditions:

Constant head nodes were flagged by negative storage values. Heads for these nodes are not recalculated during iteration. No flow nodes were specified as having zero transmissivity. Recharge was represented as injection wells in exposed nodes.

A.5.7 CALIBRATION

The model was not calibrated.

A.5.8 UNCERTAINTY ANALYSIS

The results of each of the 70 simulations using the generated parameter values were compared to a head surface interpolated from head values reported by Olson (1984). Kriging was used to interpolate these heads to the nodal locations for comparison, so that an estimate of interpolation variance, in addition to an interpolated head, was calculated for each nodal point. An error index (discussed in Appendix C) was calculated for each regional model run using the model head surface, the kriged head surface, and the interpolation variance. The authors present the error index for each of the 70 runs, but make no attempt to find a correlation between this index and the model parameters.

A.5.9 RESULTS

Hydraulic Heads

Figure A.5.2 shows the calculated potentiometric surface in the four model layers for one of the 70 regional model runs. Flow directions in the alluvium are east towards the Columbia. In the basalt units, flow is to the southeast.

Figure A.5.3 shows the calculated heads for the corresponding local model in two layers near the hypothetical repository, along with a vertical section through the repository. Flow in these layers is generally to the southeast.

The error index associated with this run was 1.7. This index (discussed in Appendix C) is the average number of standard deviations by which simulated heads differ from interpolated data.

Fluxes

None reported.

Travel Times

The travel times calculated for the 70 runs range from 7000 to 500,000 years. Note that travel times to the accessible environment (as defined by EPA) were reported, not travel times to a natural discharge point.

Significance to Licensing

All reported ground-water travel times were greater than 1000 years.

A.5.10 EVALUATION

The system analyzed in this report is hypothetical. Many of the following remarks discuss the suitability of this system as a representation of the BWIP site, which was not one of the authors' concerns in developing their model. Any incompatibilities result from discrepancies between the BWIP site and the authors' hypothetical site, rather than discrepancies between the authors hypothetical site and their model.

Conceptual Model:

The assumption that the geologic units have a uniform thickness over the extent of the model is unsupported with BWIP data. The assumption of homogeneity considering the wide ranges of reported conductivities for the represented units is also questionable. Homogeneity at the scale of the model is possible in spite of local variations in conductivity, but has not been demonstrated at BWIP. Hydrologic units are assumed to correspond to these idealized geologic units. BWIP test results do not justify this assumption.

Boundary Conditions:

Most of the regional model boundaries are defined by the physical limits of the basalts. The remaining boundaries are Dirichlet boundaries with the head values interpolated from measured heads by a kriging technique. Although estimates of the interpolation variance are available, the effect of the uncertainty in boundary condition values on the model results was not reported. No internal

discontinuities of the hypothetical formations were included in the regional model. Universal connection (over the Rattlesnake Hills, for example) may not be a realistic representation of the conditions at BWIP.

Local scale boundaries are interpolated from the results of the regional model. This process produces a fixed potential field around the local model boundary which is more detailed than the regional model results, and consistent with them. The possibility of using other methods to calculate boundary heads which would also be consistent is not addressed. There is consequently no way to evaluate the uncertainty in the local boundary heads.

Calibration

No calibration was attempted. By making multiple runs using sets of parameters sampled from the reported ranges the authors' expect to produce a run which will match the measured heads. If the conceptual model is not appropriate, a set of parameters resulting in reproduction of measured heads may not be produced.

Uncertainty Analysis

A multiple linear regression analysis was performed to discover which of the sampled parameters had the most impact on the performance measure of interest, estimated integrated discharge to the EPA-defined accessible environment. The authors did not include in their analysis the impact of uncertainty in interpolated regional boundary conditions, the uncertainty in calculated local boundary conditions, or uncertainty in their conceptual model itself, such as the assumptions of uniform thickness, continuity, and homogeneity. As an estimate of the uncertainty of the predicted discharge rates as applied to BWIP, the analysis is consequently incomplete.

Results

The head surface shown in figure A.5.2 has the lowest error index of the 70 runs made. The error index of 1.7 may be interpreted as meaning that an average model head is outside the 90% confidence band for the interpolated head. This particular run, which had the lowest error index of the 70 simulations, cannot be considered an accurate representation of the flow system indicated by the data used for calibration. Since this data was in fact BWIP water levels, this simulation is also inadequate as a model of BWIP.

Given that the LHS sampling procedure used in this study provides a statistically complete coverage of the ranges of model parameters and their combinations, the failure of these samples to produce a calibrated model implies that either the parameter ranges, or the conceptualization of the system, are inappropriate.

Significance to Licensing

Because of the discrepancy between the model results and the measured data, and the consequent possibility that the conceptual model is invalid as a representation of BWIP, the reported travel times should not be considered representative of BWIP.

**Table A.1.1 Baseline Material Hydraulic Conductivities
used for
Calculating Basalt Composite Conductivities**

Basalt	% of Total Basalt Thickness	K (ft/d)	Layer Values (m/d)		
			Kv	Kh	Kv/Kh
Saddle Mountains					
Basalt	60	10^{-6}			
Interflow	20	10	1.7E-6	4	4E-7
Interbed	20	10			
Wanapum					
Basalt	60	10^{-6}			
Interflow	35	10	1.7E-6	4	4E-7
Interbed	5	10			
Grande Ronde					
Basalt	60	10^{-6}			
Interflow	39	10^{-2}	1.7E-6		4
Interbed	1	10			

*Data from RHO-BWI-80-100

**Table A.1.2 Ratios of Kv to Kh used to Produce
Model-Calculated Heads in RHO-BWI-80-100**

Basalt	Simulation 1 (see figure)	Simulation 2 (see figure)
Saddle Mountains	2×10^{-3}	2×10^{-5}
Wanapum	8×10^{-3}	8×10^{-5}
Grande Ronde	3×10^{-2}	3×10^{-4}

Table A.2.1 MAGNUM3D Values for Hydraulic Parameters

Layer	Horizontal Conductivity (m/s)	Vertical Conductivity (m/s)	Effective Porosity
Saddle Mountains	1.0×10^{-8}	1.0×10^{-11}	.01
Wanapum	1.0×10^{-9}	3.0×10^{-12}	.01
Grande Ronde	1.0×10^{-9}	1.0×10^{-12}	.01

Table A.2.2. Material Properties

Material type	Horizontal conductivity (m/s)	Vertical conductivity (m/s)	Effective porosity
1	3.5×10^{-4}	3.5×10^{-8}	0.06
2	1.8×10^{-5}	3.5×10^{-9}	0.06
3	5.3×10^{-4}	3.5×10^{-8}	0.06
4	7.1×10^{-6}	3.5×10^{-10}	0.06
5	1.8×10^{-6}	3.5×10^{-10}	0.6
6	1.4×10^{-5}	1.4×10^{-10}	0.06
7	3.5×10^{-8}	3.5×10^{-11}	0.001
8	3.5×10^{-8}	3.5×10^{-12}	0.001
9	3.5×10^{-9}	3.5×10^{-12}	0.001
10	3.5×10^{-9}	3.5×10^{-13}	0.001
11	6.0×10^{-7}	4.6×10^{-10}	0.06
12	4.2×10^{-6}	4.2×10^{-9}	0.06
13	1.8×10^{-6}	3.9×10^{-10}	0.06
14	6.0×10^{-6}	4.6×10^{-10}	0.06
15	2.1×10^{-6}	3.9×10^{-10}	0.06
16	3.2×10^{-7}	9.2×10^{-10}	0.001

Table A.2.3. Annual Pumpage Rates Used in the Initial
MAGNUM-3D Pasco Basin Simulation

Pumpage	Rate (m ³ /yr)
Saddle Mountains pumpage from area 1	5.6 x 10 ⁶
Saddle Mountains pumpage from the remainder of the basin (including areas 2 and 3)	2.2 x 10 ⁷
Wanapum pumpage from area 1 (Badger Mountain)	6.5 x 10 ⁶
Wanapum pumpage from area 2	6.5 x 10 ⁶
Wanapum pumpage from area 3 (Rye Grass Coulee)	2.8 x 10 ⁶

Table A.2.4 Hydraulic Head Data

Borehole	Basalt Formation (Straddled Zone) (m above MSL)	Head (m above MSL)	3-D (2D) Model Identification**
DB-12	Saddle Mountains/ Mabton (28.0 to -13.7)	122.5	Top of Wanapum (DB-12a)
DB-13	Saddle Mountains/ Mabton (-180.3 to -217.3)	128.5	Top of Wanapum
DB-14	Saddle Mountains/ Mabton (-91.1 to -126.8)	128.6	Top of Wanapum
DB-15	Saddle Mountains/ Mabton (-64.1 to -114.1)	124.0	Top of Wanapum
DC-6	Grande Ronde (-607.8 to -699.5)	130.7	Top of Grande Ronde
DC-7/8	Grande Ronde (-1089.6 to -1131.4)	123.32	Top of Grande Ronde (DC-8a)
DC-12	Wanapum/ Priest Rapids (-213.6 to -233.9)	123.7	Top of Wanapum
	Grande Ronde/ Vantage (-517.8 to -530.6)	124.6	Top of Grande Ronde
DC-14	Saddle Mountains/ Mabton (-173.1 to -204.5)	148.8	*Top of Wanapum
	Wanapum/ Priest Rapids (-208.2 to -239.9)	151.2	*Top of Wanapum
	Grande Ronde/ Vantage (-523.7 to -588.7)	142.0	*Top of Grande Ronde

Table A.2.4 (continued)

	Grande Ronde (-595.3 to -610.5)	131.1	*Top of Grande Ronde
DC-15	Wanapum/ Priest Rapids (-183.2 to -268.0)	117.0	Top of Wanapum
	Wanapum/Roza- Frenchman Springs (-302.7 to -326.4)	117.5	(DC-15a)
	Wanapum/ Frenchman Springs (-436.5 to -452.6)	117.9	(DC-15b)
	Grande Ronde/ Vantage (-486.8 to -515.1)	107.3	*Top of Grande Ronde
	Grande Ronde (-516.9 to -547.4)	118.3	*Top of Grande Ronde
	Grande Ronde (-734.9 to -751.6)	119.2	(DC-15c)
	Grande Ronde/ Umtamum Flow (-866.5 to -882.1)	112.17	(DC-15d)
	Grande Ronde (-883.6 to -917.4)	117.0	(DC-15e)

*In some cases the head values for two consecutive hydrologic intervals are given, particularly where the difference is sufficiently large to indicate that the measurement nearest the interface may not be representative.

Table A.2.5. Results of Different Boundary Conditions

Specified head, left boundary (m)	RMSE value (m)	Maximum difference (m)	2nd Maximum difference (m)
205	6.9	11.3	1.2 (DB-12a)
170	5.0	9.3	8.4 (DB-12a)
130	3.6	7.0	5.1 (DB-12a)
125	3.6	6.7	4.8 (DB-12a)
115	3.4	6.1	4.0 (DB-12a)
105	3.4	5.5	4.7 (DC-8a)

*All maximum differences occur at DC-15d.

Table A.3.1 Model Parameters for
Rigdon and others, 1981

Hydraulic Parameters - General

Layer	Hydraulic Conductivity (m/s)		Effective Porosity (%)	Thickness
	Horizontal	Vertical		
1	1.18E-3	1.18E-4	10	90
2	1.41E-5	1.41E-6	2	215
3	7.1E-5	7.1E-6	4	29
4	3.5E-7	3.5E-8	4	9
5	7.1E-5	7.1E-9	2	61
Confining beds	7.1E-10	7.1E-10	2	402

Hydraulic Parameters - Near the Columbia River

Layer	Vertical
	Hydraulic Conductivity (m/s)
1	1.18E-1
2	1.41E-3
3	7.1E-3
4	3.5E-5
5	7.1E-6
Confining beds	7.1E-7

Table A.4.1 Initial and Calibrated Hydraulic Parameters

	<u>INITIAL</u>	<u>CALIBRATED</u>
Layer 1 T	3E3ft ² /d	1E4ft ² /d
Layer 2 T	8E3ft ² /d	7E3ft ² /d
Layer 1-2 Kv	1E-3ft/d	1.01E-3ft/d - Average
Layer 1 - alluvium Kv	1E-2ft/d	6.9E-3ft/d - Average
Lakes and Rivers Kv	1E-2ft/d	1E-2ft/d
Seepage Face K	1E-2ft/d	1E - 2ft/d

**Table A.4.2 Porosities Used in Ground-Water
Travel Time Calculation**
(Reproduced from Dove and others, Table B.27)

Modeled Hydrologic Unit	Equivalent Porous Medium Effective Porosity		
	<u>Minimum</u>	<u>Average</u>	<u>Maximum</u>
Alluvium	--	0.10	--
Saddle Mountain	0.06	0.095	0.12
Wanapum	0.05	0.07	0.10
Grande Ronde	0.05	0.06	0.07

Table A.4.3 Average, rms, Maximum and Minimum Error
 Comparisons Between Well Data and Model
 Predictions and Well Data and the
 Interpreted Potentials for Layer 1
 (Reproduced from Dove and others, Table B.26)

	<u>1958</u>		<u>1968</u>		<u>1978</u>	
	<u>Model</u>	<u>Inter- preted</u>	<u>Model</u>	<u>Inter- preted</u>	<u>Model</u>	<u>Inter- preted</u>
Average	4	79	96	116	105	108
rms	97	116	127	149	138	146
Maximum Positive Error	280	150	761	738	511	444
Maximum Negative Error	442(?)	-649	-646	-471	-473	-519

All values are in feet

Table A.4.4 Summary of Comparison Statistics Between Model-Predicted Potential Distributions Interpreted from Water Level Data Four Illustrative Model Calibration Runs and the Base (Comparisons are shown for both the current condi scenario and the preman scenario. All values are in ft) (Reproduced from Dove and others, Table B.31)

<u>Run Description</u>	<u>Scenario Description</u>	<u>Number of Positive Differences</u>	<u>Maximum Positive Difference</u>	<u>Average Positive Difference</u>	<u>Number of Negative Differences</u>	<u>Maximum Negative Difference</u>	<u>Average Negative Difference</u>	<u>Average Absolute Difference</u>	<u>Root Mean Squire Difference</u>
Run 1	Current Conditions	742	1454	66	1124	-674	-125	101	142
	Preman	778	1144	60	1088	-685	-119	94	133
Run 2	Current Conditions	1014	2965	135	852	-809	-148	141	214
	Preman	1060	2341	137	806	-733	-143	140	203
Run 3	Current Conditions	895	1021	75	971	-688	-133	105	134
	Preman	933	795	72	933	-698	-125	98	124
Run 4 (Base Case)	Current Conditions	991	948	100	875	-658	-135	116	135
	Preman	1050	735	95	816	-666	-125	108	119
Run 5	Current Conditions	995	627	87	871	-576	-122	103	112
	Preman	1066	971	96	800	-583	-118	106	118

Table A.4.5 Calculated Fluxes in the Regional Model

<u>Layer</u>	<u>Flow to Overlying Layer</u>	<u>Flow to Underlying Layer</u>	<u>Flow to Constant Heads</u>
Alluvium	X	0.11	X
1	0.71	0.64	0.176
2	0.32	X	0.725

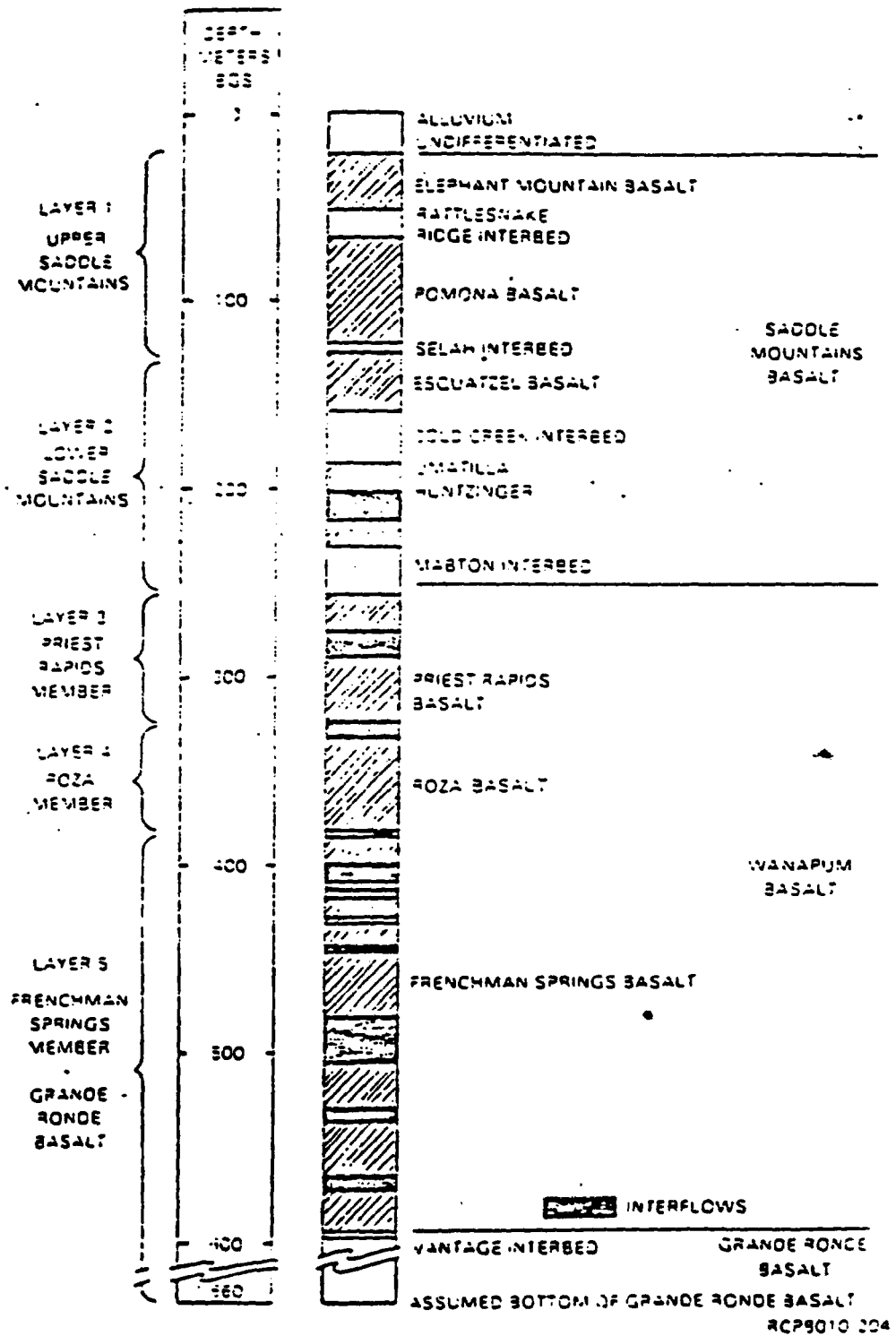


FIGURE A.1.1 Vertical Layering for Pasco Basin Three-Dimensional Model at Well DC-15.

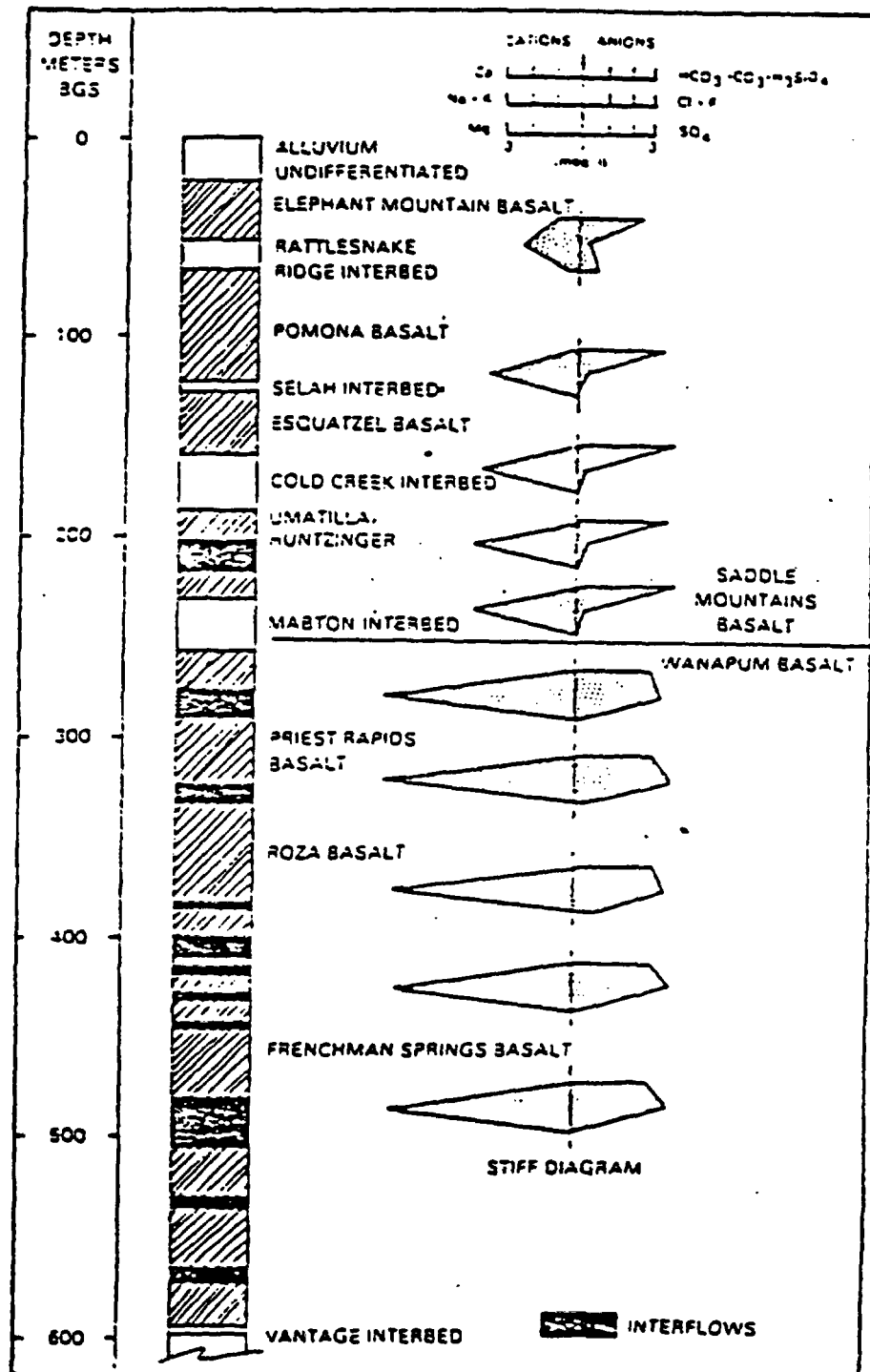


FIGURE A.1.2 Preliminary Hydrogeologic and Hydrochemical Data within the Saddle Mountains and Wanapum Basalts at Borehole DB-15.

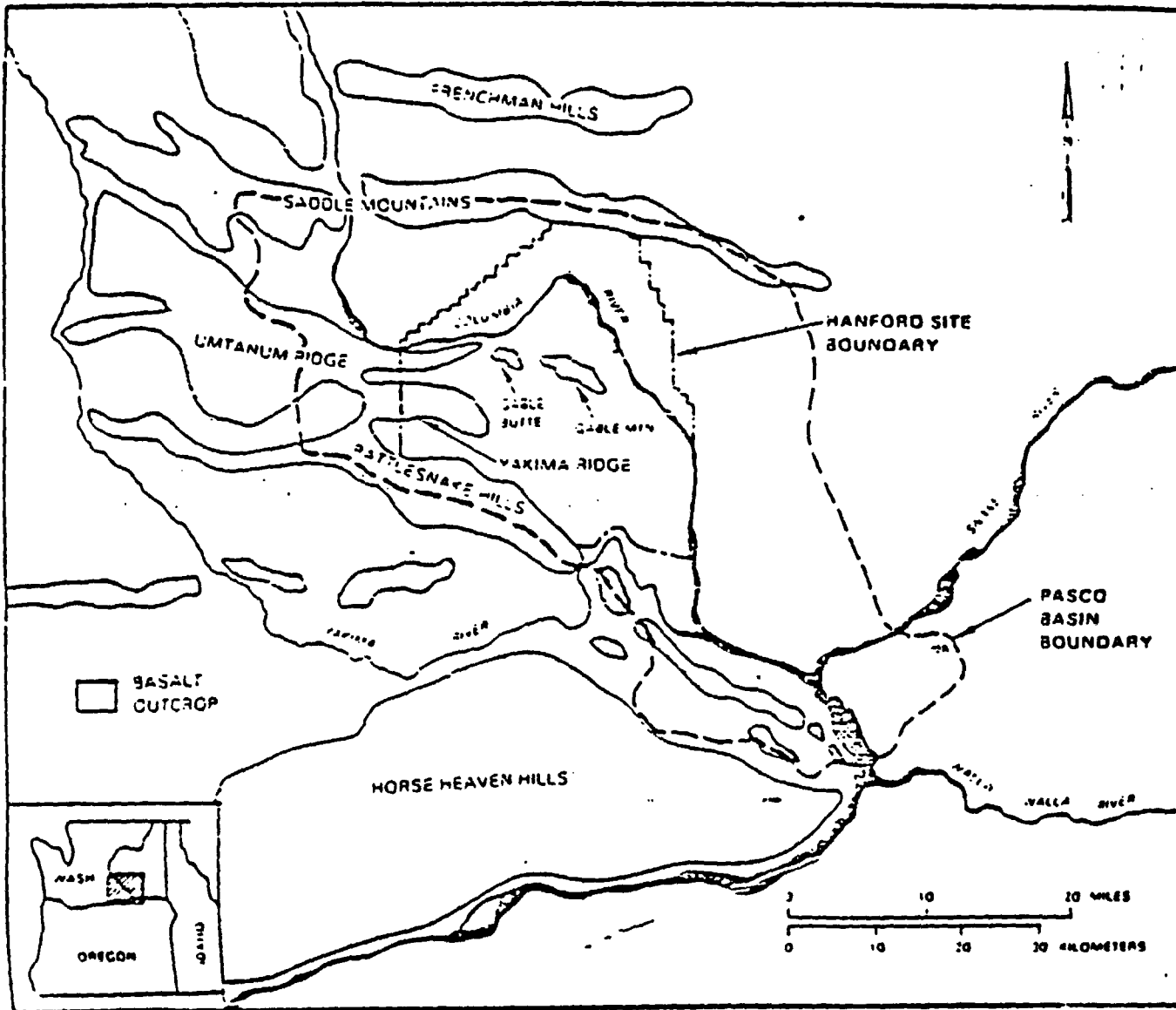


FIGURE A.1.3 Pasco Basin and Hanford Site.

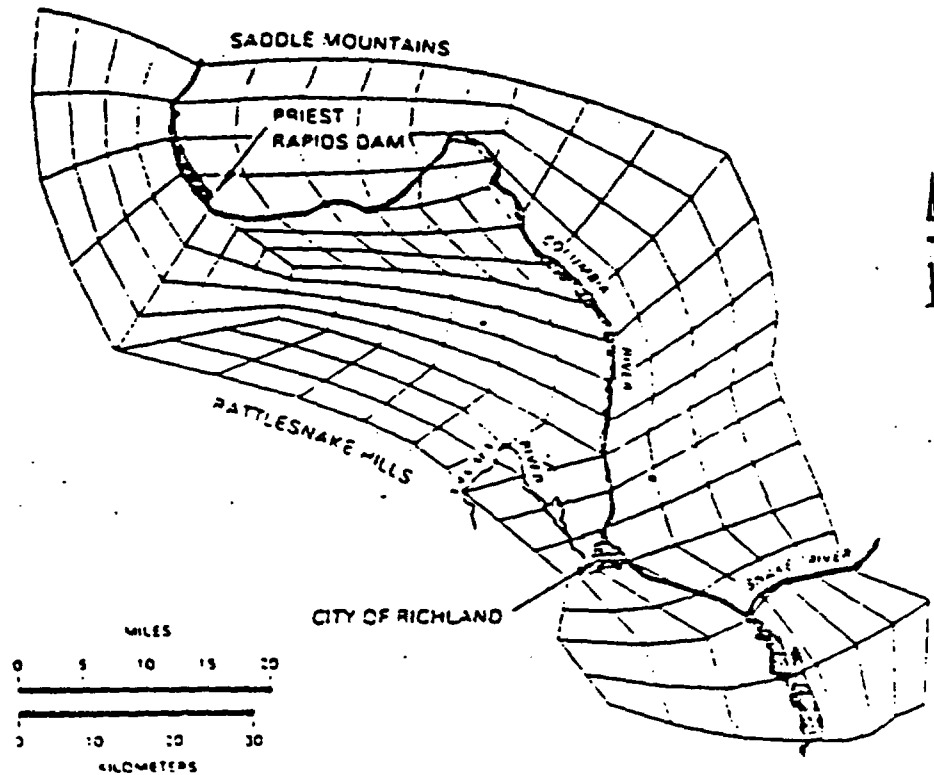


FIGURE A.1.4 Plan View of Three-Dimensional Finite Element Network for Pasco Basin.

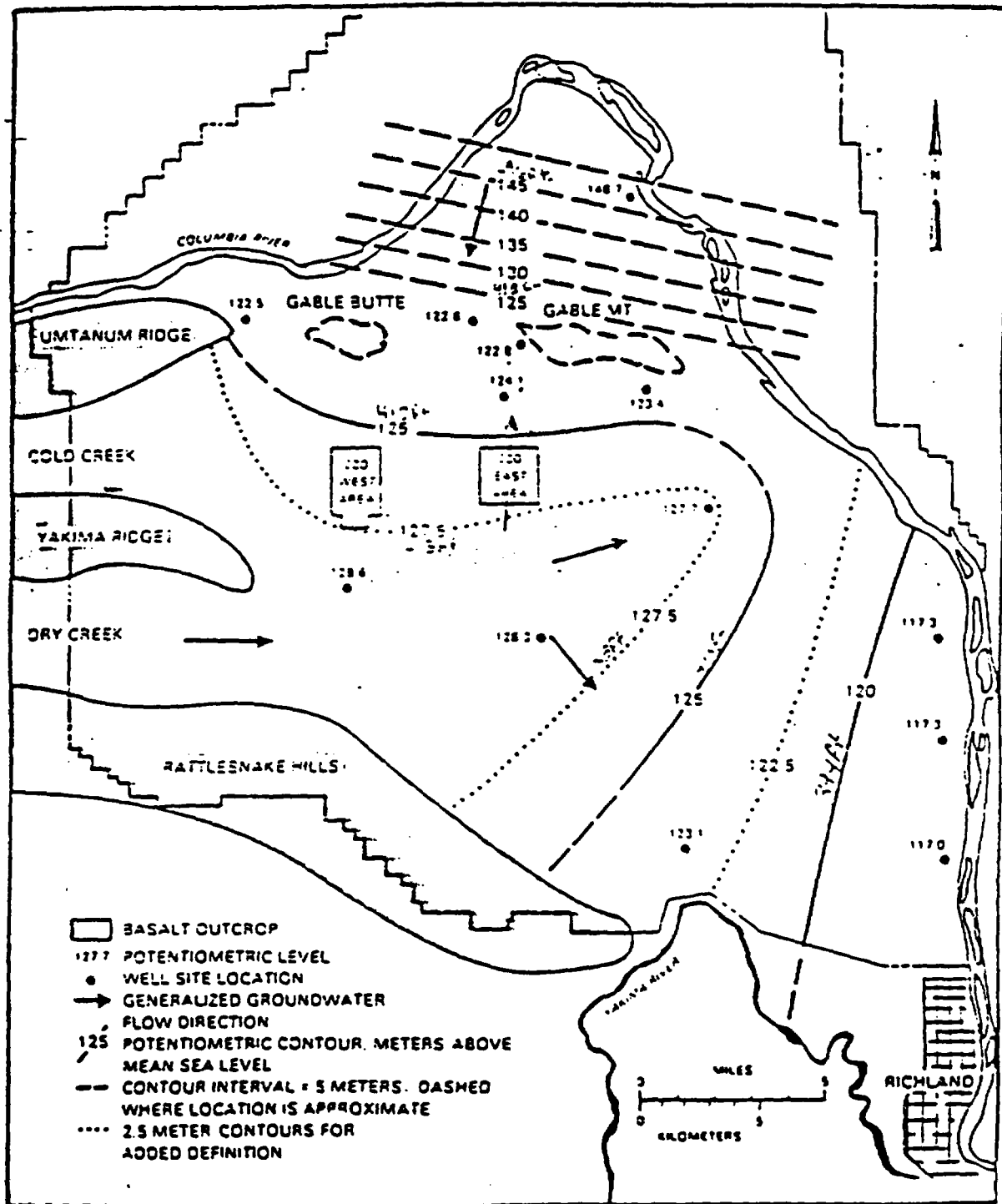


FIGURE A.1.5 Potentiometric Map for and Inferred Flow Directions of Groundwater within the Mabton Interbed beneath the Hanford Site.

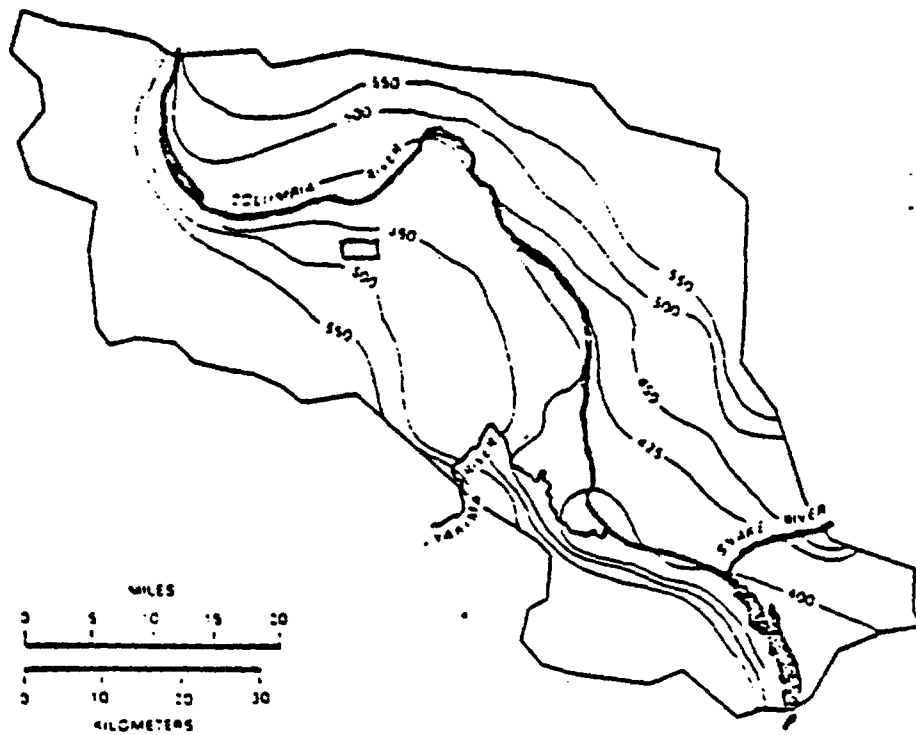


FIGURE A.1.6 Model-Calculated Heads, Top of Wanapum Basalt K_z/K_x from 10^{-2} to 10^{-3} .

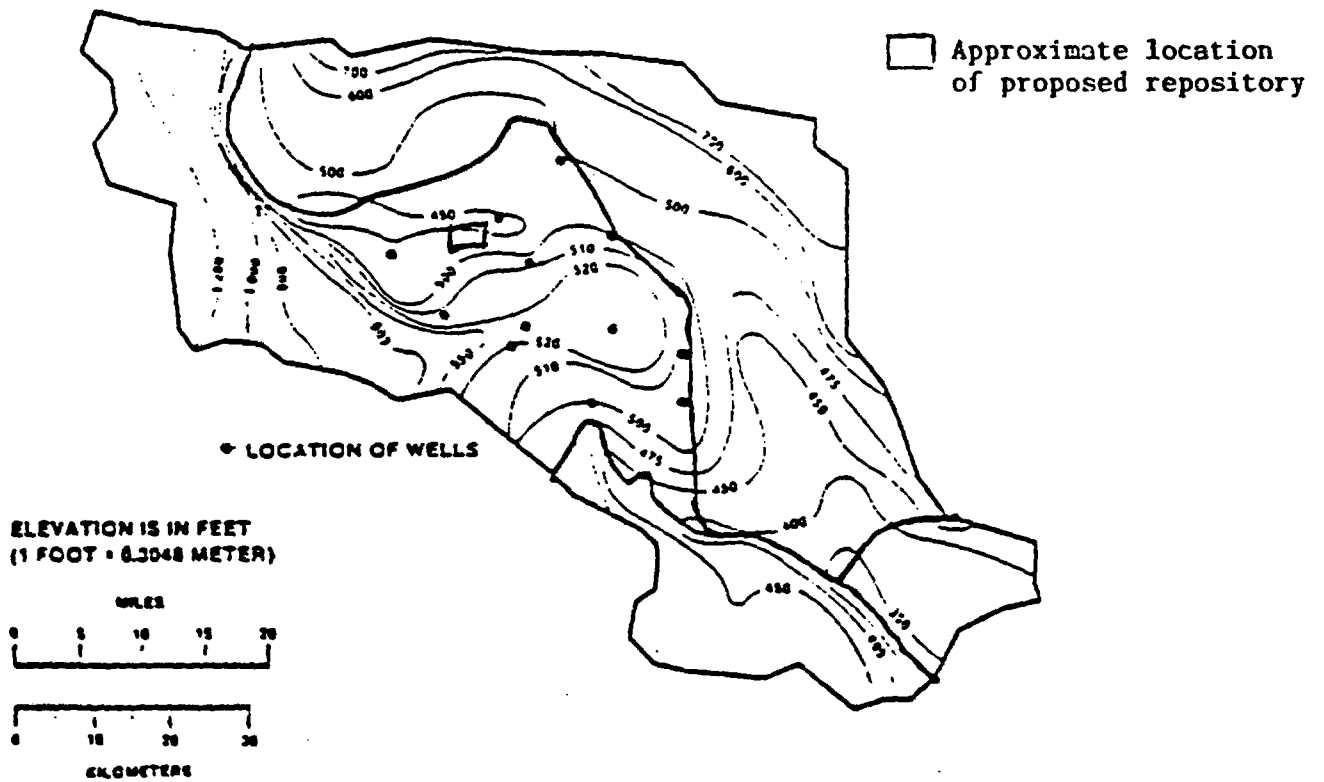


Figure A.1.7 Model-Calculated Heads, Top of Wanapum Basalt K_z/K_x from 10^{-4} to 10^{-5} .

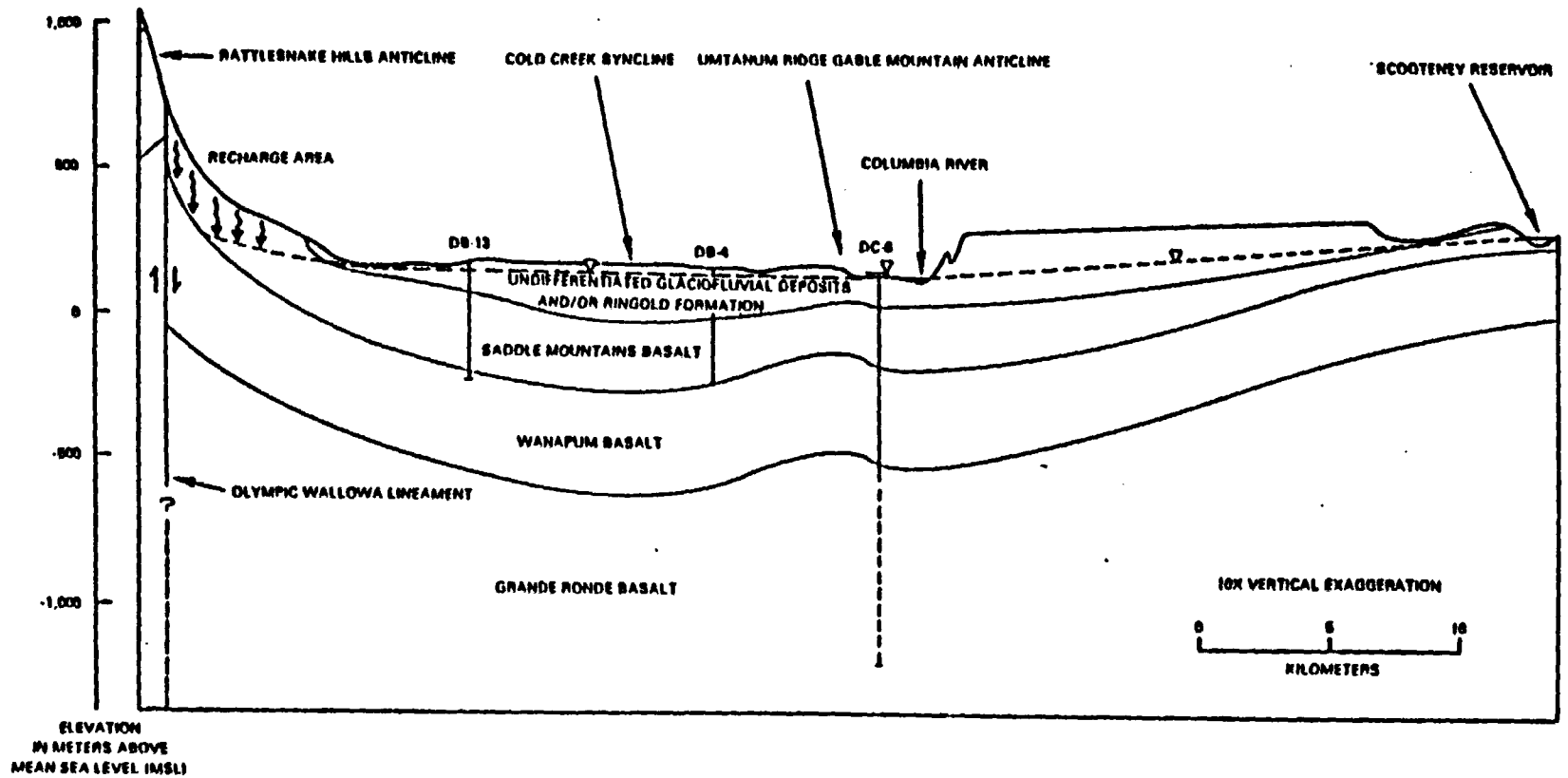


FIGURE A.2.1 Typical Vertical Cross Section of the Pasco Basin (adapted from cross section B-B' in Plate III-11 of Gephart and others, 1979).

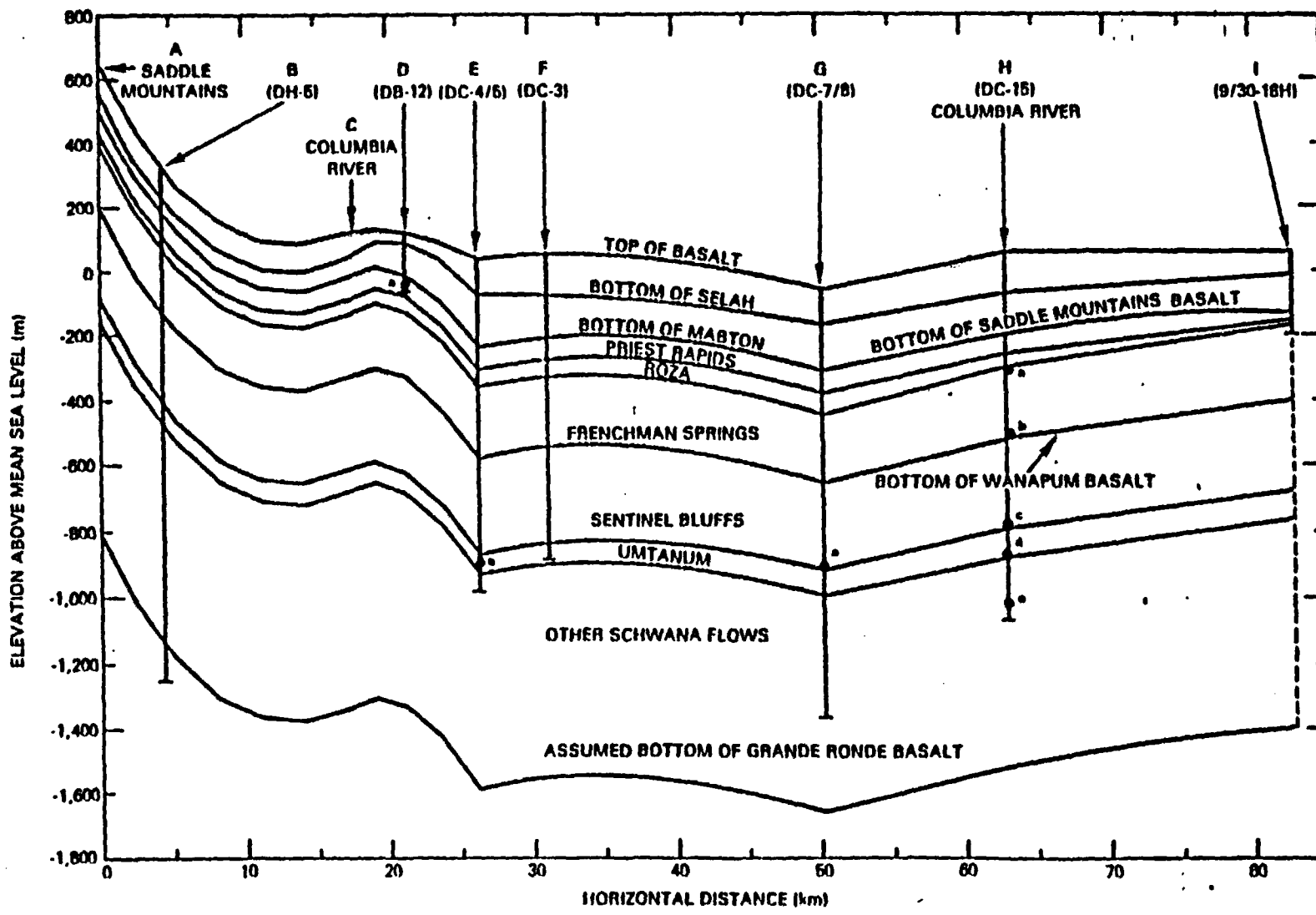


FIGURE A.2.2 Cross-Section View Showing Vertical Layering.

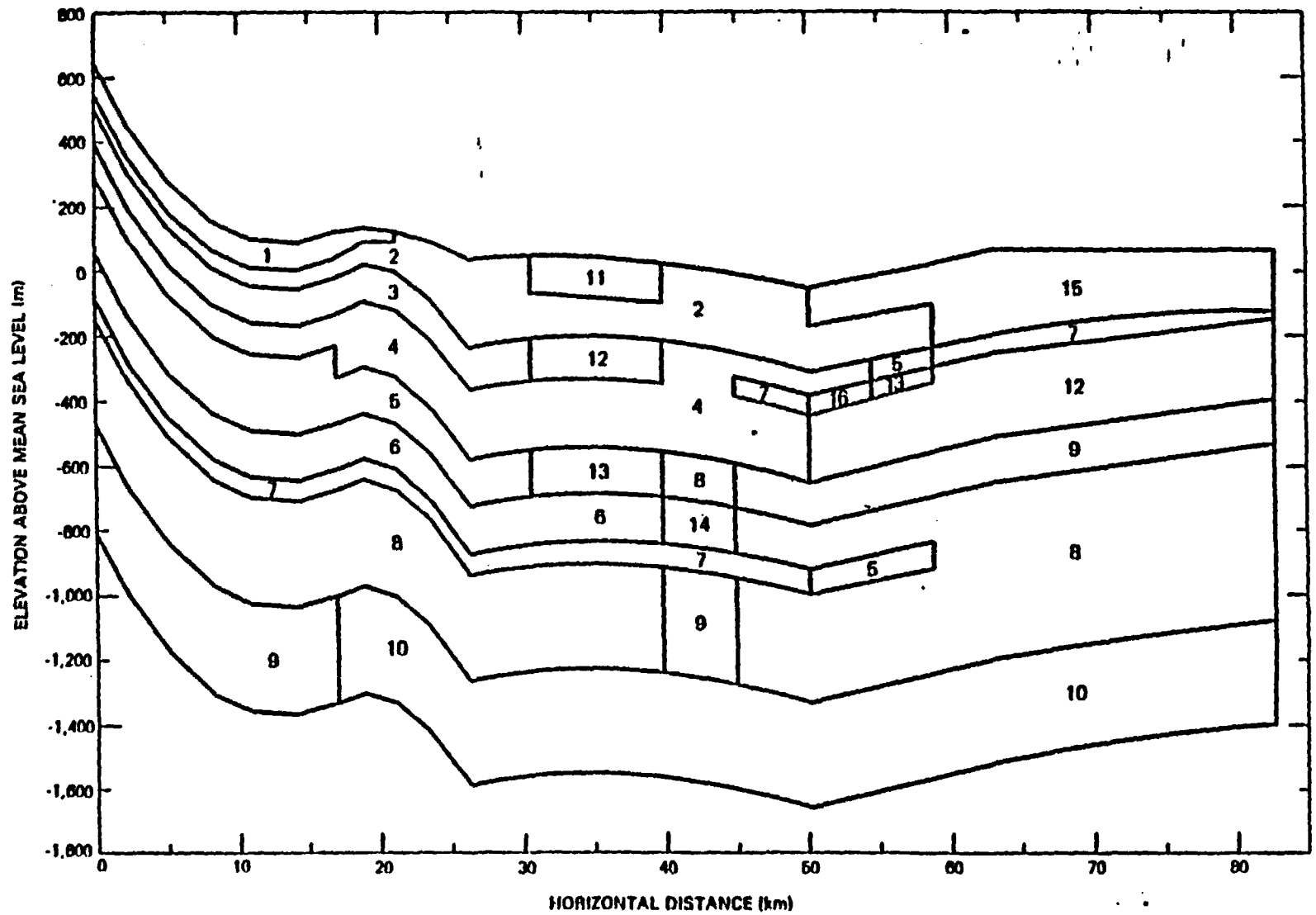


FIGURE A.2.3 Material Type Distribution.

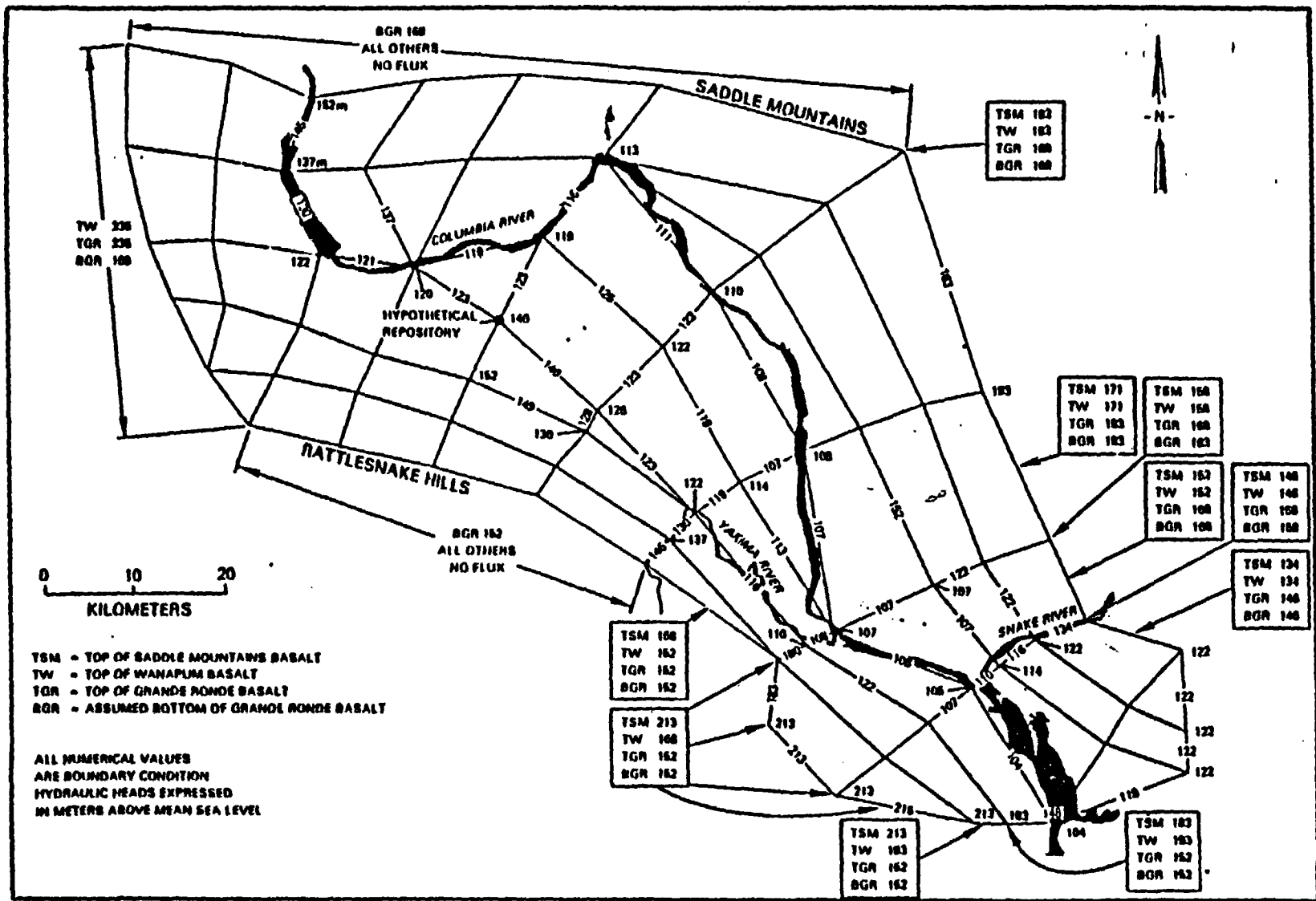


FIGURE A.2.4 Plan View of the Pasco Basin Three-Dimensional Finite-Element Network Showing Head Boundary.

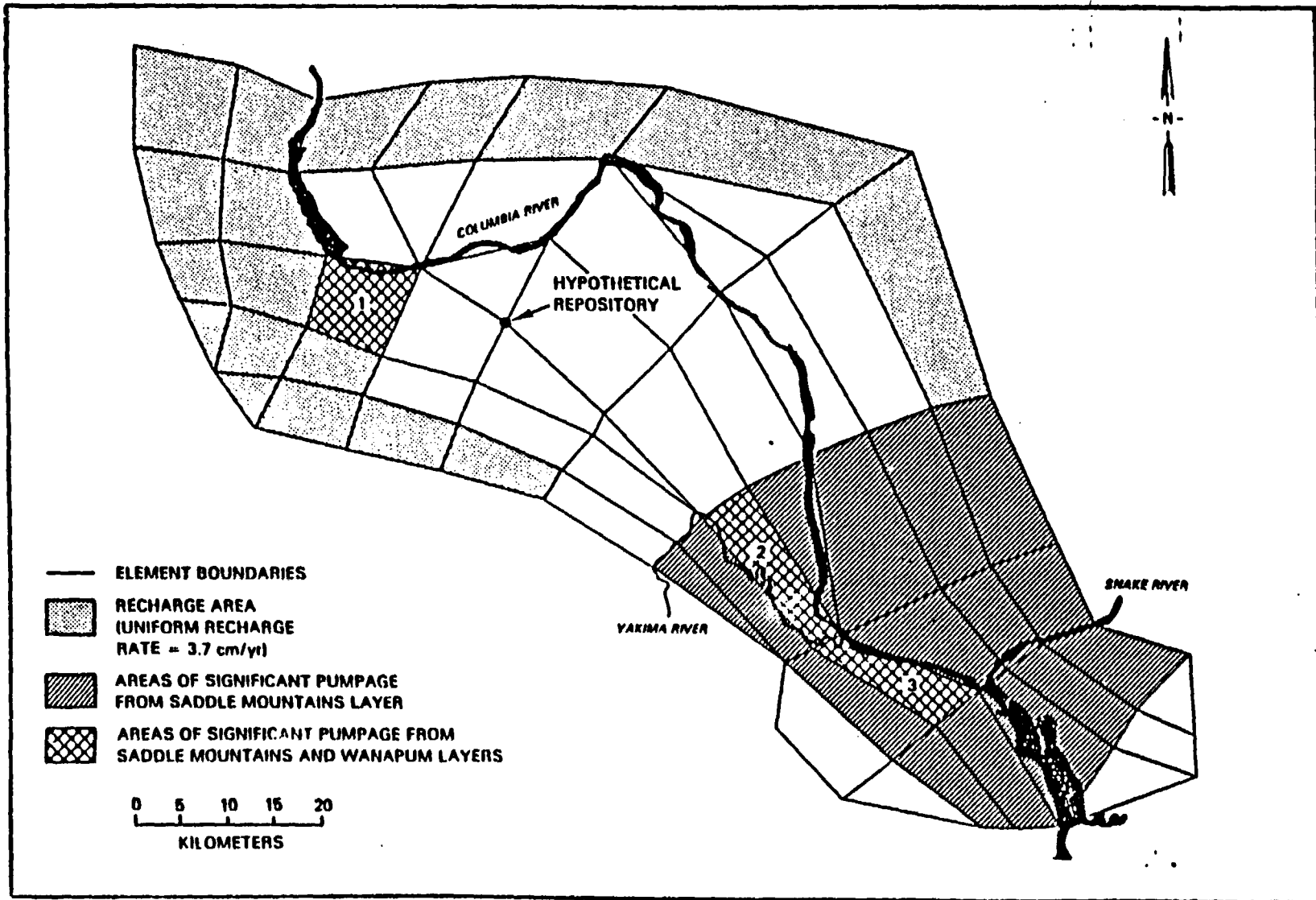


FIGURE A.2.5 Plan View of the Pasco Basin Three-Dimensional Finite-Element Network Showing Recharge and Pumping Areas and Major Rivers.

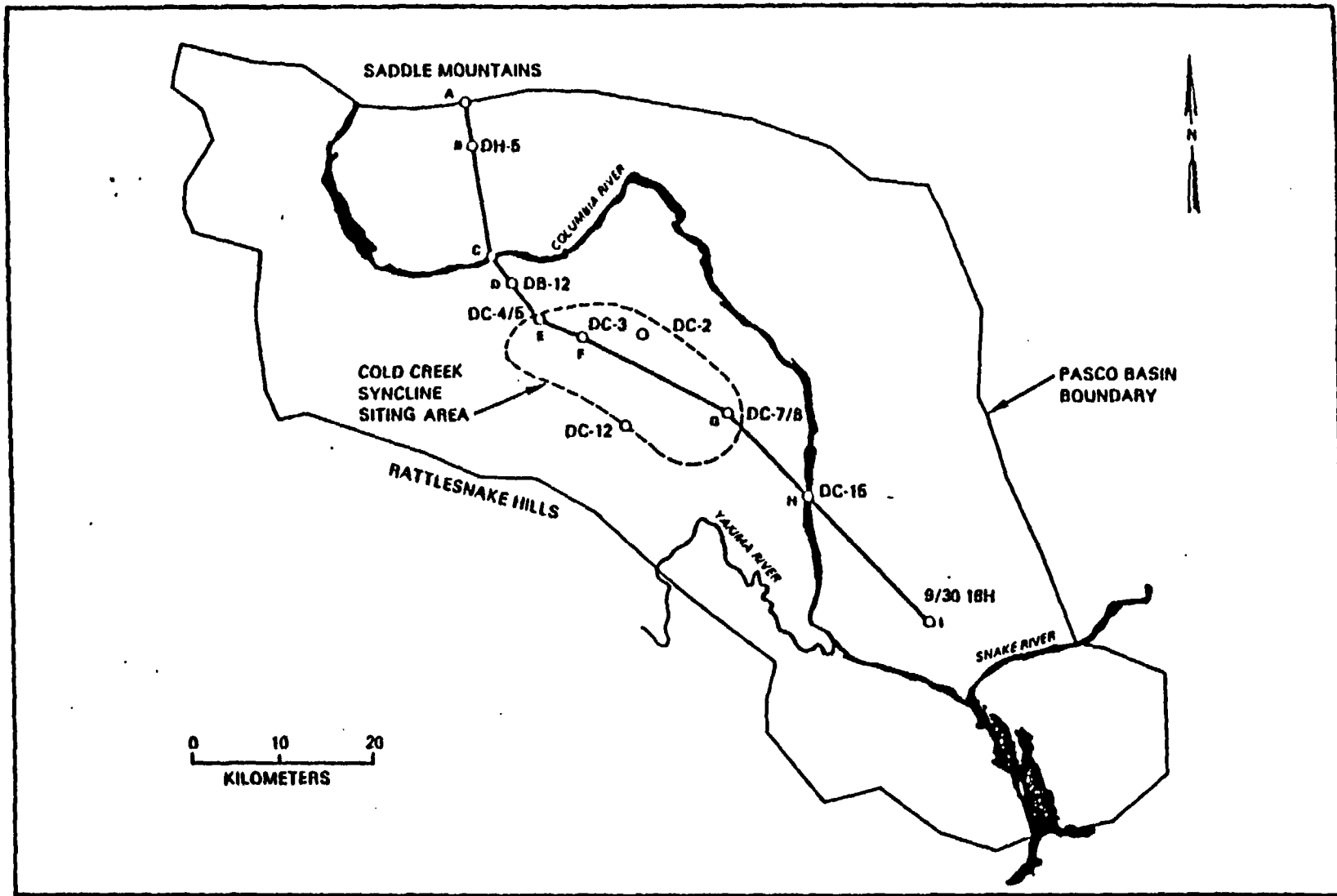


FIGURE A.2.6 Plan View of Two-Dimensional Cross-Section Model.

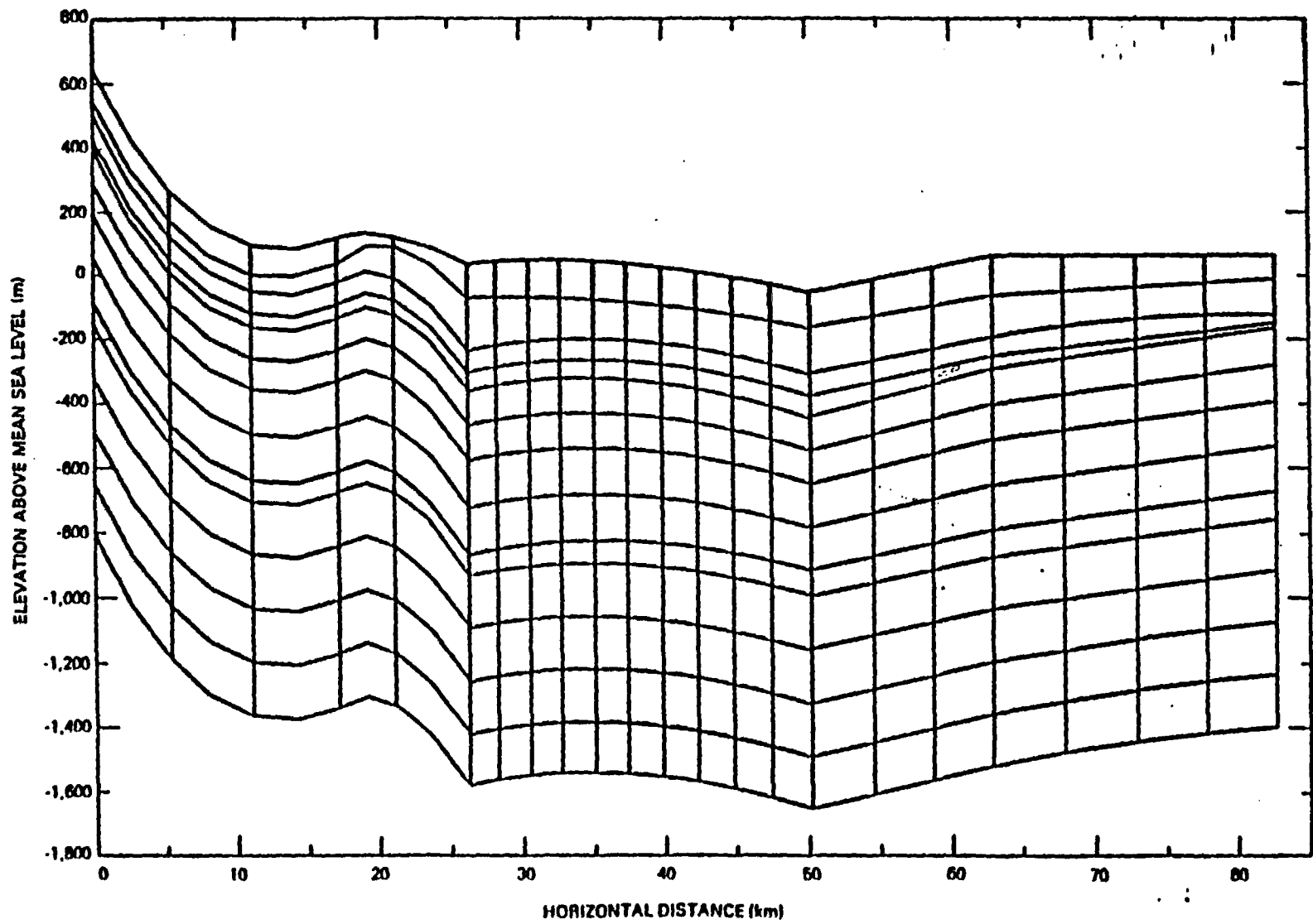


FIGURE A.2.7 Cross-Section Model-Finite-Element Network.

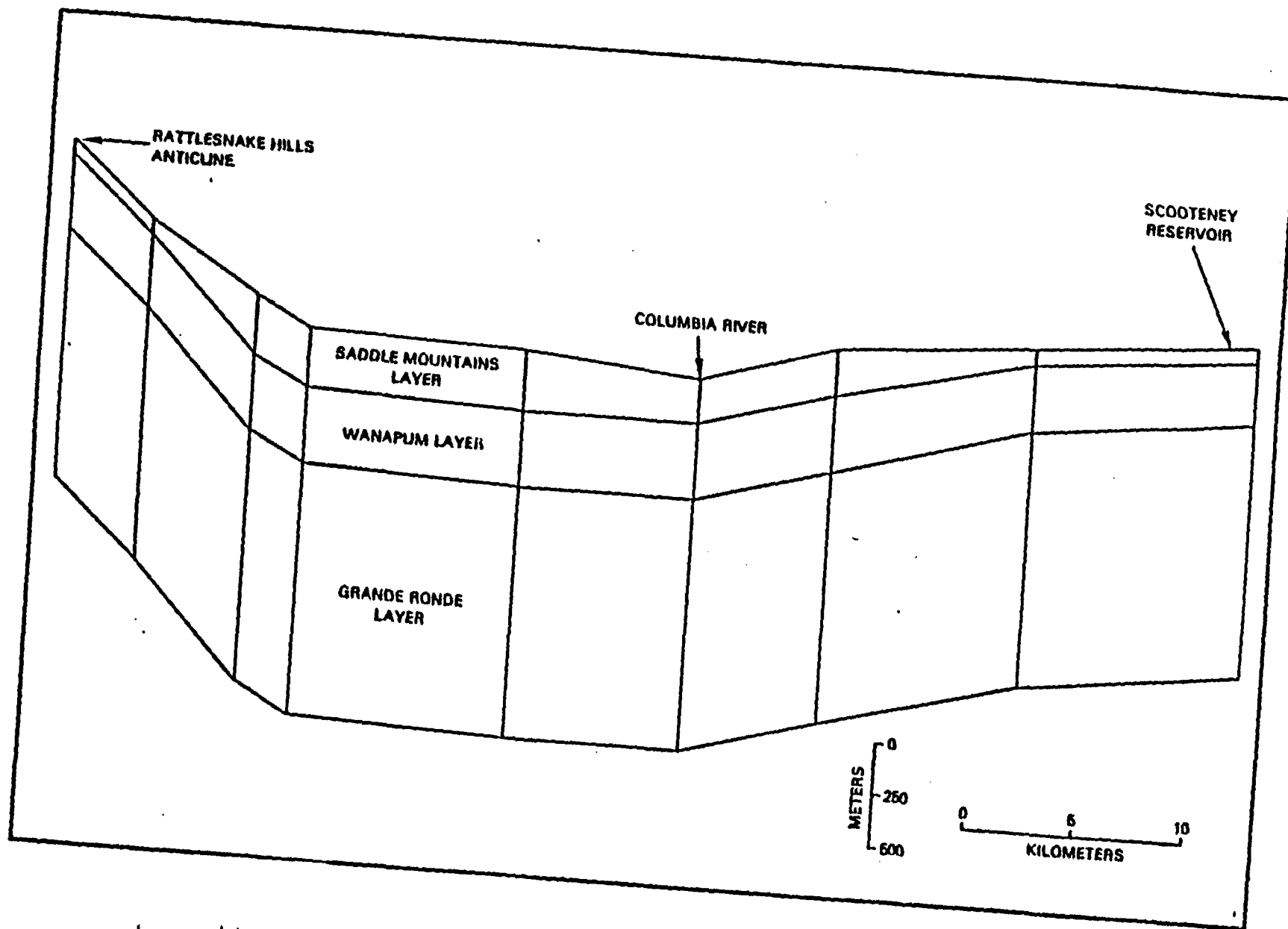


FIGURE A.2.8 Typical Vertical Cross Section of the Pasco Basin Three-Dimensional Finite-Element Network (corresponds to Figure 4 2.1).

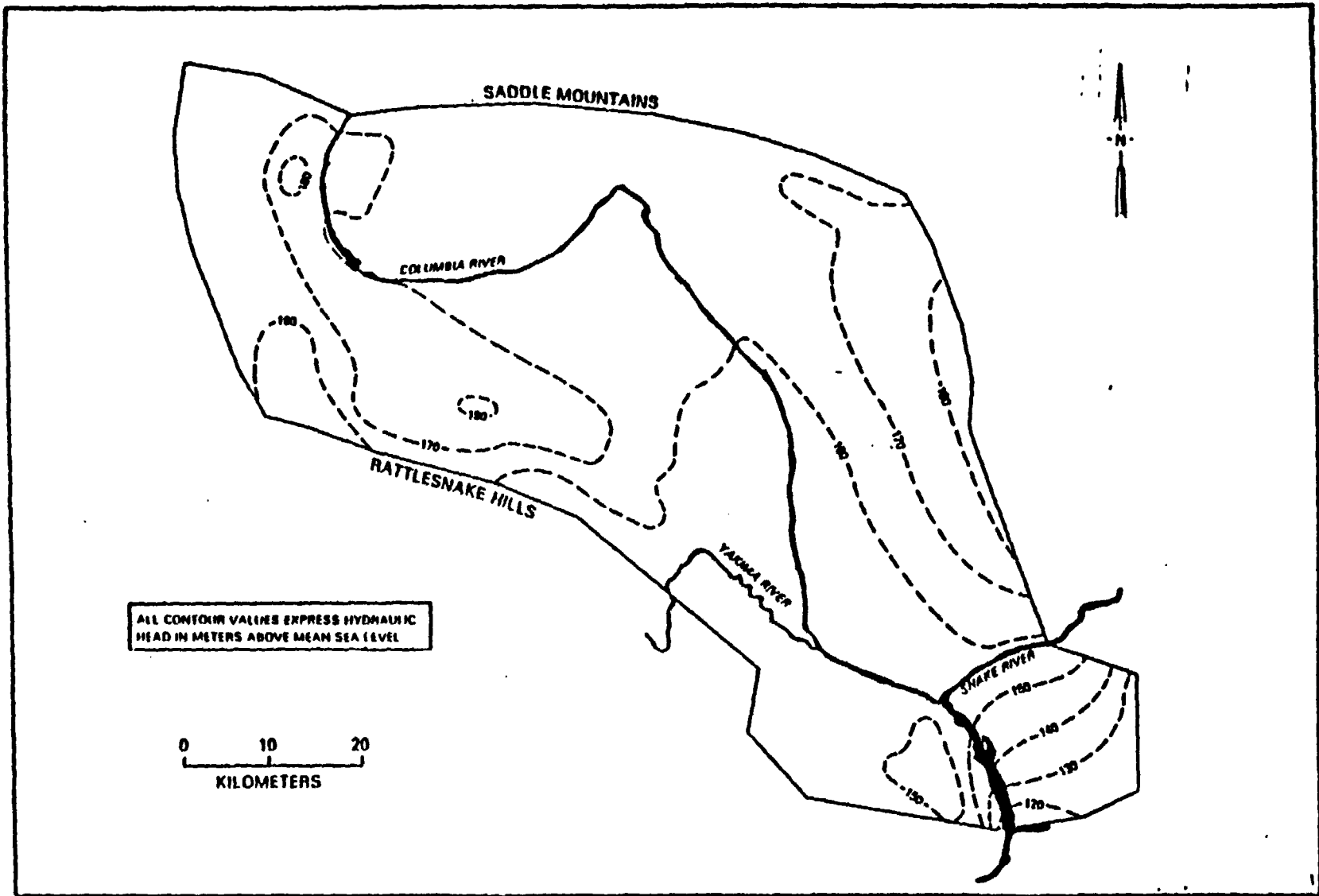


FIGURE A.2.9 Hydraulic Head Contours at Bottom of Grande Ronde Basalts--Pumpage Case.

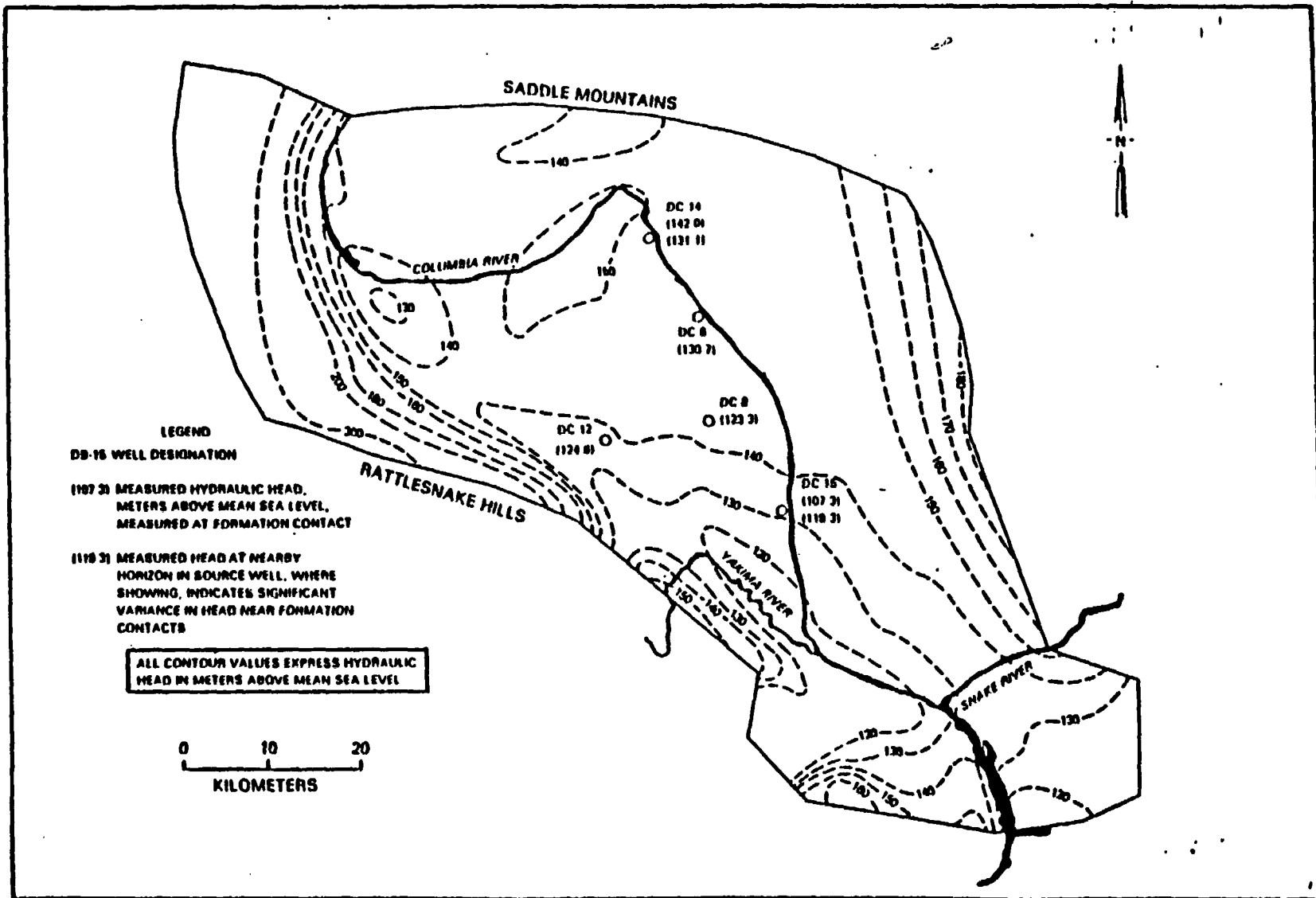


FIGURE A.2.10 Hydraulic Head Contours of Top of Grande Ronde Basalts--Pumpage Case.

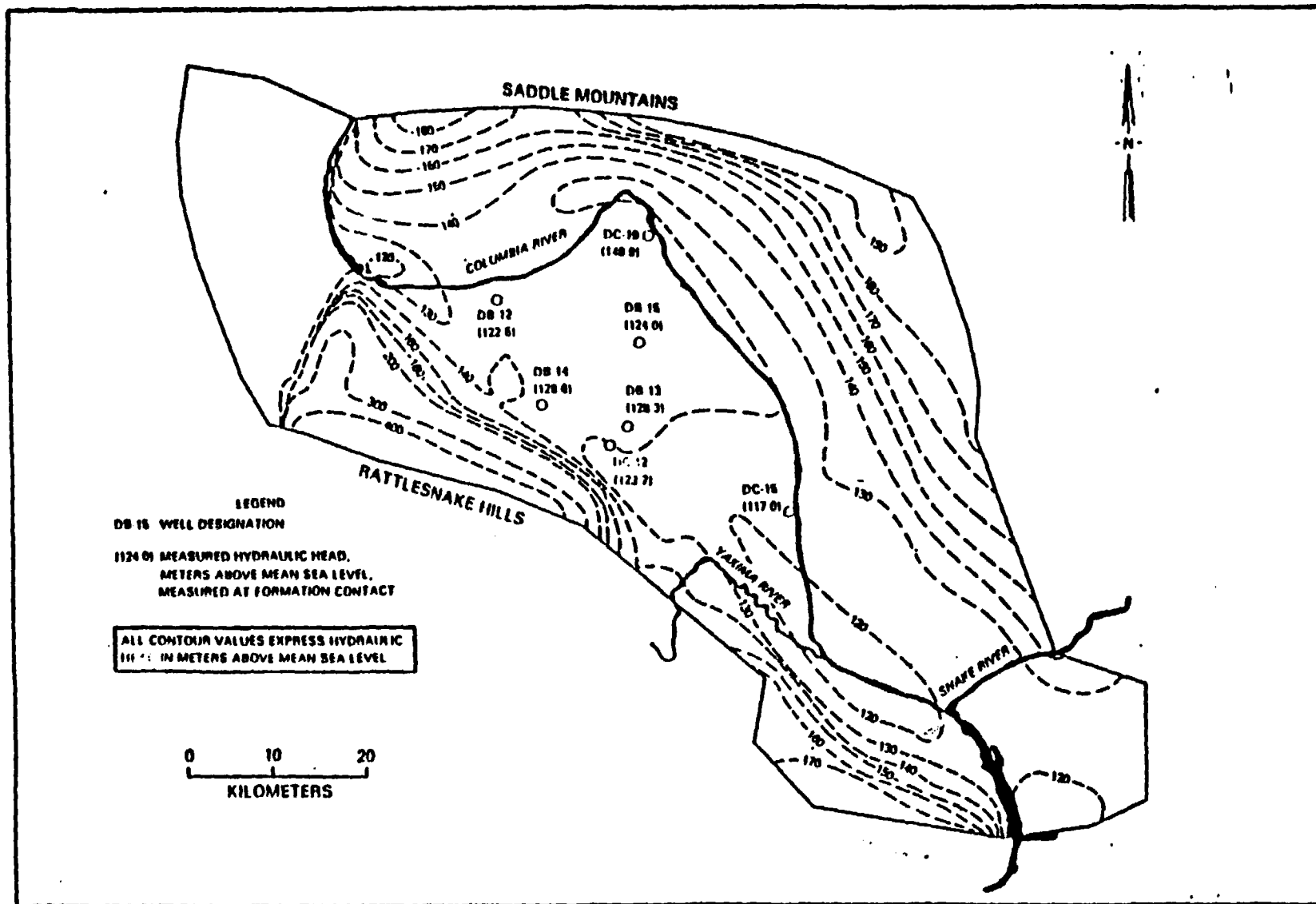


FIGURE A.2.11 Hydraulic Head Contours at Top of Wanapum Basalts--Pumpage Case.

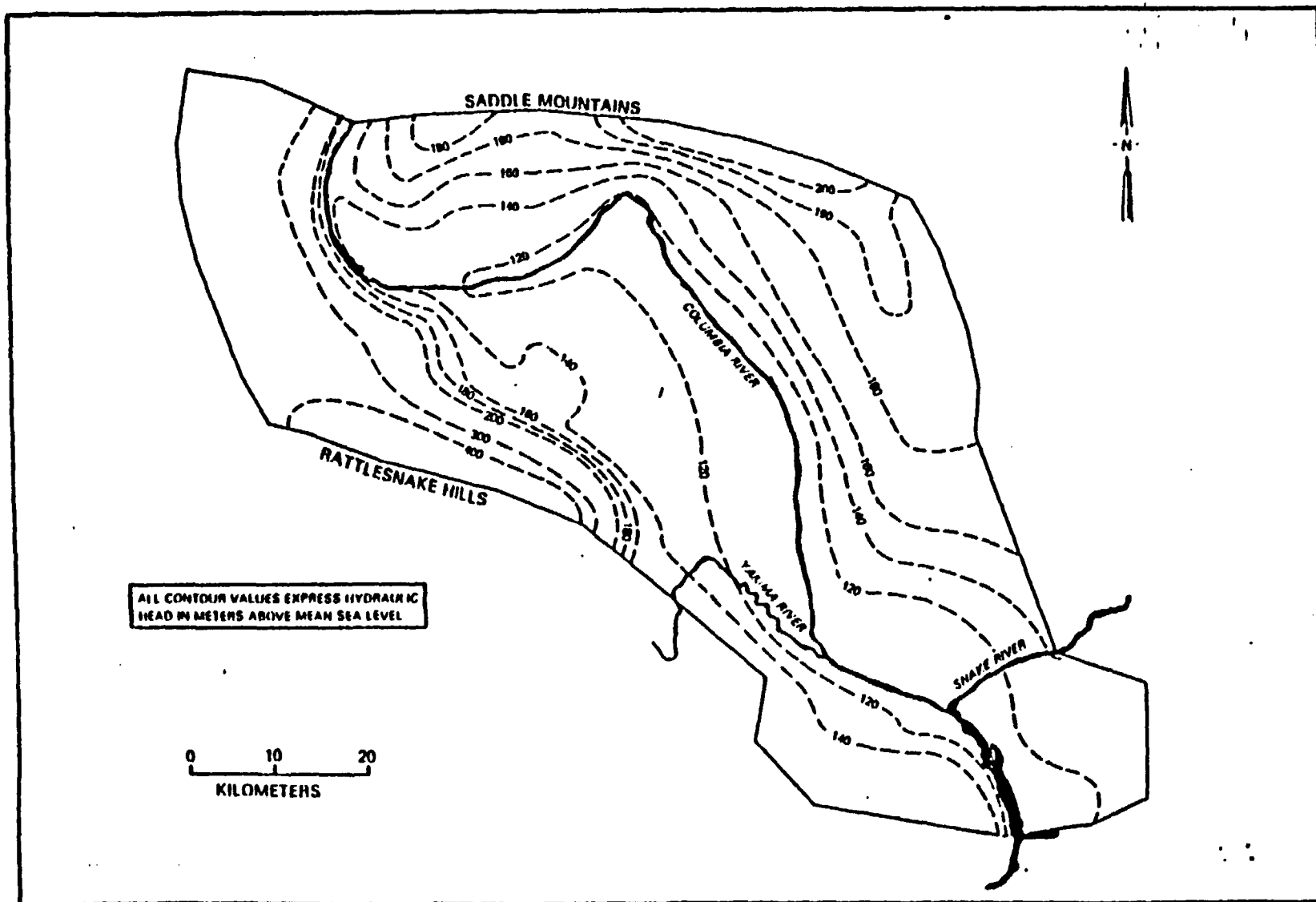


FIGURE A.2.12 Hydraulic Head Contours at Top of Basalt Sequence--Pumpage Case.

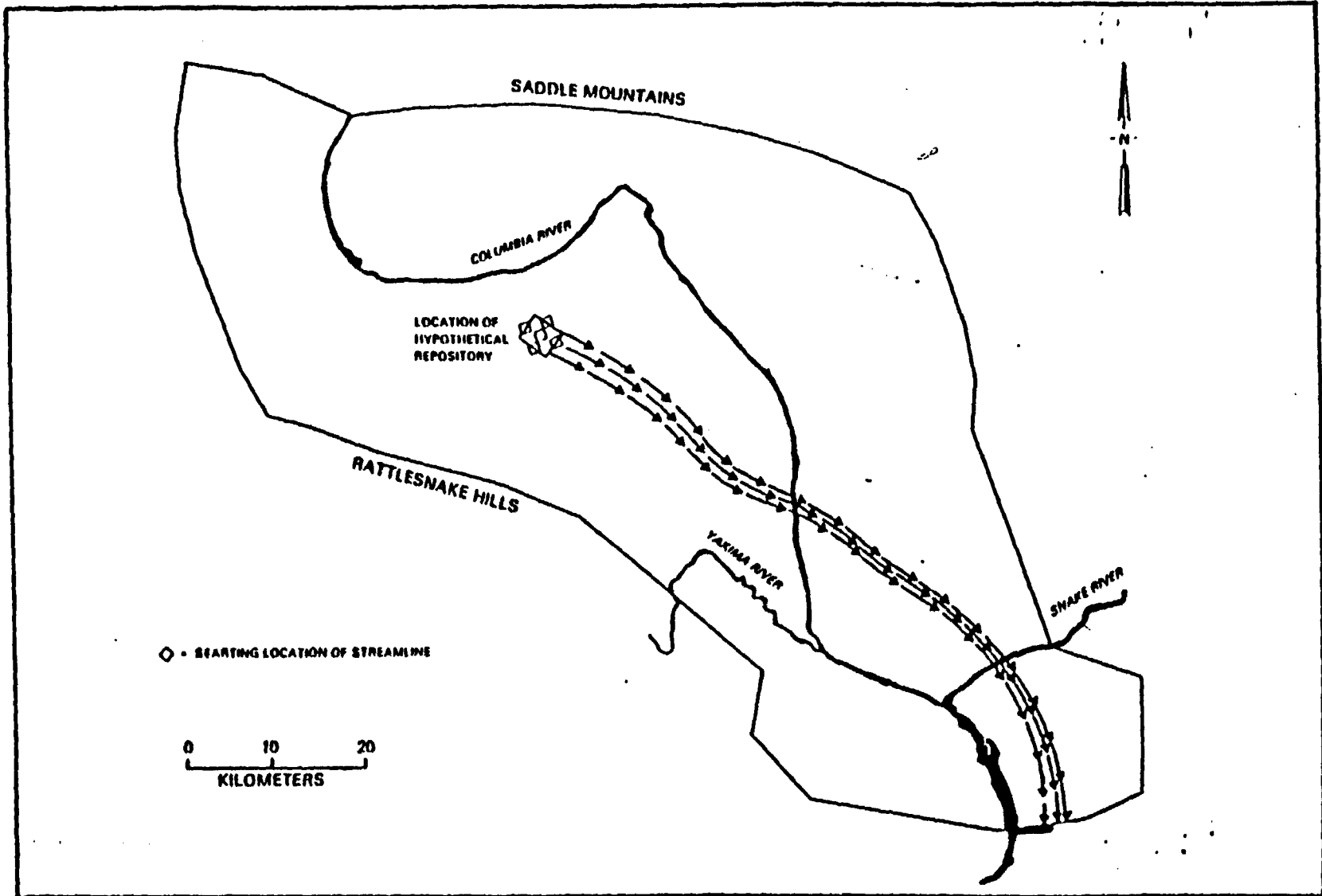


FIGURE A.2.13 X-Y Projection of Streamlines from Hypothetical Repository to Boundary.

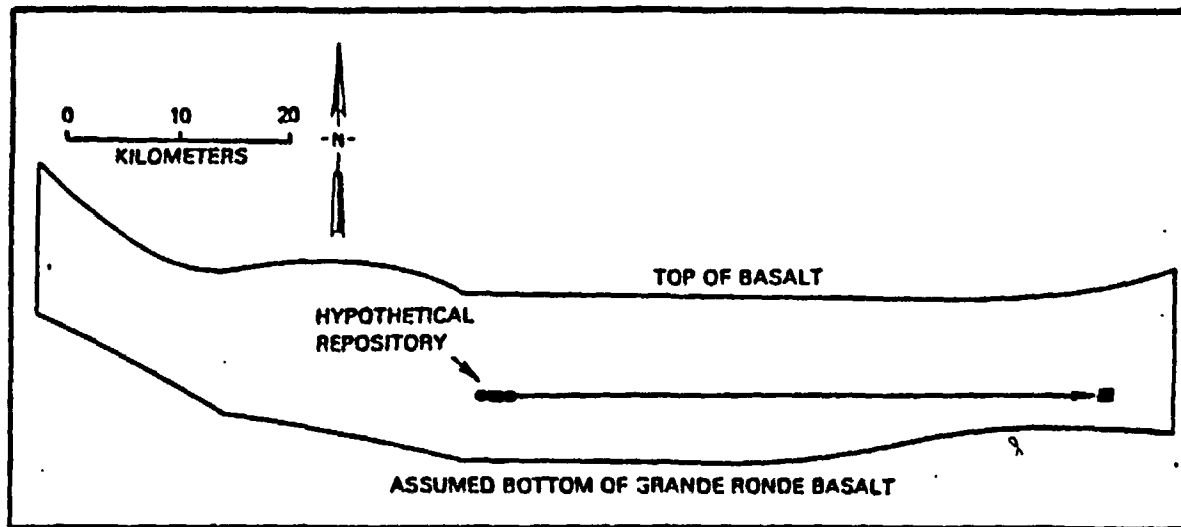


FIGURE A.2.14 X-Z Projection of Model-Calculated Streamline.

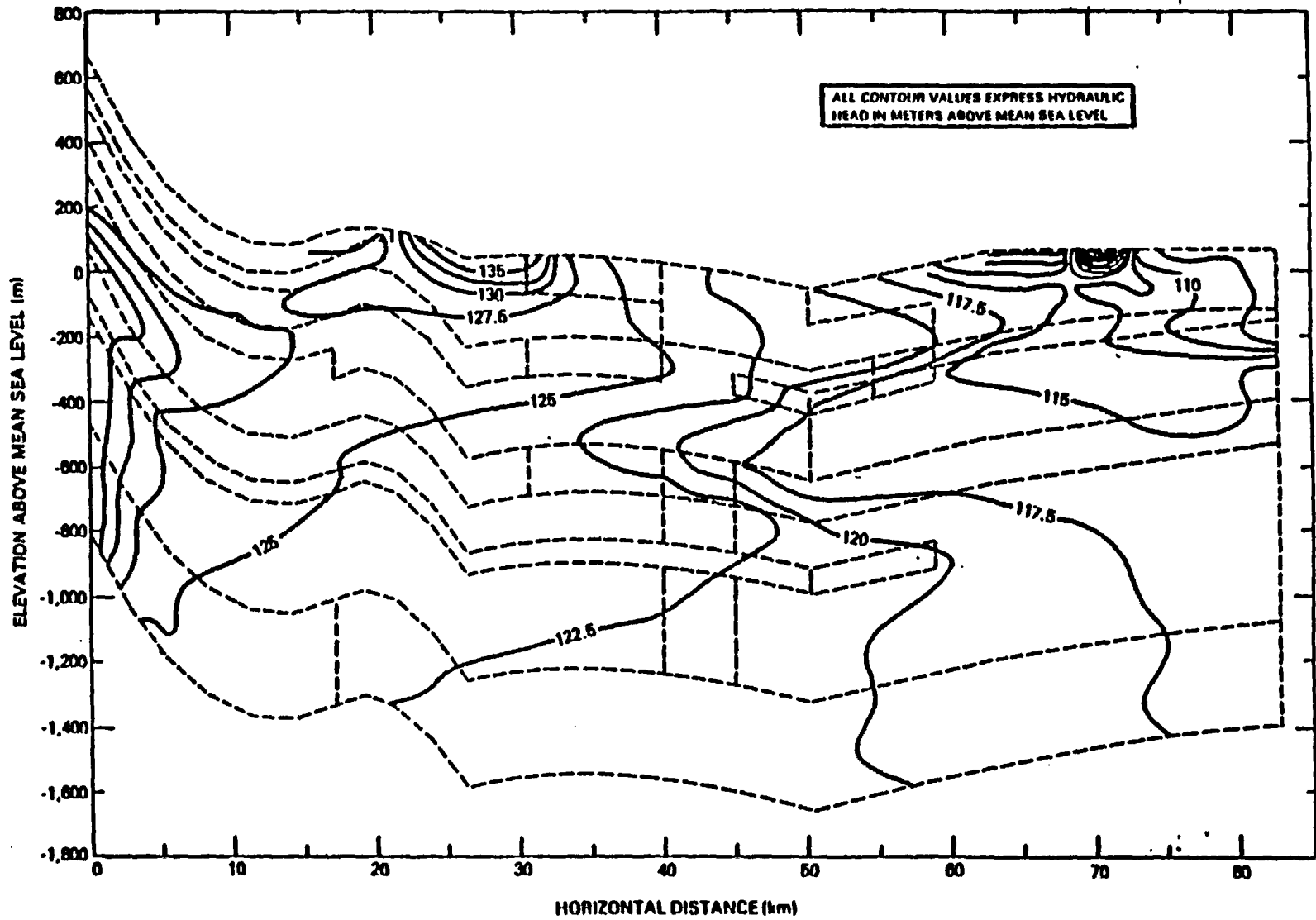


FIGURE A.2.15 Head Contours--Base Case.

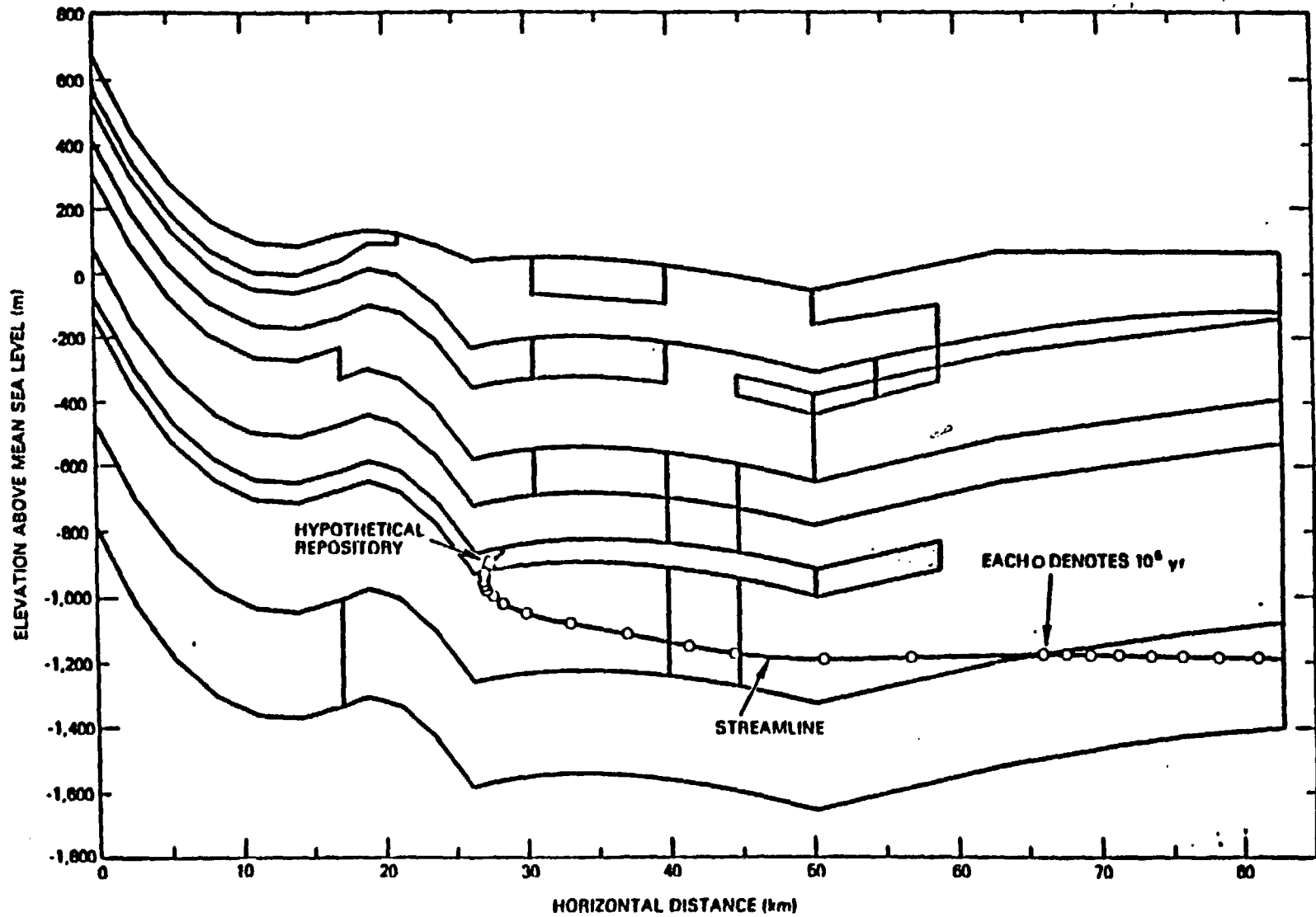


FIGURE A.2.16 Streamline from Hypothetical Repository--Base Case.

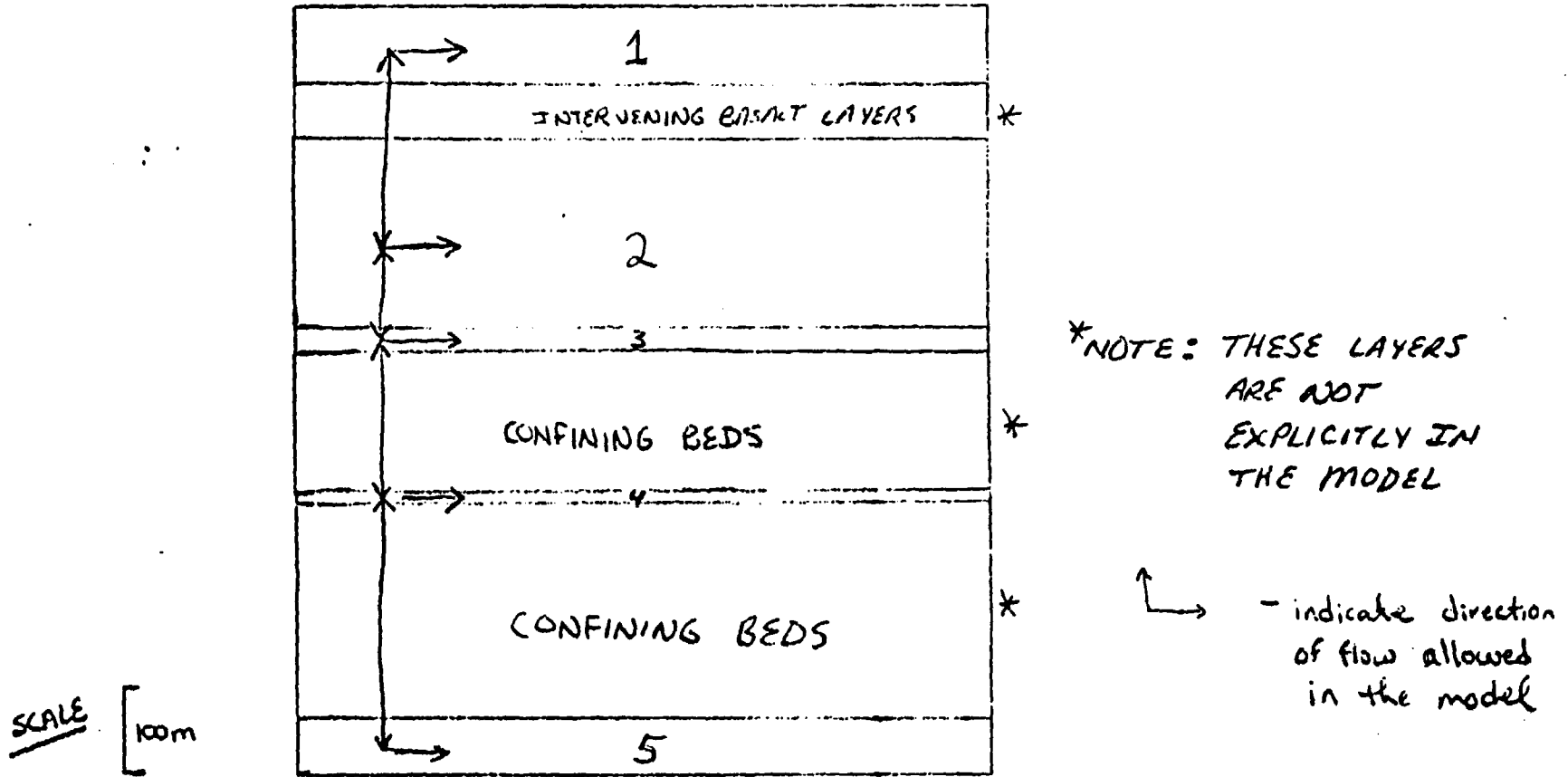


FIGURE A.3.1 Layering Scheme for LATA-RHO-04-02-A Model

22-141 50 SHEETS
22-142 100 SHEETS
22-144 200 SHEETS

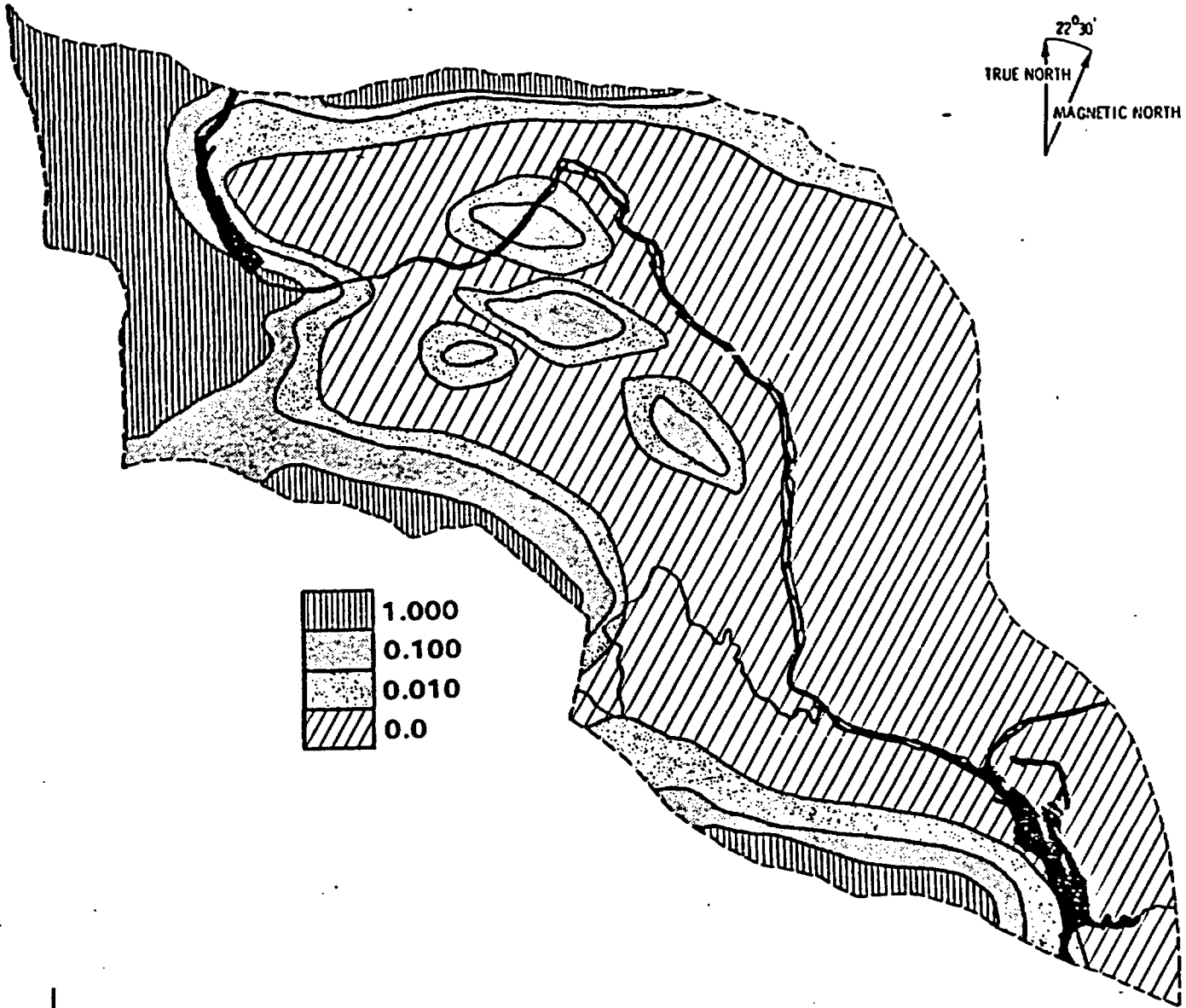
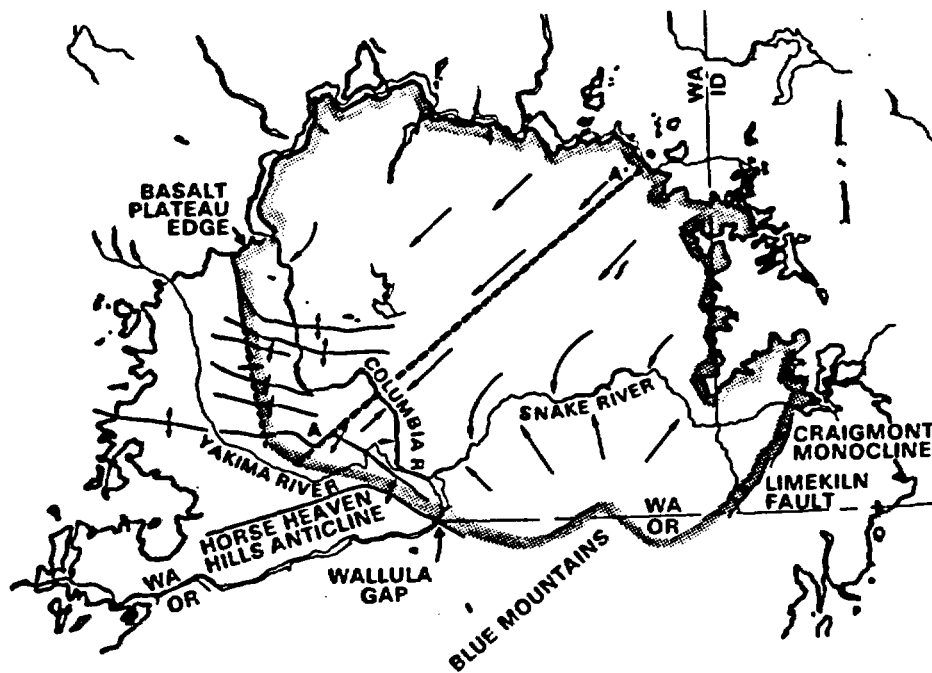


Figure A.4.1 Assumed Regions of Equal Deformation Associated with Structures within the Local Model Area (Scale is from 0 to 1 with 1 representing areas of greatest deformation). (from Dove and others, 1982)



ANTICLINE 
 BASALT EDGE 
 GROUNDWATER FLOW DIRECTION 
 MODEL BOUNDARY 

SCALE

 0 50
 km

Figure A.4.2 Regional Model Boundary (from Dove and others, 1982)

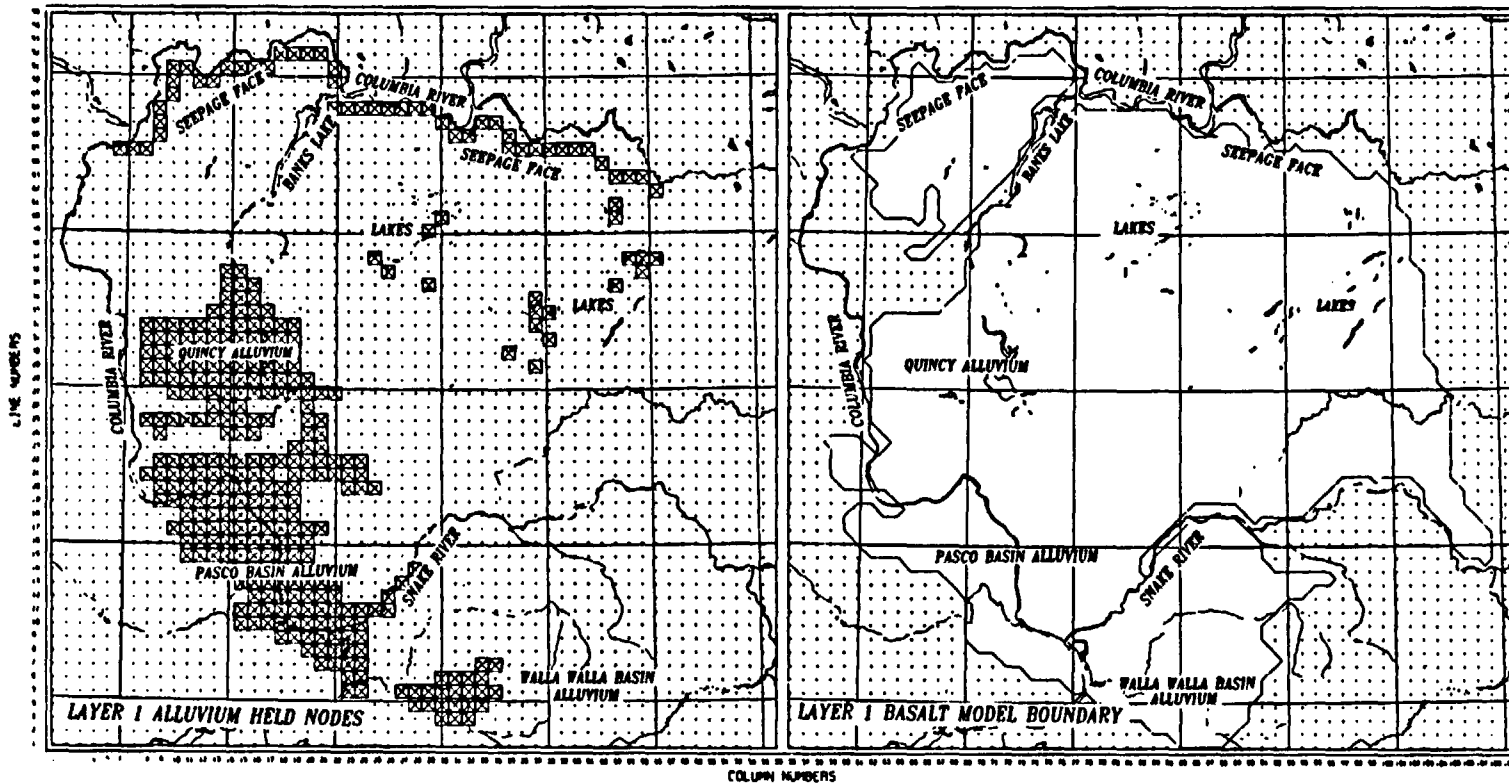


Figure A.4.3 Model Boundaries and Constant Hydraulic Heads for the Saddle Mountains/Wanapum Basalts (Layer 1) (from Dove and others, 1982)

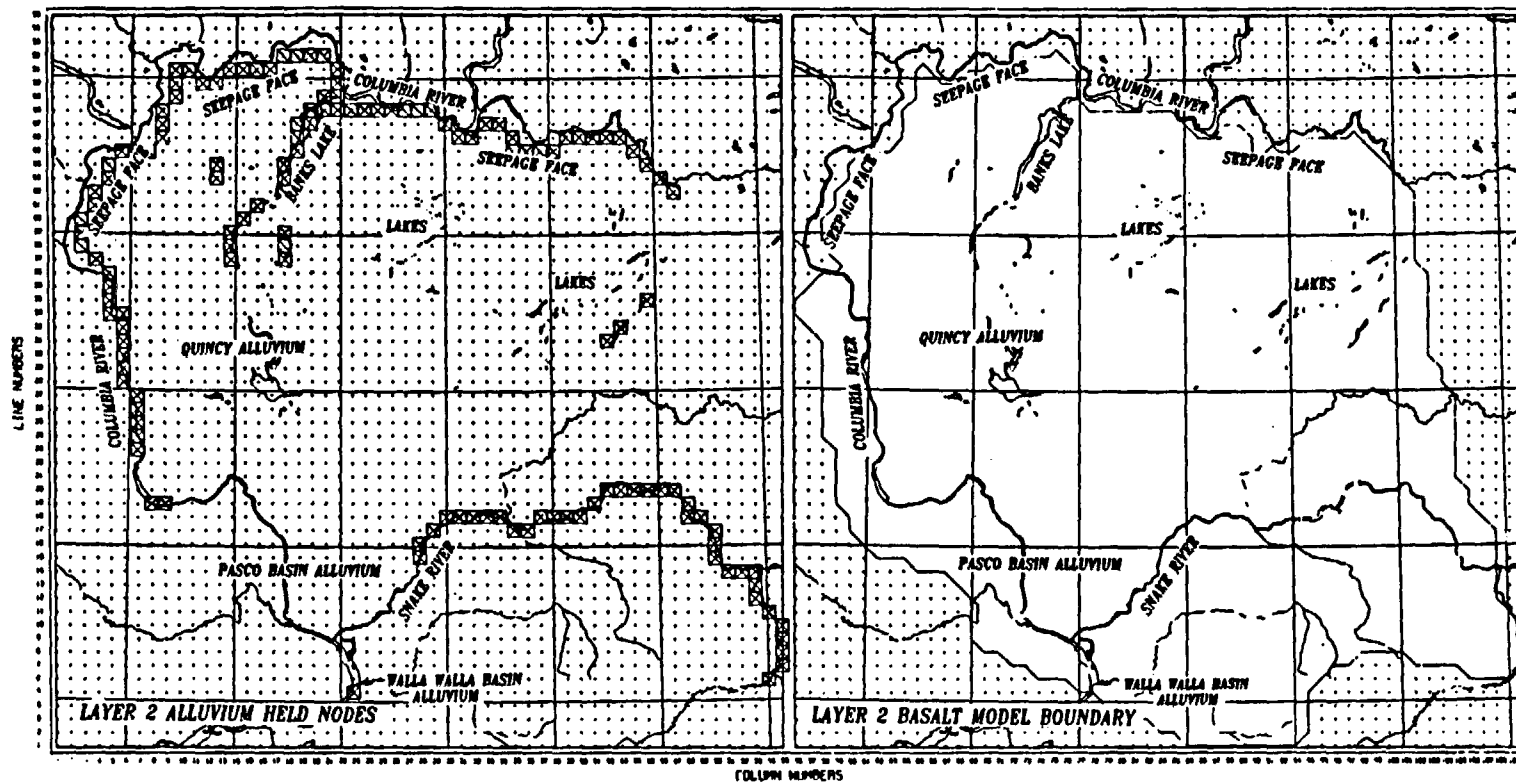


Figure A.4.4 Model Boundaries and Constant Hydraulic Heads for the Grande Ronde Basalts (Layer 2) (from Dove and others, 1982)

22-141 50 SHEETS
22-142 100 SHEETS
22-144 200 SHEETS

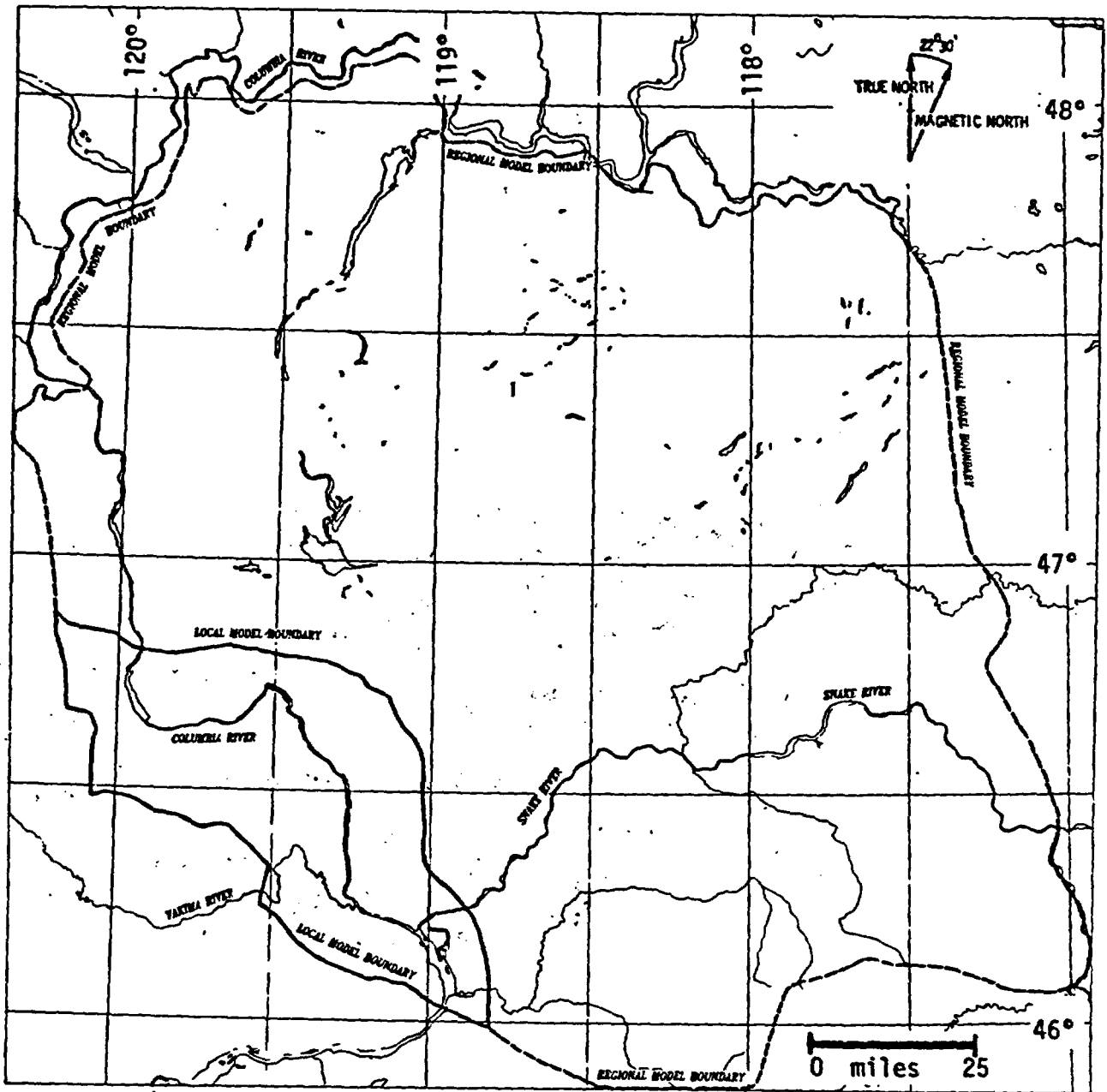


Figure A.4.5 Regional and Local (Pasco Basin) Model Boundaries
(from Dove and others, 1982)

22-141 50 SHEETS
22-142 100 SHEETS
22-144 200 SHEETS

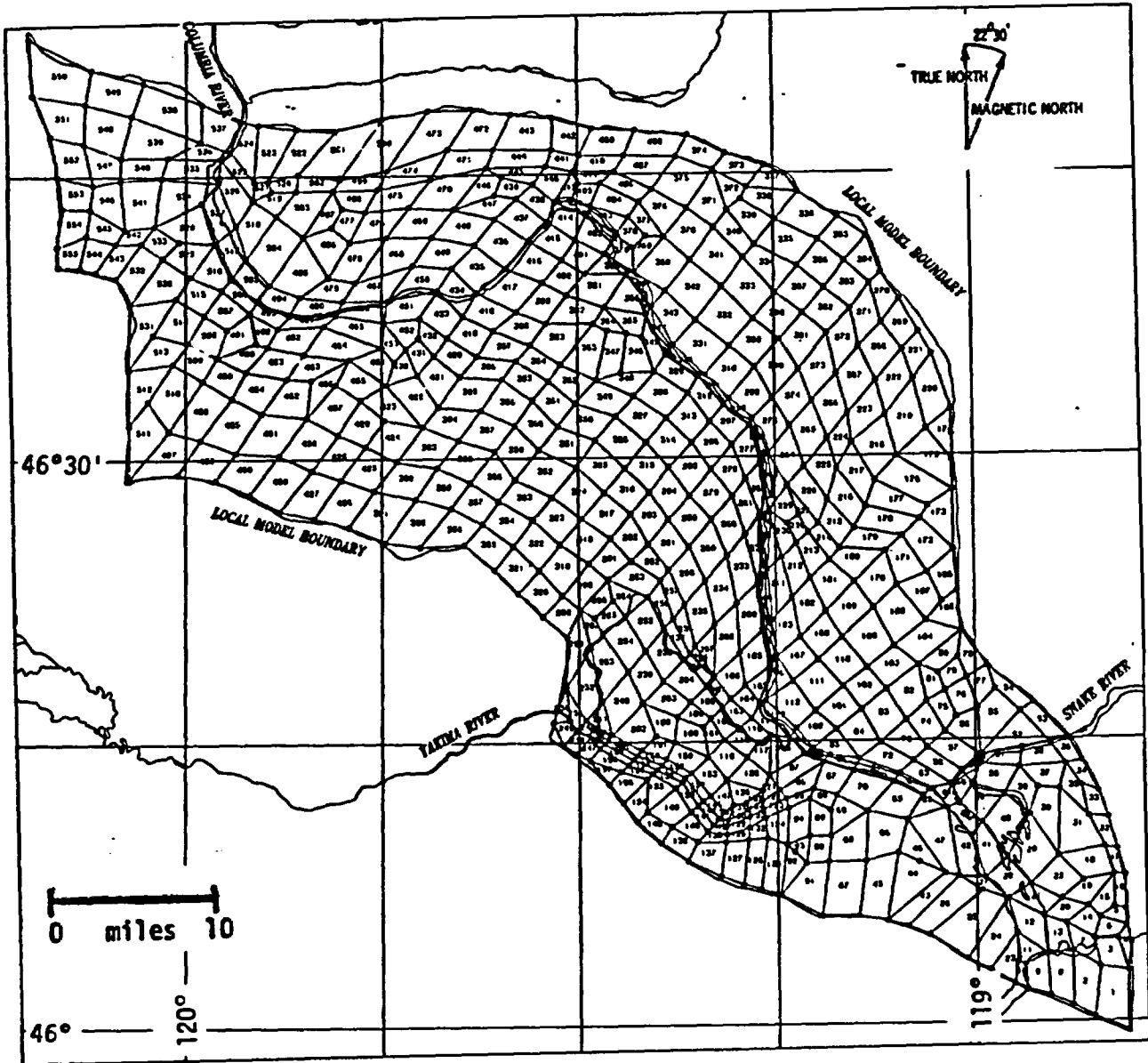


Figure A.4.6 Finite-Element Grid used in the Pasco Basin Model
(from Dove and others, 1982)

22-141 50 SHEETS
22-142 100 SHEETS
22-144 200 SHEETS

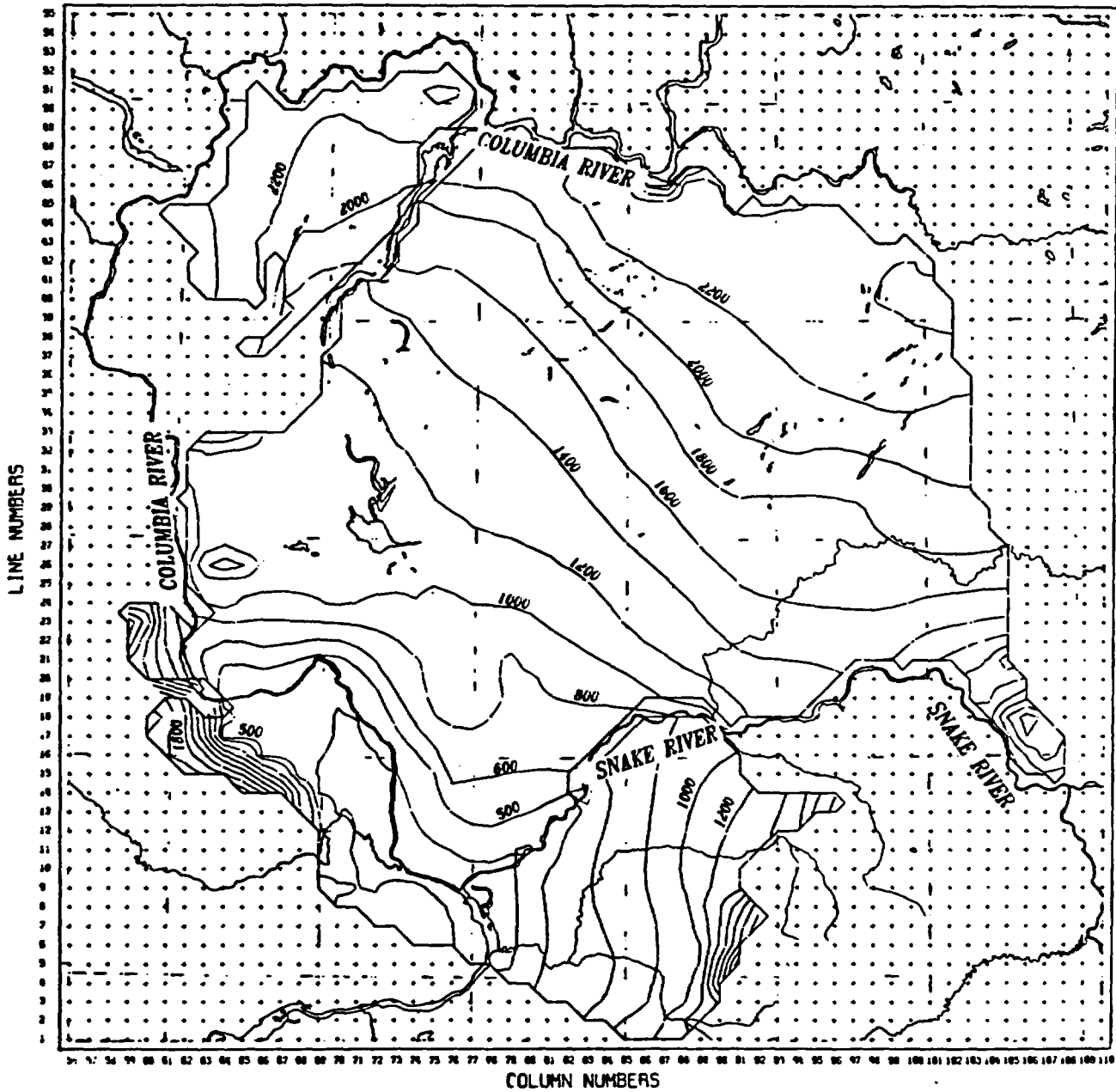


Figure A.4.7 Model-Predicted Hydraulic Heads for the Saddle Mountains/Wanapum Basalts Layer (values are in feet above MSL) (from Dove and others, 1982)

22-141 50 SHEETS
22-142 100 SHEETS
22-144 200 SHEETS

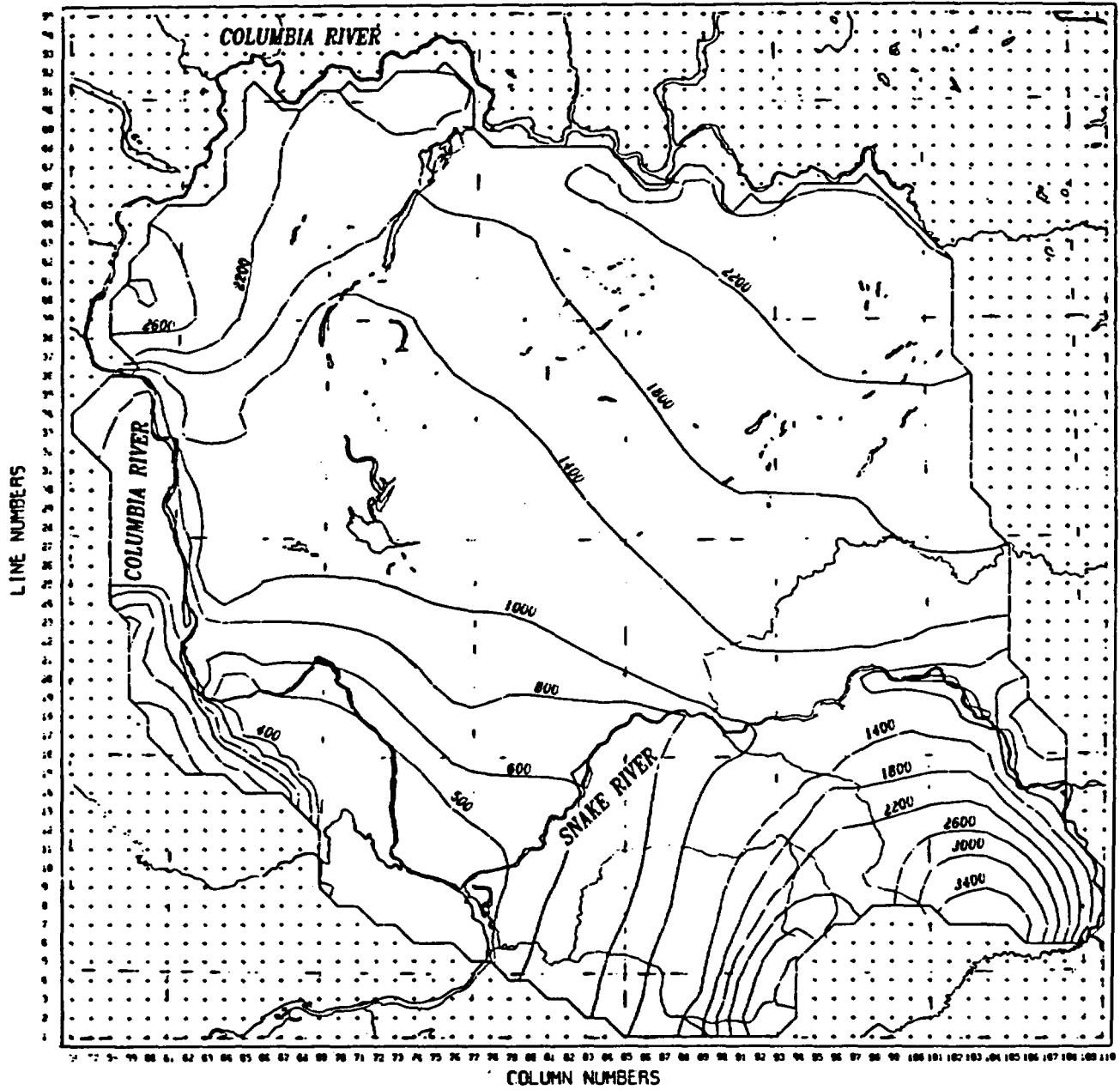


Figure A.4.8 Model-Predicted Hydraulic Heads for the Grande Ronde Basalts Layer (values are in feet above MSL) (from Dove and others, 1982)

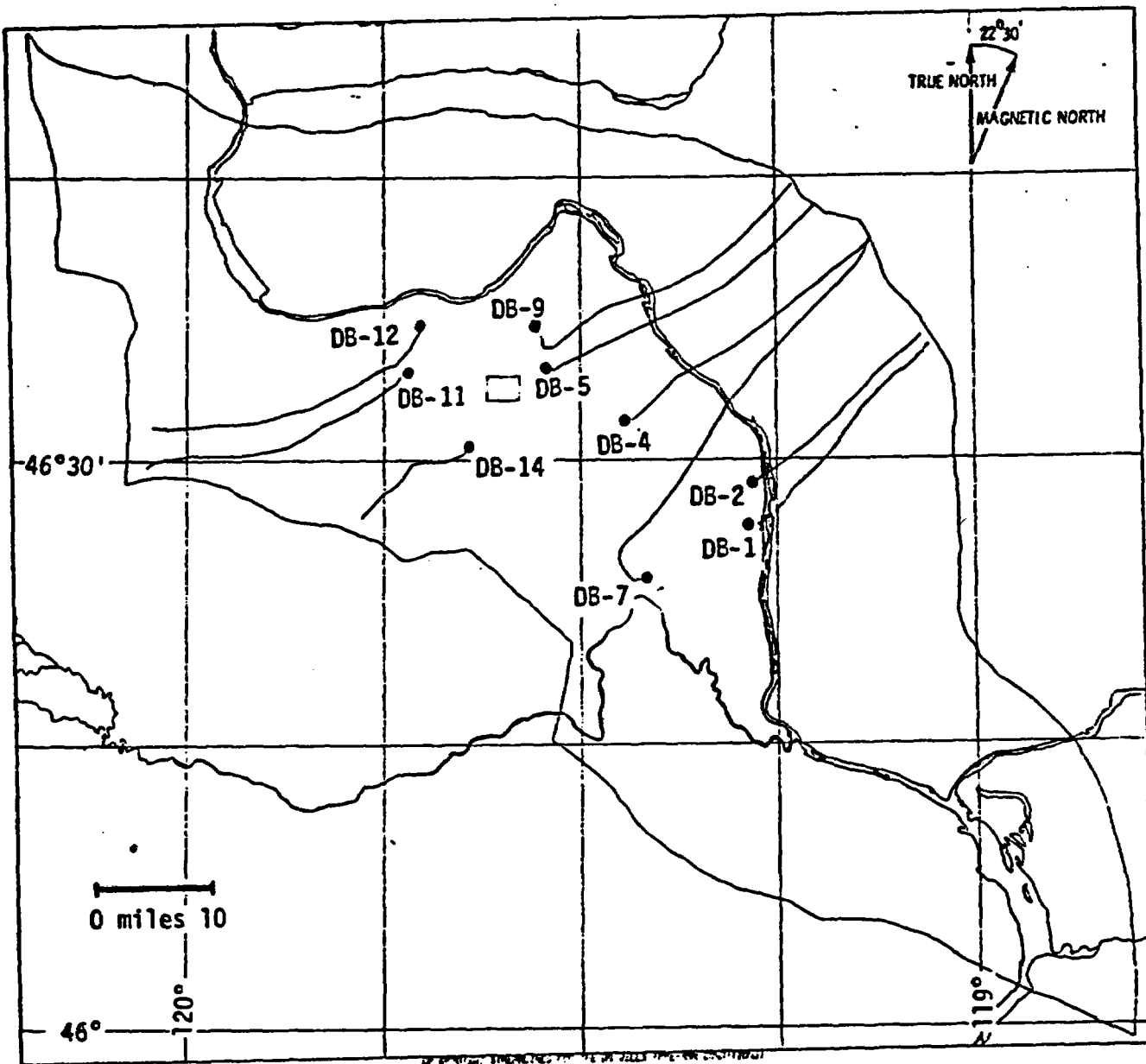


Figure A.4.9 Flow Directions in the Pasco Basin (from Dove and others, 1982)

22-141 50 SHEETS
22-142 100 SHEETS
22-144 200 SHEETS

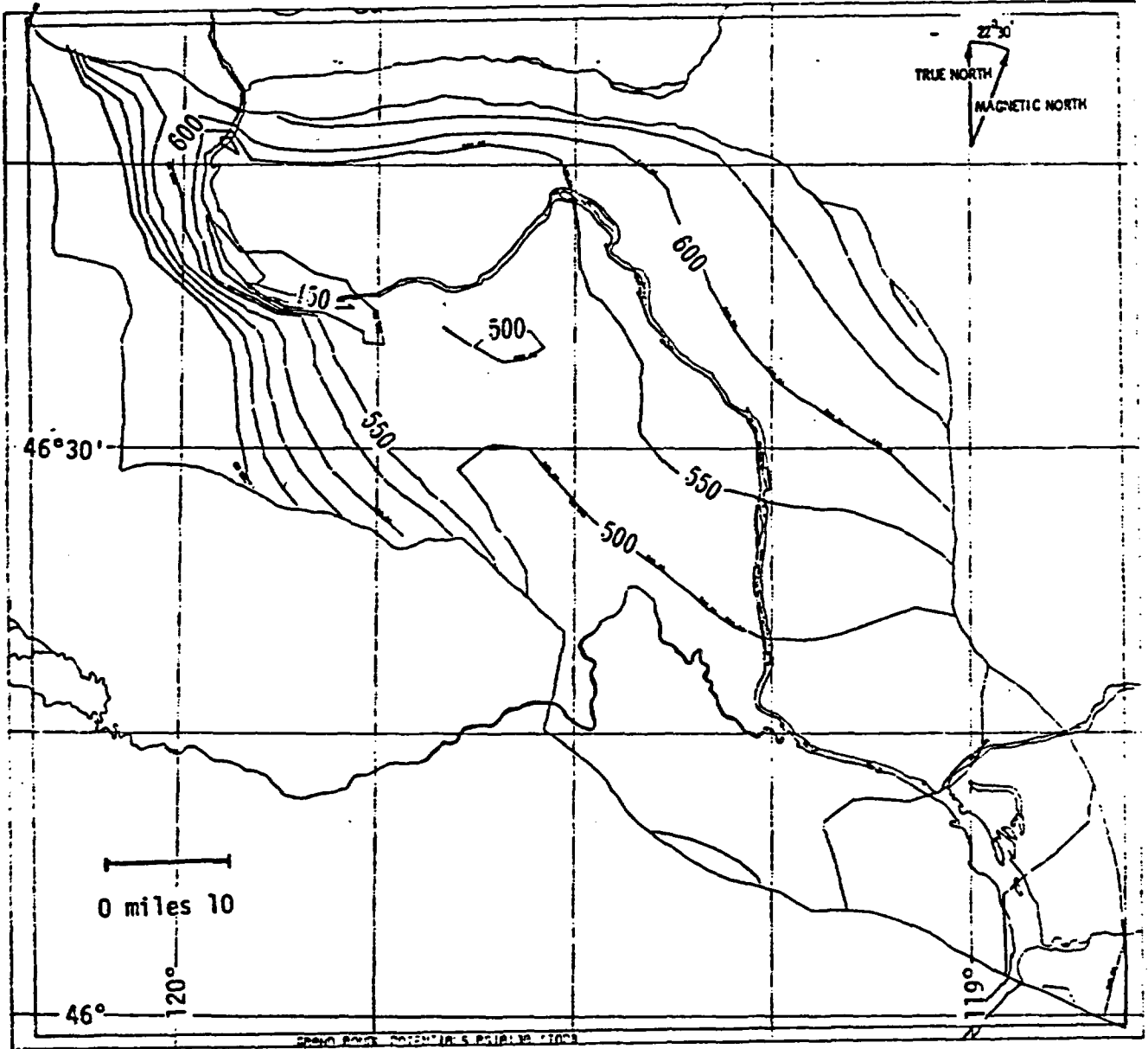


Figure A.4.10 Simulated Hydraulic Heads for the Top of the Grande Ronde for "Preman Conditions" (values are in feet above MSL) (from Dove and others, 1982)

22-141 50 SHEETS
22-142 100 SHEETS
22-144 200 SHEETS

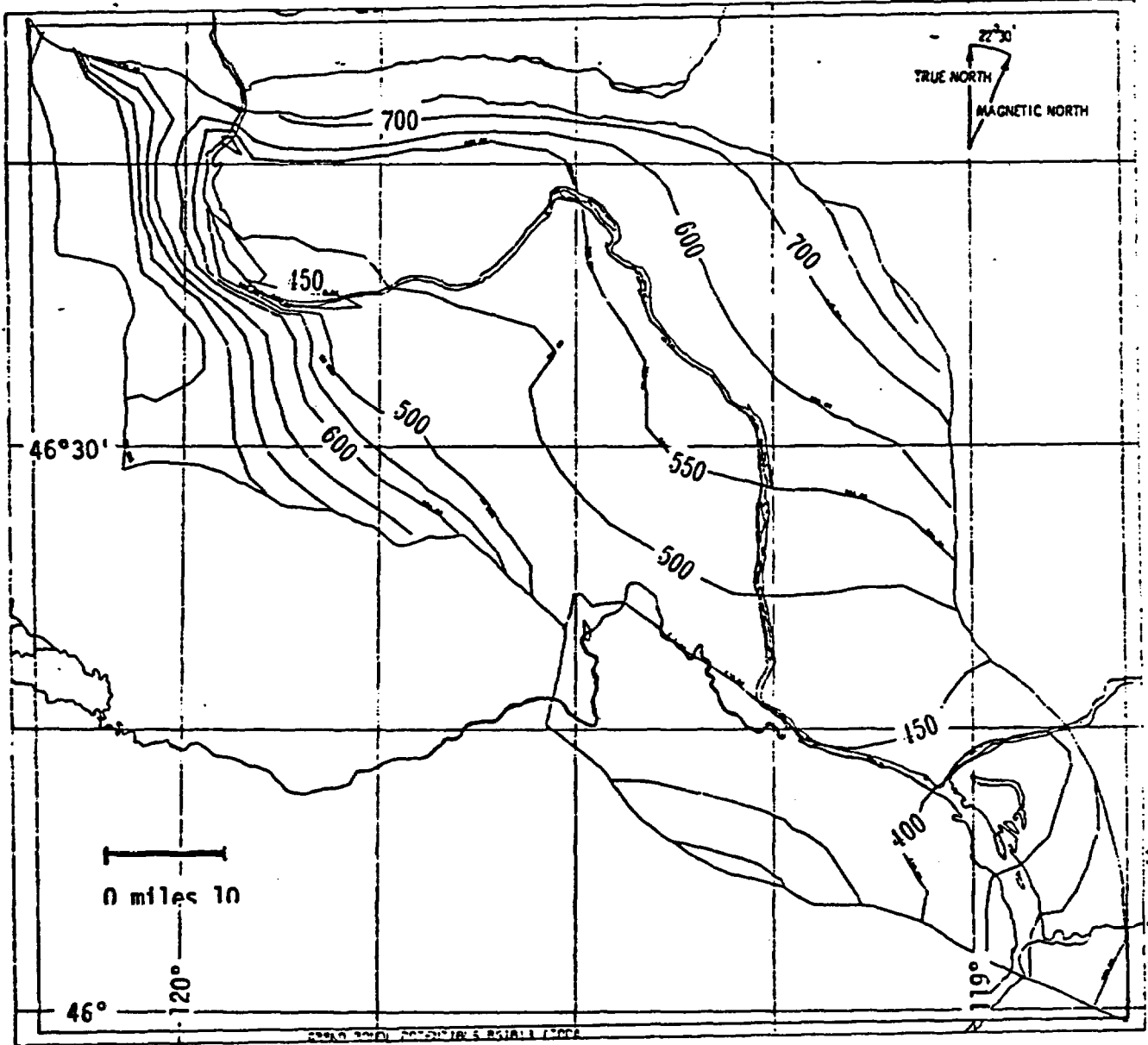


Figure A.4.11 Simulated Hydraulic Heads for the Top of the Grande Ronde for "Current Conditions" (values are in feet above MSL) (from Dove and others, 1982)

22-141 50 SHEETS
22-142 100 SHEETS
22-144 200 SHEETS

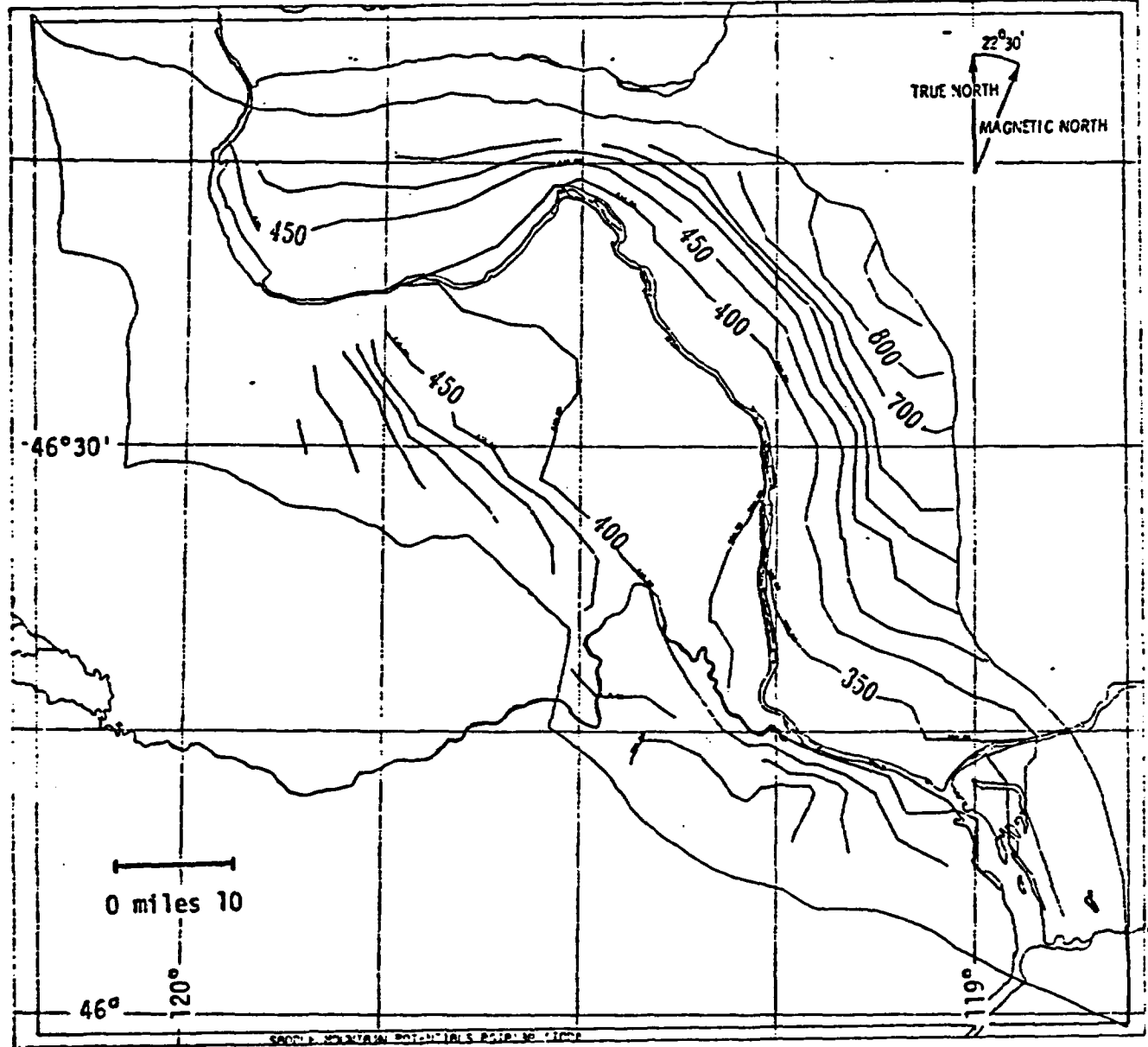


Figure A.4.12 Simulated Hydraulic Heads for the Top of the Saddle Mountains for "Preman Conditions" (values are in feet above MSL) (from Dove and others, 1982)

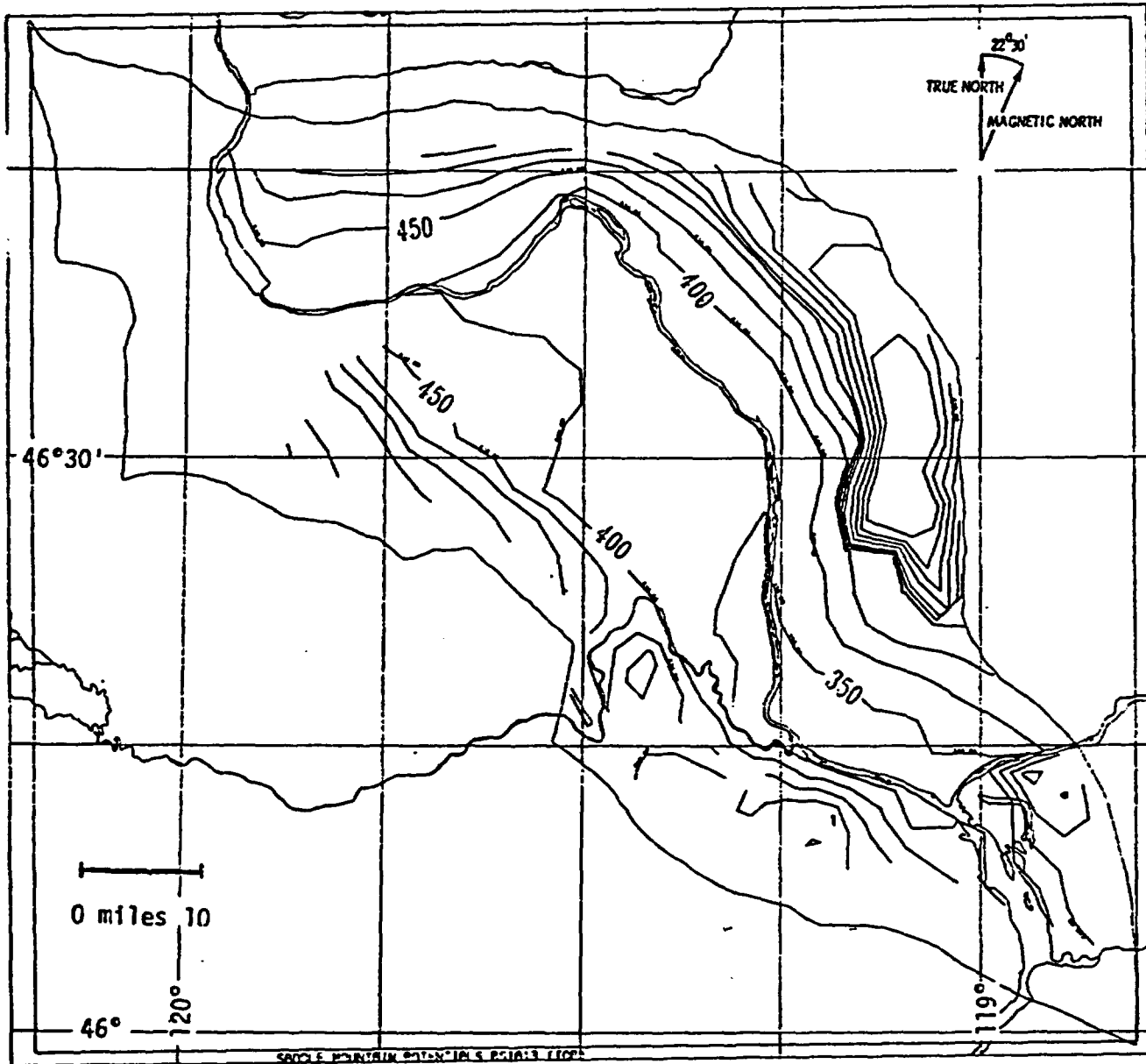
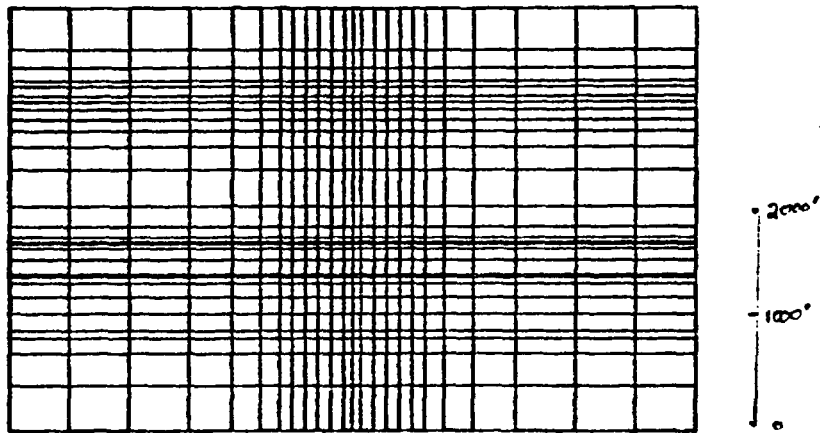
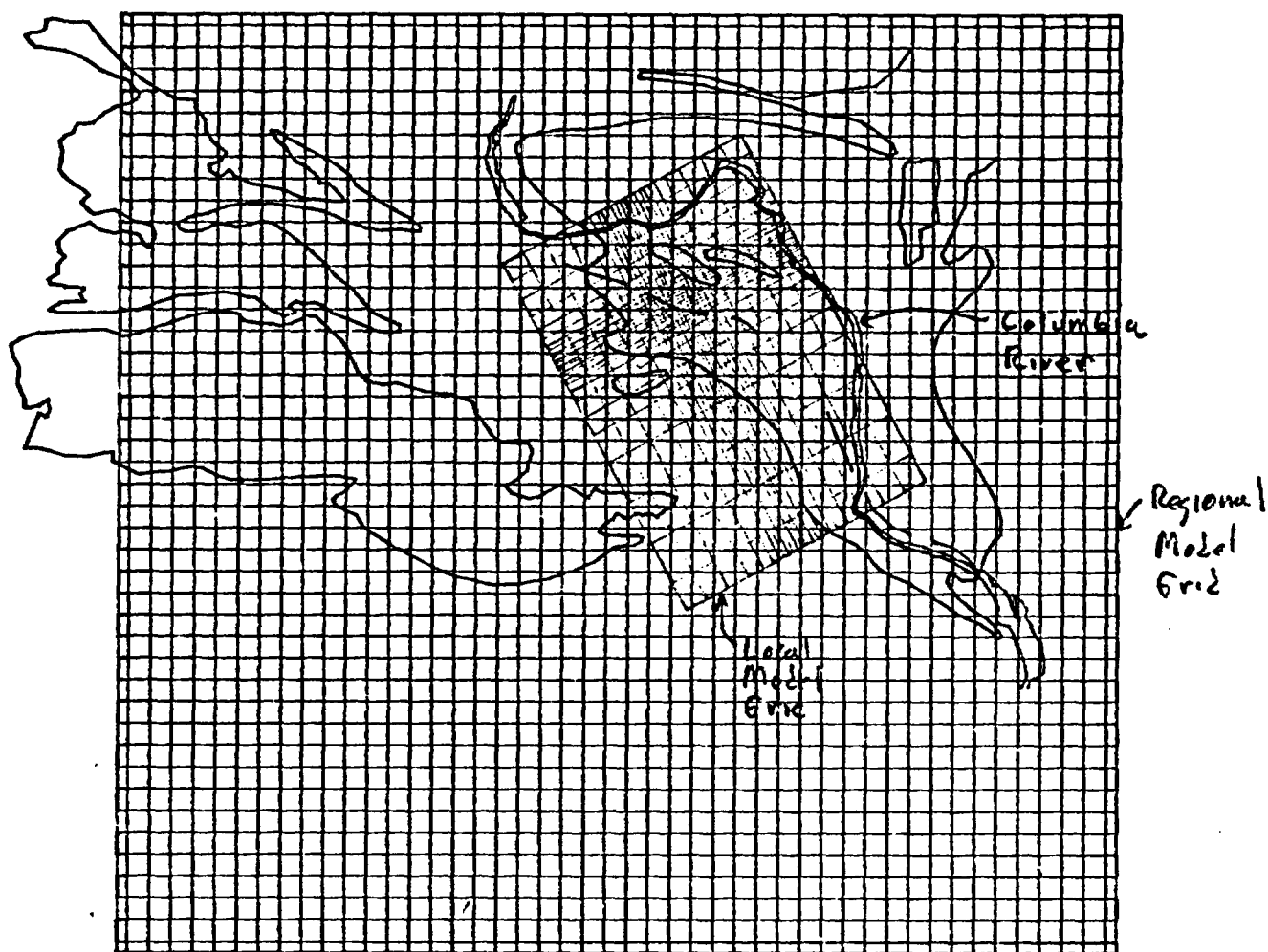


Figure A.4.13 Simulated Hydraulic Heads for the Top of the Saddle Mountains for "Current Conditions" (values are in feet above MSL) (from Dove and others, 1982)

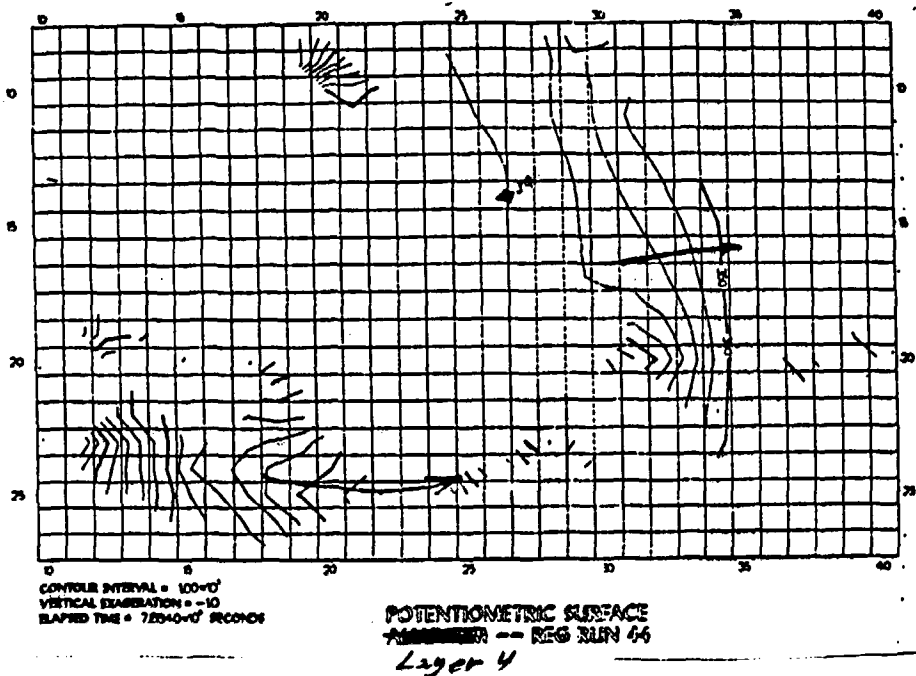


a) Local Scale Model Layering

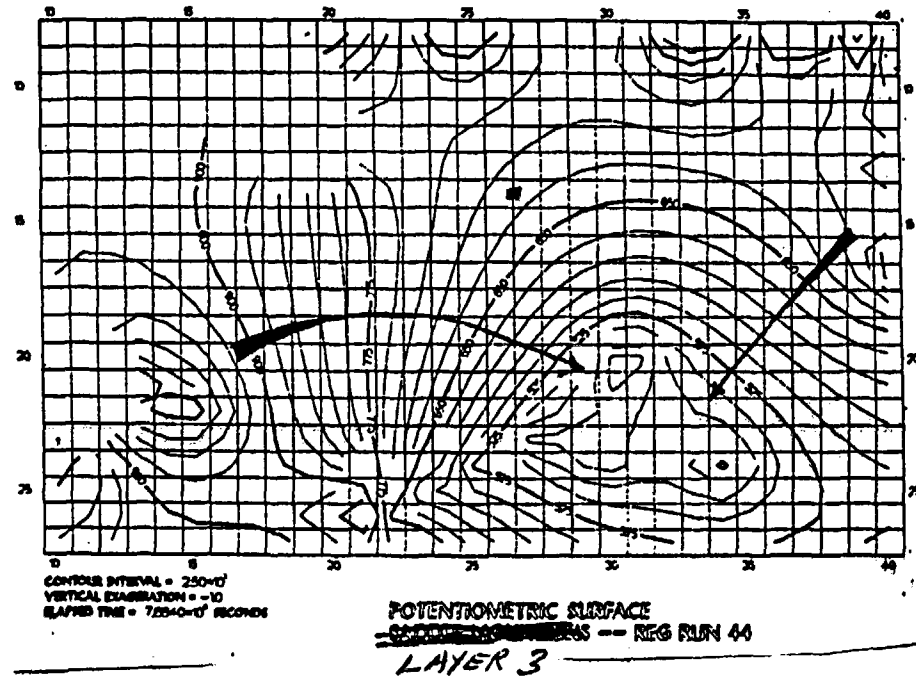


b) Relationship Between the Regional and Local Grids

Figure A.5.1 Local Scale Model Grid



744



780

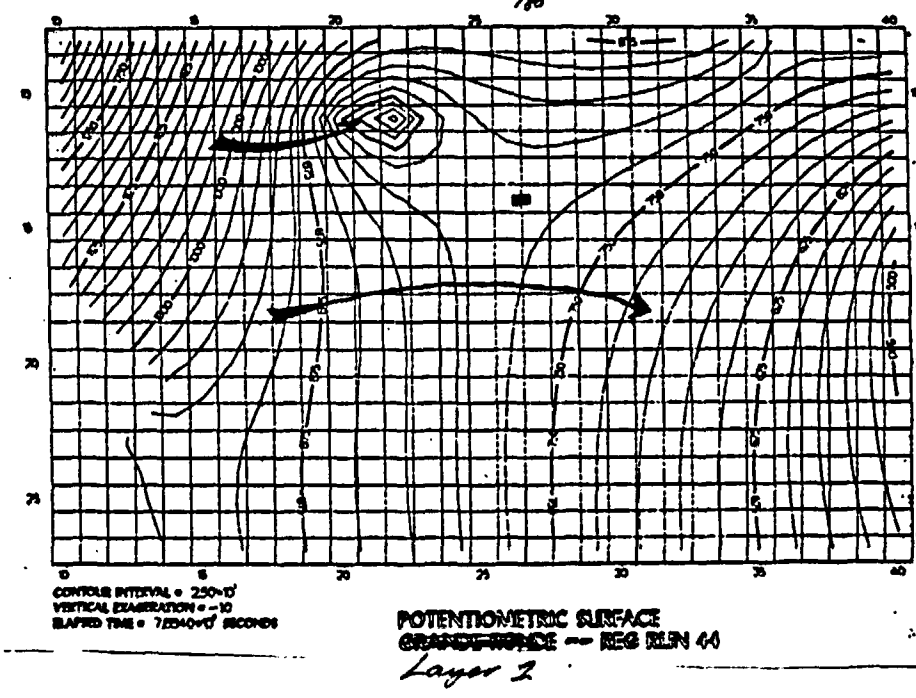
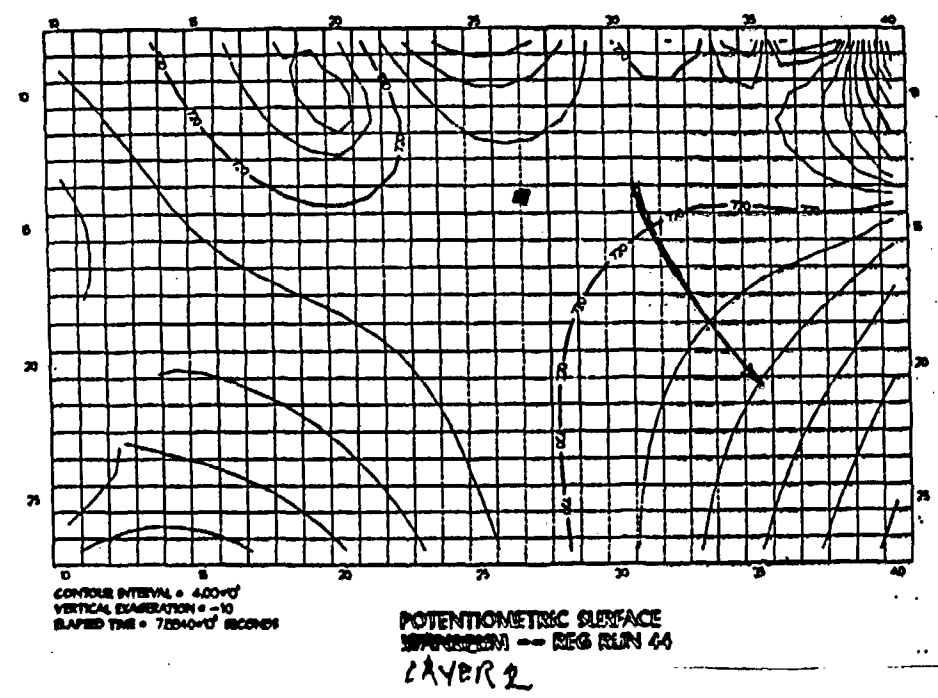
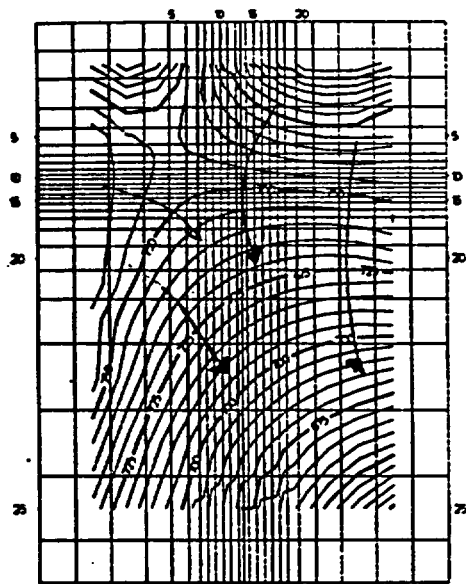
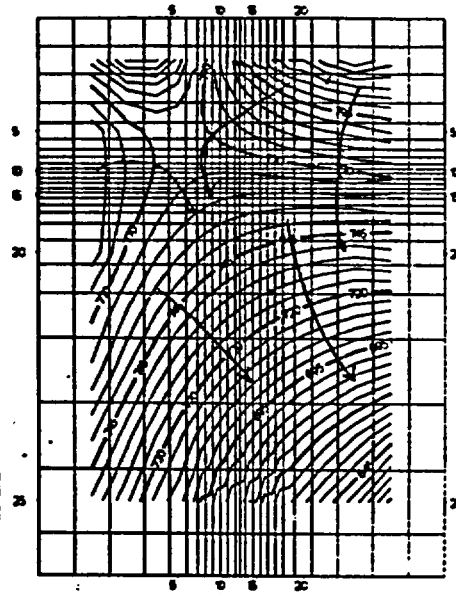


Figure A.5.2 Potentiometric Surface for Layers 1,2,3, and 4
 for the Run Having the Lowest Error Index
 (from Bonano and others, 1986)



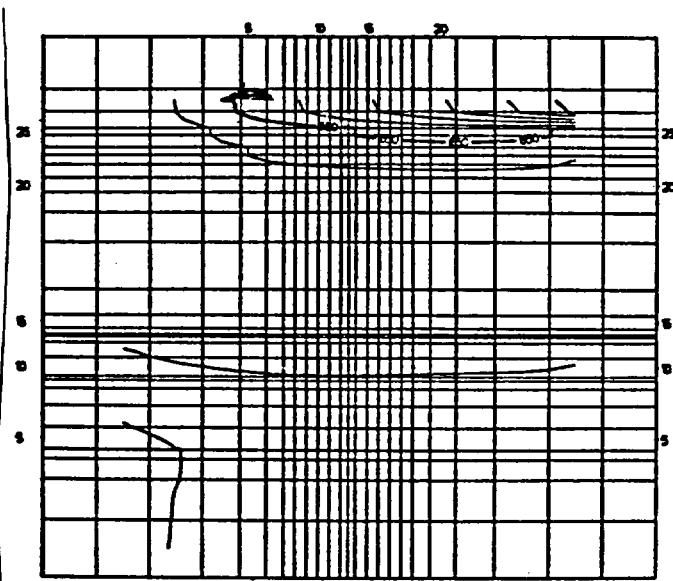
CONTOUR INTERVAL = 500-ft
 VERTICAL EXAGGERATION = 10
 ELAPSED TIME = 85400-yr SECONDS

**LOCAL POTENTIOMETRIC SURFACE
 LAYER 9 -- LOCAL RUN 44**



CONTOUR INTERVAL = 500-ft
 VERTICAL EXAGGERATION = 10
 ELAPSED TIME = 85400-yr SECONDS

**LOCAL POTENTIOMETRIC SURFACE
 LAYER 7 -- LOCAL RUN 44**



CONTOUR INTERVAL = 500-ft
 VERTICAL EXAGGERATION = 300
 ELAPSED TIME = 85400-yr SECONDS

**LOCAL VERTICAL CROSS SECTION
 THROUGH ROW D -- LOCAL RUN 44**

Figure A.5.3 Potentiometric Surface from the Local Scale Model in the Flow Tops adjacent to the Hypothetical Repository, and in a Section Through the Hypothetical Repository (from Bonano and others, 1986)

Appendix B
Theoretical Background of Kriging

Kriging is an interpolation procedure named for D. R. Krige, who applied the technique to the estimation of mineral reserves. Unlike least-squares interpolation techniques, kriging restitutes measured values at the observation points, as well as providing an estimate of the accuracy of interpolated values.

The goal of any interpolation procedure is, given a number of observations of a field Z at the points x_i , to estimate the value of the field at some point where an observation is not available. In the kriging approach the interpolated value Z^* of the field Z at a point x_0 is calculated as a linear combination of some subset of the available observations:

$$Z^*(x_0) = \sum_{i \in I} w_i Z(x_i) \quad (B-1)$$

Usually the subset I consists of observations made in the neighborhood of x_0 . The w_i are the weights given to each observed field value $Z(x_i)$. These weights are calculated to give an unbiased, minimum variance estimate of $Z(x_0)$, that is

$$\langle Z(x) - Z^*(x) \rangle = 0, \text{ and} \quad (B-2)$$

$$\langle [Z(x) - Z^*(x)]^2 \rangle = \text{minimum} \quad (B-3)$$

Where the indicated averaging is performed over the domain of interest. Equations (B-2) and (B-3) are unsolvable as such, because the value of the field $Z(x)$ is only known at discrete points. By making assumptions about the field Z , (B-2) and (B-3) can be transformed into a tractable system of equations relating the unknown coefficients w_i to the observations $(x_i, Z(x_i))$. In the development of Kafritsas and Bras (1984), Z is assumed to be an intrinsic function of order k . Further, the residual $Z(x) - Z^*(x)$ is assumed to be a generalized increment of order k .

The following discussion of generalized increments of order k and intrinsic random functions of order k was adapted from 'The Practice of Kriging' by Kafritsas and Bras (1984):

Consider a linear operator G on Z defined as follows:

$$G(Z) = \int Z * g(dx) \quad (B-4)$$

The operator G is a generalized increment of order k if, for any field Z

$$G(Z + P_k) = G(Z) \quad (B-5)$$

where P_k is any polynomial of order k . P_k may be written as

$$P_k = \sum b_m f_m \quad (B-6)$$

with b_m being any constant multiplier, and f_m any simple monomial of the form:

$$f_m = x_1^{b_1} x_2^{b_2} x_3^{b_3} \dots x_n^{b_n} \quad (B-7)$$

with

$$\sum_{i=1}^n b_i \leq k \quad (B-8)$$

Because G is linear, an equivalent condition to (B-5) is

$$G(f_m) = 0 \quad (B-9)$$

for every f_m of order less than or equal to k .

A field Z is said to be an intrinsic function of order k if the following conditions hold:

$$\langle G(Z) \rangle = 0 \quad (B-10)$$

for every generalized increment G of order k ; and there exists a function K such that for any two generalized increments G and G' of order k ,

$$\langle G(Z) G'(Z) \rangle = \iint K(x-y) G(dx) G'(dy) \quad (B-11)$$

K , called the generalized covariance, relates variance to vector separation.

As a consequence of these assumptions, equation (B-2) will be satisfied if

$$\sum_{i \in I} w_i * f_m(x_i) = f_m(x_0) \quad (B-12)$$

for every monomial f_m of order less than or equal to k . In other words the coefficients w_i are constrained to interpolate any polynomial of order k or less with zero residual. These assumptions also allow the expected variance constraint (B-3) to be written as follows:

$$\begin{aligned} <[Z(x) - Z^*(x)]^2> = \\ \sum_{i_1 \in I} \sum_{i_2 \in I} w_{i_1} w_{i_2} K(x_{i_1} - x_{i_2}) - 2 \sum_{i \in I} w_i K(x_0 - x_i) \\ + K(0) = \text{minimum} \end{aligned} \quad (B-13)$$

The solution of (B-13) for the w_i obviously depends on the generalized covariance function K . This function can be estimated from the available data, as described below. Minimizing (B-13) subject to the constraints (B-12) gives the following system of equations:

$$\begin{aligned} \sum_{i \in I} w_{i_1} K(x_{i_1} - x_{i_2}) + \sum_{m=1}^{l(k)} u_m f_m(x_{i_2}) \\ = K(x_0 - x_{i_2}) \quad , i_2 \in I \end{aligned} \quad (B-14)$$

$$\sum_{i \in I} w_i f_m(x_i) = f_m(x_0) \quad , m=1..l(k) \quad (B-15)$$

Where u_m are Lagrange multipliers, and $l(k)$ is the number of monomials of order less than or equal to k .

The central problems in applying this technique are determining an appropriate order k and generalized covariance K . Delfiner (1976) states that almost all practical fields can be characterized as intrinsic functions of order 0, 1, or 2 with generalized covariances having the form:

$$K(h) = c_0(h) + a_1|h| + a_3|h|^3 + a_5|h|^5 \quad (B-16)$$

where $\delta(h) = 1$ for $h = 0$, $\delta(h) = 0$ for $h \neq 0$, $|h|$ is the separation distance, and c and $\{a_i\}$ are undetermined coefficients. In the program AKRIP (Kafritsas and Bras, 1984), these coefficients are iteratively calculated for each order and each assumed form of generalized covariance. Iteration is controlled by the estimated residuals from a defining relationship for generalized covariance. Once coefficients have been calculated for each form of the covariance function, each function is used to estimate variance at each observation location from data points surrounding that location. The function giving the lowest variance estimate at the greatest number of points is selected. Note that the covariance function must be selected prior to solving equations (B-14) and (B-15), and that selecting the covariance function based on minimum variance prediction is unrelated to the minimum variance condition imposed on the w_i by equation (B-2).

Once a generalized covariance has been selected the weights w_i are calculated for each point at which an interpolated value is required. The interpolated value is then calculated from these weights and the observed values. Interpolated variance is estimated from the expression for $[Z(x) - Z^*(x)]^2$ in terms of the generalized covariance.

Reference:

- Kafritsas, J. and Bras, R. L. 1984. The Practice of Kriging (Second Edition). Technical Report No. 263. Ralph M. Parsons Laboratory, Department of Civil Engineering, M.I.T.
- Delfiner, P., 1976. Linear Estimation of Non-Stationary Spatial Phenomena, in Guarascio and others, Advanced Geostatistics in the Mining Industry, NATO Advanced Study Institute Series, Reidel Publishing Co., Boston.

Appendix C
Application of Kriging to BWIP head data

A. The Use of Kriged Heads

Measurements of hydraulic head in the three basalt groups were provided indirectly by the USGS through DOE (Olson, 1984). The kriging program AKRIP (Kafritsas and Bras, 1984) was then used to interpolate head values at the center of the model nodes. These interpolated values were used in both constructing input to the BWIP model, and in evaluating the model results.

In addition to the water level elevations reported by Olson, river elevations were used to interpolate heads. These river data were not used to estimate the generalized covariances, as the spatial correlation of river elevations would be different than the spatial correlation of heads in the basalts.

Fixed head boundary nodes were used in the areas of the model where the simulated units extended beyond the model boundaries (figure C.1). Using fixed head nodes at these locations permits flow components normal to model boundaries in those areas where the model boundaries do not coincide with the physical boundaries of the basalts. The head value for each of these fixed head nodes was the kriged head at the location of the node.

The interpolated heads were also used to provide a measure of the agreement between model results and the observed heads. The model-calculated head at each location, n , was compared to the interpolated head as follows:

$$E_n = \frac{|Hm_n - Hi_n|}{1 + \sigma_n} \quad (C-1)$$

where Hm_n is the model-calculated head at node n , Hi_n is the kriged head at node n , and σ_n is the standard deviation of interpolation estimated by AKRIP. The quantity $(1 + \sigma_n)$ was used rather than σ_n alone to prevent numerical problems at nodes coinciding with data points, where the standard deviation of interpolation is 0. This normalized error was calculated for each node in the active areas of the model, and averaged for each layer. A composite average for the entire model was also calculated. The resulting error index can be interpreted as the average number of standard deviations by which the model results differ from the interpolated heads.

The error index specified by (C-1) provides an indication of the agreement of the model results with the observed data. A low value of the error index could indicate similarity between head values at many locations, making the numerator of (C-1) small,

or scarcity of data, making the interpolation variance, and consequently the denominator of (C-1), large. In the latter case a simulated head field with a low error index would still have considerable uncertainty associated with it. The degree to which the model represents the actual flow system depends on both the agreement between model results and observations, estimated by the error index, and the sufficiency of the observations to characterize the flow system.

B. The Calculation of Kriged Heads

In order to interpolate values for grid nodes, the relationship between the grid coordinate system and the observed head coordinate system must be known. The coordinates of the reported 1984 data, although given in feet, are referred to an unknown origin. They have the wrong order of magnitude to be given in either state planar or Hanford coordinates, the two commonly used coordinate systems for BWIP data. All efforts at identifying the person responsible for compiling the data were unsuccessful, as were inquiries after possible locations for the origin used in reporting the observed heads. We ultimately decided to plot the reported data at the same scale as existing maps showing selected well locations, and estimate the location of the data origin by overlaying the plot of reported well locations on our maps. Confidence in the origin estimated in this way was supported by it's location along the Willamette base line

Once the relationship between the data and grid was established AKRIP was used to estimate heads and interpolation variance at each model node. The uniformly large interpolation variances prompted an examination of the input data. Observed heads in the Wanapum and Saddle Mountains units seemed to be divided into two groups: high heads generally in the northwest and southwest corners (where recharge from rainfall is significant); low heads in the central, and eastern parts of the modeled region. Based on this observation the data for each of these layers was divided into two groups: observed heads greater than 700 feet, and those less than 700 feet. A generalized covariance was calculated for each group separately. Each group was then used to estimate a head at each model node. A single kriged head surface was obtained from the two sets of interpolated heads in the following way: the head for a given node came from either the set of nodes kriged using data above 700 feet, or the set using data below, depending on the variance of interpolation. The interpolation variance for each set at the given node was compared, and the head from the set with the lower variance selected.

The desired outcome was that a node near a cluster of data from one group would be assigned the head interpolated from the heads in that group. Combination based on estimated variance was designed to accomplish this, as a value interpolated from nearby

heads should have a lower variance associated with it than a value interpolated from a more distant set of measurements. The data in the two groups showed a higher degree of correlation than the combined data, as expected, however the combined interpolated heads were later discovered to have some undesirable characteristics. Interpolated values for a given node usually differed by hundreds of feet, so that when heads from different sets were used in adjacent nodes unrealistic gradients were generated. Boundary head values varied radically in these regions of transition. Once this problem was detected, we decided to use the entire data set in spite of the larger variance.

Subsequently, a number of problems associated with the kriged heads were discovered in attempting to calibrate the model. Inspection of the contour map of kriged heads in the Saddle Mountains layer revealed a predicted head of 2100 feet in the northwest corner of the model where the highest measured head was 1700 feet. We checked the data used in kriging against the listing supplied from the USGS, and discovered typographical errors in the data for each formation. Correcting these errors didn't correct the erroneously high head in the Saddle Mountains. On re-kriging using the corrected data, a second order ($k=1$) variance structure was found to best characterize the data for the Wanapum. When this structure was used for interpolation, the calculated heads ranged from -400 to 7000 feet when the observed data range was 200 to 1500 feet. This problem was eliminated by using an inferior alternate variance structure with $k=0$. Before the input data was corrected the optimal variance model for the Saddle Mountains was also second order. The interpolated value of 2100 feet in the northwest apparently arose from the second order variance model.

A new kriged head surface was generated using the corrected data and first order variance structures. Boundary conditions were enforced using the new kriged heads. As it became apparent that homogeneous model layers could not produce the areal variation in gradient direction and magnitude evident in the contours of the kriged heads, we attempted to identify geologic structures associated with the regions of apparent discontinuity. This effort required a consideration of the observed heads and their locations, including river elevations. These elevations were recovered from the model output, and found to be grossly in error. Elevations enforced at the river nodes had apparently been taken from a kriged head surface, rather than from river elevation data. In attempting to relate structural features to apparent discontinuities in the flow field the measured heads were found to be incorrectly located with respect to the grid. The error in the locations using the origin along the Willamette base line was identified by the consequent displacement of the cluster of wells near the RRL. Using the pattern of these wells, it was possible to associate well designations with the supplied measurement points. The coordinates of these wells were also known in Hanford coordinates, which allowed the location of

the origin of the supplied data to be calculated with respect to the Hanford coordinate system.

Once the data were plotted in the correct location, the influence of structural features on the head surface became apparent. The following conclusions were made after considering structural data and extant water level data, and were used in reconstructing the BWIP model:

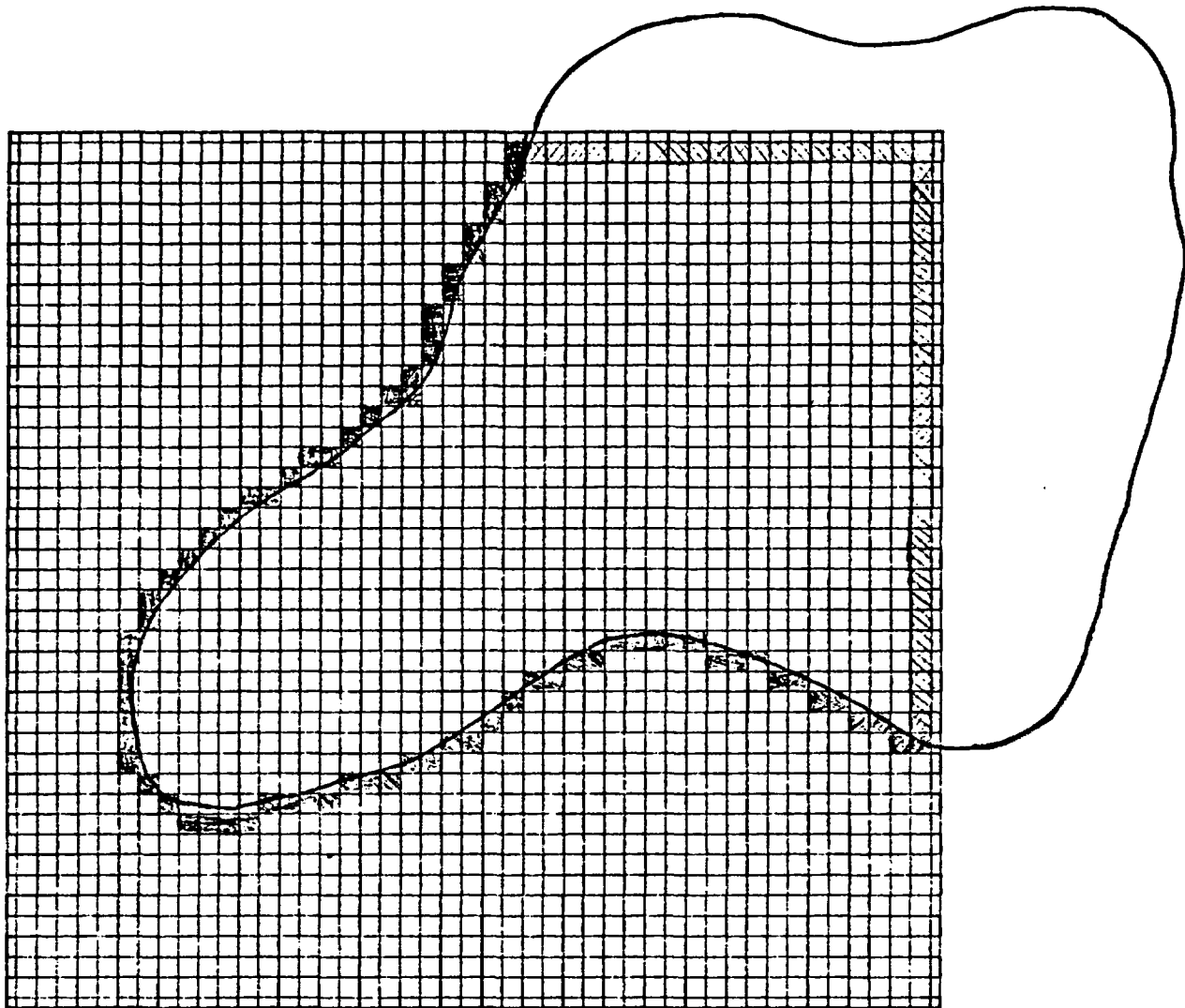
The Horse Heaven structure separates the flow system in the Horse Heaven basin from systems to the north in both the Saddle Mountains and Wanapum basalts. No hydrologic data exists in this area for the Grande Ronde.

The Rattlesnake Hills, Yakima, and Umtanum anticlines bound three troughs of the exposed Wanapum basalt in the northwest. These independent systems are joined to the east approximately where the bounding features turn to the south.

The Saddle Mountains basalt is discontinuous across the Rattlesnake anticline. This discontinuity effectively isolates the Saddle Mountains in the Yakima Basin from the Saddle Mountains formation in the Pasco Basin. The two systems are joined in the vicinity of Badger Mountain.

The Yakima, Horse Heaven, and Pasco basins appear to be composed of distinct parts of both the Saddle Mountains and Wanapum basalts. Head data collected for these formations in one basin should be independent of data collected for the same formation in another basin. For this reason, the head data for the Wanapum and Saddle Mountains layers were divided into three groups based on well location. Additionally Pasco Basin data in both formations which had apparently been significantly influenced by irrigation recharge were considered separately, as were Wanapum data in the northwest corner of the model, where the basalts are exposed and interrupted by the Yakima, Umtanum, and Rattlesnake Hills anticlinal features. The data in each group were kriged separately (generalized covariances are shown in figure B.2). Model nodes were assigned to one of the groups based on node location. The interpolated value for that node came from the data for the group to which it was assigned.

The resulting combined kriged head surface (figures 7.46a - 7.48a) shows none of the undesirable irregularities of the surface made from groupings based on head measurement. Drastic variations in head between adjacent nodes occur only across discontinuities in the formation.



No-Flow Boundaries

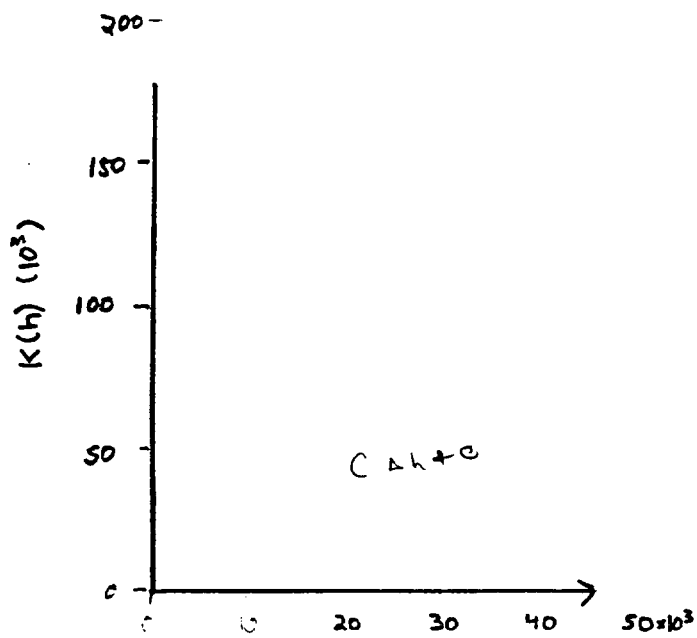


Hypothetical Basalt Boundary

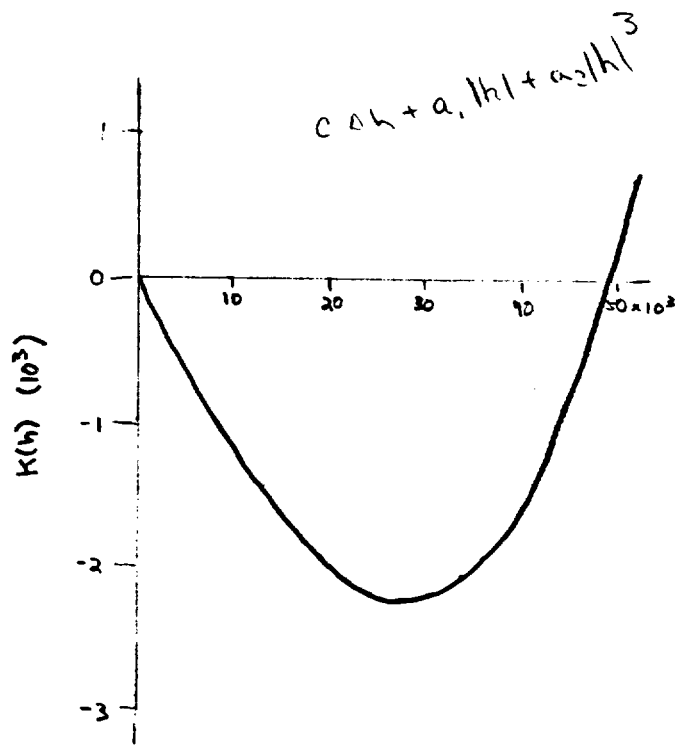


Constant Head Boundaries

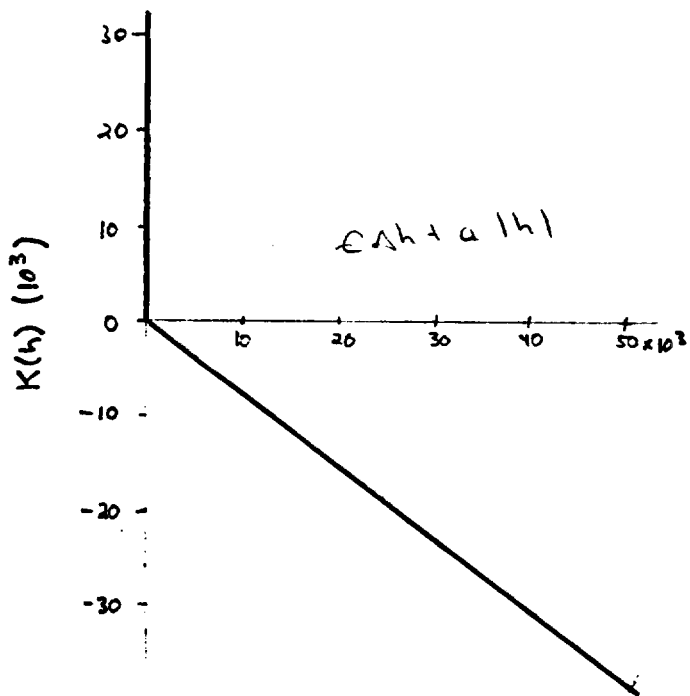
Figure C.1 - Use of Constant Heads at a Model Boundary for a Hypothetical Basalt Layer



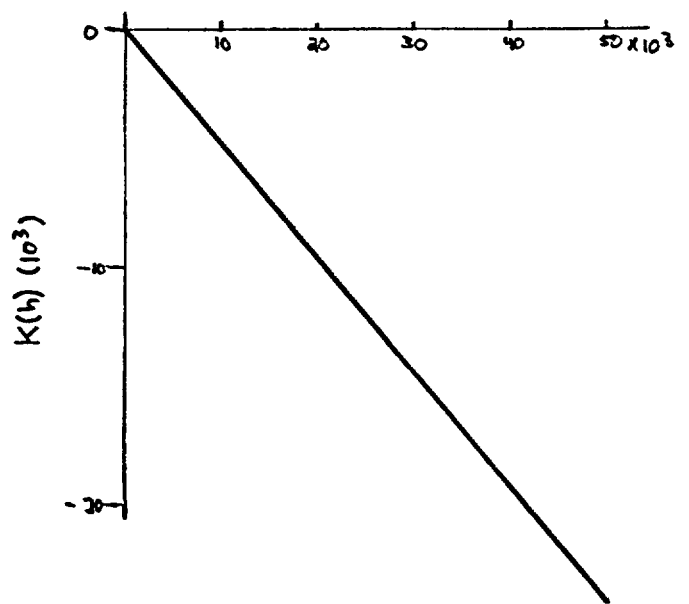
A. Wanapum - Horse Heaven Hills



C. Wanapum - Yakima

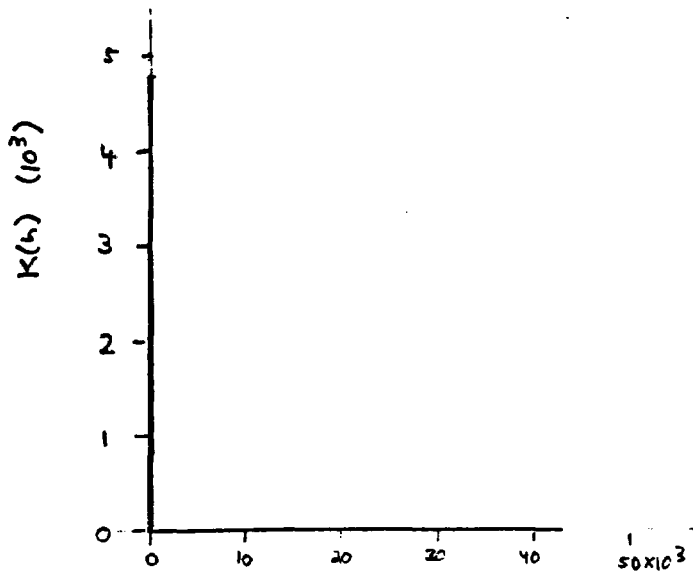


B. Saddle Mtns. - Horse Heaven Hills

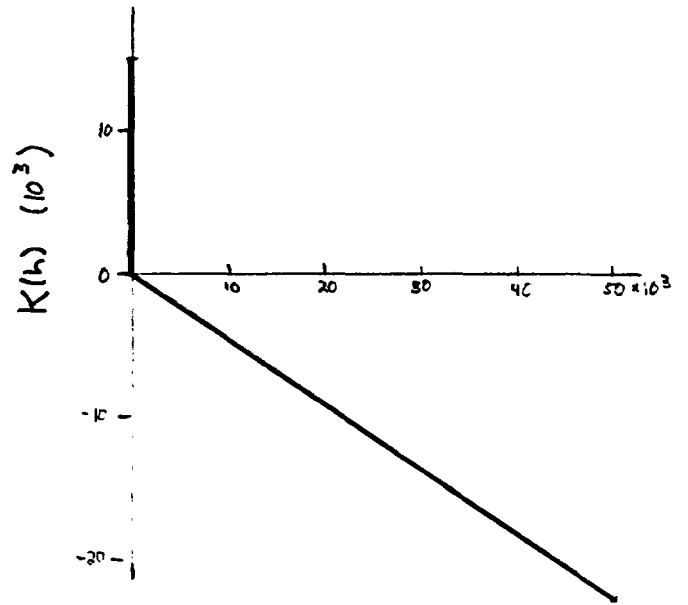


D. Saddle Mtns. - Yakima

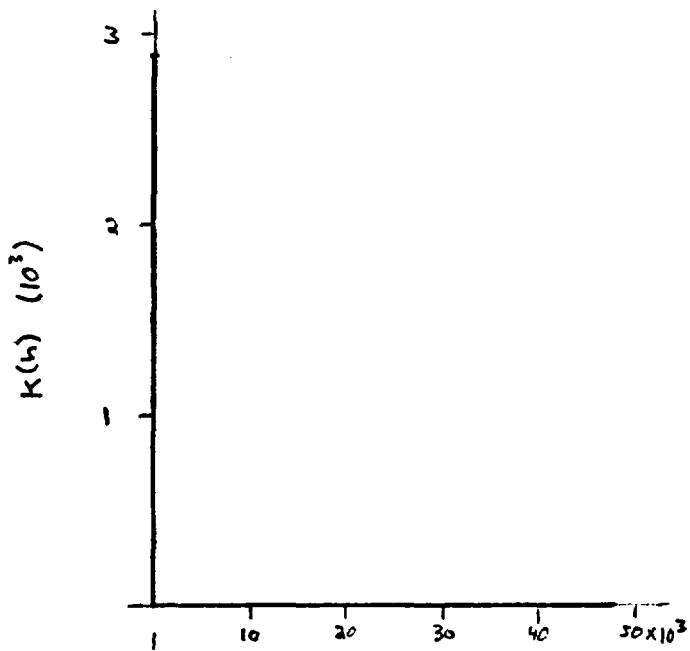
Figure C.2 - Generalized Covariance Functions for the Saddle Mountains, Wanapum, and Grande Ronde Basalts



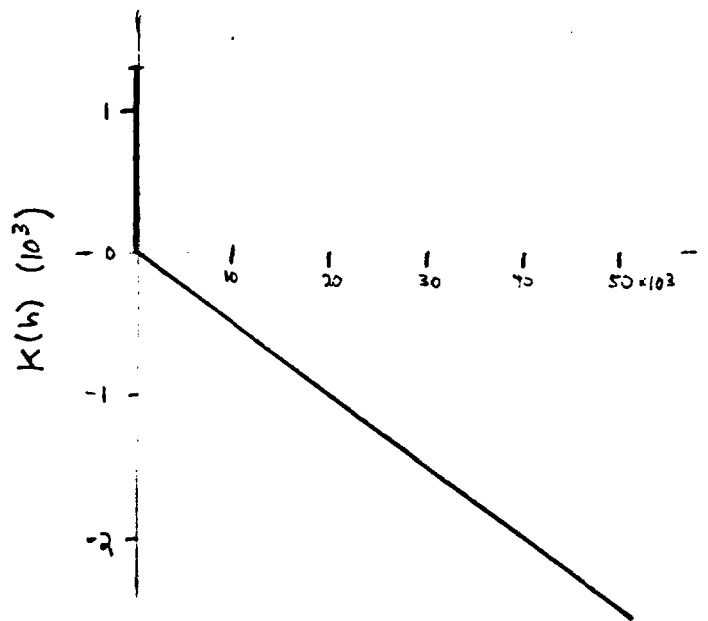
E. Wanapum - Pasco Basin South and West of Columbia River



G. Wanapum - Pasco Basin North or East of Columbia River

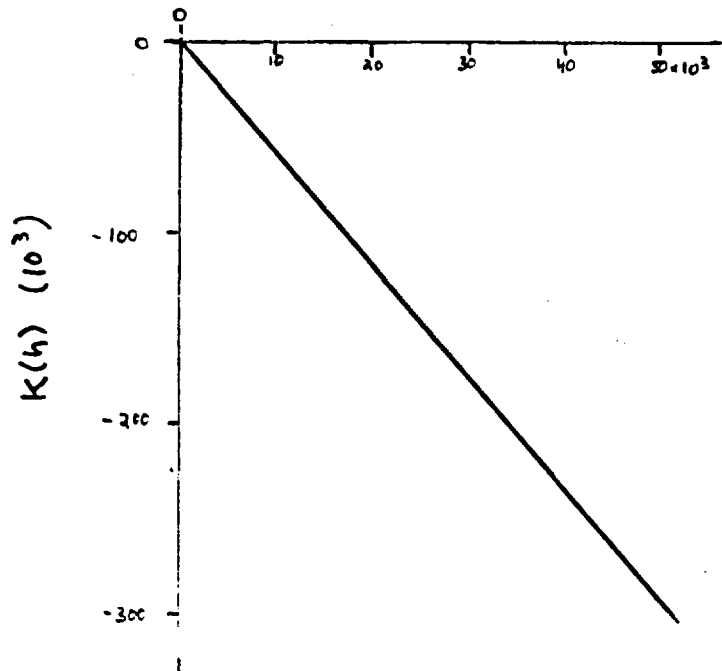


F. Saddle Mtns. - Pasco Basin South and West of Columbia River

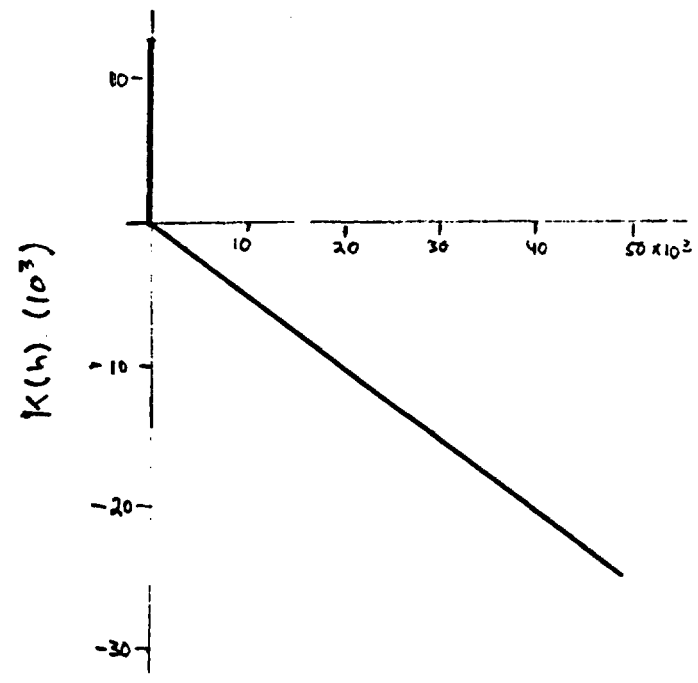


H. Saddle Mtns. - Pasco Basin North or East of Columbia River

Figure C.2 (Continued)



I. Wapapa - Exposed



J. Grande Ronde

Figure C.2 (Continued)